TURBULENCE AND DRAG REDUCTION WITH

POLYMER ADDITIVES

By

ALAN WHITE, B.Sc.,M.Sc.,C.Eng.,M.I.Mech.E.

A Thesis submitted for the Degree of Doctor in Philosophy through the Council for National Academic awards at Hendon College of Technology. (Part of the proposed Middlesex Polytechnic.)

JULY, 1972

FOREWORD.

Quite remarkable reductions of frictional drag can be obtained under turbulent flow conditions by dissolving small traces of certain additives in a liquid solvent. The discovery of the effect dates back nearly twenty five years from the present time and was observed quite independently both in the U.S.A. and this country with quite different substances.

Towards the end of World war II a group of researchers were involved in the development of incendiary weapons for the U.S. Army Chemical Warfare Service, and in 1945 it was discovered that under turbulent pipe-flow conditions, a viscous Napalm-gasolene gell offered less flow resistance than the untreated gasolene. Due to wartime security regulations the publication of these results was rather unorthodox and scattered, and lagged the actual discovery date by a number of years, the first available publication being a U.S. Patent filed by Karol Mysels in 1949, (1).

During 1947 the friction reduction effect was independently observed in this country by B.A.Toms and J.G.Oldroyd, who were working with the Fundamental Research Laboratory of Courtoulds Ltd. They were concerned with the shear dependent behaviour of high polymer solutions in small bore tubes, and using a solution of polymethylmethacrylate in monochlorobenzine found that the flow

resistance of the solution was less than that of the solvent alone under turbulent flow conditions, and at the same flow rate. The experimental results of Toms and an analysis by Oldroyd were presented in 1948 at the First International Rheology Congress (2).

TABLE 1.

Year	Cumulative total No. of publications.
1949	3
1953	3
1954	4
1955	5
1956	5
1957	6
1958	7
1959	9
1960	9
1961	12
1962	18
1963	24
1964	42
1965	79
1966	140
1967	190
1968	210
1969	280
1970	320
1971	400

A rough cumulative total of unclassified world literature directly related to drag reduction.

Although interest in this phenomenon is now worldwide, the initial developments following the original discoveries were very slow. Table 1 shows a cumulative count of unclassified documents relevent to drag reduction, year by year up to the present time, and is based on information collated by Savins (3). Widespread research activity in this field did not really get under way until the mid 1960's when Hoyt and Fabula working with the U.S. Naval Ordnance Test Station, investigated a whole range of water soluble high polymers. They showed that with some of these additives extremely large friction reductions were possible with just a few parts per million by weight of the polymer in solution. A.G. Fabula presented a paper on his work at the Fourth International Congress on Rheology in August 1963 (4), and J.W.Hoyt presented some further aspects of the work in a joint paper with A.G.Fabula at the Fifth Symposium on Naval Hydrodynamics in September 1964 (5).

Results by other workers with rather more concentrated drag reducing solutions were appearing by this time, and clearly there were now great possibilities for economical exploitation of the phenomenon in a number of practical applications, although the mechanism of the effect was not understood. The whole subject now presented a most interesting and challenging topic for research which was seized upon by both industrial and academic

scientists and engineers.

Most of the early research activity with very dilute drag reducing solutions was confined to the U.S.A., and a general awareness of the phenomenon in the U.K. followed publications early in 1965 by A.Emerson (6) and G.E.Gadd (7). The author's interest in this subject was stimulated after reading these works, and drag reduction research at Hendon College of Teachnology was initiated almost immediately thereafter. Thanks are due to Dr. Gadd for the provision of samples of Guar gum and Polyox, which enabled some preliminary pipe-flow experiments to be carried out while bulk supplies of polymers were on order, and which facilitated early publication of the results in 1966.

When it was decided to register the present work for a Ph.D. degree under the Council For National Academic Awards, Dr. G.E.Gadd of the N.P.L. Ship Division, and Dr. H.Barrow of Liverpool University agreed to supervise the work, and Dr. V.G.Pisolkar agreed to act as internal college adviser. Acknowledgement is made to these people for useful discussions and advice during the course of this research. Acknowledgement is also made to Dr. R.J. Beale, then head of the Mechanical Engineering Dept. at Hendon College of Technology, and to his successor Dr. E.P. Booth for the provision of research facilities.

This Thesis describes the research with drag

reducing additives which was carried out on a part time basis between 1965 and the present date. As is inevitable with such a rapidly expanding field of study, between 85 and 90% of the published work of others in this field has occurred since the commencement of the present research.

When the work was started surprisingly little was known about the drag reduction phenomenon in detail. At an early stage it was decided to attack the problem on a broad front in order to provide as much data as possible for likely practical applications and to throw light on the mechanism causing the effect. The initial approach had of necessity to be largely empirical. The work is concerned with internal flows through rough and smooth pipes, external flow over bluff bodies and other anomolous effects involving heat transfer cavitation and submerged jets. The Thesis is conveniently presented in sections which are linked together with a general discussion.

Many of the results herein have been previously published by the author in a number of scientific journals and symposia transactions. In some instances similar findings have been reported by other workers almost simultaneously, which is not surprising with such a rapidly developing topic. It is therefore very difficult to designate with certainty to any worker the priority for several of the discoveries.

A collection of the publications by the author

are presented in the flap at the end of this Thesis, and the dates of publication will provide some indication of the time scale of the subject development during the course of this study.

NOMENCLATURE

a	Pipe radius
Cd	Drag coefficient $D/\frac{1}{2}\rho U_o^2 S$
Cp	Specific heat
D	Drag force
d	Pipe internal diameter
f	Friction factor $\tau_w/\frac{1}{2}\rho V^2$
h	Heat transfer film coefficient. (Heat transfer rate/ area x bulk mean temp. diff.)
K'	Fluid consistency index for non-Newtonian fluid.
k	Thermal conductivity.
l	Pipe test length
Nu	Nusselt number hd/k
n'	Flow index for non-Newtonian fluid
Pr	Prandtl number $\mu Cp/k$
p	Pressure
Ra	Dimensionless pipe radius $au^*/\upsilon = Re\sqrt{f}/8$
Ro	Dimensionless distance from pipe wall to edge of linear sublayer.
R_1	Dimensionless distance from pipe wall to edge of interactive zone.
Re	Reynolds number Vd/υ

Re'	Generalized Reynolds number defined in text
S	Cross sectional area
St	Stanton number $h/\rho VCp = Nu/RePr$
u	Local instantaneous axial velocity
U	Local temporal mean velocity
Uo	Free stream velocity
u'	Axial turbulent perturbation velocity
u*	Friction velocity $\sqrt{\tau_w/\rho}$
U^+	Dimensionless velocity U/u^*
V	Mean flow velocity
y	Distance from wall
Y^+	Dimensionless distance from wall yu^*/υ
α	Thermal diffusivity $k/\rho Cp$
ε_R	Heat eddy diffusivity
ε_m	Momentum eddy diffusivity
μ	Viscosity
υ	Kinematic viscosity
ρ	Density
τ	Shear stress
τ_w	Shear stress at wall

N.B. Other symbols are defined in the text where necessary.

C O N T E N T S

------oOo------

LIST OF FIGURES

(1.0) INTRODUCTION.

(1.1) General

Experiments in recent years have demonstrated the possibility of reducing turbulent skin friction in liquids by dissolving small traces of certain macromolecular additives, such as polymers or other molecular associations.

A polymer is a substance whose molecules consist of a large number of units of a few types. These units which consist of a number of atoms are joined by covalent bonds. If the units are joined into a continuous chain we have a linear polymer, which may or may not have side branches. Alternatively the units may be joined into a two or three dimensional network. It is the former type which is found to be effective in drag reduction, the latter class generally being insoluable.

Molecules may also be joined together through weaker bonds to form associations. Where the molecules of such associations are orientated in solution they are referred to as micelles. Certain micellar solutions are also found to be effective in drag reduction.

The main objects of the present study have been to investigate the flow characteristics of such dilute solutions in order to throw light on the drag reduction mechanism and to provide data for possible practical application. Most of the work described in this thesis is con-

cerned with pipe flows and boundary layers, but in addition some other anomolous features of dilute high polymer solutions are also discussed.

Before proceeding to the main theme it is of interest by way of introduction to consider briefly the dynamics of drag from the historical viewpoint. Having discussed reasons for wishing to reduce drag and techniques previously employed, we will then describe work with drag reducing additives prior to the commencement of the present study. Important work by others in this field since this time will be introduced into the main text at relevant places where comparison with the present findings is desirable and where this influenced the development of work by the author.

In order to keep this dissertation to a readable length, a complete review of all work in this field willnot be given, particularly since a number of recent reviews and bibliographies are readily available. In fact annual summaries of world literature on this topic have been monitored and prepared by the U.S. Naval Ship Research and Development Center since 1967 under the title "Progress in Frictional Drag Reduction." A comprehensive bibliography of publications up to June 1970 has also been prepared by the University of Exeter (See list of bibliographies).

(1.2) The Dynamics of Drag - An Historical Summary.

Our present day civilisation depends on the motion of fluids to an enormous degree, and fluid motions affect our everyday lives to an extent far greater than would be apparent from cursory consideration.

When a fluid moves relative to a solid surface a force is exerted on the surface in the direction of motion, which is called in current terminology the drag force. Drag was the earliest fluid dynamic force to become apparent to man, but despite this fact knowledge about its nature has been slow to accumulate and hard won. The development of this knowledge from early times can be traced in several of the published histories of fluid mechanics such as Rouse and Ince (5), Von Karman (9), Giacomelli and Pistolesi (10) Goldstein (11) and Tokaty (12).

Man has made use of water wind and weather almost since pre-historic times and it is indeed surprising that a coherent and detailed knowledge of fluid flows has only emerged since the beginning of the present century. Even today we do not have the complete picture, especially where turbulent motions are concerned. From the wealth of accumulated knowledge we may single out perhaps four major steps forward which have significantly influenced our understanding of the dynamics of drag. (This procedure always depends to some extent on personal preference) These are:-

i) The development of the exact equations of motion for a viscous fluid, i.e. the so called Navier-Stokes equations.

It was Newton who in 1726 proposed the law which governs viscous friction. This was later generalized into a system of equations by Navier in 1826, Poisson in 1831, Saint Venant in 1843, and finally by Stokes in 1847.

ii) The discovery of the characteristic differences between laminar and turbulent flows, and the significance of Reynolds number.

Hagan clearly recognised the difference back in 1854, and even before this time Stokes (1843) had remarked that sometimes flows were unstable and that the motion could be quite changed by a disturbance. It was Reynolds who in 1883 quantified the effect by careful observation, and deduced the criterion VL/ν, later named in his honour by Arnold Sommerfeld (1908).

Reynolds also generalised the Navier-Stokes equation to take account of macroscopic momentum exchange in turbulent flows. Extra terms appear in the equation which involves products of velocity fluctuations, now known as Reynolds stresses. Boussinesq allowed for turbulent fluctuations by the introduction of an eddy coefficient.

iii) The Boundary Layer Concept.

In 1904 Prandtl showed that for low viscosity fluids the viscous effects were only significant in a thin layer adjacent to a solid surface, and outside of which the flow could be described with good accuracy by inviscid fluid mechanics. Within the boundary layer the Navier-Stokes equation becomes simplified to be amenable to

solution for laminar flows. With this concept turbulent flows also become somewhat more manageable. To some extent the existance of a boundary layer had been mentioned before Prandtl, Rankine (1864), Froude (1874), Mendeleyev (1880), Lanchester, but with no equations and no other deductions relevant to an understanding of drag such as Prandtl's explanation of boundary layer separation in regions of adverse pressure gradient.

iv) Similitude

The theory of dynamical similarity was first applied to fluid dynamical systems by Stokes in 1851, and in more detail by Helmholtz in 1873. By writing the Navier-Stokes equation in terms of reference physical quantities and perturbations therefrom, a functional relationship between dimensionless groups results for similar hydrodynamic and thermal boundary conditions, which may then be solved empirically if not analytically. Rayleigh in 1892 and subsequent years showed that these dimensionless parameters could be deduced on purely dimensional reasoning, and the theory of dimensional analysis was subsequently developed by Riabouchinsky (1911) and Buckingham (1914), into the π theorem.

These major advances contributed greatly to our present day understanding of drag and to the interpretation and application of much empirical data. Furthermore from this knowledge of the physics of frictional drag we may then consider possible means to achieve a reduction in its magnitude.

(1.3) Drag and possible reduction methods.

Frictional drag results in a corresponding dissipation or degradation of energy, and for many years

scientists and technologists have considered methods to minimize this effect. Success in drag reduction can result in a number of benefits, depending on the situation. For example we may achieve reduced power consumption of a vehicle (land or otherwise), or increased speed or size for the same power. (Indeed it is only by minimizing drag that heavier than air flight is possible). The reduction of friction in pipes and channels can result in improved throughput, reduced pumping power, or reduced duct size. Again reduction of drag force can result in lighter structures.

All this results in improved performance and economics, and possibly equally important in the overall sense, a reduction in the rate at which world fuel resources are utilized.

It is convenient to separate the total drag force into components: skin friction drag and pressure drag. The former being due to viscous shear stresses and the latter due to normal stresses (pressure variation over the surface). Pressure drag can be further split up into wake drag (form drag), induced drag and wave drag components, as in the traditional scheme below:-

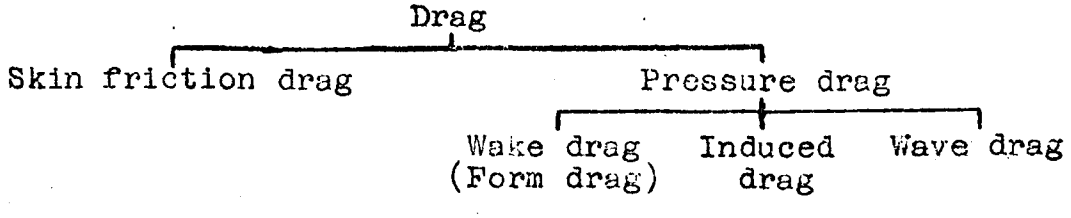

Wake drag occurs with flows over bluff bodies and in diffusing channels in regions where the adverse pressure gradient is relatively high. This causes a reverse flow and separation of the boundary layer (as explained by Prandtl) and consequently limits further pressure recovery. The result is a high drag force on the surface and a characteristic eddying wake downstream.

Early attempts at drag reduction sought to minimise this effect, and immediate benefits are achieved by fairing or streamlining to reduce the adverse pressure gradient. This streamlining principle has been known for a very long time (although not understood). Leonardo da Vinci (1452-1519) said that man should learn from the fishes since these live in the water and are shaped to move in it easily, and he also sketched some streamlined bodies of low resistance and boat hull designs. Sir George Cayley (1773-1857) realized that the downstream portion of an obstruction was important from the resistance point of view. He also copied nature in the design of early model flying machines and it is significant that his measurements of the shape of a trout coincide very closely with a modern low drag aerofoil shape (9).

Suitable streamlining can result in immense drag reductions, and as an extreme example we may note that by fitting correctly designed fairings to a disc the flow resistance may be reduced by up to around 95%. (Correspon-

ding reductions are possible in pipe flow by fairing an orifice plate into a venturi-tube). In this example the pressure drag has been practically eliminated and all that remains is skin friction, consequently any further drag reduction can only be achieved by minimizing the latter component.

A number of other methods of reducing form drag have been proposed and used practically. All depend on some form of boundary layer control such as:-

i) Moving surfaces

ii) Boundary layer suction

iii) Downstream blowing, either with a separate device or through slots or ducts from some higher pressure region in the flow.

For further details see for example Schlichting (13), Goldstein (14), Hoerner (15), or Tokaty (12).

Turning briefly now to the other two components of pressure drag we may note that wave drag is caused by the production of pressure waves (shock waves) in compressible fluids or surface waves on liquid surfaces. The effect may be minimized by suitable design i.e. slender sharp pointed bodies. In the case of aircraft wings, the formation of shock waves may be postponed to higher speeds by means of 'sweepback' and for ships the wavemaking resistance can be reduced (over a limited speed range) by utilizing a submerged bulbous bow.

Induced drag only occurs with bodies which produce a lift force. Here fluid flows around the edge of the body from the high pressure underside to the low pressure region above and results in the formation of a trailing vortex, the energy of which is related to the induced drag force. It is possible to minimize this effect on aerofoils by using a high aspect ratio (large span/chord) and elliptic loading, according to the theories of Prandtl and M.Monk (9), but the effect will only disappear with a lifting body of infinite span. It is not always recognized that any asymmetric body may have an induced drag component, for example it is present in the drag force on a land vehicle.

Having seen that it is possible to eliminate, or at least minimize pressure drag we are still left with the problem of reducing skin friction. In some situations this component may be quite large, and in pipe flows it is frequently the only component.

Following Prandtl's statement of the boundary layer concept, Riabouchinsky planned to eliminate the boundary layer by means of a moving wall (12). It is indeed conceptually possible to remove skin friction entirely by this method, but with an arbitiary shaped body the surface velocity must vary in order to maintain zero relative motion, and this is not really possible from the technological point of view.

Numerous other techniques for reducing skin friction have beenactively studied for several decades, and since turbulent boundary layers are more energy dissipative than laminar flows, most proposals seek to stabilize the laminar situation. Some early success was achieved in the development of laminar flow aerofoils (9), which are shaped to maintain a favourable pressure gradient over a large portion of the chord length and so delay transition. It is significant to note that nature has shaped many marine animals on this principle.

Alternative proposals for reducing skin friction include the use of soft complient surfaces (which nature appears to have adopted for dolphins), suction to control boundary layer growth, heat transfer, two phase flow ideas, and the use of additives to modify the boundary layer structure. A review and extensive bibliography for these methods has been presented by Lumley (16), see also the paper by Hoyt (17). A decade or so ago the author demonstrated the possibility of stabilising turbulent pipe flow and reducing pressure loss by rotation of the pipe wall (18), (19).

From all these possible techniques, the use of additives seems very attractive, particularly after it was shown that just a few parts per million of certain soluble contaminents could reduce skin friction by over 70% (5). The work described in the following pages is devoted to studies of the flow characteristics of such dilute solutions.

(1.4) Skin friction reduction with soluble additives.

Records of skin friction variations in turbulent boundary layers exist since the end of the last century, from tests over the years on a standard ship model in the Admiralty tank at Haslar (20). At times these fluctuations in drag have been quite significant as is seen in fig.1, taken from reference (20), although early analysis of the liquid from the tank detected no apparent difference from pure water. For the want of a logical physical explanation these drag variations became known as 'Tank Storms.' We shall return to this topic later since it is only comparatively recently that an explanation has been proposed.

Credit for the first drag reduction experiment with an additive should probably be assigned to Hele-Shaw. Around the turn of the century he was interested in the skin friction on marine animals and tried to simulate their soluble slime in a pipe flow by the addition of fresh bile to water. This somewhat bizarre solution resulted in a reduced pressure drop when compared with the water alone, (21) These results have remained generally unknown.

The possibility of reducing liquid skin friction by the diliberate addition of some soluble contaminent was re-discovered independently both in the U.S.A. and in this Country over 25 years ago.

Towards the end of the second world war, K.Mysels and co-workers were developing incendiary weapons for the

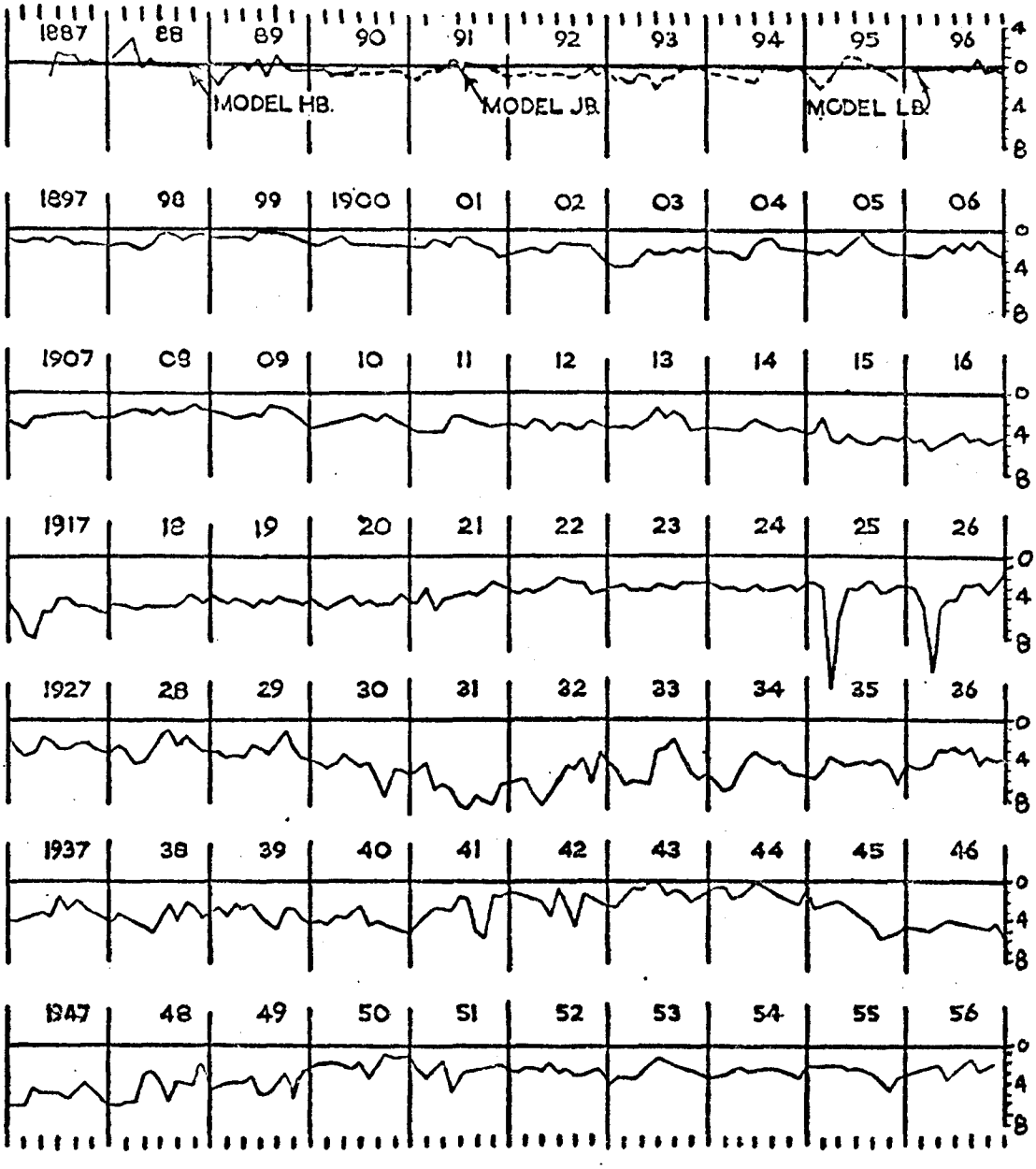

TEST RESULTS WITH A STANDARD MODEL AT AEW TOWING TANK, HASLAR (Ref. 20)

Fig. 1

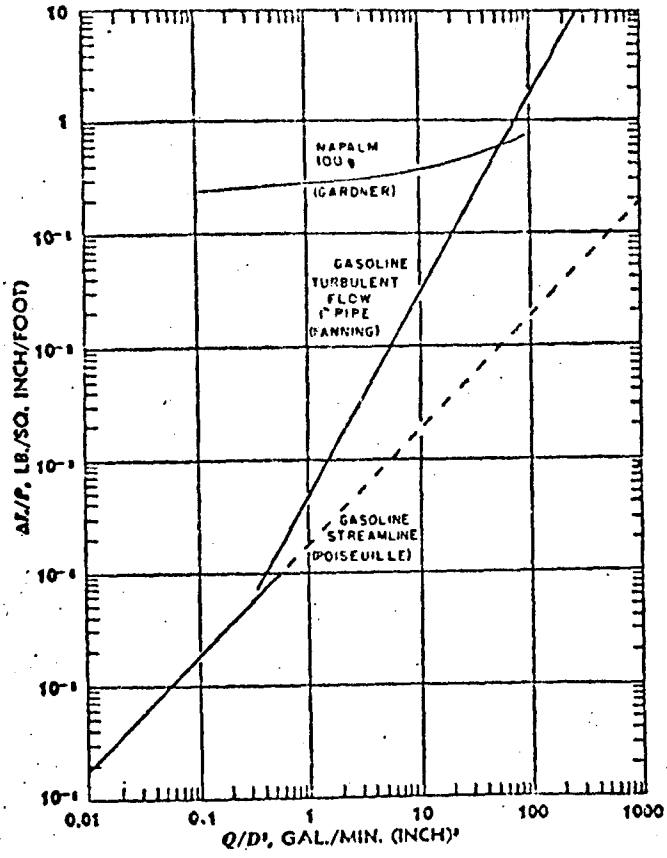

Figure 2. Relation of Pressure Drop to Flow

(Ref. 22)

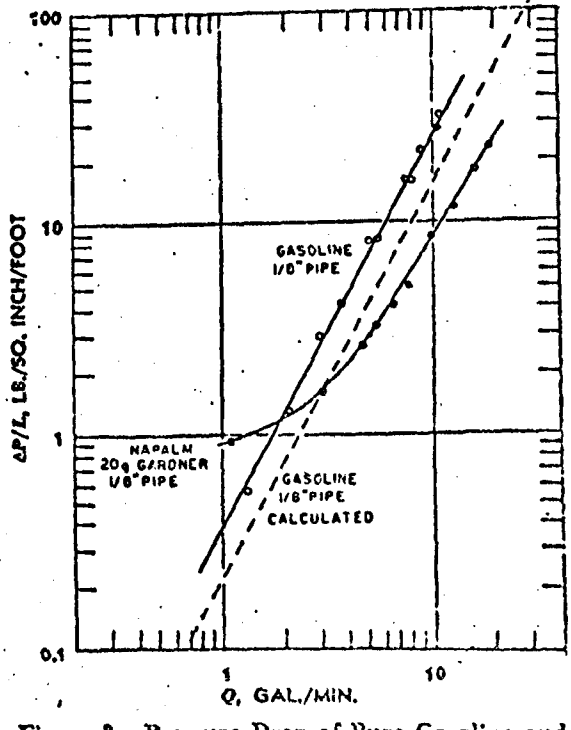

Figure 3. Pressure Drop of Pure Gasoline and Dilute Jelly

(Ref. 22)

U.S.Government when they observed that the pipe flow pressure loss of Napalm thickened gasolene was less than that for untreated gasolene at high rates of flow. Although several experiments were carried out the phenomenon was not fully investigated because of the war time situation, and publication of the results was delayed for a number of years due to secrecy regulations. The first available publication is a patent filed in 1947 by Mysels (1), and the work was subsequently described in a short paper presented by the group, Agoston, et.al. (22). Figs.2 and 3 are taken from this reference and show quite significant drag reduction in the turbulent flow regime, particularly for the smaller pipe size. From the historical point of view the story behind this early discovery has recently been published by Mysels (3).

The friction reduction phenomenon was discovered independently in this Country during 1947 by B.A.Toms and J.G.Oldroyd when they were working with the Courtoulds lab. and studying the shear dependent behaviour of high polymer solutions in pipe flow. It was found that a solution of polymethyl methacrylate (Perspex) in monochlorobenzene required a lower pressure gradient than the solvent alone to produce the same flow rate, in turbulent flow. These results were published in 1948 (2), and in common with the earlier findings exhibited a pronounced diameter effect, the drag reduction being greater in tubes of small diameter.

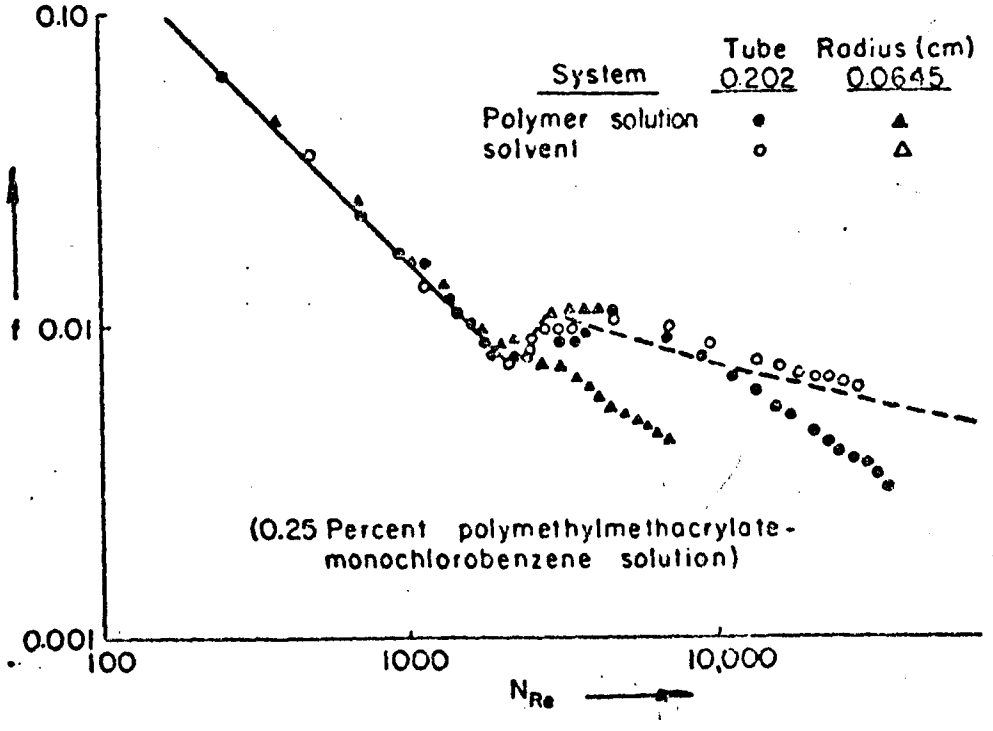

DATA OF B.A.TOMS.

(As replotted by Savins)

Fig. 4.

Fig.4 shows Toms' results as plotted in conventional friction factor form by Savins (23).

These early papers were followed by over a decade of virtual inactivity in this friction reduction field. Much progress was however being made in the understanding of non-Newtonian fluid behaviour. For detailed surveys see text by Wilkinson (24) or Skelland (25).

Real fluids may be divided into two main classes:-

i) Newtonian fluids

ii) Non-Newtonian fluids.

Newtonian fluids are those for which the viscosity is absolutely independent of the shear rate, i.e. is an absolute constant for each Newtonian fluid at a given pressure and temperature.

Non-Newtonian fluids are those in which the viscosity at a given pressure and temperature is a function of the velocity gradient, and possibly also the time that the fluid is subjected to shear or the rate of change of the shear rate.

It is convenient to sub divide non-Newtonian fluids into three classes:-

i) Time independent

ii) Time dependent

iii) Viscoelastic.

A detailed account may be found in refs. (24) and (25). It is emphasized that the non-Newtonian fluids

cannot be described by the Navier-Stokes equation.

In 1955, Metzner and Reed (26) proposed a generalized Reynolds number, Re', as a similarity criterion for time independent non-Newtonian fluids, and showed that laminar pipe flow data was successfully correlated by the expression:-

$$f = 16/Re' \qquad \text{----------(1.1)}$$

where $Re' = D^{n'}V^{2-n'}\rho/\gamma$ and $\gamma = K'8^{n'-1}$

The flow index n' and the fluid consistency K' are easily determined from laminar pipe flow measurements since by definition $\tau_w = K'(8V/D)^{n'}$

We may note that for a Newtonian fluid n' = 1, and K' becomes the viscosity. Re' then reduces to Re.

Although data in laminar flow were correlated by equation 1.1, results in the turbulent regime exhibited friction factors below those predicted by the Blasius expression $(f = 0.08/Re)^{.25}$ or by the Karman-Prandtl law, $(1/f^{\frac{1}{2}} = 4.0\ \ln(Re.f^{\frac{1}{2}}) - 0.4)$ even when expressed in terms of the generalized Reynolds number.

An important generalization of the Karman-Prandtl expression was made by Dodge and Metzner in 1959 (27), who proposed the semi-empirical correlation for turbulent pipe flow:-

$$1/f^{\frac{1}{2}} = \left[4.0/(n')^{0.75}\right]\ln\left[Re'f^{(1-n')/2}\right] - 0.4/(n')^{1.2} \qquad \text{--------- (1.2)}$$

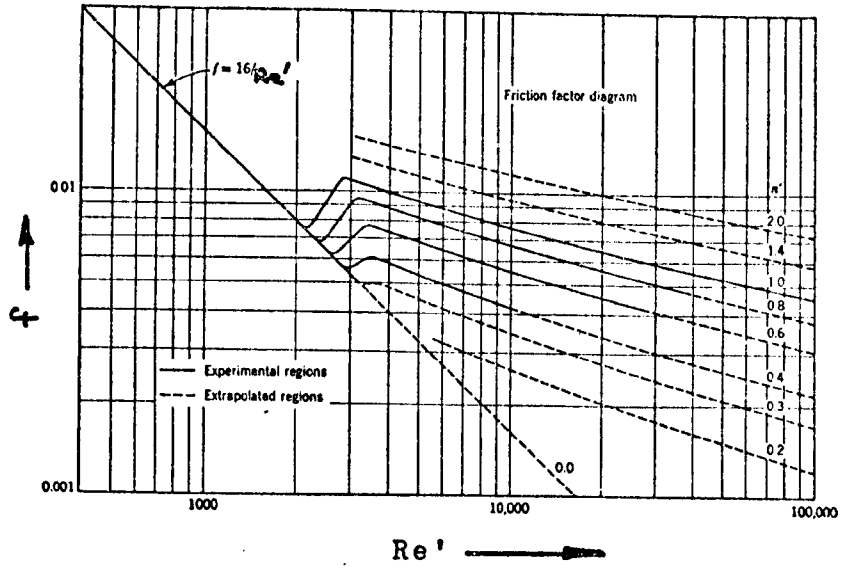

GENERALIZED PIPE FRICTION CHART.
(Dodge and Metzner)

Fig. 5.

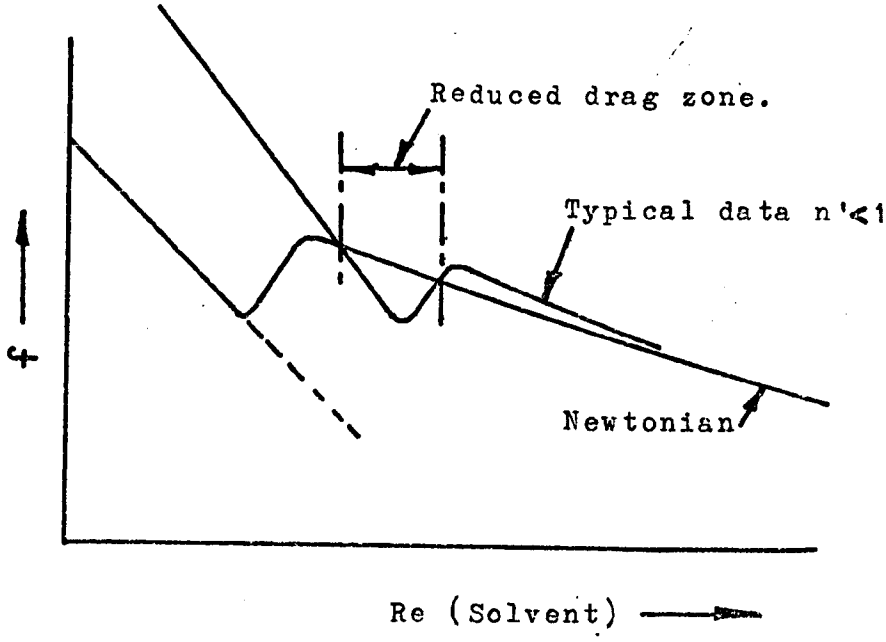

Fig. 6.

This reduces to the familiar Karman-Prandtl law in the Newtonian case when $n' = 1.0$.

The Dodge-Metzner generalized pipe friction chart is shown in fig.5, and appears to correlate most of the data from purely viscous non-Newtonian fluids quite successfully, and there is also some evidence that the transition Reynolds number is increased somewhat for fluids with a low flow index.

Since the turbulent friction factors for purely viscous non-Newtonian materials lie below those for Newtonian fluids, it would appear that the addition of some contaminent (either solid or soluble) to a base Newtonian fluid might yield a shear thinning substance (low n') and a reduction in pressure drop. Generally however, the 'thickening' action of such additives seems to outweigh the shear thinning properties, and nearly always result in an increase in the actual pressure drop.(34).

We must therefore take care to define drag reduction by an additive as the reduction in friction for the same flow rate of solution and solvent. Drag reduction will therefore only be apparent on a friction factor chart expressed in terms of the solvent Reynolds number.

By comparing the generalized Reynolds number with the solvent value at the same flow velocity, we have:-

$$Re' = \frac{\rho D^{n'} V^{2-n'}}{K' 8^{n'-1}} \qquad Re(s) = \frac{\rho(s) V D}{\mu}$$

$$\text{So,} \quad \frac{Re(s)}{Re'} = \frac{\rho(s)}{\rho} \cdot \frac{K'}{\mu} \cdot \left(\frac{D}{V}\right)^{1-n} \cdot 8^{1-n'}$$

For most practical situations we find from the above that Res > Re'. Hence points on a line for n' < 1 in fig.5 will in general be shifted to the right if plotted in terms of the solvent properties. The general effect is depicted in fig.6, and for moderately thickened fluids drag reduction is still obtained over a limited range of flow rate. This type of friction reduction with purely viscous fluids is clearly apparent from data by Shaver (28), and was also reported but not explained by Hershey and Zakin (29)

Although the Dodge-Metzner expression was successful in correlating most of the non-Newtonian data, Dodge noted that solutions of carboxmethylcellulose (CMC) in water produced anomolous results, which did not fit the correlation and which gave very much lower values of friction factor. This same effect was also apparent from parallel results by Shaver and Merrill (28). Furthermore, the friction factor values for the anomolous fluids depended on the pipe diameter, the values being lower with small bore pipes, and also the friction reduction only occurred in the turbulent flow regime. These phenomena are all consistent with the early drag reduction results by Mysels et.al. and Toms. At an early date the effect of

drag reduction by soluble additives became known as the Toms phenomenon, Fabula (4), presumuably while the work by Mysels et.al was largely un-noticed. More recently Savins (3) has proposed that the effect should be shown as the MOT phenomenon, which is fully endorsed by the author in view of the early contributions by Mysels, Oldroyd and Toms.

An early discussion of drag reduction possibilities was made by Savins (23) and practical application to oil well drilling operations was described by Ousterhout and Hall (30), and Lummus et.al. (31), during the early 1960's.

Interest in the MOT effect was greatly increased during this period when other possible practical applications became apparent. The U.S.Naval Undersea Warfare Center became interested in the use of additives to reduce the propulsion power requirements for underwater weapons etc. and it was here that Hoyt and Fabula made some noteworthy discoveries.

Hoyt and Fabula (5), used a disc rotating in a large reservoir to investigate a whole range of water soluble polymers and showed that with some of these, very large friction reductions were possible with just a small trace of the polymer in solution. Previously drag reduction was observed with relatively concentrated solutions which were both shear thinning and viscoelastic, but it was now found

that some additives produced a greater friction reduction in very dilute solutions which were not shear thinning, and had viscosity values only slightly greater than water. It was soon after the arrival of Hoyt and Fabula's paper in this country that the present work was started.

(1.5) Notes on the physics of shear flow turbulence.

Before proceeding with a description of the present experiments it is useful to include a brief account on the physics of turbulent shear flows. This will then provide some basis for discussion of the experimental results. It should be emphasized that at the present time complete physical explanations on the nature of turbulence are not available.

Detailed accounts of turbulentflows are given in texts by Bradshaw (51), (this is a particularly readable introduction), and Hinze (52), and in papers by Kline (53), (72), (73), Lighthill (54) and Phillips (55). Numerous other important works are cited in these publications.

Turbulence may be expected in a fluid whenever there is a shear flow and the inertial effects are much larger than the viscous effects. The ratio (inertia force/ viscous force) is the Reynolds number. The onset of turbulence occurs as a consequence of instability in the main flow. At Reynolds numbers below some critical value which

depends on the geometry of the flow boundaries, any disturbance introduced into the flow will decay downstream from its point of introduction. Above the critical Reynolds number however, disturbances may be amplified and the effects of small disturbances can be detected well downstream. Turbulence may be described as a random field of vorticity and can only be properly described in statistical terms.

Turbulent flows are dominated by large eddies whose wavelength is the same order of magnitude as a boundary layer thickness or pipe radius. These eddies seem to arise from some sort of instability in the shear layer close to the wall, leading to the growth of a preferred type of three dimensional disturbance. This 'bursts' away from the wall and grows downstream as is clearly seen from the hydrogen bubble pictures of Kline et.al. (53), (72), (73), and from the present work, figs.85 and 86. These large bursts of vorticity are then stretched by the mean flow velocity gradient and break up into smaller and smaller eddies until eventually the smallest are dissipated into heat energy by viscosity, Bradshaw (51). However, the turbulence in the main flow certainly triggers off instabilities in the wall layer, thus replenishing the production of turbulent kinetic energy. We have therefore a continuous spectral cascade process from production at relatively

low wave numbers (frequencies) to dissipation at high wave numbers.

A useful schematic diagram representing the production, spectral transfer and decay of turbulence in this limit cycle has been published by Kline (53) and is reproduced below:-

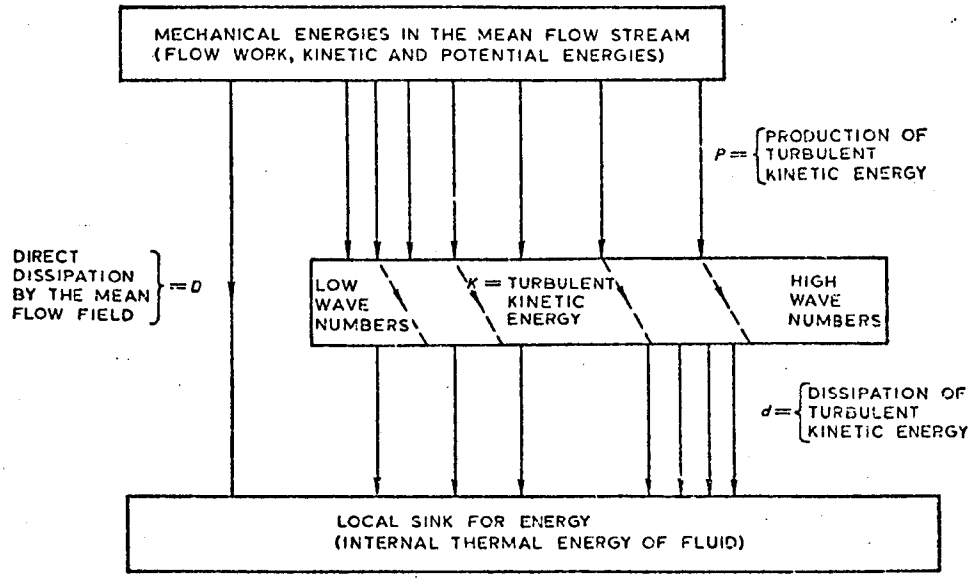

A guide to the relationship between the different contributions to the energy content of a Newtonian turbulent flow may be obtained from the turbulentkinetic energy equation, Bradshaw (51), Hinze (52), Kowalski (56).

Starting with the Navier-Stokes equation for steady incompressible flow with zero body forces:-

$$U_j \frac{\partial U_i}{\partial x_j} = \frac{1}{\rho} \frac{\partial p}{\partial x_i} + \nu \frac{\partial^2 U_i}{\partial x_j \partial x_j}$$

and the continuity equation:-

$$\frac{\partial U_i}{\partial x_i} = 0$$

we note that these non-linear equations cannot be generally solved for turbulent flow. (Here in tensor notation the suffices i, j, take the values 1, 2, 3, corresponding to the x, y, z directions.)

The above equations may be put into the Reynolds form by writing quantities in terms of time mean values and perturbations therefrom (51), (56)

$$\rho \overline{U_j} \frac{\partial \overline{U_i}}{\partial x_j} + \frac{\partial}{\partial x_j}\left(\rho \overline{u_i' u_j'}\right) = -\frac{\partial \bar{p}}{\partial x_i} + \nu \frac{\partial^2 \overline{U_i}}{\partial x_j \partial x_j}$$

$$\frac{\partial \bar{v}}{\partial x_i} = 0 \quad ; \quad \frac{\partial \overline{u_i'}}{\partial x_i} = 0$$

The terms $\rho \overline{u_i' u_j'}$ are referred to as Reynolds stresses.

Multiplying the Reynolds equation by $\overline{U_i} + u_i'$ and time averaging leads to the turbulent kinetic energy equation:-

$$\underset{\text{(i)}}{\frac{\rho}{2} \overline{U_j} \frac{\partial \overline{u_i'^2}}{\partial x_j}} + \underset{\text{(ii)}}{\frac{\rho}{2} \frac{\partial \overline{u_i' u_j'}}{\partial x_j}} + \underset{\text{(iii)}}{\rho \overline{u_i' u_j'} \frac{\partial \overline{U_i}}{\partial x_j}}$$

$$= \underset{\text{(iv)}}{-\frac{\partial \overline{u_i' p}}{\partial x_i}} + \underset{\text{(v)}}{\frac{\mu}{2} \frac{\partial^2 \overline{u_i'^2}}{\partial x_j \partial x_j}} \underset{\text{(vi)}}{- \mu \overline{\left(\frac{\partial u_i'}{\partial x_j}\right)^2}}$$

The six terms of this equation may be interpreted as follows:-

i) Convection of the Kinetic energy associated with turbulent velocities by the mean velocity gradients.

ii) Convection of kinetic energy of the turbulent velocities by the fluctuating components of velocity.

iii) Production of turbulent kinetic energy by the interaction of Reynolds stresses and the mean velocity gradients.

iv) Transport of turbulent kinetic energy by pressure fluctuations.

v) Transfer of turbulent kinetic energy by viscous interaction of turbulent eddies.

vi) Viscous dissipation of turbulent kinetic energy into heat.

These represent terms that we would like to measure. This has been carried out with gases (Klebanoff,- in boundary layers; Laufer,- in pipe flow) see refs.(51) and (52), but such measurements are extremely difficult in liquids and even more so in polymer solutions. At present we have to content ourselves with less detailed investigations. As far as drag reduction is concerned terms iii and vi appear to be the most important.

Some energy is also dissipated from the mean flow directly by viscosity. This dissipation is given (53) by:-

$$D = \rho\nu\left(\frac{\partial U_i}{\partial x_j} + \frac{\partial U_i}{\partial x_i}\right)\frac{\partial U_i}{\partial x_j}$$

The production of turbulent kinetic energy, term iii may be written as (53):-

$$P = \rho\varepsilon_m\left(\frac{\partial U_i}{\partial x_j} + \frac{\partial U_j}{\partial x_i}\right)\frac{\partial U_i}{\partial x_j}$$

From these we see the ratio:-

$$\frac{P}{D} = \frac{\varepsilon_m}{\nu}$$

This relationship may easily be determined from mean velocity profile measurements (see eqn. 2.11.iii).

In common with other aspects of fluid mechanics, dimensional analysis plays an important part in the study of turbulent flows, particularly where data correlations are concerned.

It may be assumed that close to the wall in a turbulent boundary layer of pipe flow, the velocity gradient depends on τ_w, ρ, ν, y. Following Bradshaw (51) simple dimensional reasoning then yields the so called "law of the wall":-

$$U/u^* = 1/k \ln y + \text{const.} \qquad (k \text{ is a constant})$$

This relationship has been used elsewhere in this thesis as a basis for data correlation.

Table 2

SUMMARY OF EARLY RESULTS IN THE DRAG REDUCTION FIELD
NOT PREVIOUSLY DISCUSSED IN TEXT

Ref.	Author	Date	System	Notes
32	Ripken and Pilch	1963	Pipe	Drag reduction with C.M.C. solutions up to 1% conc. All concentrations studied were shear thinning. Solutions susceptible to degradation.
33	Elata and Tirosh	1963	Pipe and Couette Viscometer	Pipe drag reduction with dilute Guar gum solutions. No apparent degradation.
34	Metzner and Park	1964	Pipe and Jet thrust	Drag reduction related to viscoelasticity through normal stress difference measurements. Relatively high polymer concentrations used, and results show pronounced diameter effect.
35	Savins	1964	Pipe	Observations of drag reduction with cellulose and vinyl polymers. Results show diameter effect. Several theories proposed for mechanism of drag reduction.
36	Lumley	1964	Theoretical	Consideration of turbulence properties indicates that viscoelasticity is responsible for drag reduction.

/Continued . . .

Table 2 (Continued)

Ref.	Author	Date	System	Notes
37	Wells	1964	Pipe	Pipe friction and velocity profile measurements with Guar gum solutions over 600 p.p.m. conc. Diameter effect and thickened viscous sublayer. Theory presented for a generalised velocity profile. Concentrations used were all shear thinning.
38	Thurston and Jones	1964	External flows	Drag reduction with soluble high polymer paints
39	Lummus and Randal	1964	Pipe	Consideration of drag reducing drilling muds for 'Project Mohole'.
40	Astirita	1964	Theoretical	Suggested that turbulence in viscoelastic fluids were less dissipitative, and produced some order of magnitude arguments in support.
41	Hoyt	1965	Capillary tube	Design of a small bore turbulent flow rheometer. Several synthetic and natural polymers showed drag reduction, including D.N.A. Degradation detected by repeated passes through instrument.

/Continued . . .

Table 2 (Continued)

Ref.	Author	Date	System	Notes
42	Hoyt and Soli	1965	Capillary Tube	Drag reduction shown possible by algal cultures. Can account for measurement fluctuations in towing tanks.
43	Pruitt and Crawford	1965	Pipe	Working with range of water soluble high polymers, showed that solutions exhibiting strong elastic effects were the better drag reducers.
44	"	1965	Pipe	Demonstrated drag reduction with polymer additives dissolved in hydrocarbon solns. (Hydraulic oil.)
45	Vogel and Patterson	1965	Body of revolution	Injection of polymer solution into boundary layer produced drag reduction. Hot film anemometer used for turbulence measurements but results not considered conclusive.
46	Wu	1965	Free turbulence	Generation and decay of turbulence produced by a grid paddle affected by C.M.C. in moderately high concentrations and by Polyox at lower concentrations.

/Continued . . .

Table 2 (Continued)

Ref.	Author	Date	System	Notes
47	Barenblatt	1965	Cylinder	Drag on cylinder reduced by moderately concentrated C.M.C. solutions. Delayed boundary layer separation.
48	Barenblatt	1965	Visual	Clusters of C.M.C. molecules held responsible for drag reduction.
49	Ruszczycky	1965	Spheres	Drag on sphere reduced in Guar gum solutions at moderately high concs.
50	Lindgren	1965	Rough pipe	Demonstration of friction reduction in rough pipe with dilute Polyox solutions.

(2.0) THE PRESENT EXPERIMENTS.

(2.1.0) PIPE FRICTION EXPERIMENTS WITH GUAR GUM SOLUTION

The initial pipe friction experiments were carried out with aqueous solutions of Guar Gum in a range of hydraulically smooth pipes. This additive was selected for the preliminary tests because it was known to be an effective drag reducer and apparently not susceptible to mechanical degradation, from previous work by Hoyt and Fabula (5) and Gadd (7). Guar Gum is a natural long chain polymer extracted from the Guar plant grown in India, Pakistan and the U.S.A. The molecular weight is around 2.0×10^5.

(2.1.1) Pipe Friction Apparatus.

A schematic layout of the pipe flow apparatus used for the initial tests is shown in fig.7. This rig consisted of a rack of drawn copper pipes with internal diameters of 3/4, 1/2 and 3/8 in. (19.05, 12.7, and 9.52mm) and with pressure tappings situated 2, 6 and 14ft. (0.61, 1.23 and 4.27m) from the entry end. Pressures were normally measured at the latter two tappings to provide as long an entry length as possible and to ensure fully developed flow. In addition a short length of 0.090 in. (2.38mm) diameter pipe was used with pressure tappings at 6 and 24 in. (152 and 610mm) from the entry.

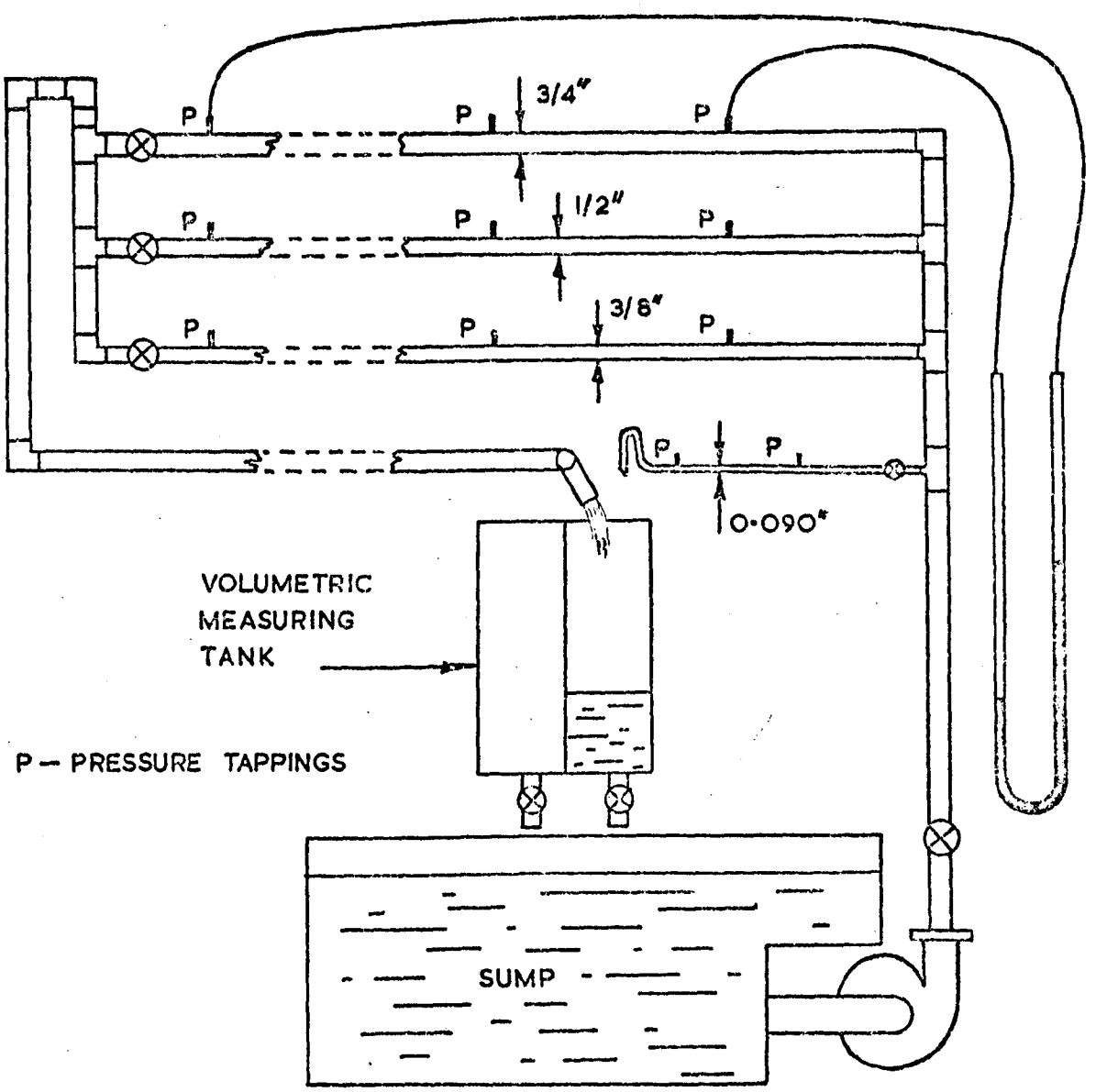

FIG. 7. SCHEMATIC LAYOUT OF TEST RIG.

Great care was taken whilst drilling the 1/16 in. (1.58mm) diameter pressure tapping holes in order to prevent burrs on the pipe interior, and the consequent measurement errors which would be caused thereby. A pilot hole of about 1/32 in. (0.78mm) was first drilled at each tapping point in the pipe, and these were opened out in stages to the final size. Any remaining raggingin the pipe bores was then removed with fine emery cloth wrapped around the end of long rods and inserted into the pipes.

Fluid was drawn from a fibreglass sump and supplied to the pipes through suitable control valves by a centrifugal pump. The flow rate was measured by collecting the pipe discharge in a volumetric measuring tank, and the fluid temperature at the exit was measured with an ordinary mercury thermometer. The pressure difference between any selected pair of pressure tappings was measured with either an inverted water manometer or with a mercury manometer.

(2.1.2) Test Procedure.

The system was filled with ordinary mains water and the pipes and manometer leads were bled to eliminate any air bubbles. Measurements of the pressure gradient along each pipe were taken over a wide range of flow rate and these results provide a possitive check on the apparatus, since they agree extremely well with those from a standard pipe friction chart.

This procedure was then repeated with solutions of Guar Gum at various concentrations up to 480 p.p.m. by weight. The weighed quantity of additive being sprinkled and stirred into the sump contents whilst the solution was circulated through the system by the pump.

A small quantity of insoluble matter (husks etc.) was found in the Guar Gum powder, but no attempt was made to filter the solution. If any degradation of the solution occurred during the tests this became apparent by a rise in the pressure loss. When this occurred the solution was immediately discarded and a fresh mixture was used. The fluid temperature during all the tests was about 25°C.

(2.1.3) The basic results.

Some typical results obtained in the 1/2 in. (12.7mm) dia. pipe are shown in fig.8, in the form of a friction factor chart. The Reynolds number was based on the solution viscosity, which was determined from measurements made with an ordinary capillary viscometer, and from laminar flow results taken from the smallest bore pipe. For the concentrations used the Guar gum solutions were found to be Newtonian under laminar flow conditions, no shear thinning could be detected, and the solution viscosities were only slightly greater than that of water. Table 3 below presents the solution viscosities relative

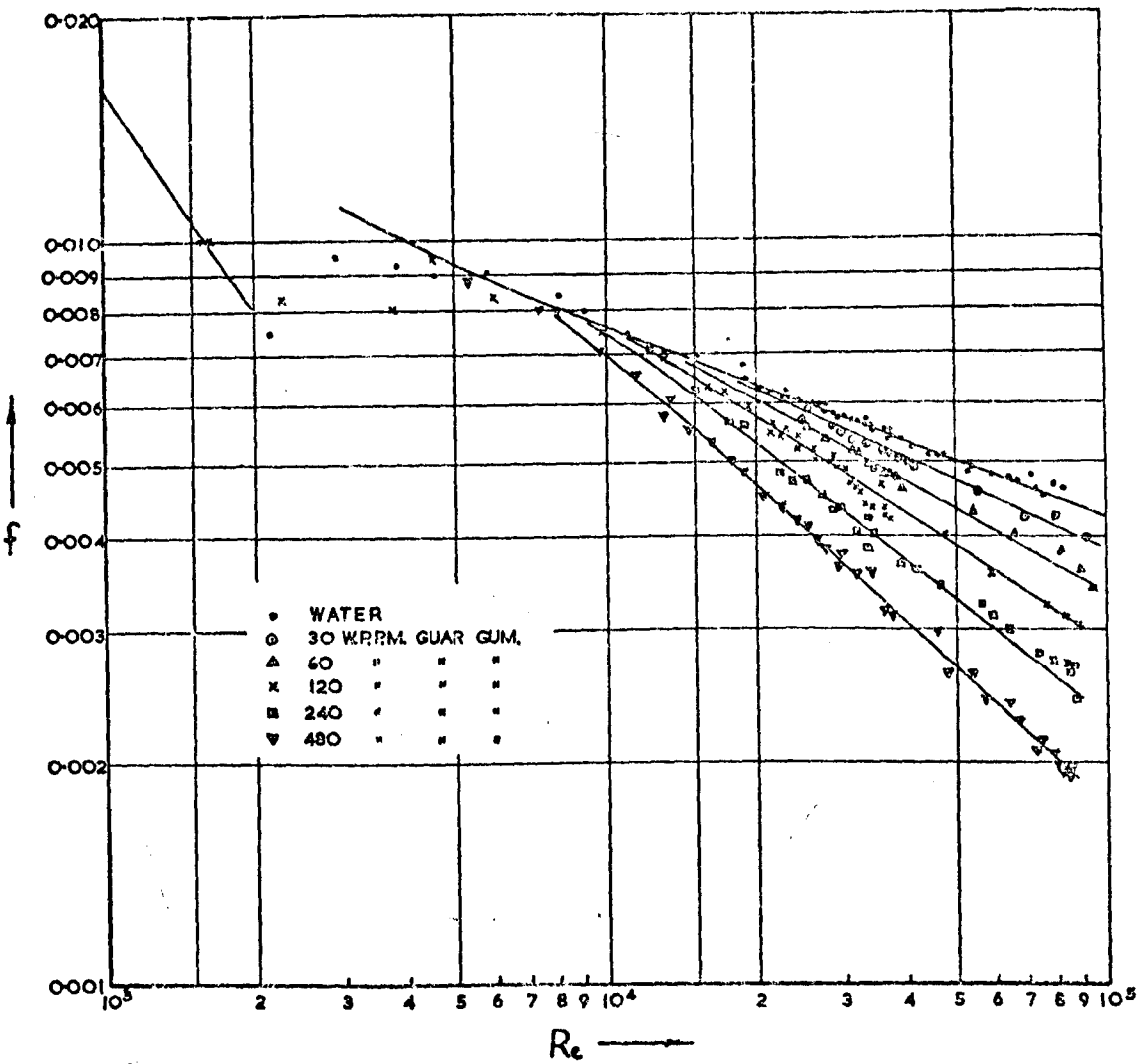

FIG. 8. RESISTANCE DATA FOR 1/2 IN. DIA. PIPE.

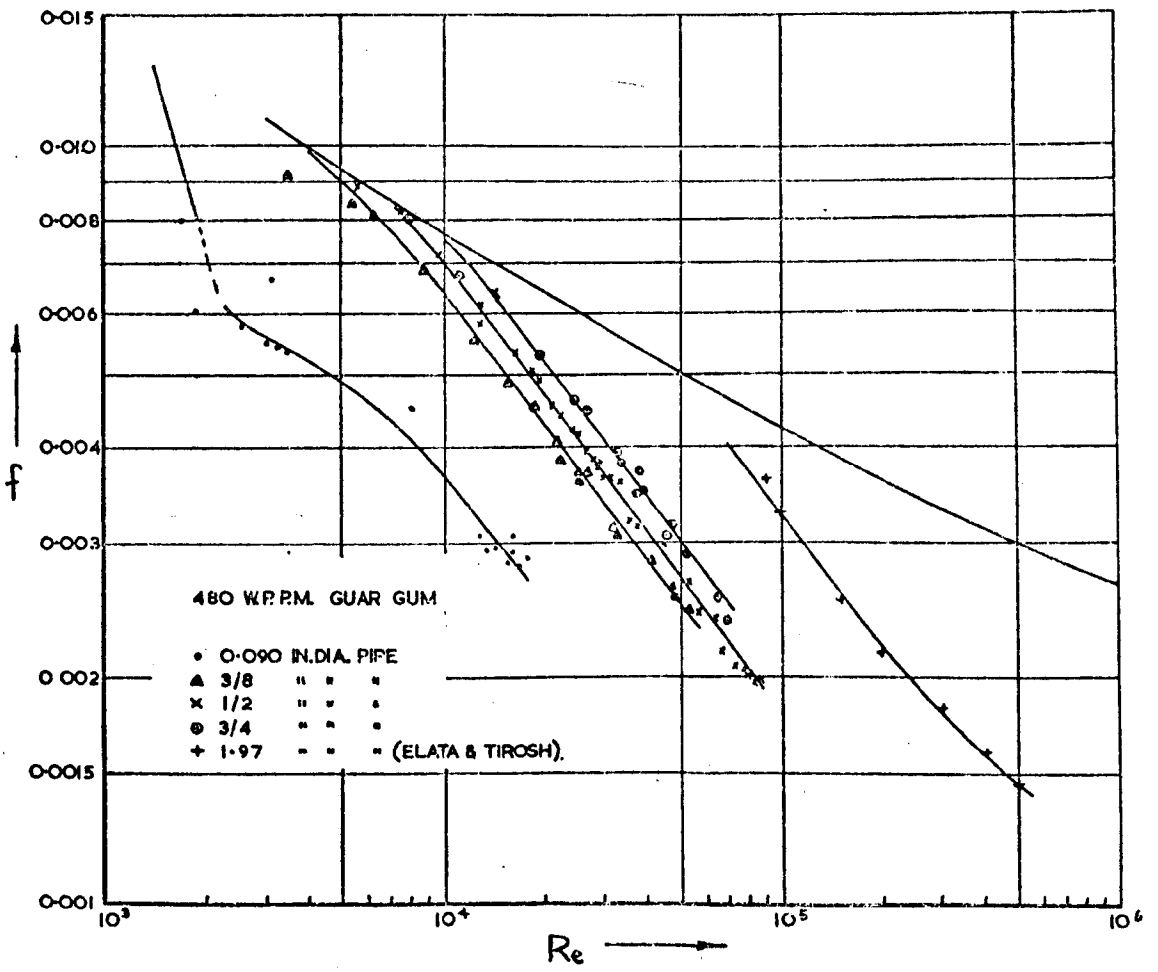

FIG. 9. EFFECT OF PIPE DIAMETER.

to water, which were used to calculate the pipe flow Reynolds numbers.

TABLE 3.

Solution Concentration (p.p.m)	Rel. Viscosity (ν/ν water)
120	1.12
240	1.20
480	1.35

Returning to fig.8 a number of features are immediately apparent. Enormous friction reductions are obtained with only small traces of the additive in solution. The drag reduction occurs only in the turbulent flow regime, and only above a threshold Reynolds number which depends to a very small extent on the solution concentration. Results with all the other pipe diameters were of similar form to these.

Fig.9 shows the flow characteristics of a fixed concentration of Guar Gum solution in the range of pipe sizes. Also included are some data cross plotted from work by Elata and Tirosh (33), which was published at this time.

As was found by a number of previous investigators using more concentrated solutions, pipe diameter has a considerable effect on the drag reduction, the reduction being greater with the smaller pipe sizes, for the same

polymer concentration and Reynolds number, Once again the results with different concentrations were similar in form to those in fig.9.

It can be seen from fig.9 that drag reduction for a given polymer concentration only occurs above a certain threshold Reynolds number which depends on the pipe size. Below this critical value the fluid exhibits normal Newtonian viscous behaviour, although for pipes of very small bore ordinary turbulent flow is never established if the threshold Reynolds number for these is less than 3,000.

(2.1.4) Some deductions from the pipe flow results.

A study of friction factor charts like fig.9 indicates that for a given polymer concentration the threshold number appears to correspond to an absolute value of the wall shear stress $\tau_{w\,crit.}$ irrespective of the pipe diameter. This is easily checked as follows:-

Using the definition of friction factor

$\tau_w = 1/2\rho v^2/f$, with the Blasius law,

$f = \text{const.} Re^{-\frac{1}{4}}$, which is valid for the Reynolds

number range of these experiments, and is applicable up to the threshold Reynolds number, it can be seen that

$$\tau_w = \text{const. } Re^{7/4}/d^2$$

So that if the threshold Reynolds number for the onset of drag reduction corresponds to a fix value of τ_w, then

$$Re(ONSET) = \text{const. } d^{8/7}$$

This relationship agrees very well with the experimental data. The fact that drag reduction only occurs above the threshold value of the wall shear stress for pipes of all diameters now suggests a possible data correlation method:-

If we again make use of the Blasius expression we find

$$\tau_w = 1/2\rho v^2 (vd/\upsilon)^{-\cdot 25}$$

i.e. $\tau_w = \text{const. } v^{1\cdot 75}/d^{\cdot 25}$ for a given

Newtonian fluid in turbulent flow.

This relationship consists of a series of straight parallel inclined lines for different diameters when plotted in the form $\ln \tau_w$ against ln.v. If data for a given polymer concentration are now superposed on this plot we find that it deviates from the solvent characteristics above $\tau_{w\,crit.}$ in a series of nearly straight parallel lines.

The idea is sketched out in fig.10 and this leads immediately to a data correlation technique. Referring to fig.10 we see that for a given wall shear stress $\tau_w, (> \tau_{w\,crit.})$, the mean flow velocities in pipes of diameter d_1 and d_2 with polymer solution are v_1 and v_2 respectively.

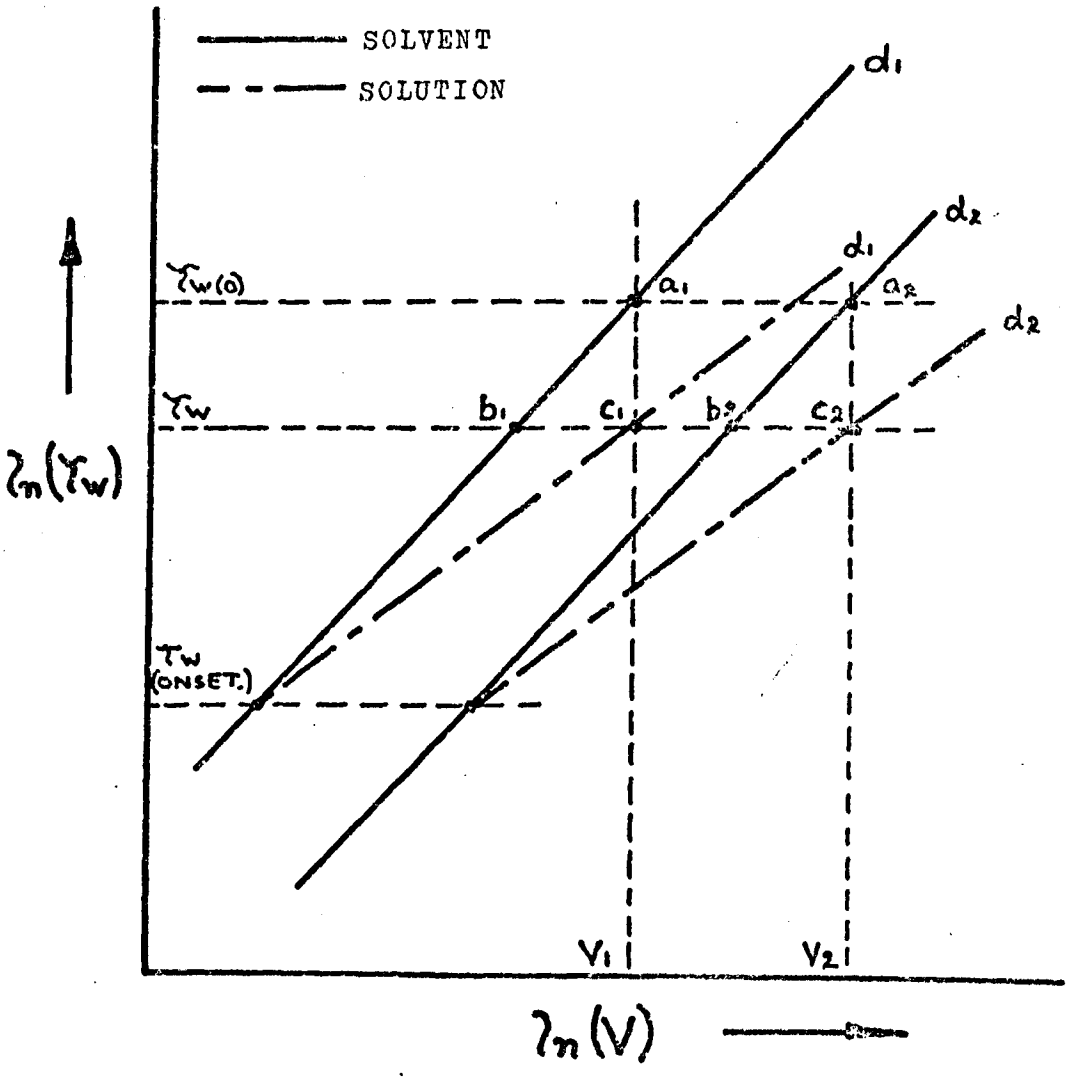

BASIS FOR EMPIRICAL DATA CORRELATION

Fig. 10.

For these SAME velocities we see that the wall shear stress for the solvent is $\tau_{w(o)}$, due to the similarity of the near triangles $a_1b_1c_1$ and $a_2b_2c_2$. Thus the drag reduction $(\tau_{w(o)} - \tau_w)$ at velocities v_1 and v_2 is independent of pipe diameter.

We are thus led to the data correlation proposed in fig.11. Here the wall shear stress for the solution is plotted against the corresponding wall shear stress for the solvent at the same mean flow velocity. Results for a 480 p.p.m. Guar Gum solution are shown together with the aforementioned data from Elata and Tirosh (33) and a single point from Hoyt (41). For the range covered the correlation seems to be remarkably good, in that nearly all the experimental points lie along a unique line irrespective of pipe diameter and the threshold wall shear stress is clearly shown.

Fig.12 shows results from all the pipe flow experiments plotted in this universal correlation form, but only relatively few typical experimental points have been shown to avoid confusion. Data from the small bore pipe tests have only been included well above transition, and with this limitation the correlation is extremely good.

Figs.13 to 15 illustrate the same correlation plotted in a slightly different form, being linear-log plots of percentage drag reduction against $\tau_{w(o)}$. These

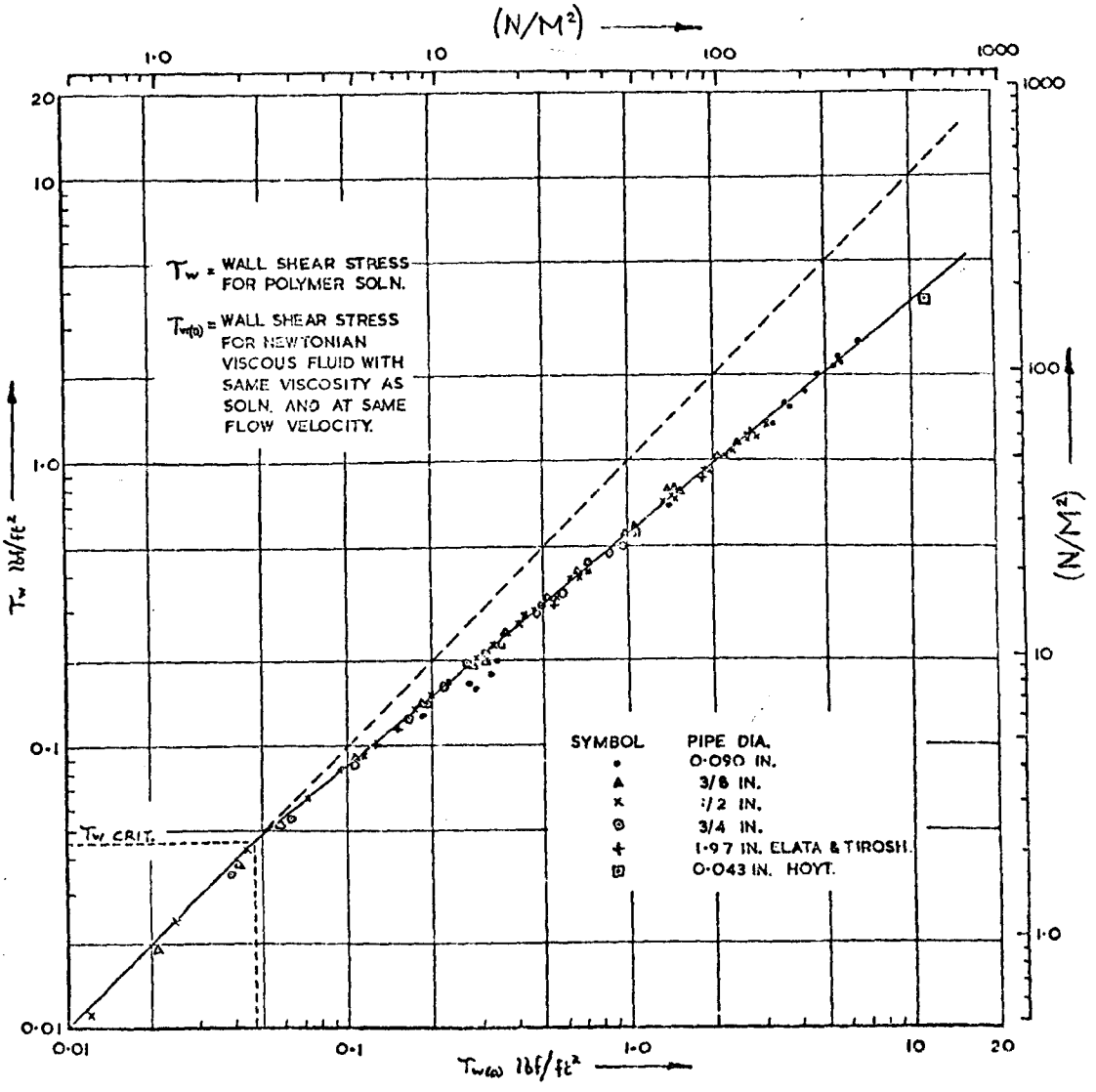

FIG. 11. CORRELATION FOR 480 W.P.P.M. GUAR GUM SOLN.

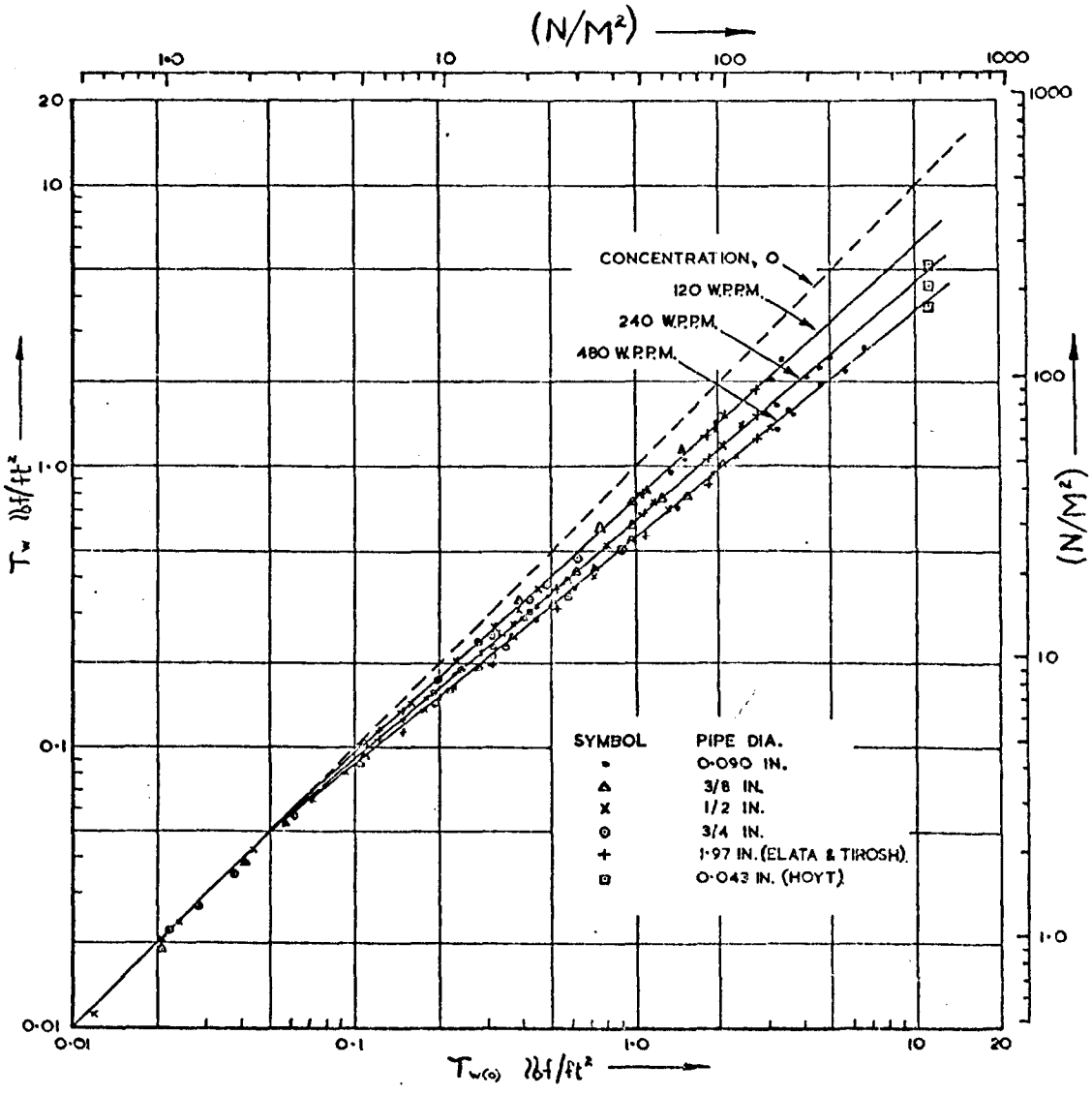

FIG. 12. PIPE FRICTION CORRELATION FOR DILUTE GUAR GUM SOLUTION.

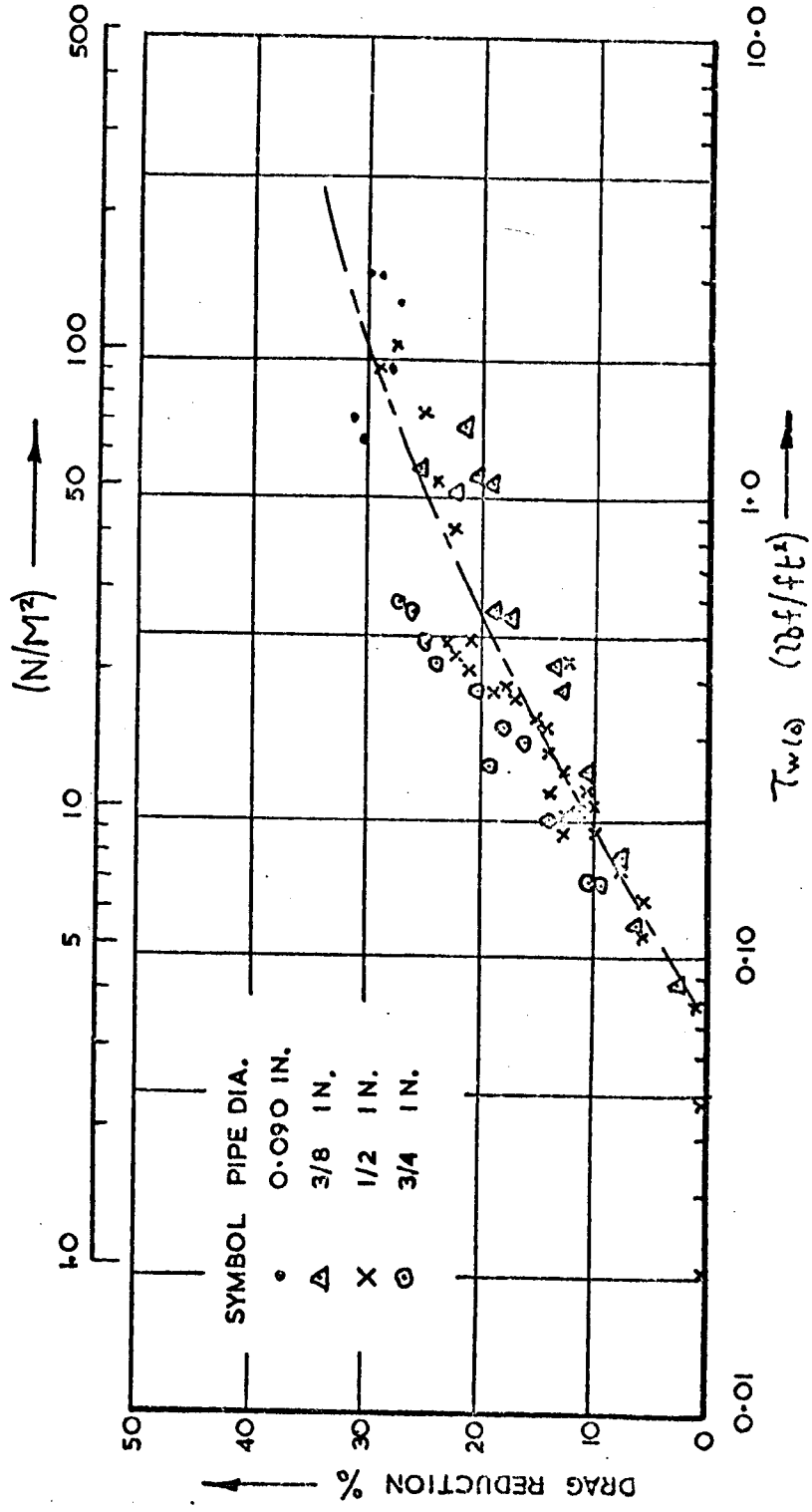

PIPE FRICTION REDUCTION 120 p.p.m. GUAR GUM SOLN.

Fig. 13.

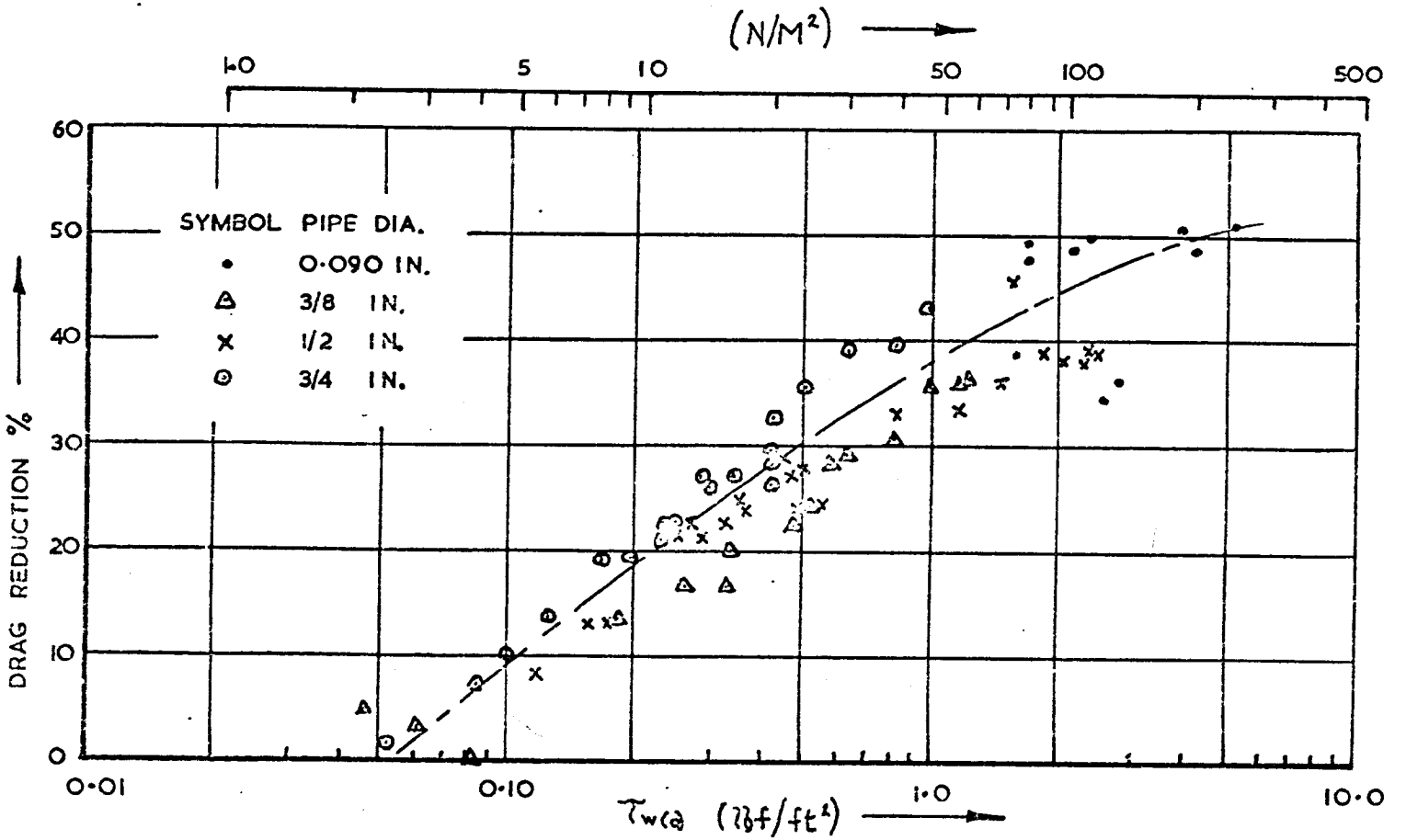

PIPE FRICTION REDUCTION. 240 p.p.m. GUAR GUM SOLN.

Fig. 14.

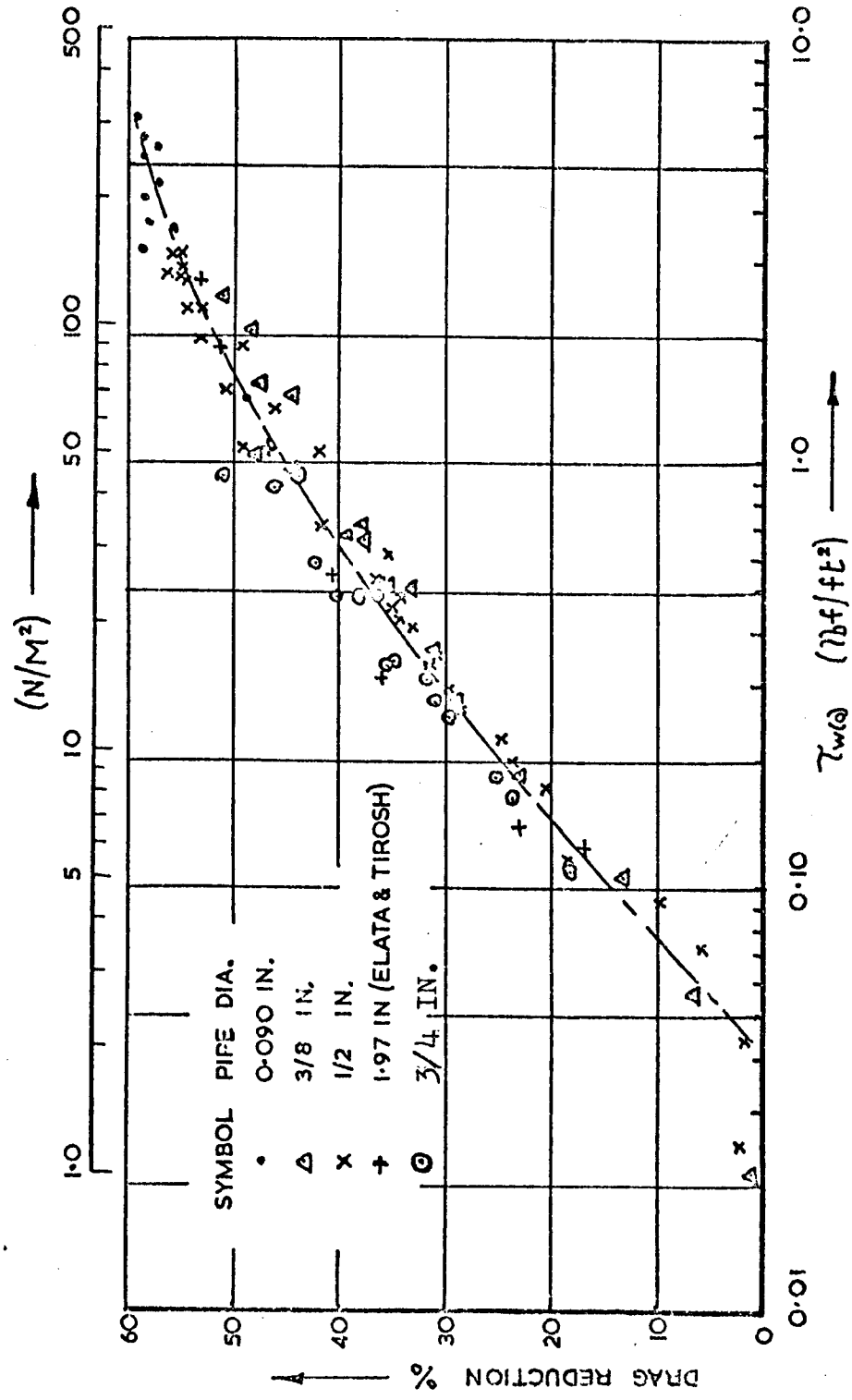

PIPE FRICTION REDUCTION 480 p.p.m. GUAR GUM SOLN.

Fig. 15.

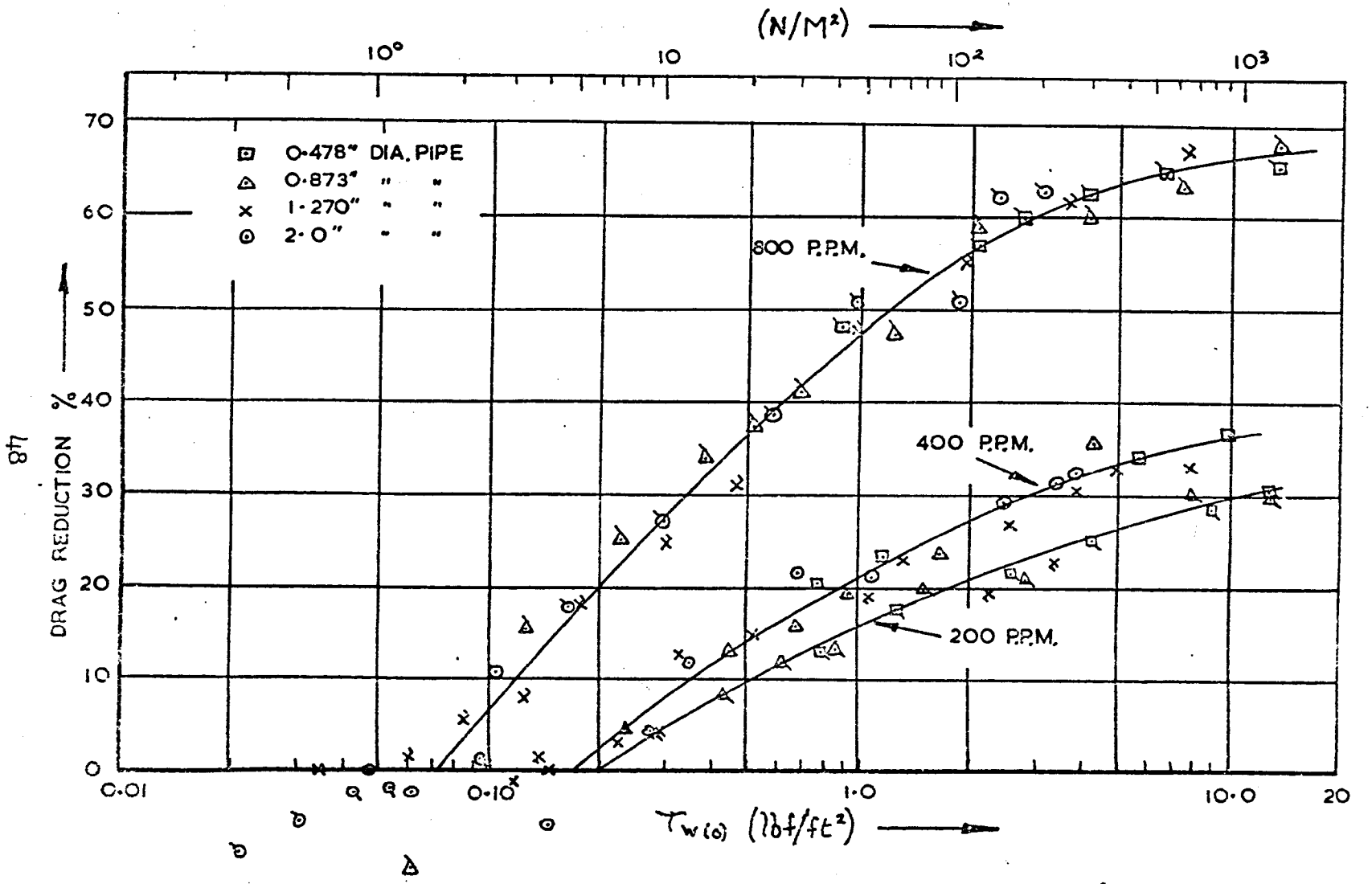

PIPE FRICTION REDUCTION WITH GUAR GUM SOLN.

(DATA OF ELATA ET. AL.)

Fig. 16

graphs show up any scatter rather better and are probably more useful for direct practical application. The scatter is due largely to measurement errors, there being no significant diameter effect.

Some further confirmation of the correlation is provided by data published by Elata, Lehrer and Kahanovitz (57), which was published in 1966. Fig.16 shows that their results correlate extremely well by the present technique.

With all these results we can see that the threshold wall shear stress is only slightly affected by solution concentration for very dilute solutions, but is reduced with higher concentrations. We will return to this point at a later stage of the discussion.

The fact that the present correlation holds over a range of pipe sizes from 0.090 in. (2.38mm) to 2.0 in. (50.8mm) diameter, (a 20 to 1 ratio), gives some confidence for cautious extrapolation to the larger sizes used in practical installations.

(2.1.5) Degradation.

The results of previous work (Hoyt and Fabula 5) and (Gadd 7) indicated that many synthetic polymer drag reducing additives were rapidly degraded by mechanical shearing and soon lost their effectiveness. Guar gum solutions however were shown to be quite stable in this respect.

As was previously mentioned the foregoing results were all obtained with freshly mixed Guar gum solution and if any degradation occurred during the tests then the mixture was discarded. Sometimes the apparatus could be run for periods approaching one hour before any serious degradation occurred, which again indicates that Guar gum is very stable with respect to mechanical shear. Often, however, degradation occurred much more rapidly. A jelly like precipitate was found at the bottom of and adhering to the sides of the fibreglass sump, which presumably reduced the effective concentration of the remaining solution. It seemed that the insoluble particles found in the Guar gum powder formed nucleii onto which the soluble polymer molecules were adsorbed. Furthermore, prior to using the fibreglass sump a few tests were carried out using a very dirty and rusty container, and it was found that very rapid degradation of the solution occurred with the formation of a jellylike precipitate. A test with a carefully filtered sample of Guar gum solution was run in the rig for a very much longer period of time before significant degradation occurred, and subsequent tests by Poreh et.al. (58) with a chemically clean rig showed no degradation over very long periods of time.

(2.2.0) PIPE FRICTION EXPERIMENTS WITH SYNTHETIC POLYMERS

A series of pipe friction experiments have also been carried out using dilute aqueous solutions of two synthetic high polymers, namely Separan NP10 - a polyacrylamide supplied by the Dow Chemical Co., and Polyox WSR 301, a poly (ethylene oxide) manufactured by Union Carbide Ltd. Both of these additives are very rapidly degraded by mechanical shearing and the closed circuit rig previously utilized could not be used. Consequently a once-through method of testing was adopted, the rack of pipes being supplied from a large roof mounted header tank, and the solutions were discarded after collection in the measuring tanks.

(2.2.1) Solution preparation.

A standard procedure was adopted for the preparation of these dilute polymer solutions. The weighed quantity of additive was dispersed in a small quantity of alcohol and was then carefully and gently stirred into a large bucket of water. Gentle stirring was continued for a period of 1/2 hour and the solution was then mixed with the water in the header tank and left for a further 1/2 hour period. Another gentle mixing then preceeded the test.

(2.2.2) The basic results.

Fig.17 shows some pipe flow results with a

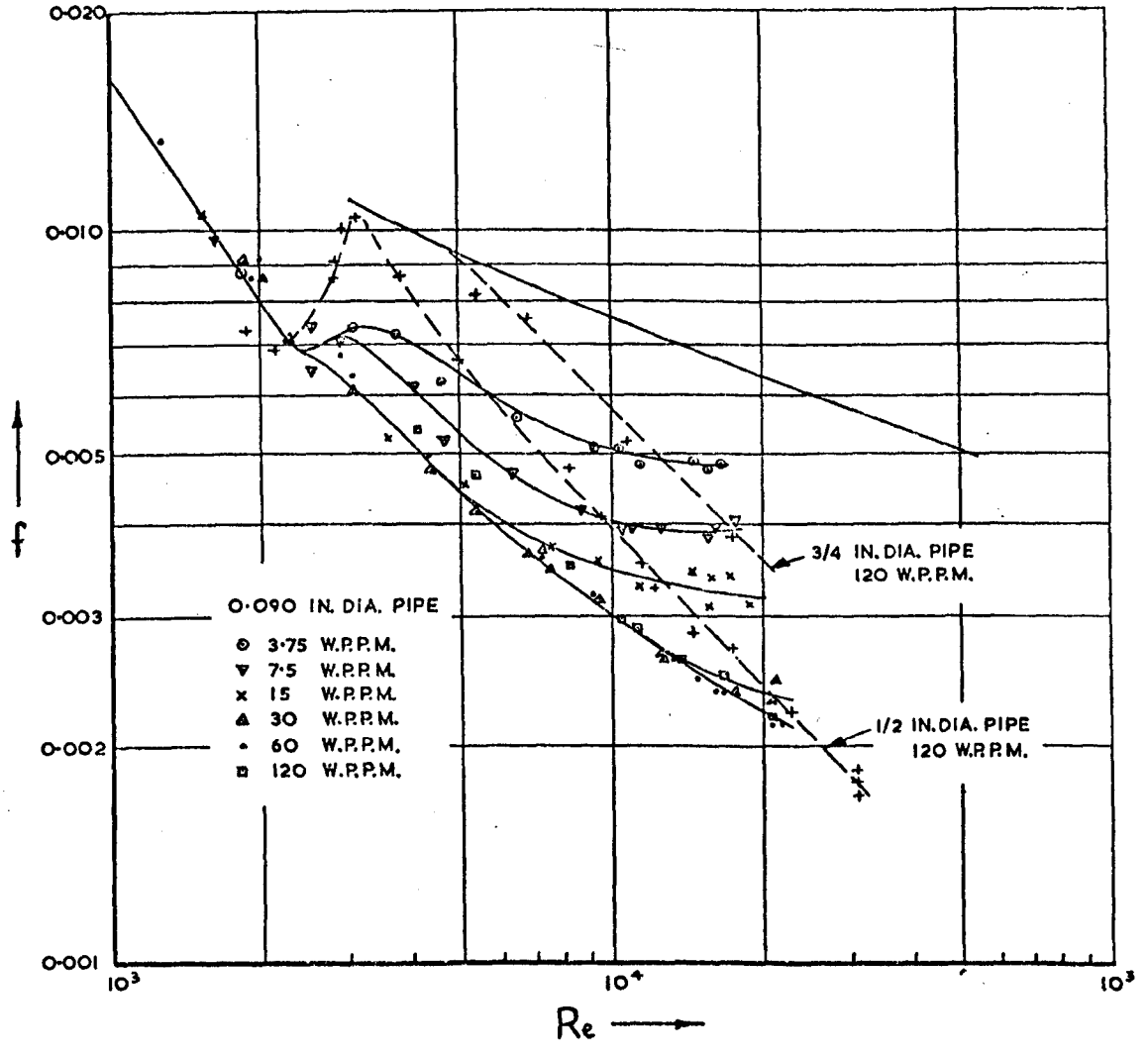

PIPE FRICTION WITH SEPARAN N.P.10 SOLN.

Fig. 17.

solution of Separan NP10 at various concentrations in pipes of various diameters. This additive is seen to be a much more effective drag reducer than Guar Gum solution although the results exhibit the same phenomena, namely a diameter effect and threshold wall shear stress. Results from the small bore pipe appear to approach a maximum drag reduction asymptote with increasing concentration and the upward trend of these results at the higher Reynolds numbers or higher shear stress values is apparently due to degradation. The relative viscosity of the solutions is shown in table 4, and at the concentrations used the solutions were found to behave in a Newtonian manner under laminar flow conditions.

TABLE 4

Solution Concentration (p.p.m)	Rel. Viscosity (ν/ν_{water})
60	1.03
120	1.07
240	1.25

Figs.18 and 19 illustrate results obtained with dilute Polyox WSR 301 solutions in pipes of 3/8 in. (9.52mm) and 3/4 in. respectively. Again the asymptotic nature of the drag reduction with increasing concentration can be seen. Furthermore the threshold wall shear stresses with these solutions are clearly very much lower than those for Separan, which in turn are less than those for Guar Gum.

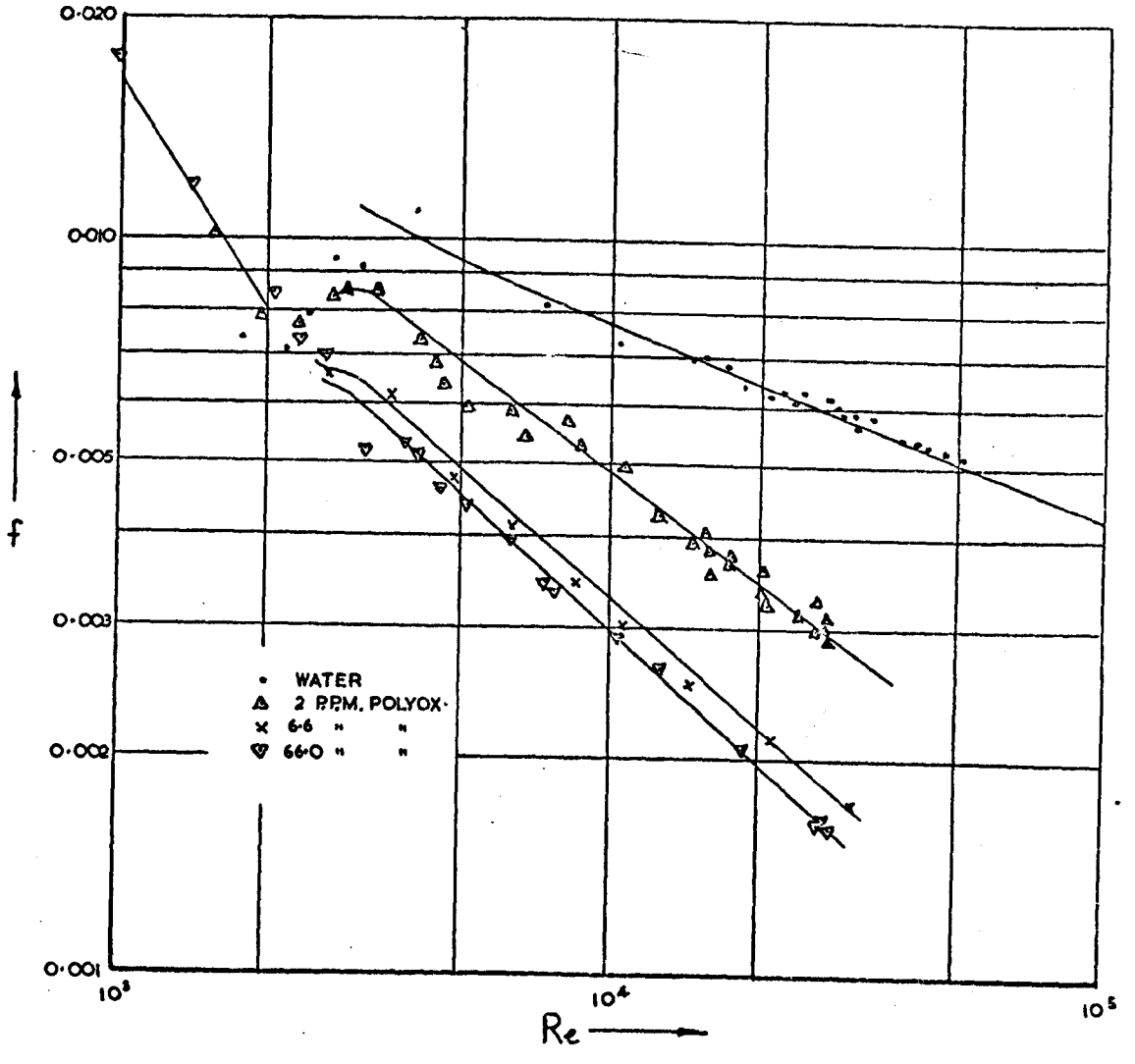

PIPE FRICTION WITH POLYOX W.S.R.301 SOLN.

(PIPE DIAMETER 3/8 IN.)

Fig. 13.

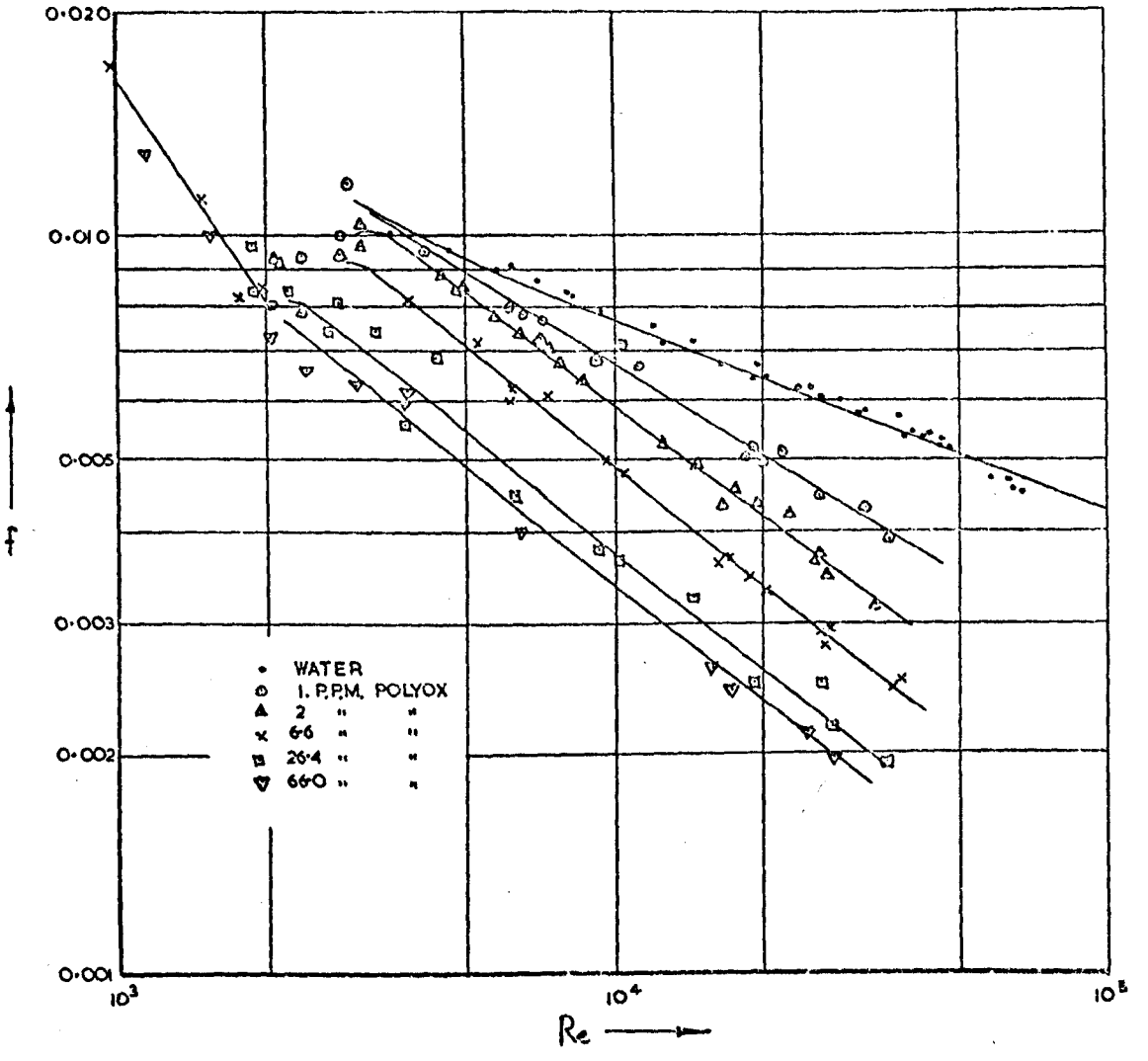

PIPE FRICTION WITH POLYOX W.S.R.301 SOLN.

(PIPE DIAMETER 3/4 IN.)

Fig. 19.

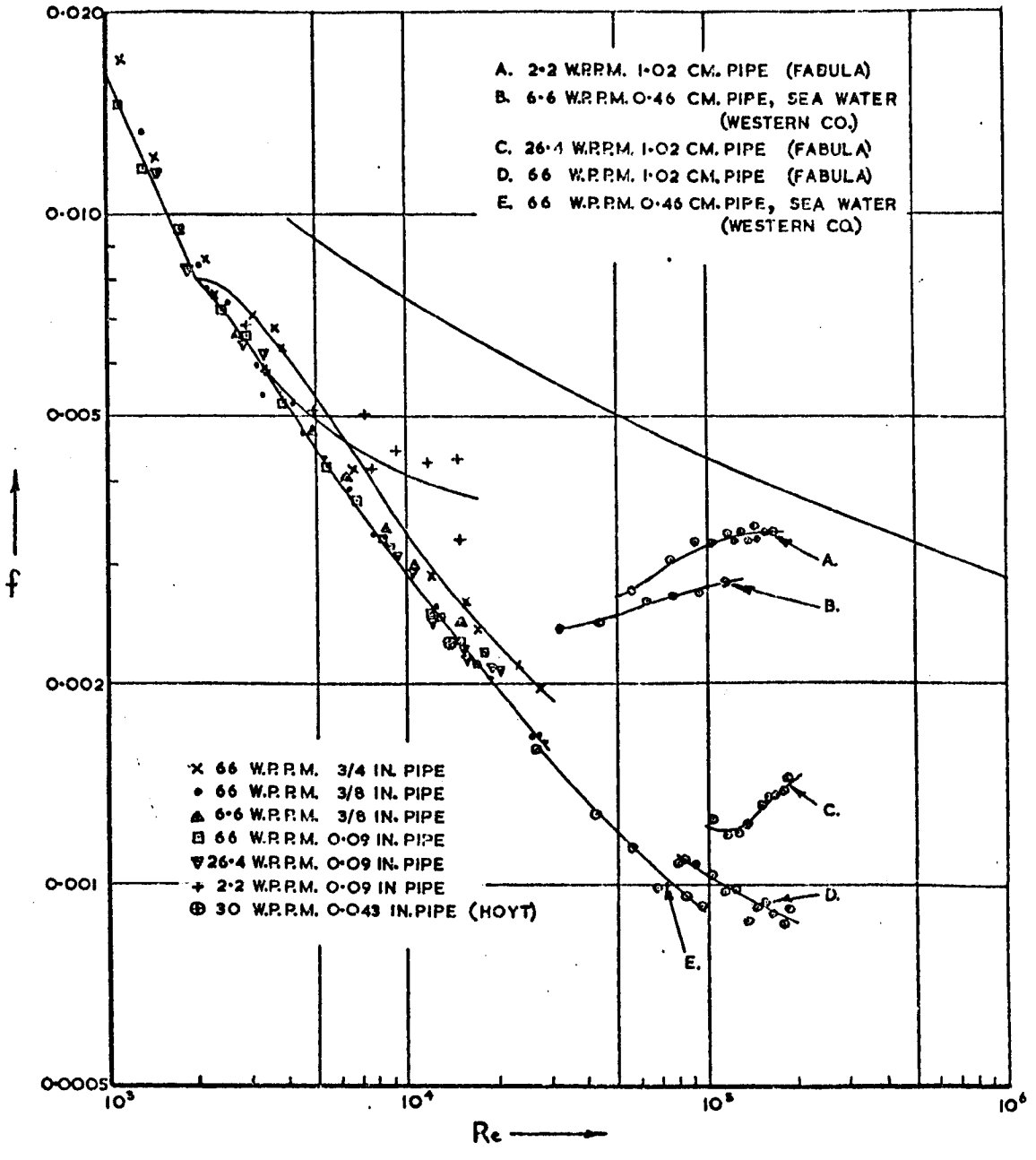

PIPE FRICTION WITH POLYOX W.S.R.301 SOLN.

Fig. 20.

Fig. 20 gathers together on a friction factor chart some of the present results with those of other workers which were available at this time. Exact correspondence would not be expected due to different mixing procedures and different batches of polymer, since the molecular weight is not guaranteed by the manufacturer. Again degradation is apparent at high shear rates, particularly with the lower concentrations.

A comparison of figs.20 and 17 indicates that the maximum drag reduction asymptote is about the same for both Separan and Polyox solutions. In fact subsequent studies by Virk et.al. (59), who analyzed a whole collection of much more recent data, showed that this maximum asymptote is the same for all polymeric drag reducing additives and represents the maximum drag reduction obtainable.

Virk et.al. (59) show that the best line through all the available data points on the asymptote are correlated by the following expression:-

$$1/\sqrt{f} = 19.0 \log_{10}(Re\sqrt{f}) - 32.4$$

This relationship fits the data in figs. 14 and 17 extremely well.

In common with the other solutions, those with polyox were also found to be Newtonian under laminar flow conditions for the dilute concentrations used. The

relative viscosities used in calculating Reynolds numbers for the preceeding figures were once again determined by capillary viscometry and from measurements in the small bore pipe. These are shown in table 5 and it is seen that the solutions are only very slightly more viscous than water.

TABLE 5

Solution Concentration (p.p.m)	Rel. Viscosity (ν/νwater)
10	1,010
26.4	1.024
30	1.028
60	1.070
66.0	1.075
120	1.145

(2.2.3) Empirical data correlation.

The success of the wall shear stress plot in correlating the Guar gum results prompted its adoption for the latter two polymers. Once again the percentage drag reduction is determined by comparing the wall shear stress of the polymer solution (τ_w) with that of the solvent ($\tau_{w(o)}$) the same mean flow velocity.

Fig.21 shows the limited data obtained with a 60 p.p.m. solution of Separan. The correlation is remarkably good, results for the 3/8 in. (9.52mm) and 3/4 in. (19.05mm) dia. pipes lying along a unique line. Degradation is apparent at the high shear end of the curve.

Results for the extremely dilute 2.2 p.p.m. and

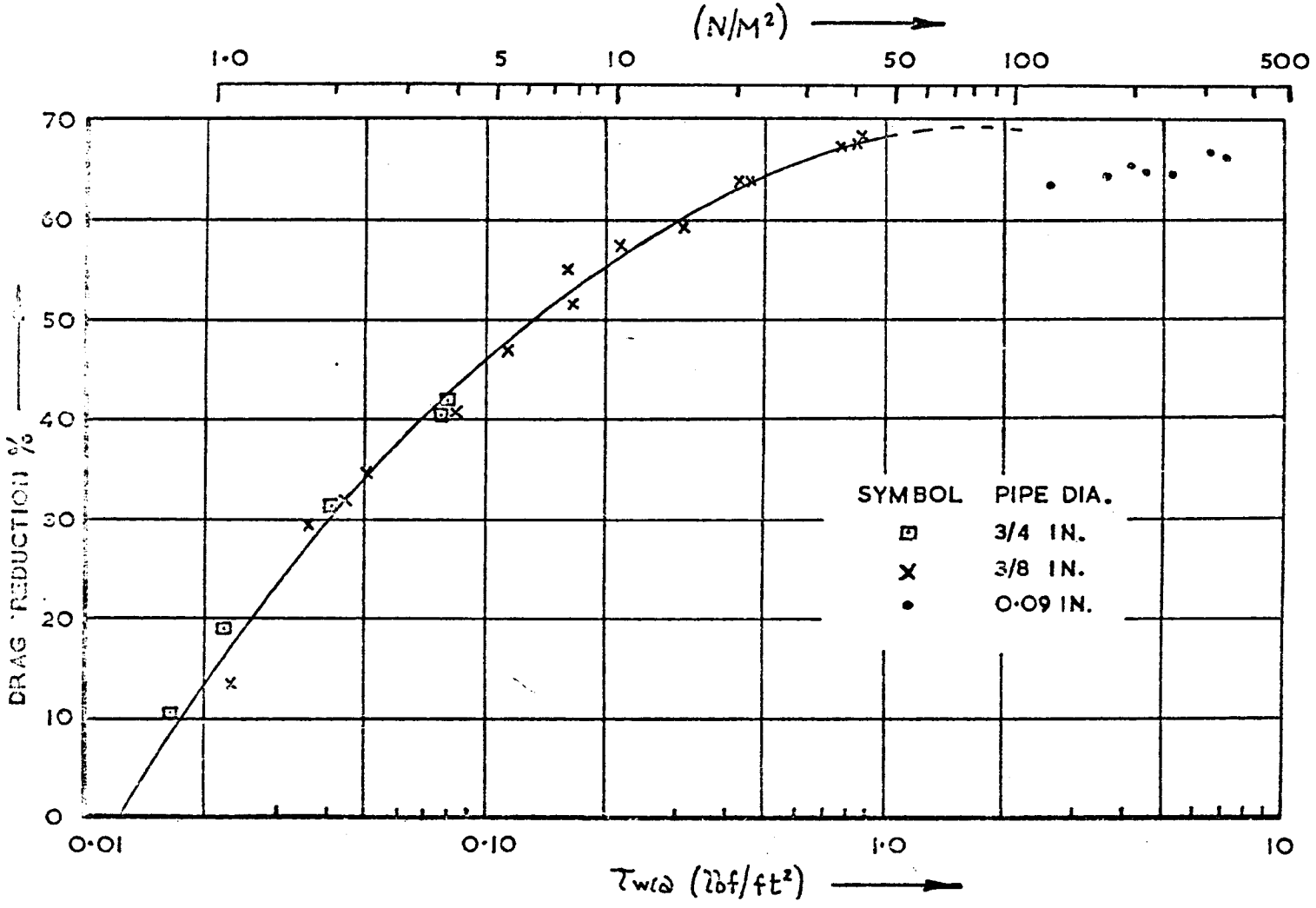

PIPE FRICTION REDUCTION SEPARAN NP10 60p.p.m.

Fig. 21.

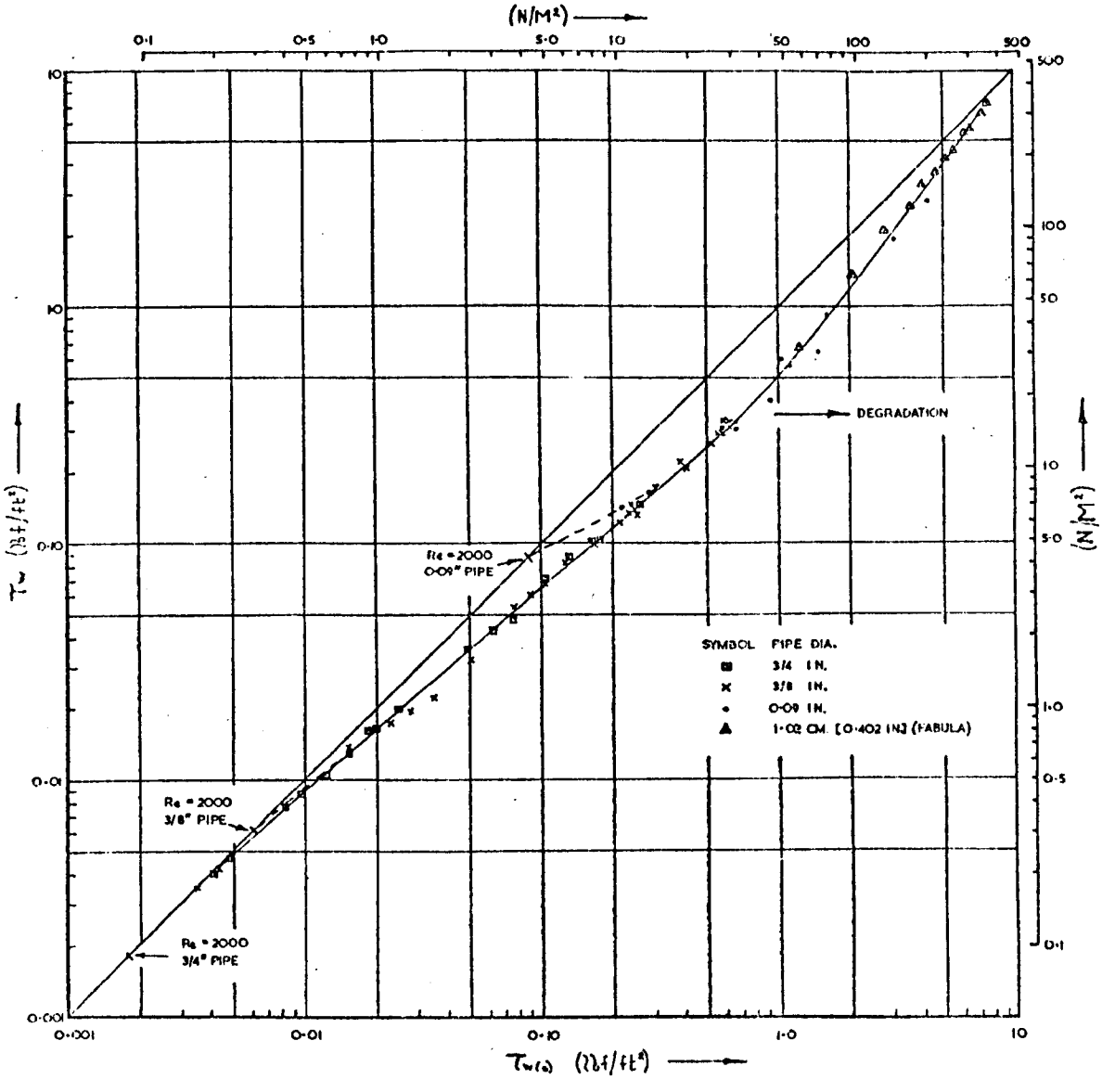

PIPE FRICTION CORRELATION.

2.2 p.p.m. Soln. POLYOX WSR 301.

Fig. 22.

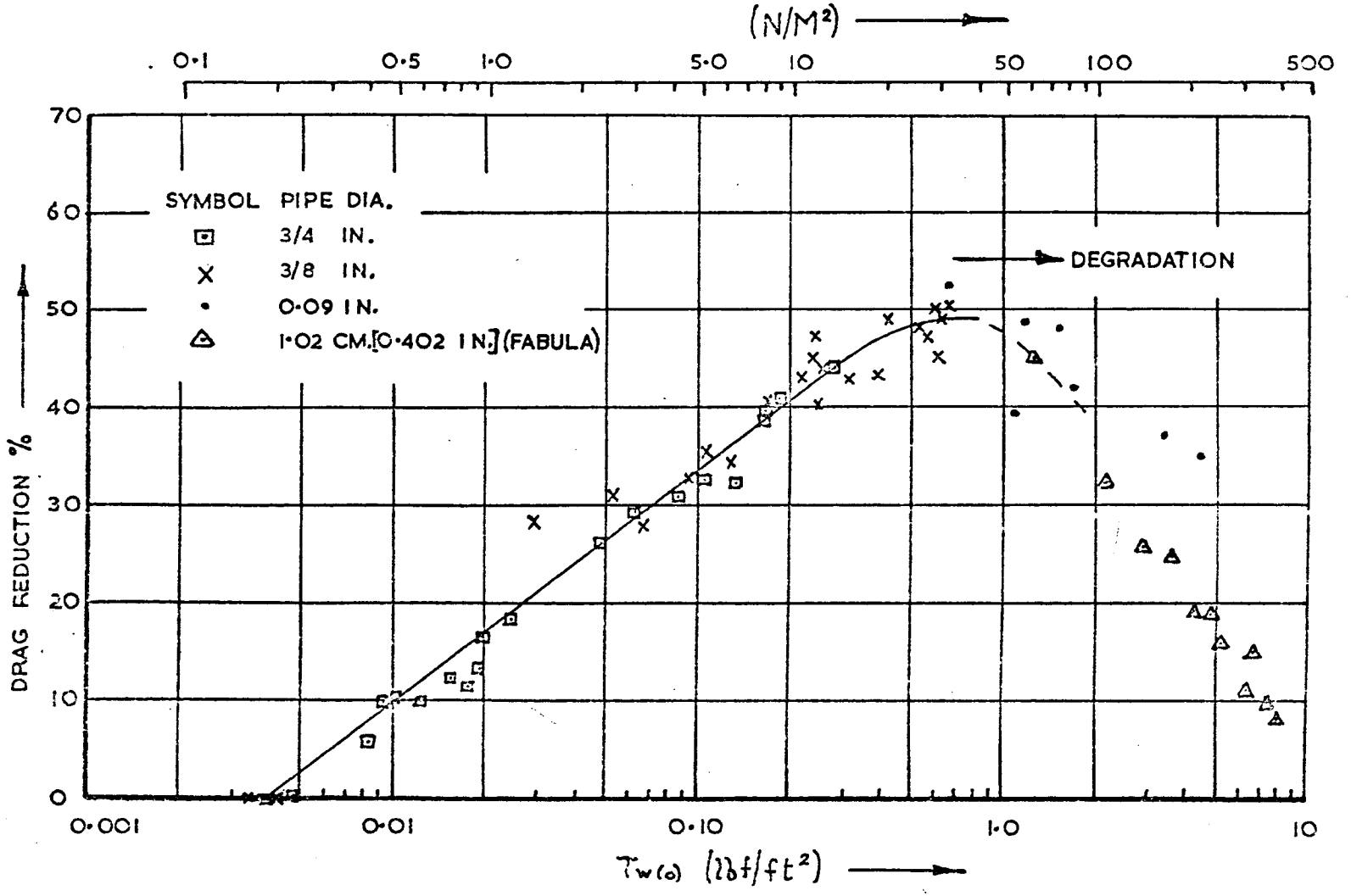

PIPE FRICTION REDUCTION 2.2 p.p.m. POLYOX WSR301 SOLN.

Fig. 23.

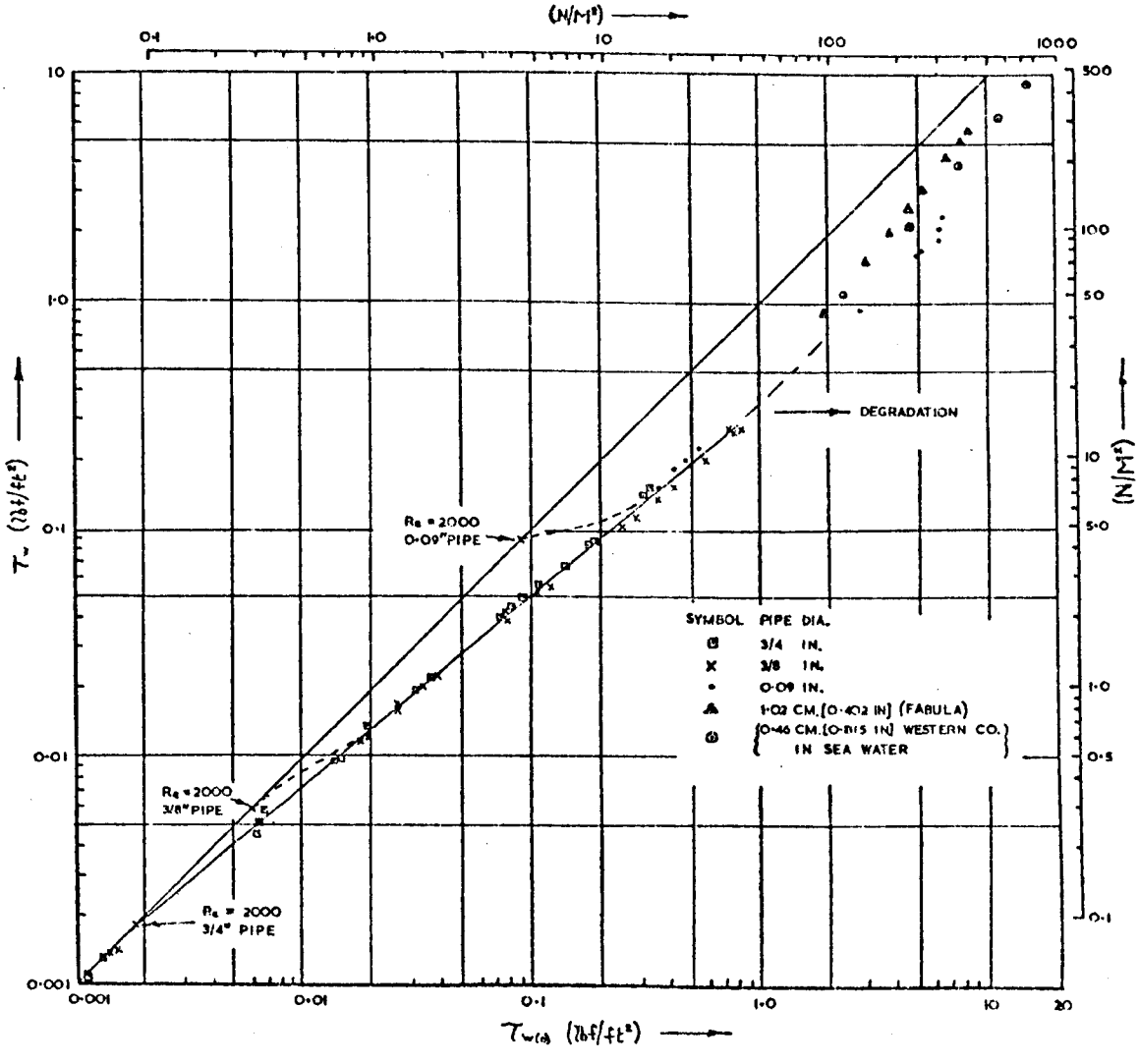

PIPE FRICTION CORRELATION

6.6 p.p.m. Soln. POLYOX WSR301.

Fig. 24.

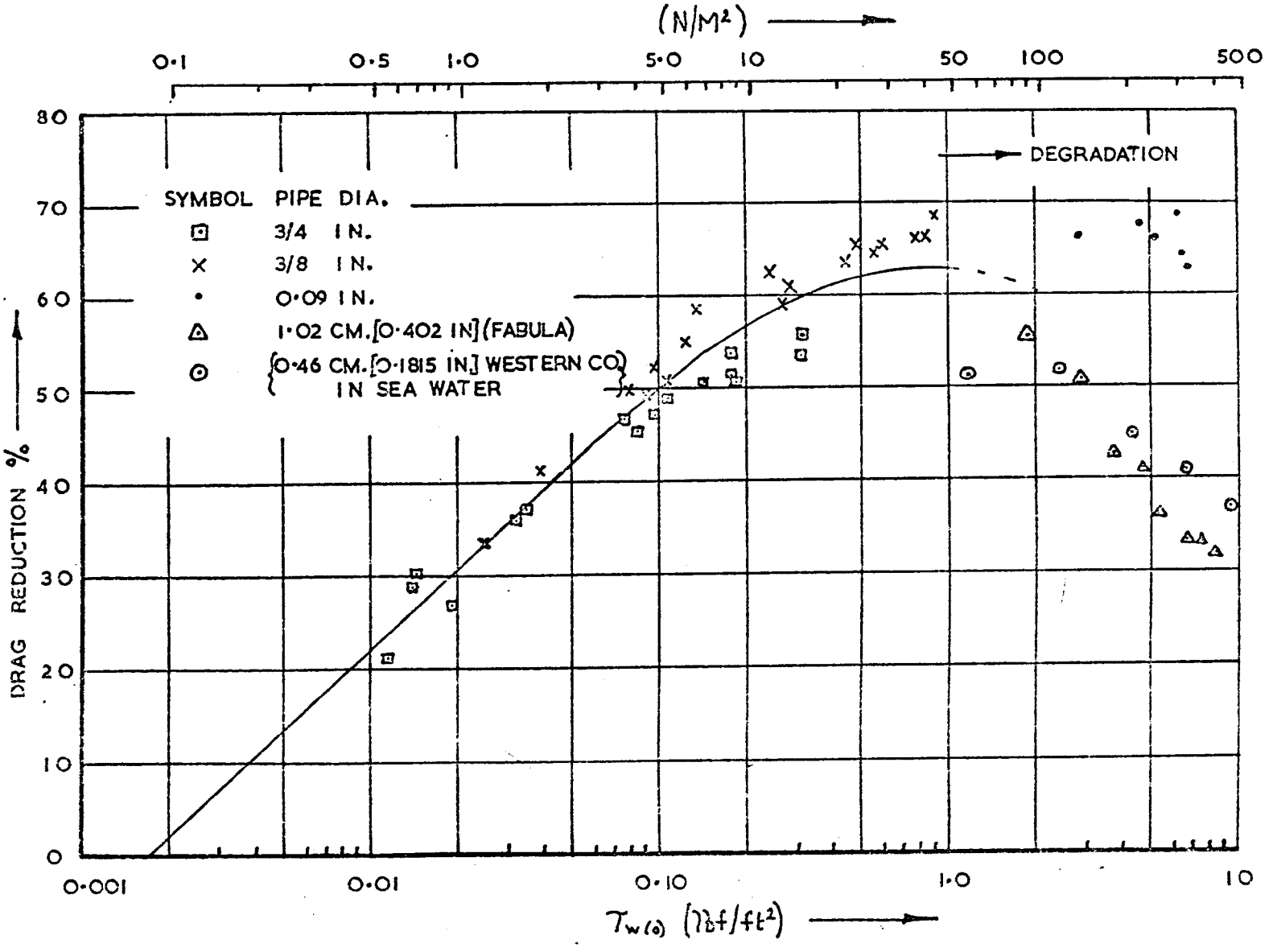

PIPE FRICTION REDUCTION 6.6 p.p.m. POLYOX WSR301 SOLN.

Fig. 25.

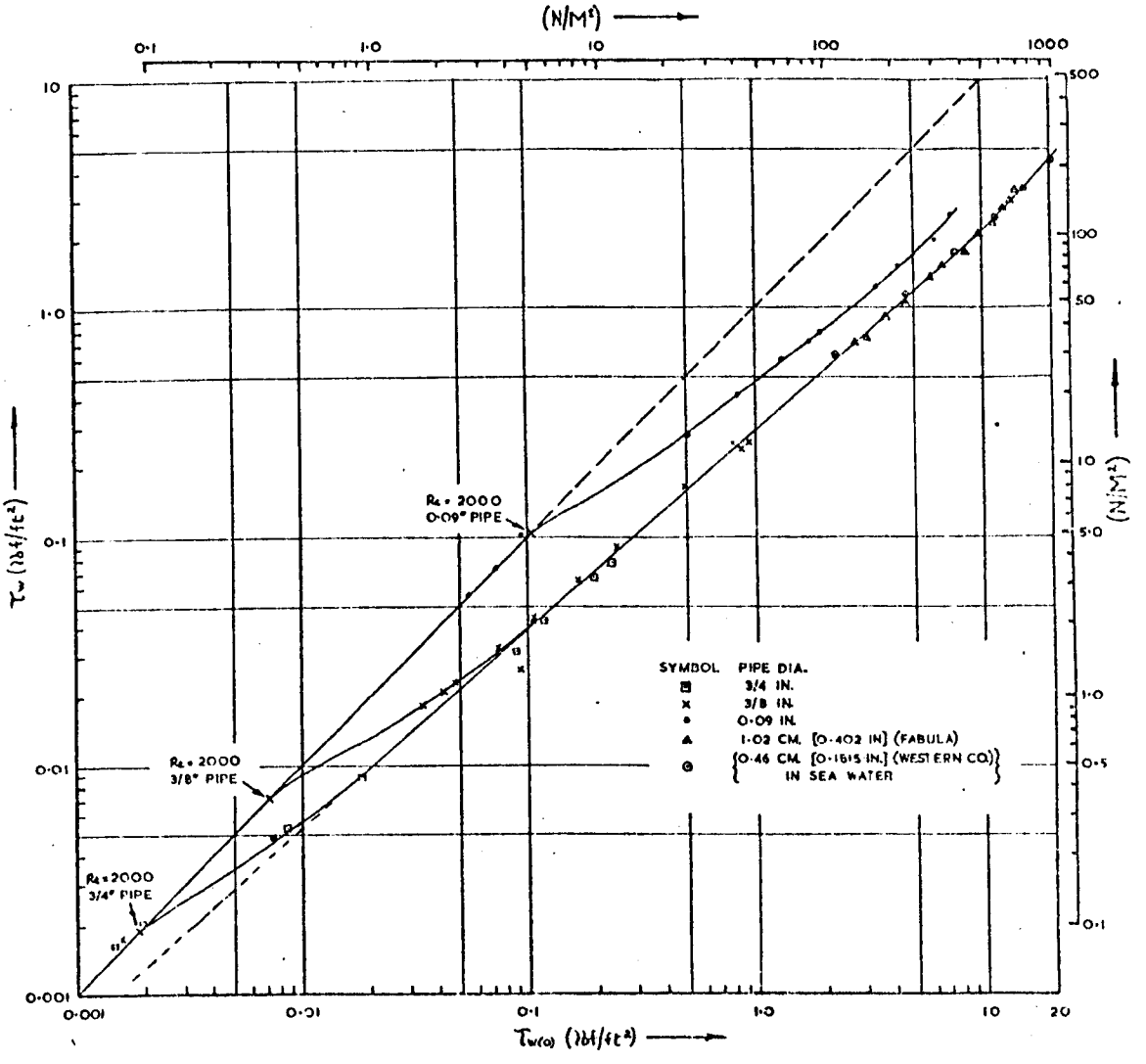

PIPE FRICTION CORRELATION.

66 p.p.m. Soln. POLYOX WSR 301.

Fig.26.

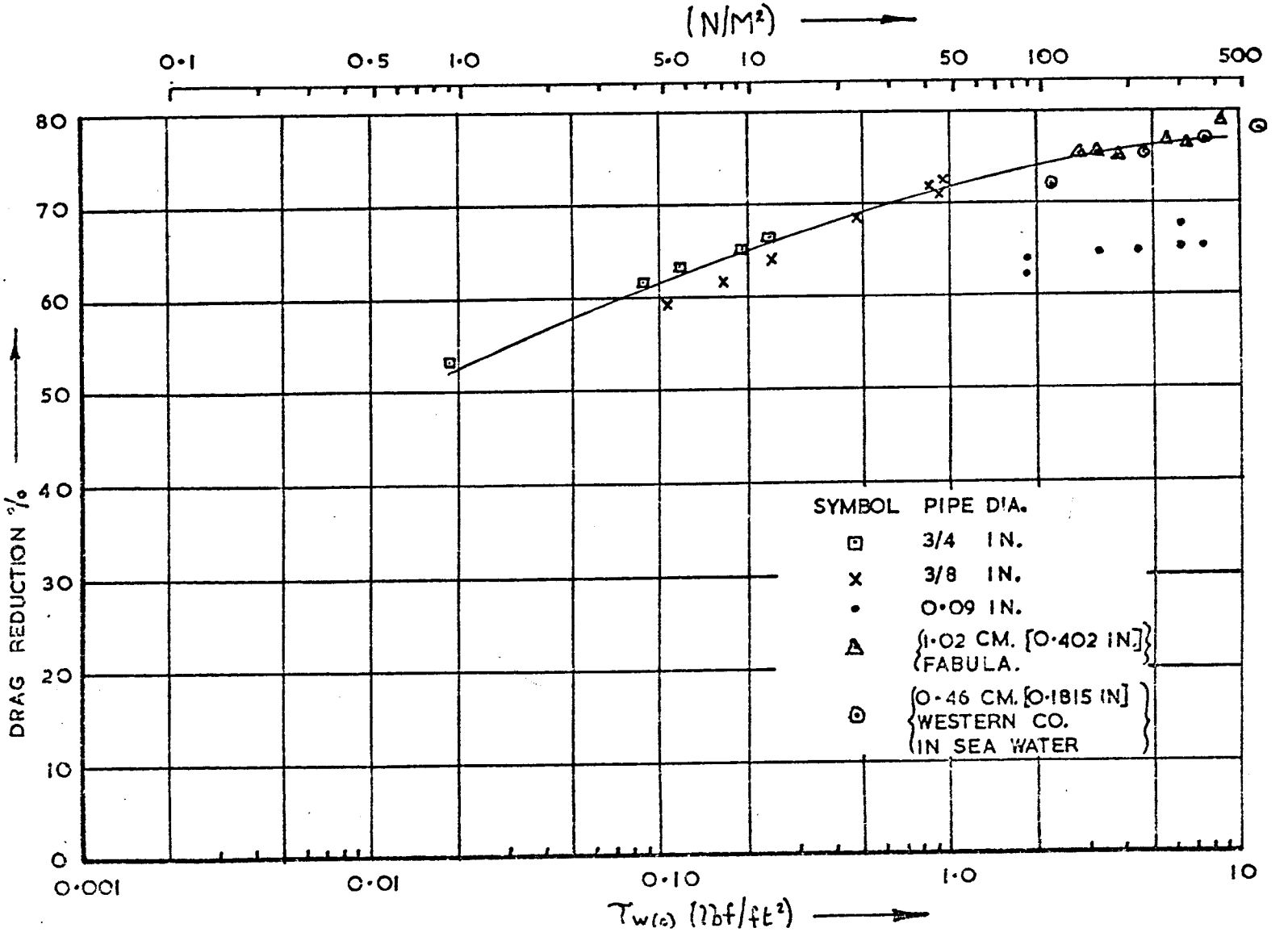

PIPE FRICTION REDUCTION 66 p.p.m. POLYOX WSR 301 SOLN.

6.6 p.p.m. solutions of Polyox are correlated quite satisfactorily in figs.22 and 25. Above a wall shear stress of about 1.0 lbf/ft^2 (48 N/M^2) degradation is very rapid, shown by the sharp fall off in drag reduction with increasing flow rate.

Data from tests with a 66 p.p.m. Polyox solution also correlate reasonably well by the present method, at least for the larger pipe sizes. Points from tests in the 0.090 in. (2.38mm) dia. pipe however, show less drag reduction at a given wall stress than those from pipes of greater diameter. This is not surprising since drag reduction in the small pipes is limited by the drag reduction asymptote, and the correlation cannot work for data on or very close to this limit, as is explained in the next section.

Another observation which can be made from the present results is the considerable variation of the threshold wall shear stress with Polyox concentration, which is much greater than that found with Guar gum solutions.

(2.2.4) Limitations of the wall shear stress correlation method.

The present data has been shown to correlate very well by comparing the corresponding wall shear stresses of solution and solvent in pipe flow at the same mean flow velocity. This technique eliminates the pipe diameter

Fig.28.

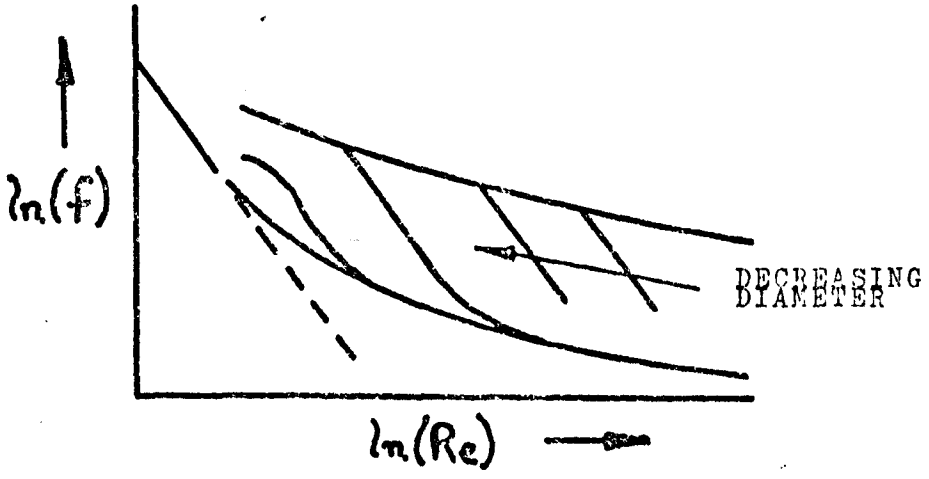

APPROACH TO ASYMPTOTIC LIMIT IN SMALL DIA. PIPES

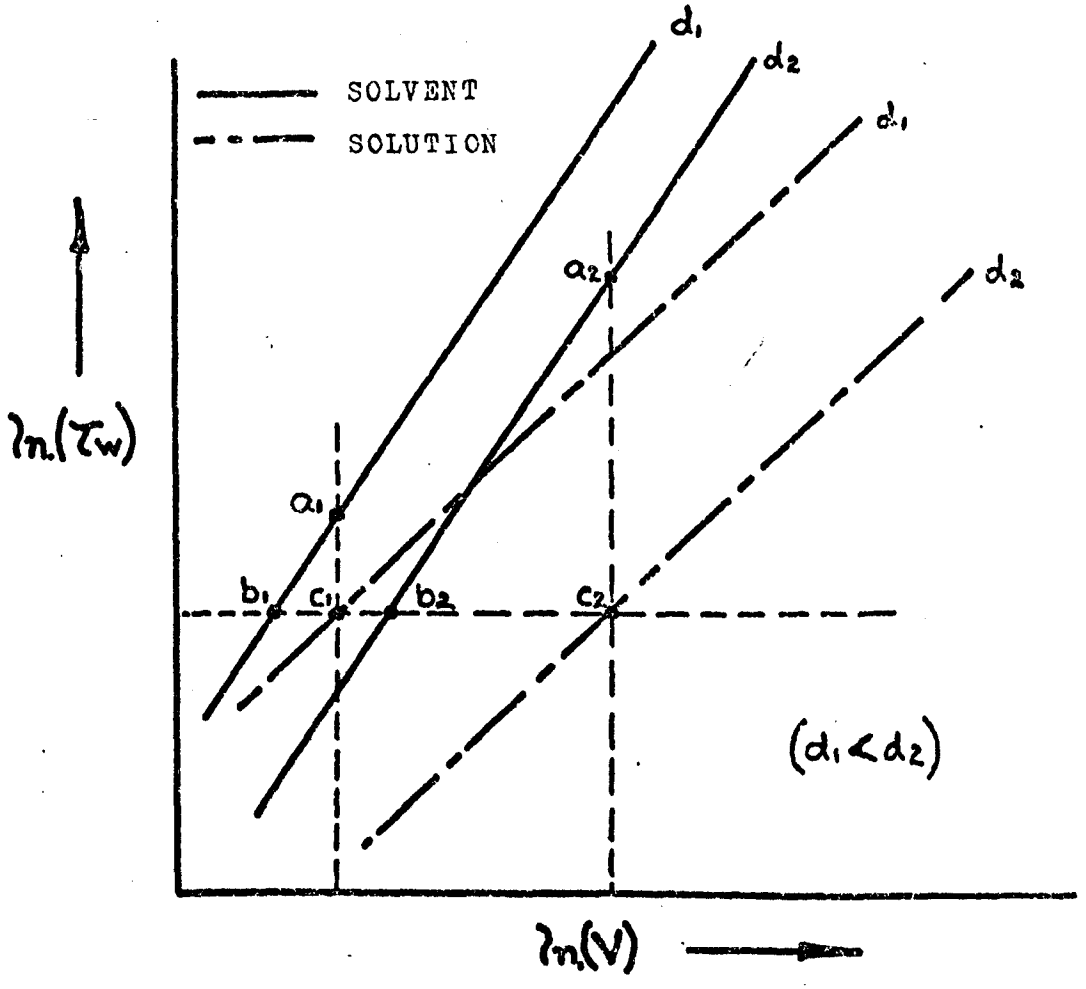

FAILURE OF CORRELATION NEAR TO ASYMPTOTE.

Fig. 29.

effect and makes possible the tentative extrapolation of results from moderate diameter pipes used in laboratory experiments to larger ones used in practical installations. The limitations of this method must be carefully noted if it is to be correctly applied.

The correlation works because of the parallelism of friction factor lines for pipes of different diameter which deviate from normal turbulent flow at the threshold wall shear stress. The drag reduction is limited by the maximum asymptote and results with small pipes may approach or reach the asymptote as is shown in fig.28. The asymptote may also be approached by increasing the concentration of a given polymer in a particular pipe.

By the correlation, the drag reduction is constant for a given wall shear stress and polymer concentration irrespective of pipe diameter, but this must fail to hold near or on the asymptote where the friction reduction would be less in a small pipe than in a larger one for the same wall shear stress. This is clearly shown in fig.29 which is a plot of wall shear stress against mean flow velocity for two pipes of diameter d_1 and d_2, showing the normal turbulent flow relationship (solid lines) and the corresponding drag reduced flow based on the asymptote (dashed lines).

Using the Blasius relationship as in fig.7, we have for turbulent flow:-

$$\tau_w = 1/2\rho v^2 f$$

$$= 1/2\rho v^2 . 0.08(vd/\nu)^{-0.25}$$

$$= 0.08(\rho/2\nu^{0.25})\ v^{1.75}/d^{0.25}$$

$$= \text{const.}_1 \ . v^{1.75}/d^{0.25}$$

A power law which fits the asymptote for Re = 4000-40000 is given by Virk et.al. (59) as $f = 0.59Re^{-0.58}$, which gives the corresponding wall shear stress as:-

$$\tau_w = 0.59(\rho/2.\nu^{0.58})\ v^{1.42}/d^{0.58}$$

$$= \text{const.}_2 \ . v^{1.42}/d^{0.58}$$

From these relationships we see in fig.29 that the asymptote lines for diameters d_1 and d_2 are more widely spaced and have a smaller slope than the corresponding lines for ordinary turbulent flow, and for a given wall shear stress we see that the drag reduction in the small pipe (a_1c_1) is less than that in the larger pipe (a_2c_2).

Based on the preceeding data the wall stress correlation would seem to be quite reliable provided that it is not used near to the asymptote or close to the transition Reynolds number.

(2.3.0) DATA CORRELATION BASED ON VELOCITY PROFILES.

(2.3.1) Two zone model

We have seen (section 1.5) that simple dimensional reasoning applied to turbulent boundary layers and pipe flows close to the wall yields the dimensionless velocity distribution known as the "Law of the wall."

By neglecting the transition or 'buffer' layer, the velocity profile on ordinary pipe flow can be approximated with good accuracy by Prandtl's two zone model, which consists of a thin linear viscous layer adjacent to the wall and a turbulent core, described by the law of the wall expression. This is shown in fig.30 and a full description may be found in any basic fluid mechanics text.

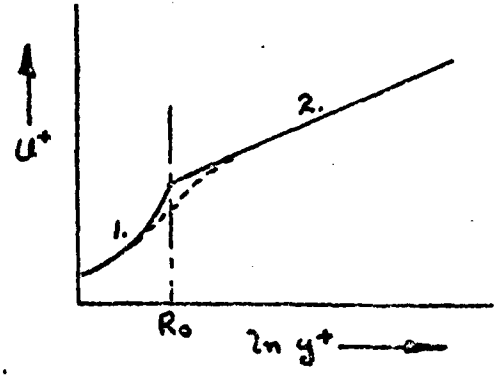

$u^+ = u/u^*$

$y^+ = yu^*/\nu$

where $u^* = \sqrt{\tau_w/\rho}$

---- Blending or buffer layer.

Zone 1 is given by $u^+ = y^+$

Zone 2 is given by $u^+ = A \ln y^+ + B$

Experiments in normal turbulent flow indicate that:-

$$A = 1/k = 2.5$$

$$B = 5.5$$

Ro comes from the intersection of zones 1 and 2 works out to be 11.6

Fig.30 THE TWO ZONE MODEL OF A NEWTONIAN TURBULENT BOUNDARY LAYER

By integrating this velocity profile between limits of the pipe radius and the axis, we can easily show (see appendix 1) that:-

$$1/\sqrt{f} = 1/(k\sqrt{2})(\ln Re\sqrt{f} - \ln 2\sqrt{2} + kRo - \ln Ro - 3/2)$$

Now pipe friction experiments in turbulent flow yield values for k and Ro from this equation which are very similar to those derived from velocity profile measurements quoted above, and this affords some degree of confidence to the use of the two zone model.

On the assumption that such a profile is universal it is apparent from the above equation that if polymer additives are to bring about a reduction in friction factor, then either k must be reduced or Ro increased, or both may possibly change.

Mean velocity profile measurements in polymer solutions are not straightforward since the calibration of instruments such as small pitot tubes or hot film anemometers may be affected by the additive and result in measurement errors. However, even quite early reliable measurements such as those by Wells (37), Ernst (60) Elata et.al. (57) and Goren and Norbury (61) showed the common significant result that with very dilute solutions the slope (A=1/k) of the logarithmic core region was unchanged by the additive and merely displaced upwards. The effect on the buffer layer was not very clear from these early results.

Correlations almost identical in form were published in 1966 by Meyer (62) and by Elata et.al. (57), which were based on these velocity profile measurements, the idea being basically as follows.

Referring to fig.31 the velocity profile for a given polymer concentration was assumed to follow through zones 1 and 3, resulting in an increased value of the dimensionless sublayer thickness from Ro to Ro'

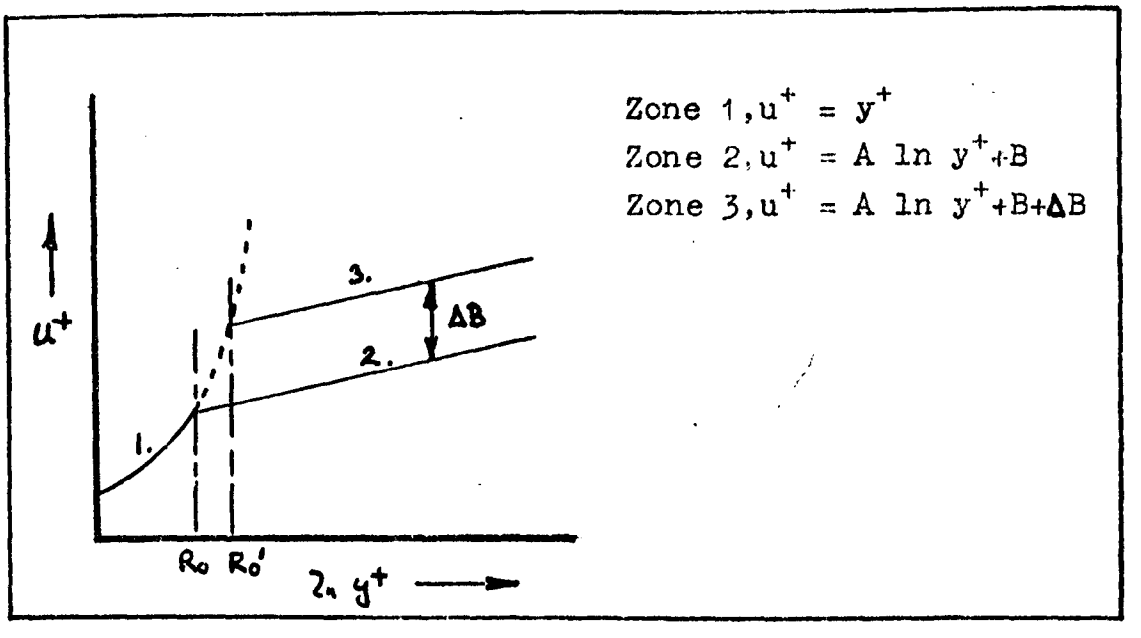

Fig.31 TWO ZONE VELOCITY PROFILE MODEL FOR DILUTE POLYMER SOLUTIONS IN TURBULENT FLOW

As before integration of this profile and assuming that Ro' is still quite small yields:-

$$1/\sqrt{f} = 1/(k\sqrt{2})(\ln Re\sqrt{f} - \ln 2\sqrt{2} + kRo' - \ln Ro' - 3/2)$$

It is now possible to deduce values for Ro' (or ΔB) from

pipe friction measurements by knowing corresponding values of f and Re.

Using both friction data and velocity profile information for a 500 p.p.m. solution of CMC (Sodium Carboxymethylcellulose) which is a moderately effective drag reducer, Ernst (60) found that ΔB was a unique function of the wall shear stress, given by:-

$\Delta B \propto \log (u^*/u^*_{threshold})$ with apparently no diameter effect. Similar work by Elata et.al. (52) with Guar gum solutions indicated a similar result, namely:-

$(Ro' - Ro) \propto \log u^{*2}$ for a given concentration

Values for the dimensionless sublayer thickness Ro' have been calculated from the present pipe friction results using this two zone model, and the results are shown in fig.32. Contrary to the results of Ernst and the statement by Elata et.al. these results show a weak but significant diameter effect. Furthermore when re-analyzed, the data of Elata et.al. also show considerable scatter when plotted in the form of fig.32, and many of the experimental points for the large pipes lie above those for the smaller ones as is found with the present data.

Although correlations of this type may work with very dilute solutions, a serious limitation is that as the concentration is increased with consequent increases in Ro',

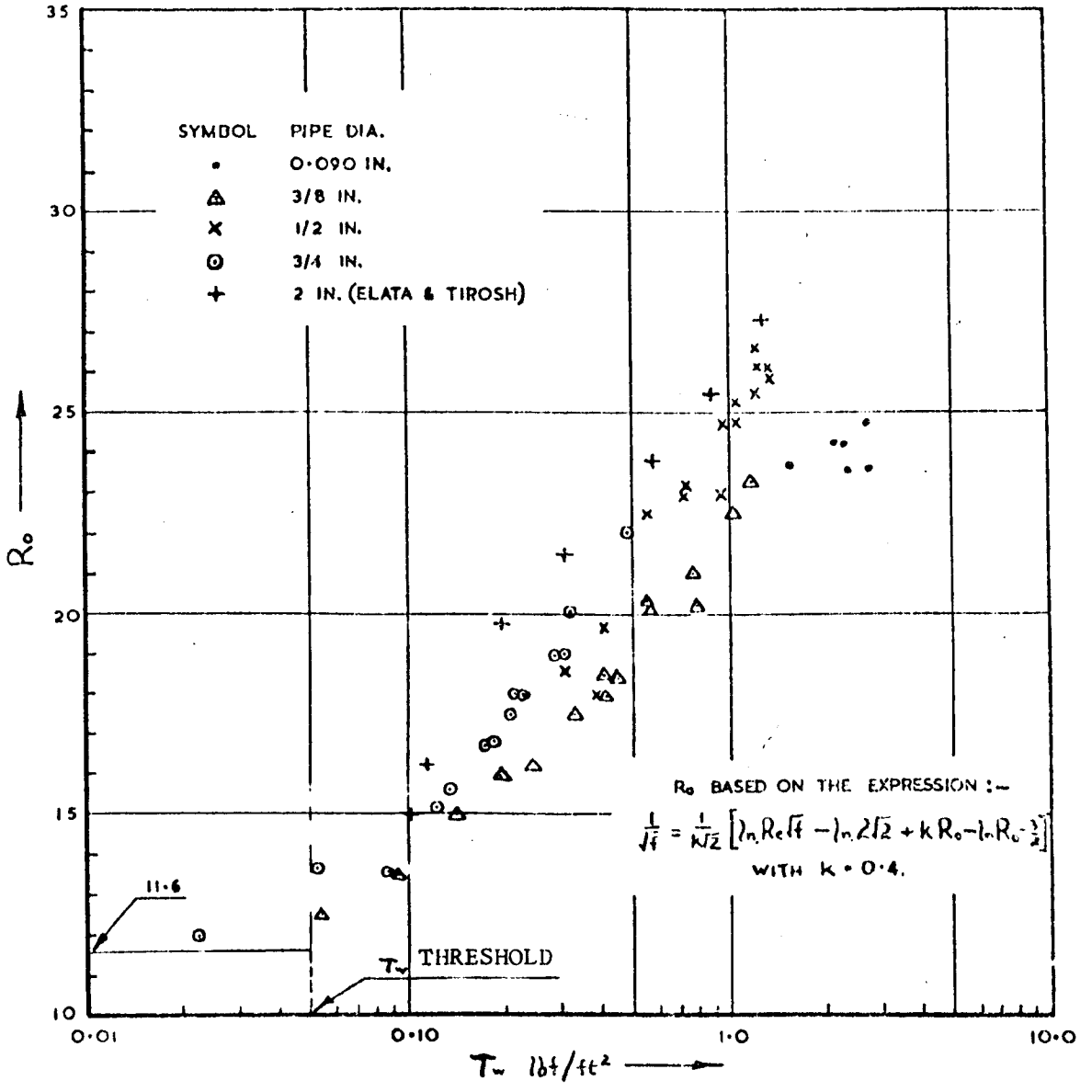

Fig 32. SUBLAYER REYNOLDS Nº WITH 480 W.P.P.M. GUAR GUM SOLUTION

the limiting case would be laminar flow with a linear profile when zone 1 reaches the pipe axis. This is certainly not the case in practice as drag reduction is limited by the maximum asymptote.

(2.3.2) The three zone velocity profile model.

The limitation of the two zone model is overcome when we consider the three zone model recently proposed by Virk et.al. (59)

The friction factor equation which fits the drag reduction asymptote for all polymers:-

$1/\sqrt{f} = 19\log_{10}Re\sqrt{f} - 32.4$ can be related to a semi logarithmic velocity law away from the wall given by:

$u+ = 11.7 \ln y^+ - 17.0$ in the same way that the Prandtl-Karman law:

$1/\sqrt{f} = 4 \log_{10}Re\sqrt{f} - 0.4$ is related to the velocity law:

$u^+ = 2.5 \ln y^+ + 5.5$ (See Virk et. al. 59)

We thus have the two zone models shown in fig.33 for the universal velocity profiles of ordinary turbulent flow and for drag reduced flow on the asymptote.

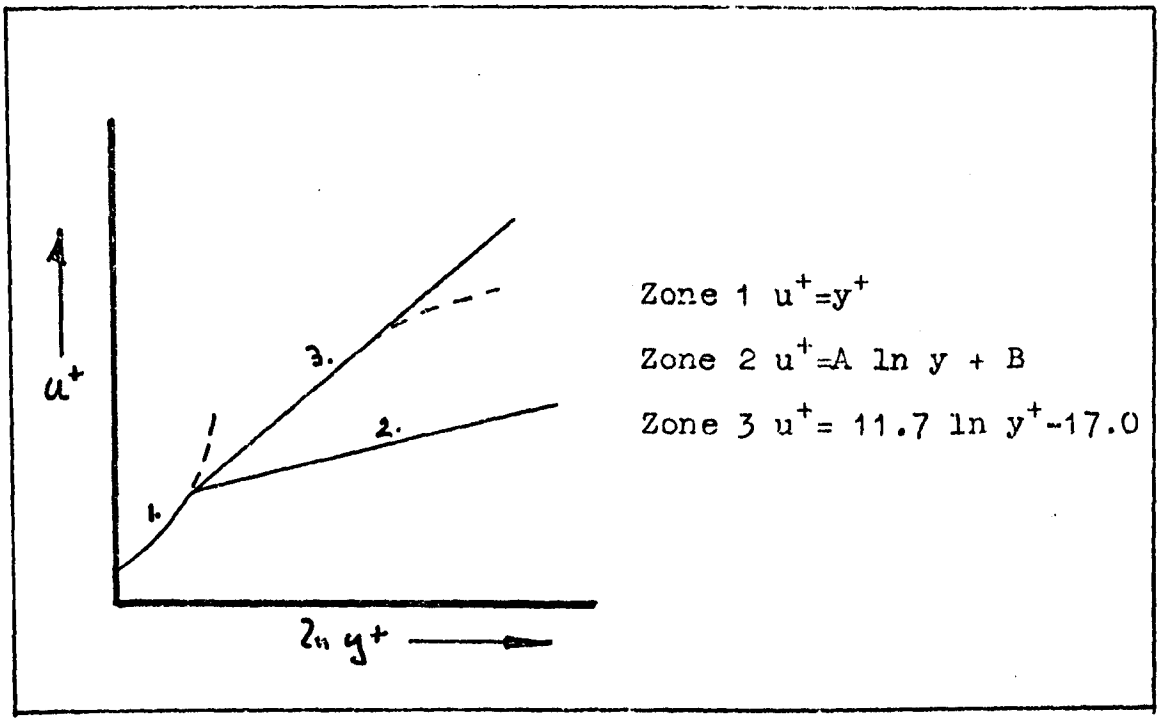

Fig.33 TYPICAL VELOCITY PROFILE WITH POLYMER ADDITIVE

Whilst no velocity profiles have been reported for conditions of maximum drag reduction*, some profiles under very high but less than the maximum have been published, for example those by Goren and Norbury (61), and their form is sketched as a dotted line on fig.33

This prompted Virk et.al. (59) to propose a three zone model 1-3-4 for the universal velocity profile, Fig.34. For zero drag reduction this is identical to the Prandtl model, and as drag reduction increases the core zone 4 diminishes in size until the asymptote zone 3 reaches the pipe axis.

* (But see Section 2.7.0 of this thesis)

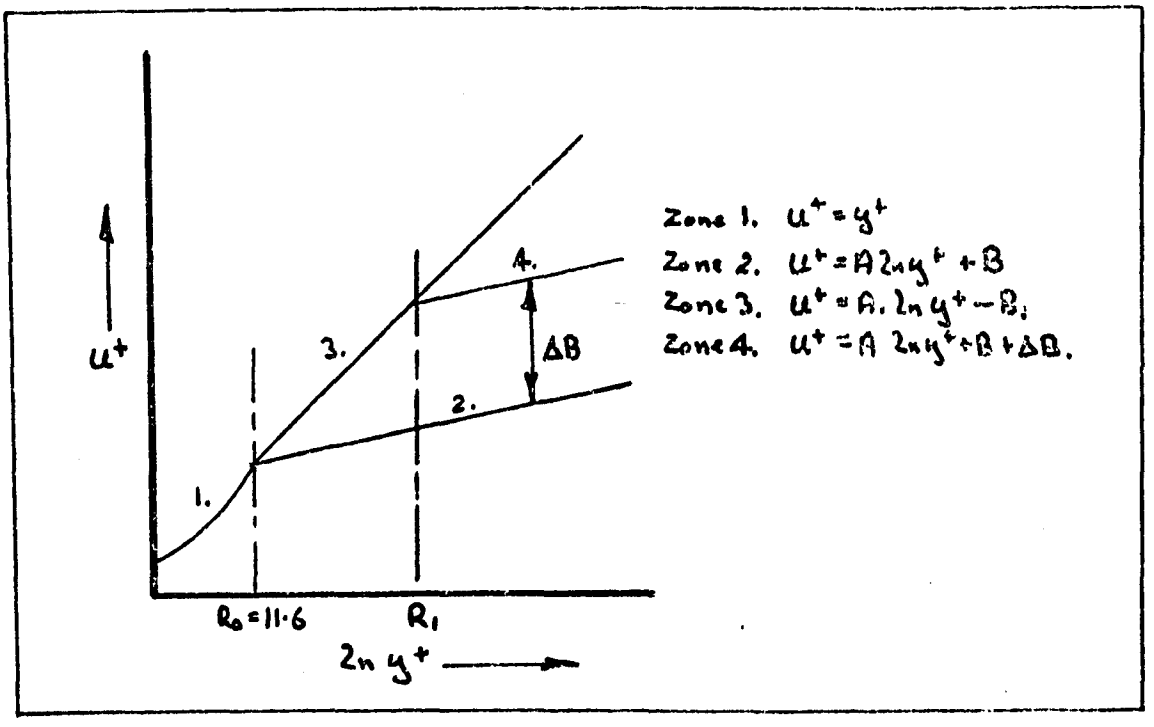

Fig.34 THREE ZONE VELOCITY PROFILE MODEL FOR DILUTE POLYMER SOLUTIONS IN TURBULENT FLOW

The three zone model may be integrated across the pipe radius to give a relationship for the friction factor, and this results in the following expression, see appendix 2:-

$$1/\sqrt{f} = 1.768 \ln Re\sqrt{f} - 16.51 + 6.5 \ln R_1 + 268.1/Re\sqrt{f} - 9.2R_1/Re\sqrt{f}$$

From a knowledge of friction factor and Reynolds number we may hence evaluate the corresponding values of R_1. These calculations have been carried through for many of the preceeding results with Guar gum, Separan and Polyox solutions. Since the calculation procedure involved an iteration process a digital computer was used.

Values for the wall layer thickness, R_1 calculated from the present Guar gum results are shown in figs.35 to 37. Despite some data scatter, for the low concentrations it seems that R_1 may be described by an expression of the form:-

$$R_1 = 11.6 + \ln(\tau_w/\tau_{w(onset)}) \times \text{const.}$$

where the proportionality constant depends on the solution concentration. This is basically similar to expressions proposed by Ernst (60) and Elata et.al. (57), for the two zone velocity profile model.

With the 480 p.p.m. solution there does seem to be a small but significant diameter effect, the value of R_1 for a given wall shear stress being slightly higher for the larger diameter pipes.

It is of interest to compare fig.37 with fig.32 which shows corresponding values of the sublayer thickness R_0' based on the two zone model. The diameter effect appears to be about the same in both figures, but the three zone model indicates nearly twice the wall layer thickness compared with the two zone model predictions.

Fig.38 presents results for R_1 based on the data by Elata et.al. (57) for three concentrations of Guar gum solution. Once again the diameter effect is indistinguishable with the lowest concentrations, and only just apparent with the 800 p.p.m. solution at high values of the wall shear stress.

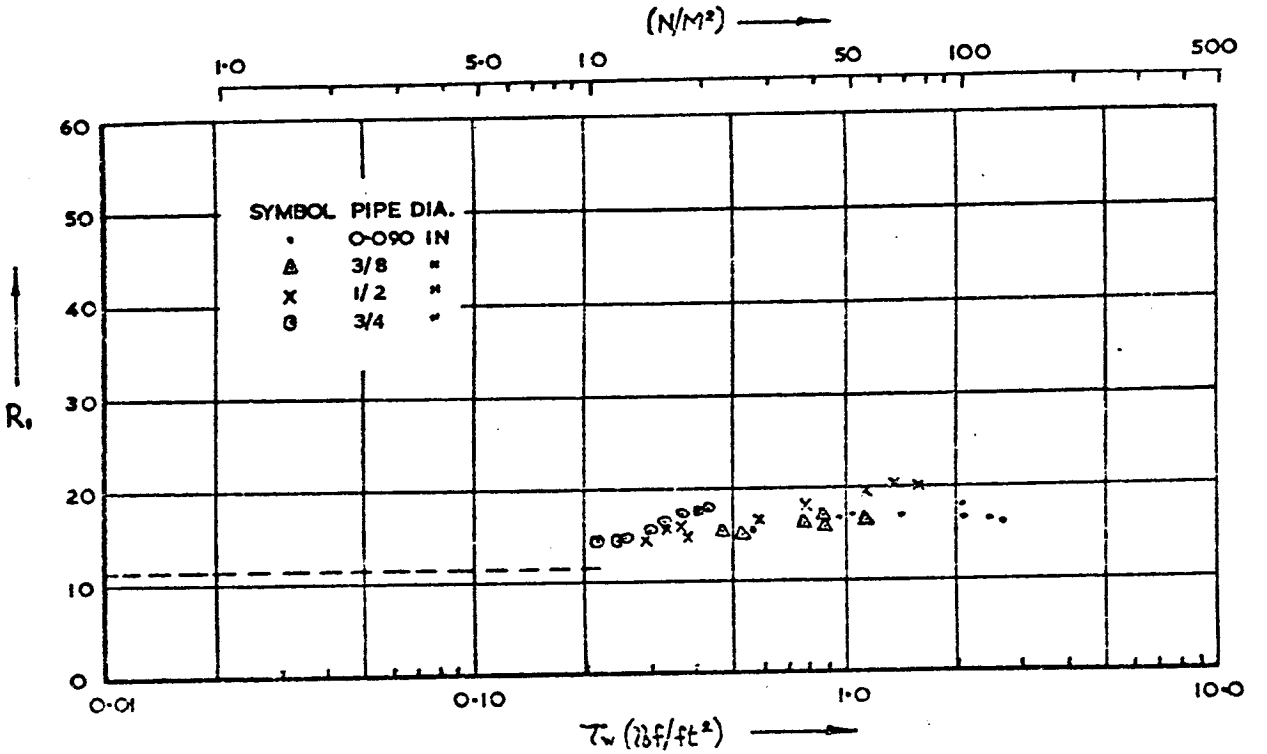

DIMENSIONLESS WALL LAYER THICKNESS 120 p.p.m. GUAR GUM SOLN.

Fig. 35.

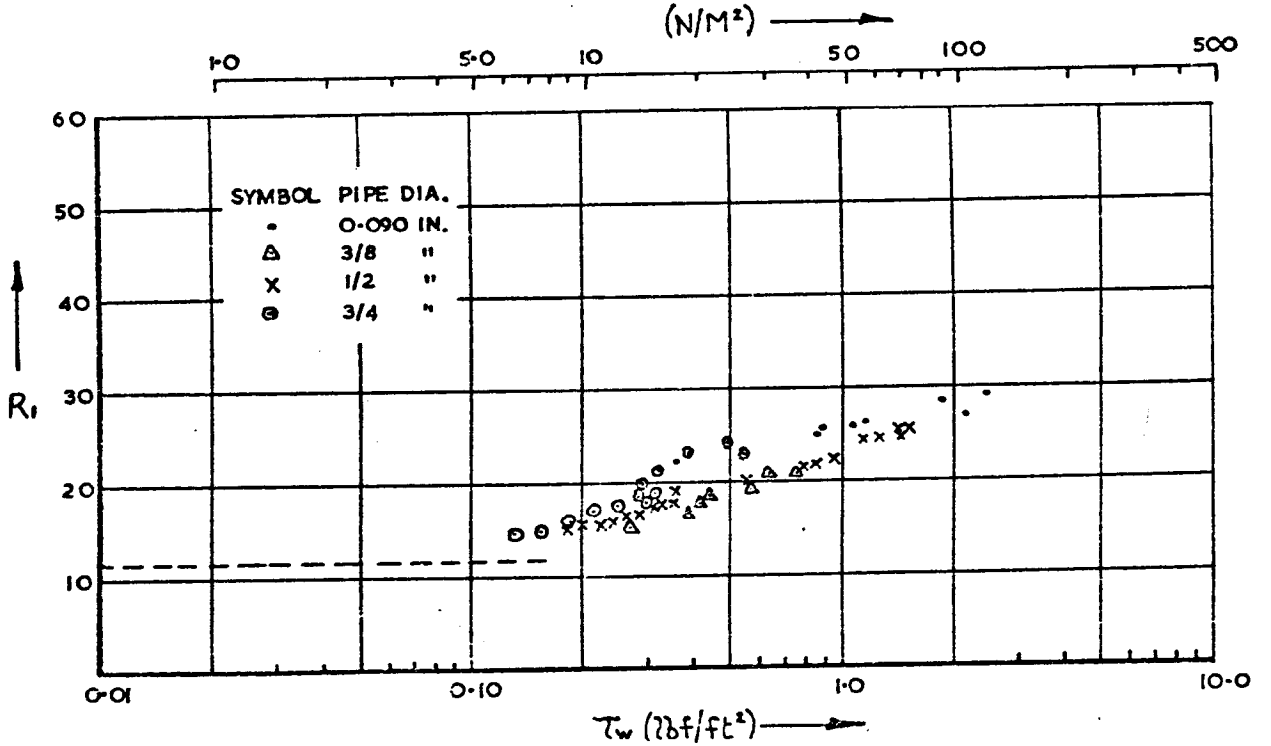

DIMENSIONLESS WALL LAYER THICKNESS.

240 p.p.m. GUAR GUM SOLN.

Fig. 36.

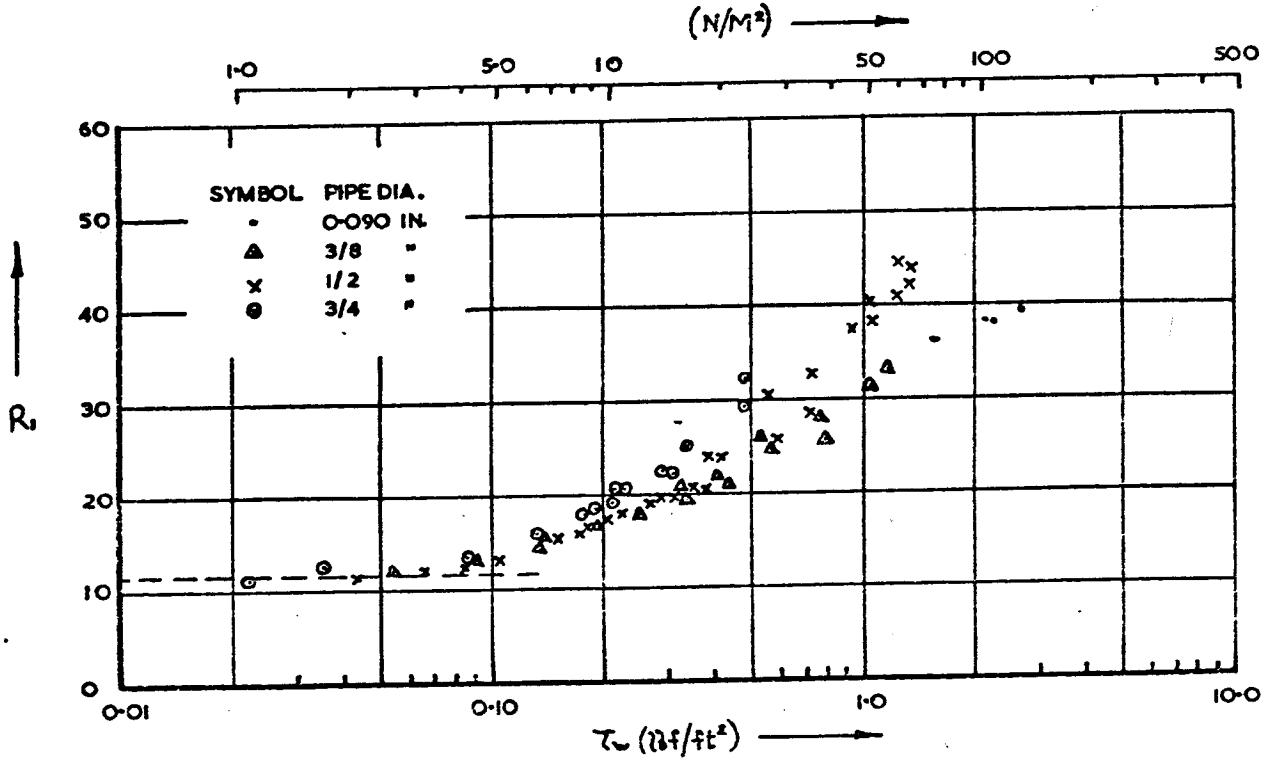

DIMENSIONLESS WALL LAYER THICKNESS.

480 p.p.m. GUAR GUM SOLN.

Fig. 37.

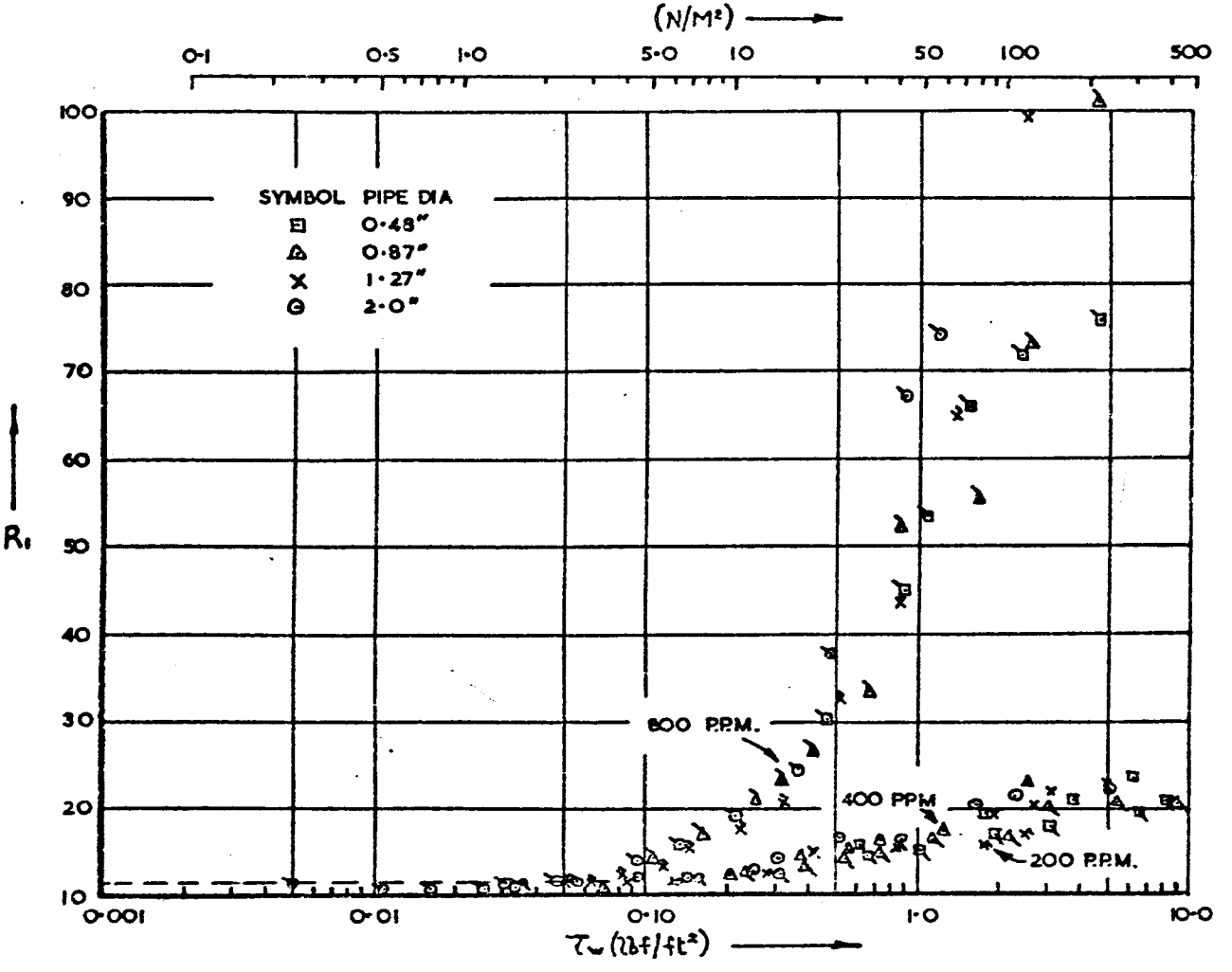

DIMENSIONLESS WALL LAYER THICKNESS WITH GUAR GUM SOLN.

(DATA OF ELATA et.al.)

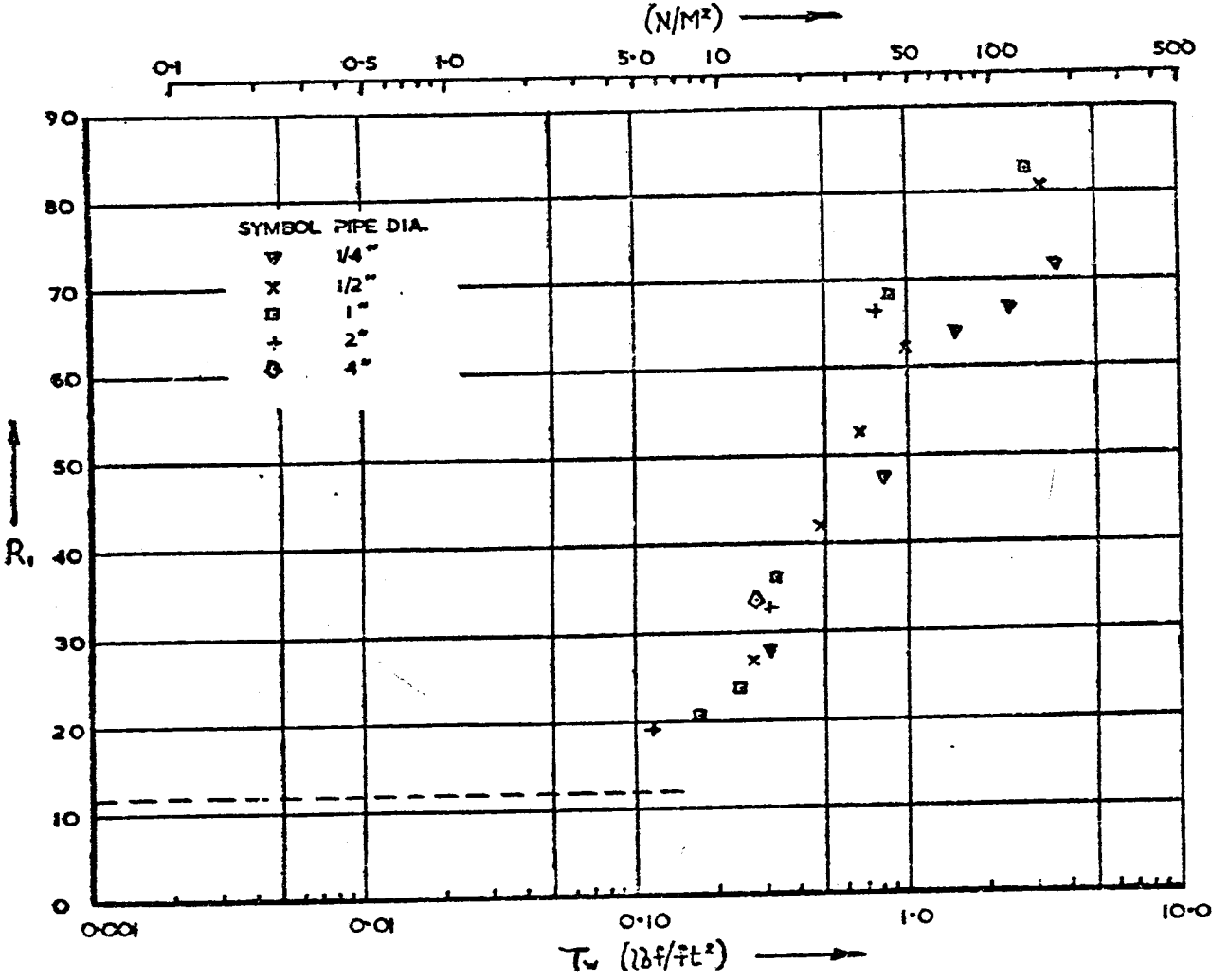

DIMENSIONLESS WALL LAYER THICKNESS FROM DATA CORRELATION.

(See Text.)

Fig. 39.

The results depicted in fig.39 were calculated to provide a compatibility test between the wall shear stress correlations described earlier, and the three zone velocity profile model. These results are determined from the line passing through data for 800 p.p.m. Guar gum solution in fig.16 and random points have been calculated for pipes of different diameter. Again we see very little diameter effect except at high wall shear stress values.

Fig.40 shows results reduced from the pipe friction measurements with 60 p.p.m. Separan solution. Data from the 3/4 in. diameter pipe are somewhat limited, but there is apparently no diameter effect between the 3/4 and 3/8 in. (19.05 and 9.52mm) pipes. It should be noted that the results from the 0.090 in. pipe lie beneath those from the larger ones for two reasons:-

i) Because the polymer is apparently undergoing degradation at the high shear stress levels in this small pipe.

and ii) Because $R_1 \rightarrow R_a$ and R_a in small bore tubes may be below the value of R_1 calculated for larger pipes.

The values for R_a (= Re f/8) are plotted in fig.40 for the small bore pipe.

Results for Polyox solution at concentrations of

2 p.p.m. and 6.6 p.p.m. are shown in fig.41. No diameter effect is seen with the very dilute solution, but for the 6.6. p.p.m. concentration values for R_1 calculated for the 3/4 in. pipe lie below corresponding values determined from 3/8 in. pipe data. It should be noted that this diameter effect is opposite to the trend with Guar gum solutions seen in fig.37 for example. Similar results are seen in fig.42 for 66 p.p.m. Polyox solution. Points from the 0.090 in. (2.38mm) pipe are once again low for the reasons cited above.

It is of interest to compute the actual thickness of the wall layer for various solutions, which may be done by determining the ratio R_1/R_a, which is the ratio of wall layer thickness to the pipe radius. Fig.43 shows results calculated for 480 p.p.m. Guar gum solution in the 1/2 in. (12.7mm) pipe, and these are shown together with an arbitrary Newtonian sublayer thickness based on $R_0 = 11.6$ for comparison. With this solution the wall layer is still relatively thin when compared with corresponding calculations for Polyox solutions shown in figs. 44 to 46. With Polyox at even quite moderate concentrations the wall layer thickness can be considerable compared with the pipe radius. This explains the reduced turbulence found in dye injection studies in small bore pipes reported by Gadd (63). In these experiments R_1 is close to Ra.

'A' — Ra = Re f/8 For 0.090 IN. Pipe.

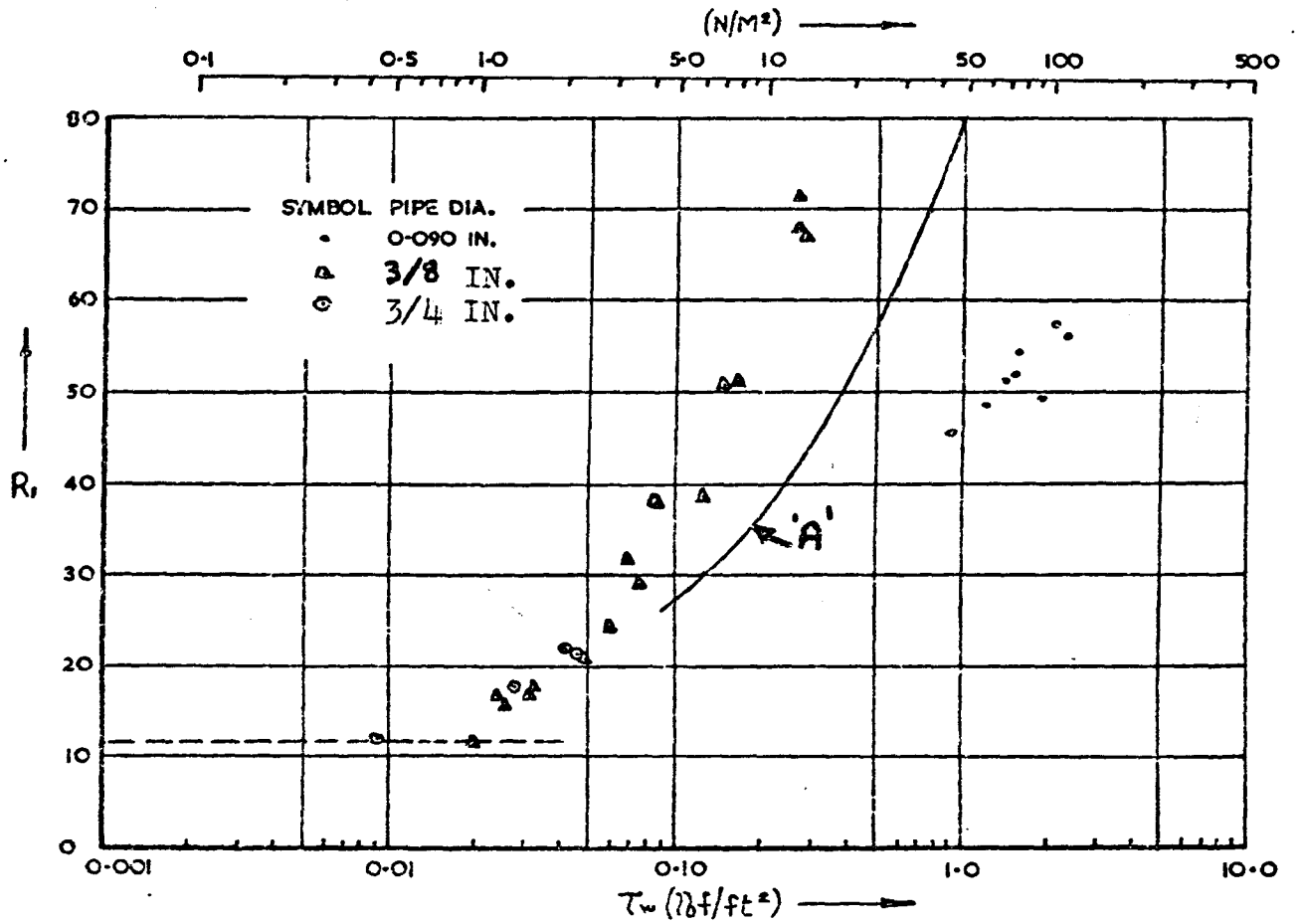

DIMENSIONLESS WALL LAYER THICKNESS.
60 p.p.m. SEPARAN NP10.

Fig. 40.

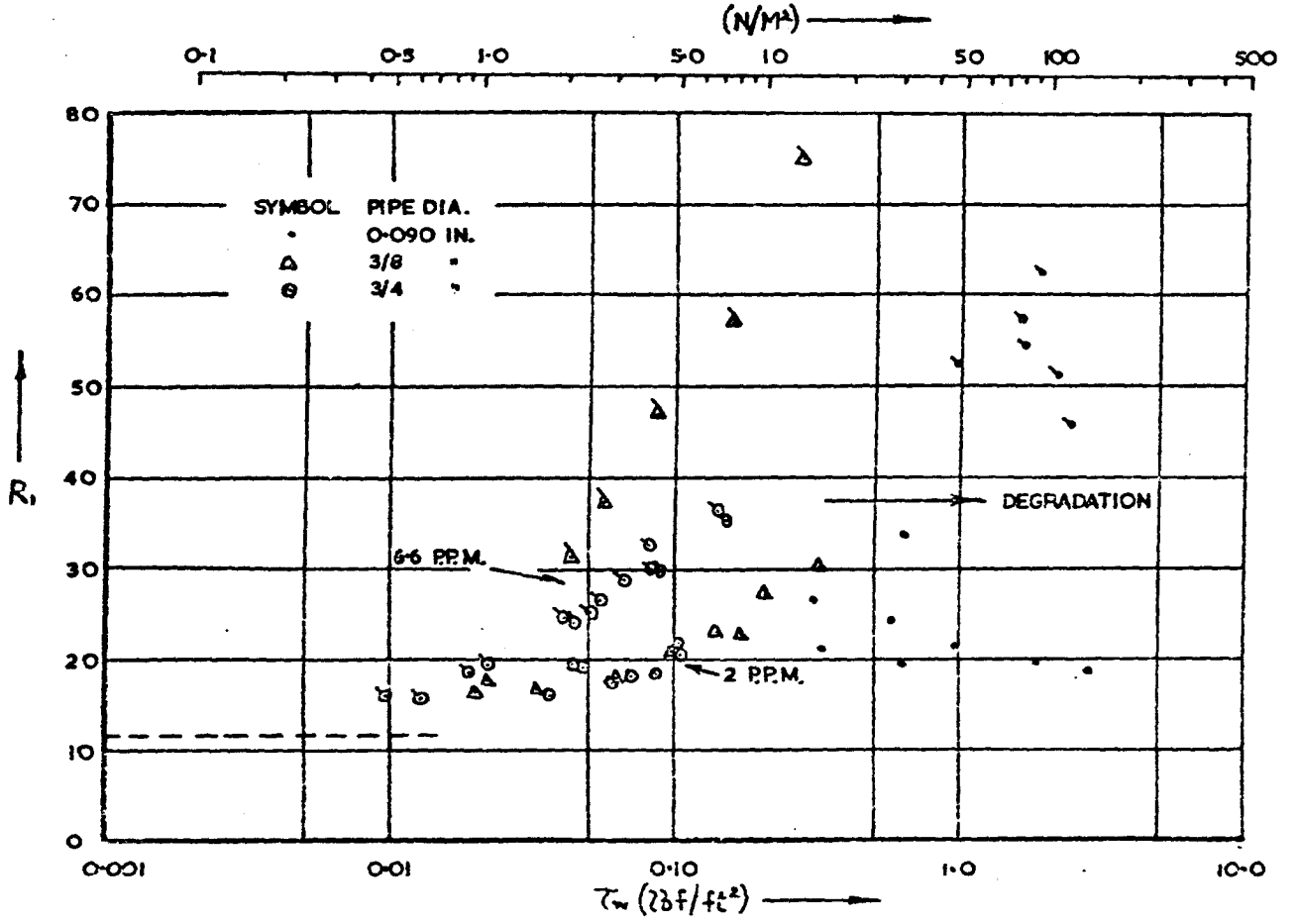

DIMENSIONLESS WALL LAYER THICKNESS.

POLYOX WSR 301 Soln.

Fig. 41.

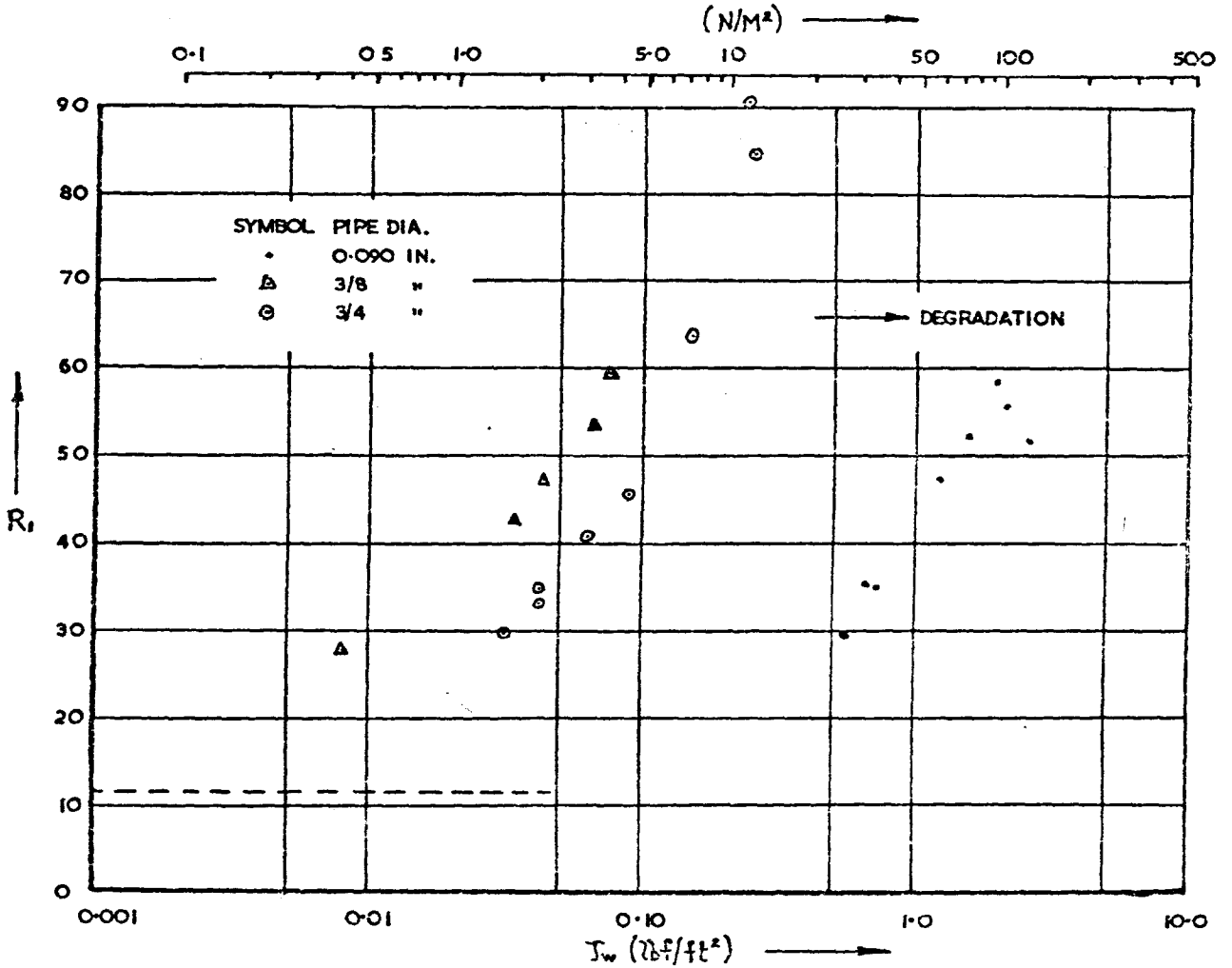

DIMENSIONLESS WALL LAYER THICKNESS.
66 p.p.m. POLYOX WSR 301 SOLN.

Fig. 42.

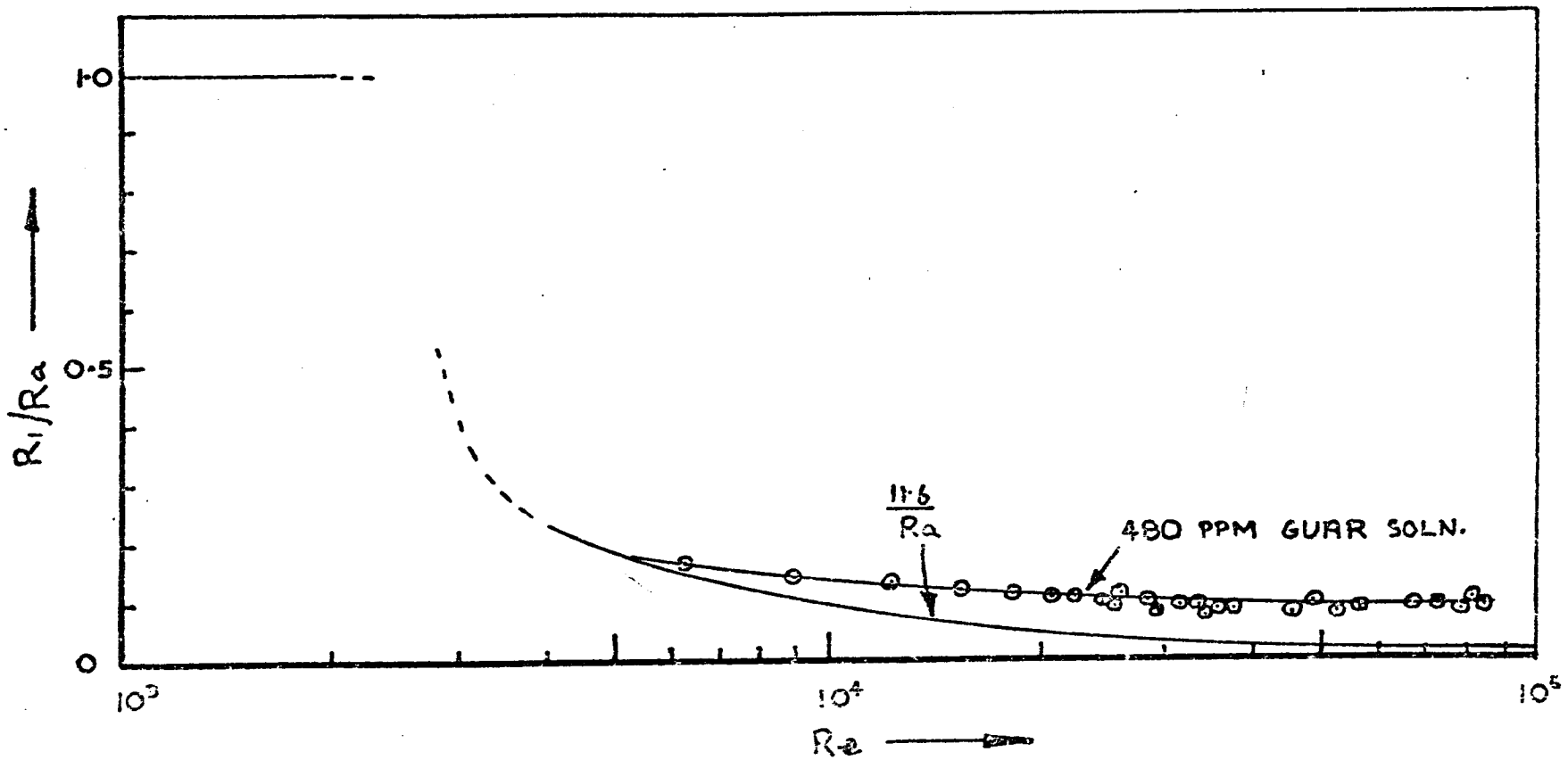

WALL LAYER THICKNESS. PIPE DIA. = 1/2 IN.

Fig. 43.

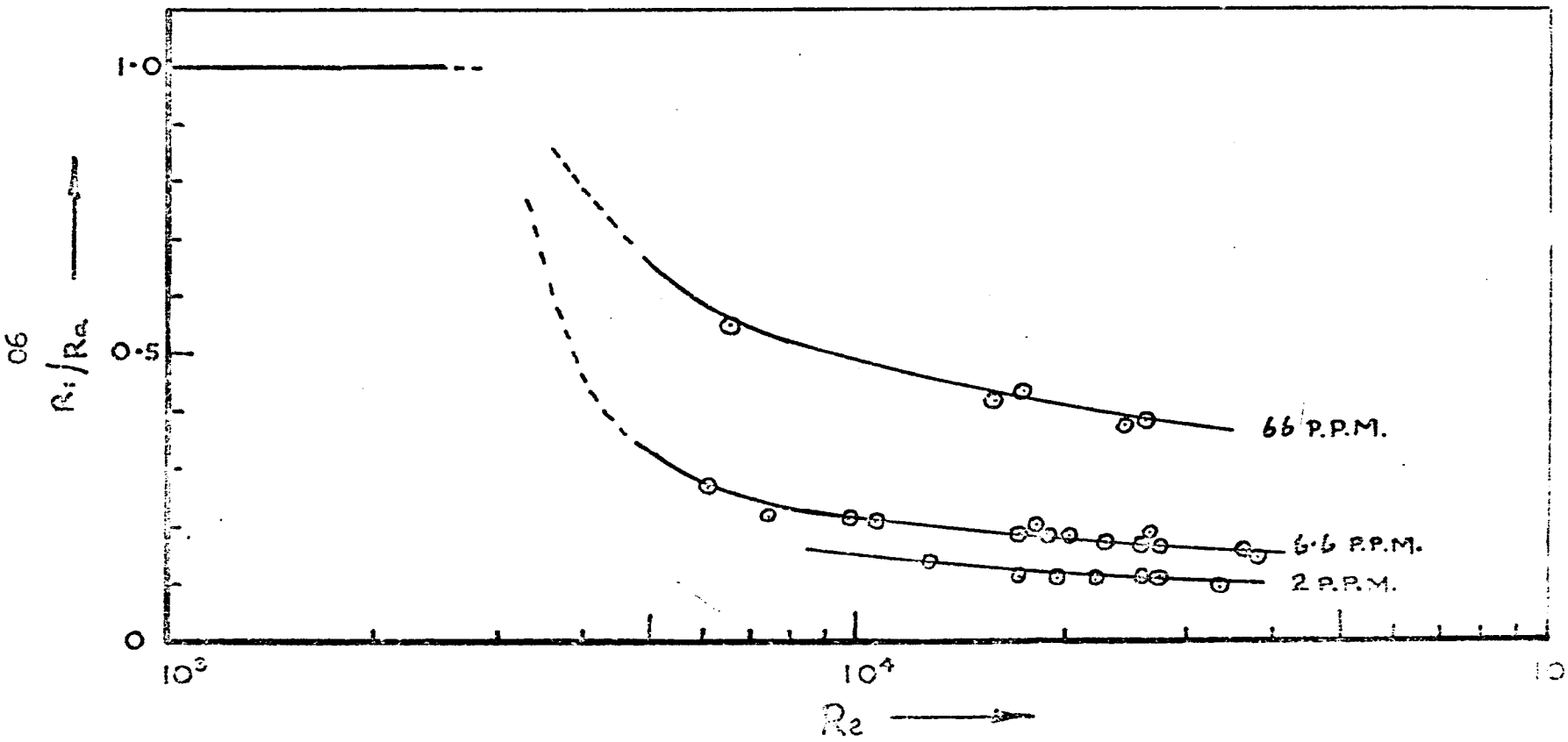

WALL LAYER THICKNESS POLYOX WSR 301 SOLN. 3/4 IN. PIPE.

Fig. 44.

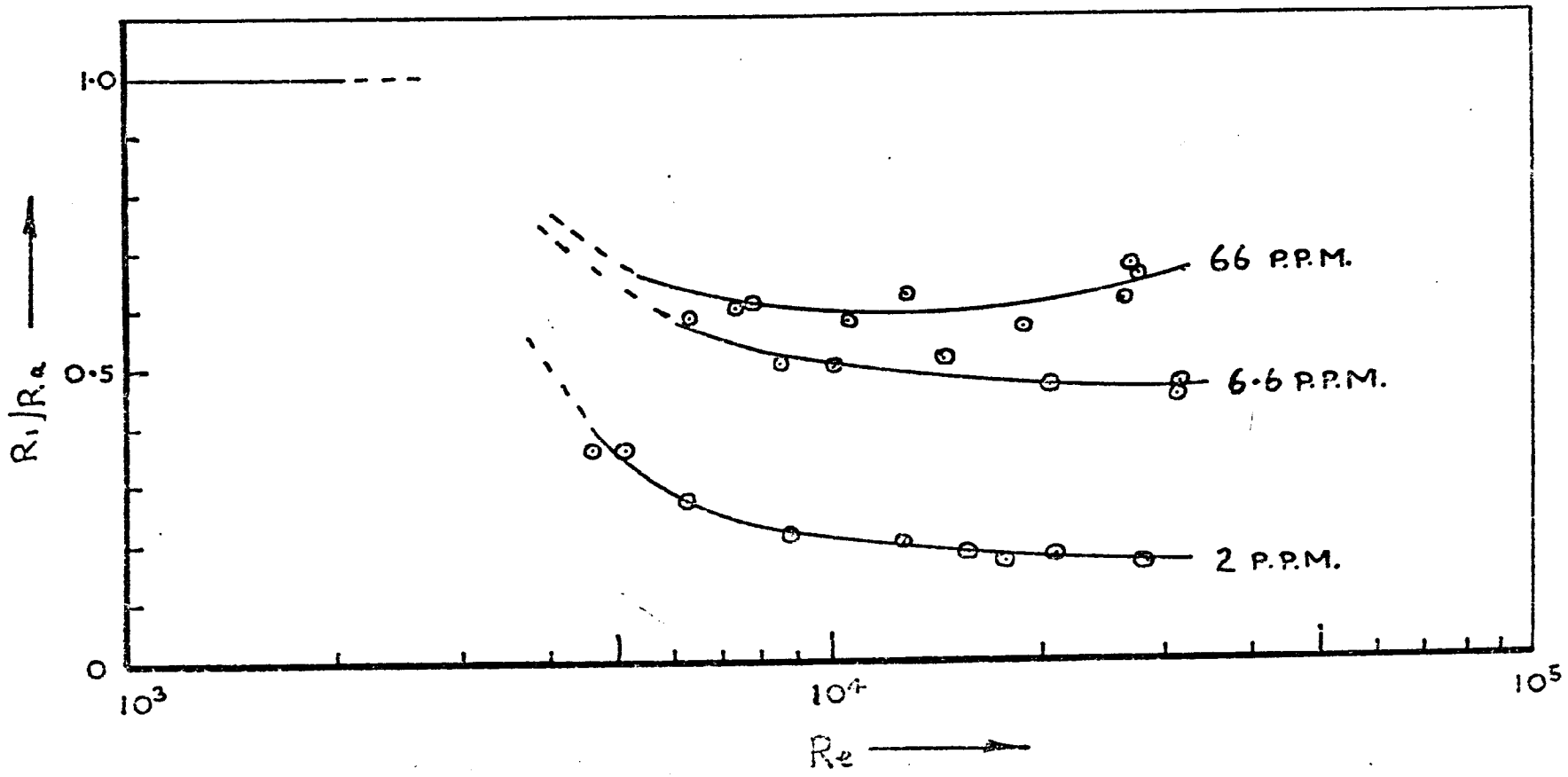

WALL LAYER THICKNESS POLYOX WSR 301 SOLN. 3/8 IN. PIPE.

Fig. 45.

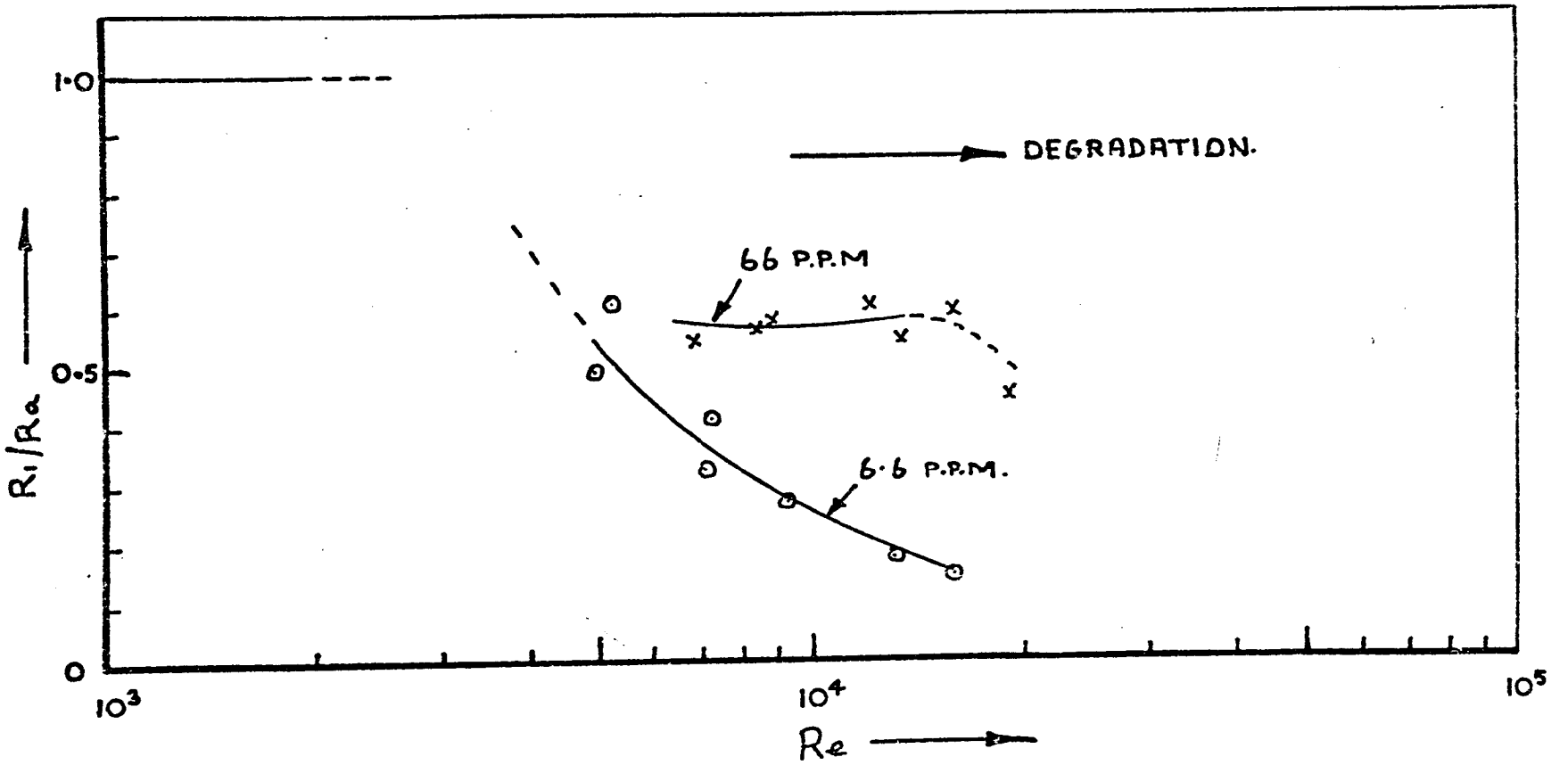

WALL LAYER THICKNESS POLYOX WSR 301 SOLN. 0.090 IN. PIPE.

Fig. 46.

(2.4.0) FLOW OF POLYMER SOLUTIONS IN PIPES WITH EXTREME ROUGHNESS

The evidence presented so far indicates that the skin friction reductions obtained in turbulent flow are related directly to a wall effect in which the polymer molecules somehow react with the turbulence processes in the 'buffer layer' causing increased thickness. In situations well away from the asymptotic condition, the core region well away from the wall seems practically unaffected by the additives since the mixing constant k obtained from the slope of the semi logarithmic velocity profile is apparently unchanged. This is not surprising since large eddies are inertial and unlikely to be affected by additive molecules.

This evidence then would suggest that "free" turbulence in the absence of a wall would be unaffected by dilute solutions of drag reducing additives, but this is not always the case. For example Wu (46) has measured the rate of spread and decay of turbulence created by a paddle which was given a single oscillation in a large tank, and found considerable suppression of free turbulence with Polyox solutions above 25 p.p.m. which was the lowest concentration he used.

Submerged jets provide another means to study the turbulence damping properties of various additives

without the influence of a wall and these sometimes show a very marked and visible reduction of small scale eddies, as is described later in this thesis.

It is possible to produce a flow with the 'wall effect' eliminated, in a rough pipe. Provided that the height of the rugosity is increased so that it extends well beyond the buffer layer into the core zone then the flow behaviour is fully turbulent or wholly inertial, the drag then being directly proportional to the square of the velocity. Observations of this flow can then test whether the turbulence structure is affected by polymer additives merely by comparing the flow resistance with and without the additives.

A suitable rough pipe was manufactured from brass rod which was axially drilled to produce a hole 0.516 in. (13.1mm) in diameter, and then tapped with an extension tap of 5/8 in. Whitworth thread form. This resulted in a slightly truncated thread with 0.055 in. (1.4mm) depth to act as the rough surface - a cross section of which is shown in fig.47. In order to ease manufacture, the pipe was fabricated from 8 in. (203mm) lengths, which were then joined together in axial alignment with collars to produce a rough section 4 ft. (1.22mm) long. Smooth entry and exit sections were provided, the bores of which were the same as the core of the threaded pipe. The entry length was 4 ft (1.22mm), and static pressure tappings were provided

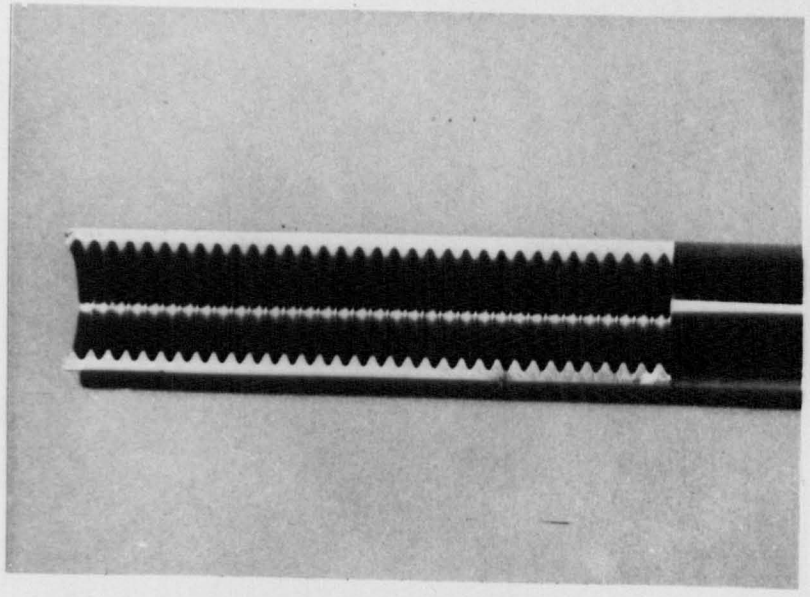

CROSS SECTION OF THREADED PIPE

Fig. 47

2 in. (50.8mm) upstream and downstream from the rough section.

(2.4.1) (a) Tests with Guar gum solution.

The rough pipe assembly was inserted into the pump-circuit previously described. Pressure loss measurements were recorded over a wide range of flow rate for both water and dilute Guar gum solution in various concentrations, and the results of these tests are shown in fig.48. The mean flow velocity and Reynolds number have been based on the core diameter of the threaded pipe. Flow characteristics of this polymer in a 1/2 in. (12.7mm) diameter smooth pipe are also shown in fig.44 for comparison.

It can be seen from fig.48 that Guar gum molecules have only a slight effect on the pressure drop along the rough pipe up to a concentration of 480 p.p.m. which was the highest used, although an enormous drag reduction was observed with the smooth pipe. In fact very slight INCREASES of drag are discernable for these solutions which could imply some very small change in the turbulence structure.

(b) Tests with Polyox solution.

Some pressure loss measurements have also been carried out for the flow of Polyox WSR 301 solutions along the rough pipe. Since this polymer is very susceptible to

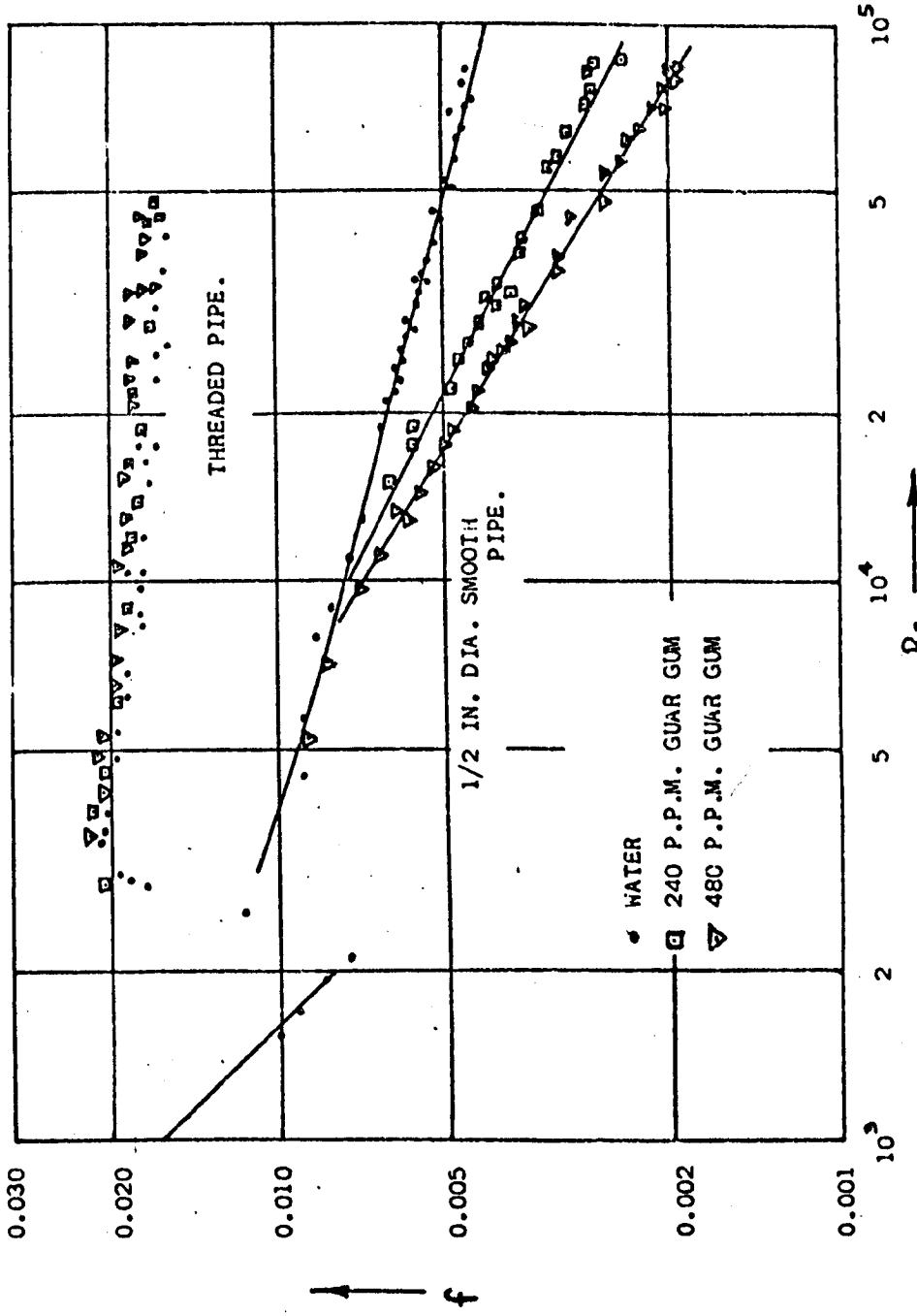

Effect of Extreme Roughness with Guar Gum Solution

Fig. 48.

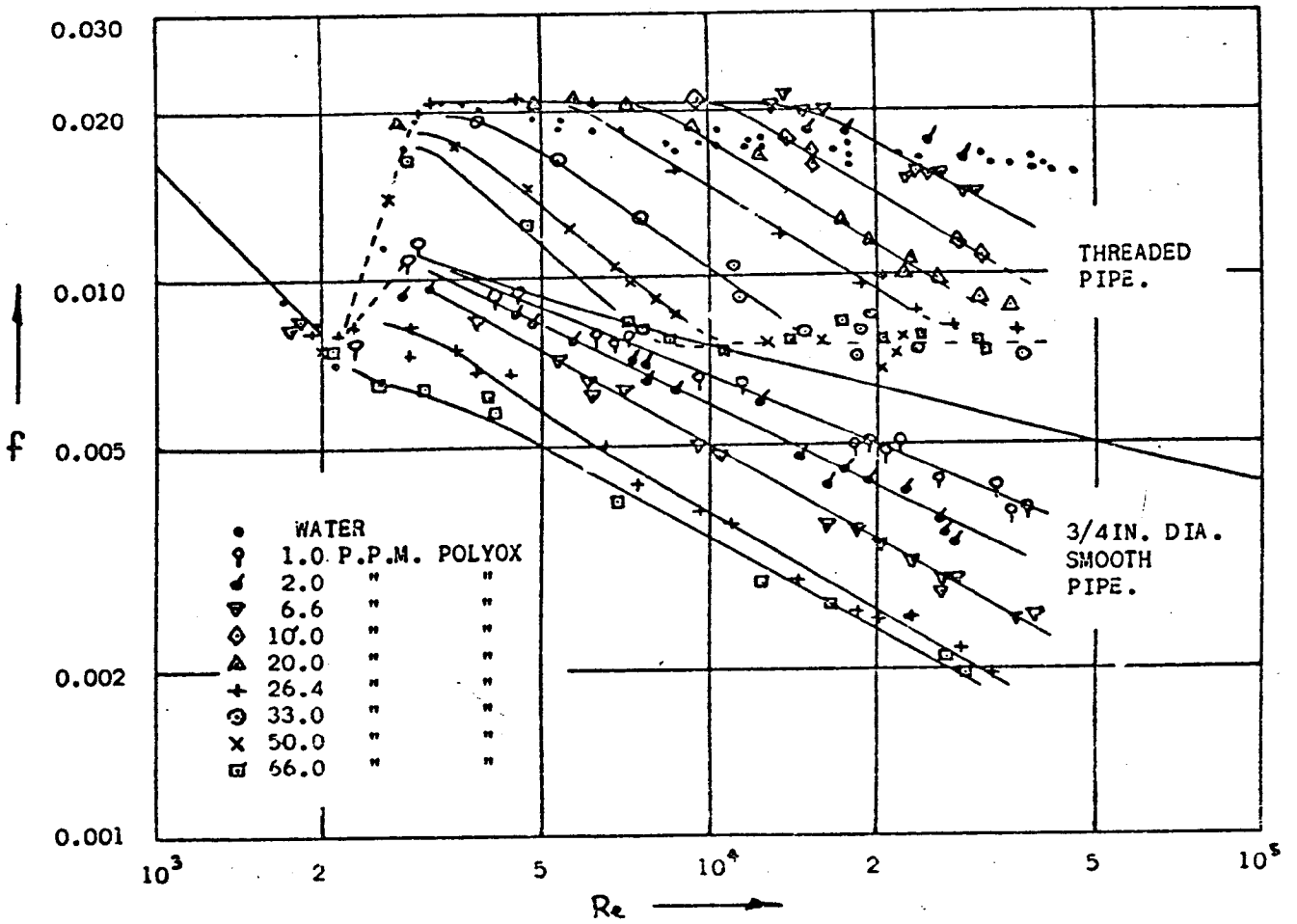

Effect of Extreme Roughness with Freshly Mixed Polyox WSR 301 Solution

Fig. 49.

mechanical degradation, a once-through method of testing was adopted, the pipe being supplied with fluid from a header tank.

Preliminary tests showed considerable scatter - much more than could be accounted for by errors of experimental measurement. The pressure loss characteristics appeared to depend somewhat on the pre-history of the polymer solution and it was only by adhering rigidly to the standard mixing procedure previously described, that any degree of repeatability could be obtained.

The results of the experiments are shown in fig.49 and despite the scatter some clear and rather unexpected trends are discernable. It is seen that the Polyox additive can result in a drag reduction for all except the very lowest concentrations. This increases with both concentration and Reynolds number and is clearly due to wall layer thickening which has previously been demonstrated to be very much greater with Polyox solution than with Guar gum. In the drag reduced zones on the friction factor chart, the wall roughness height is certainly not great enough to ensure a fully inertial flow.

It must be stated that these rough pipe experiments were carried out with a different batch of Polyox to the previously described smooth pipe tests and the comparative smooth pipe results shown in fig.49. This latter batch was more effective as a drag reducer and produced

even greater increases in the wall layer thickness. This is seen by comparing the 'fresh' results in fig.54 with those in figs.44 and 45. With this newer batch the wall layer increases very rapidly at the higher values of wall shear stress or Reynolds number, and the onset of drag reduction occurs when the wall layer overcomes the wall roughness. This takes place at lower Reynolds numbers with increasing concentration.

Below the onset of drag reduction we have a fully inertial flow and in this region the drag is seen to be considerably increased, very much more so than with the Guar gum solutions. Once again this would indicate a change of the core region turbulence structure. Drag increases have also been reported by Kalashnikov et.al. (64), (65) in a fully rough couette flow experiment.

These results were first published by the author some time ago, before the extent of wall layer thickness was fully appreciated, and the tentative explanations for drag reduction in the rough pipe discussed in refs. (P.4) and (P.10)* are now considered suspect.

* (See publications at end of this thesis).

(2.5.0) THE EFFECT OF AGING ON DRAG REDUCTION WITH DILUTE POLYOX SOLUTIONS

Brennen and Gadd (66) found differences between the properties of freshly mixed solutions and those which had been stored for some time. They found that detectable elastic effects (normal stress differences) disappeared after storing dilute solutions for several days although drag reduction measured in a rotating cylinder device was hardly affected. Very small changes were also observed in the viscosities of these solutions. Differences in the behaviour between freshly mixed and aged solutions have been found in connection with the drag of spheres and wall attachment experiments - these are discussed later in this thesis.

In view of this it was decided to repeat some of the previous pipe flow experiments, this time using aged solutions. Flow resistance tests were carried out in three pipe sizes, 1/4 in. (6.35mm), 1/2 in. (12.7mm) diameter and the threaded pipe, using the once-through method of testing, the pipes being fed from an 80 gallon (350 litre) fibre-glass tank situated in the roof of the laboratory. Larger pipes could not be used because of the limited capacity of the header tank.

Fig.50 shows results obtained with a 30 p.p.m. solution of Polyox WSR 301 which had been stored for seven days in the roof tank prior to conducting the tests.

During storage the tank was completely covered with a black cloth since it is known that sunlight can bring about degradation of the polymer (7).

Fig.51 shows results from a freshly mixed solution using the same batch of polymer, for comparison purposes.

Fig.52 shows these results in the form of the wall shear stress correlation. It is clearly seen that aging has considerably increased the threshold wall shear stress below which no drag reduction occurs, and furthermore there is no detectable diameter effect in this plot, since results with the aged solution in the 1/4 in. (6.35mm) and 1/2 in. (12.7mm) pipes lie on a unique line. It is interesting to note that the slopes of the lines in fig.52 for both fresh and aged solutions are roughly parallel.

Values of the wall layer thickness (R_1) using the three zone velocity profile model have been calculated from these pipe friction measurements and are depicted in fig.53. We see that the wall layer is very much thinner with the aged solution than with the freshly mixed one, and we also see that there appears to be a unique relationship between R_1 and τ_w for the aged solution with no detectable diameter effect.

Differences in the physical thickness of the wall layer between fresh and aged solutions are shown in fig.54

and this can explain the drag reduction found in the rough pipe only with the freshly mixed solutions. The aged solution caused a drag increase in the rough bore pipe but only for Reynolds numbers above about 10^4.

These aging effects can be brought about artificially by prolonged gentle mixing (66) and we apparently have the paradoxical situation that if the solutions are mixed too perfectly then we may achieve reduced drag reduction.

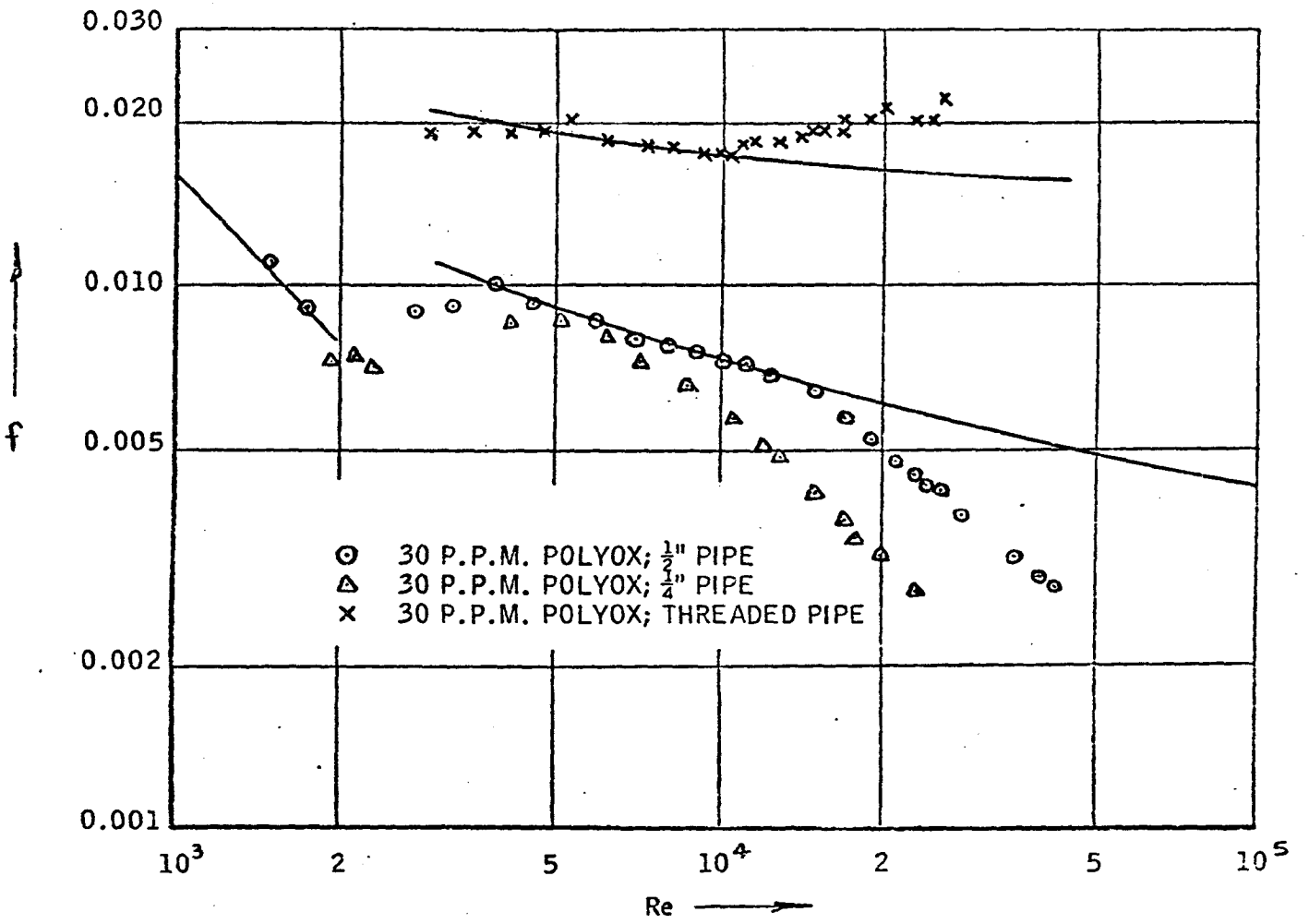

PIPE FLOW CHARACTERISTICS - POLYOX W.S.R.301 (AGED FOR 7 DAYS).

Fig. 50.

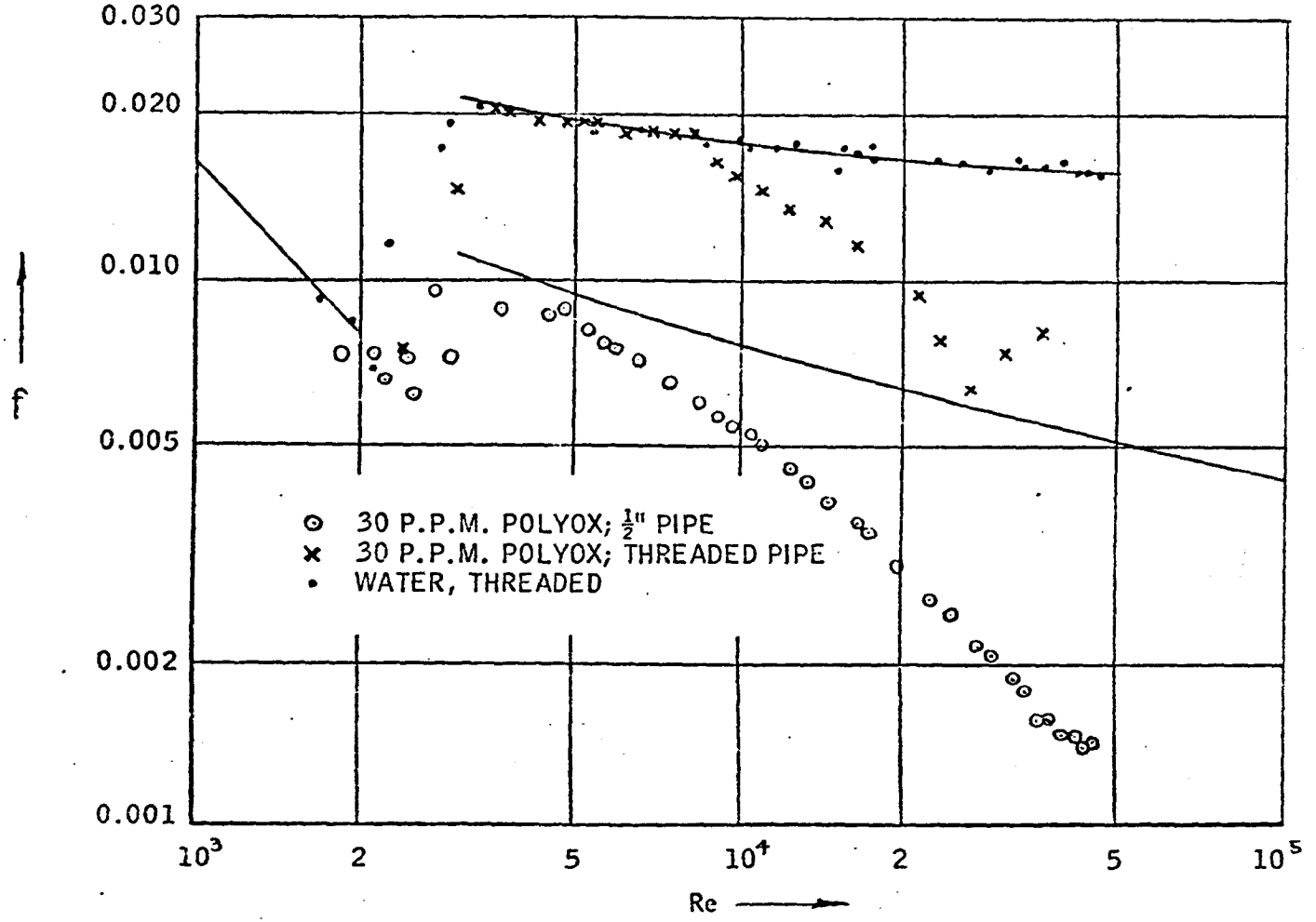

PIPE FLOW CHARACTERISTICS - POLYOX W.S.R.301 (FRESHLY MIXED).

Fig. 51.

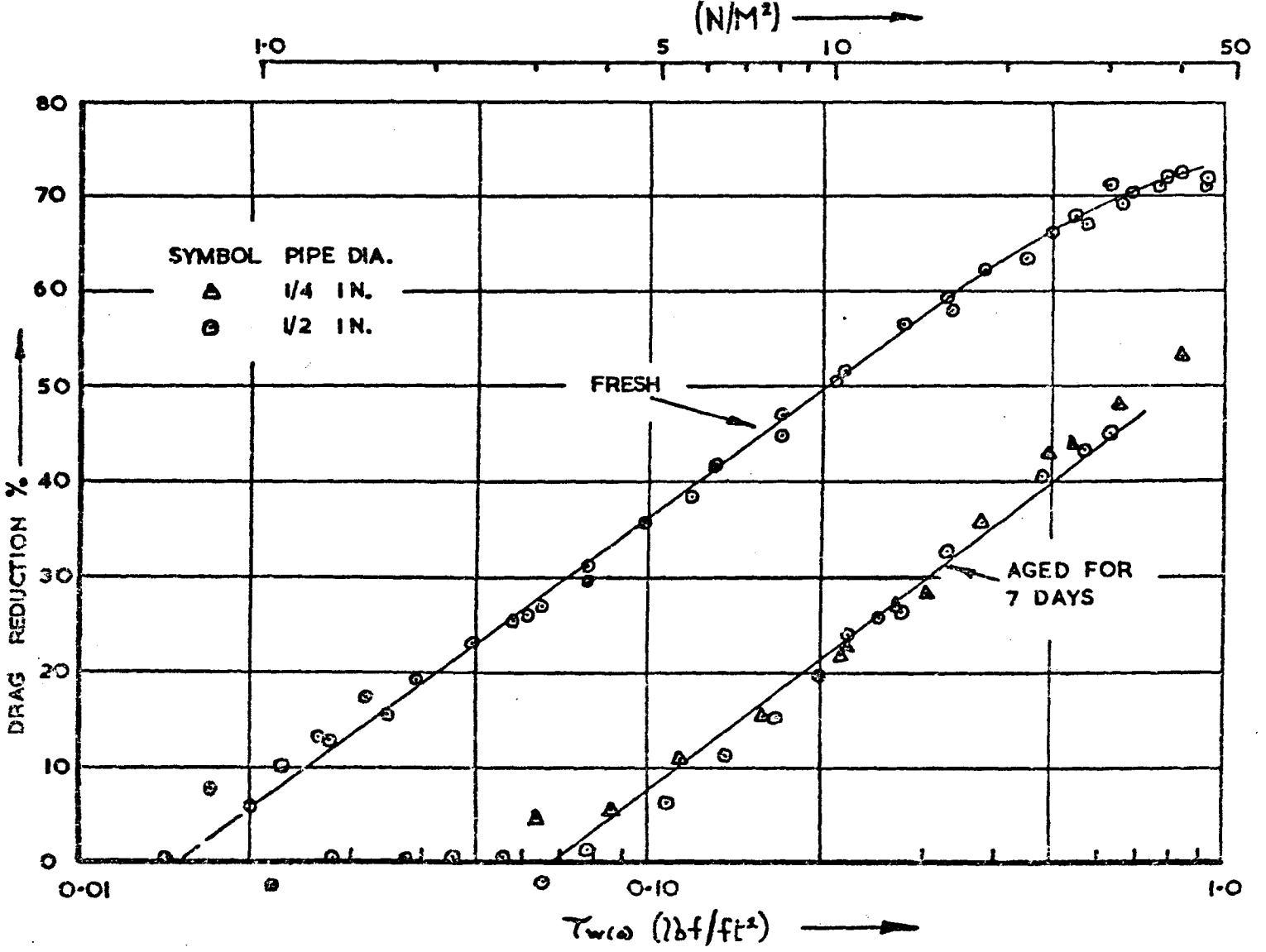

PIPE FRICTION REDUCTION POLYOX WSR301 SOLN.

Fig. 52.

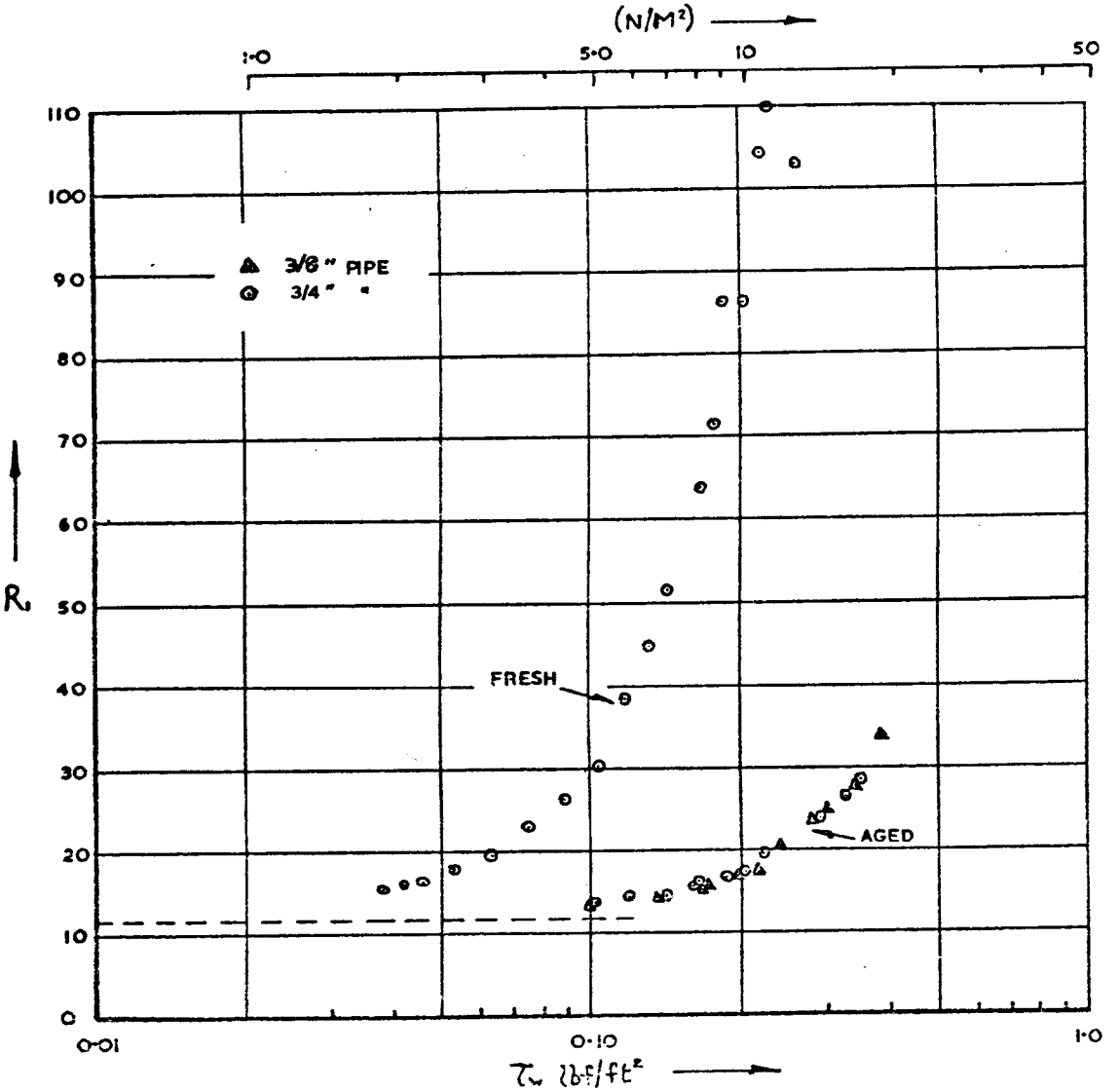

DIMENSIONLESS WALL LAYER THICKNESS POLYOX WSR 301.

Fig. 53.

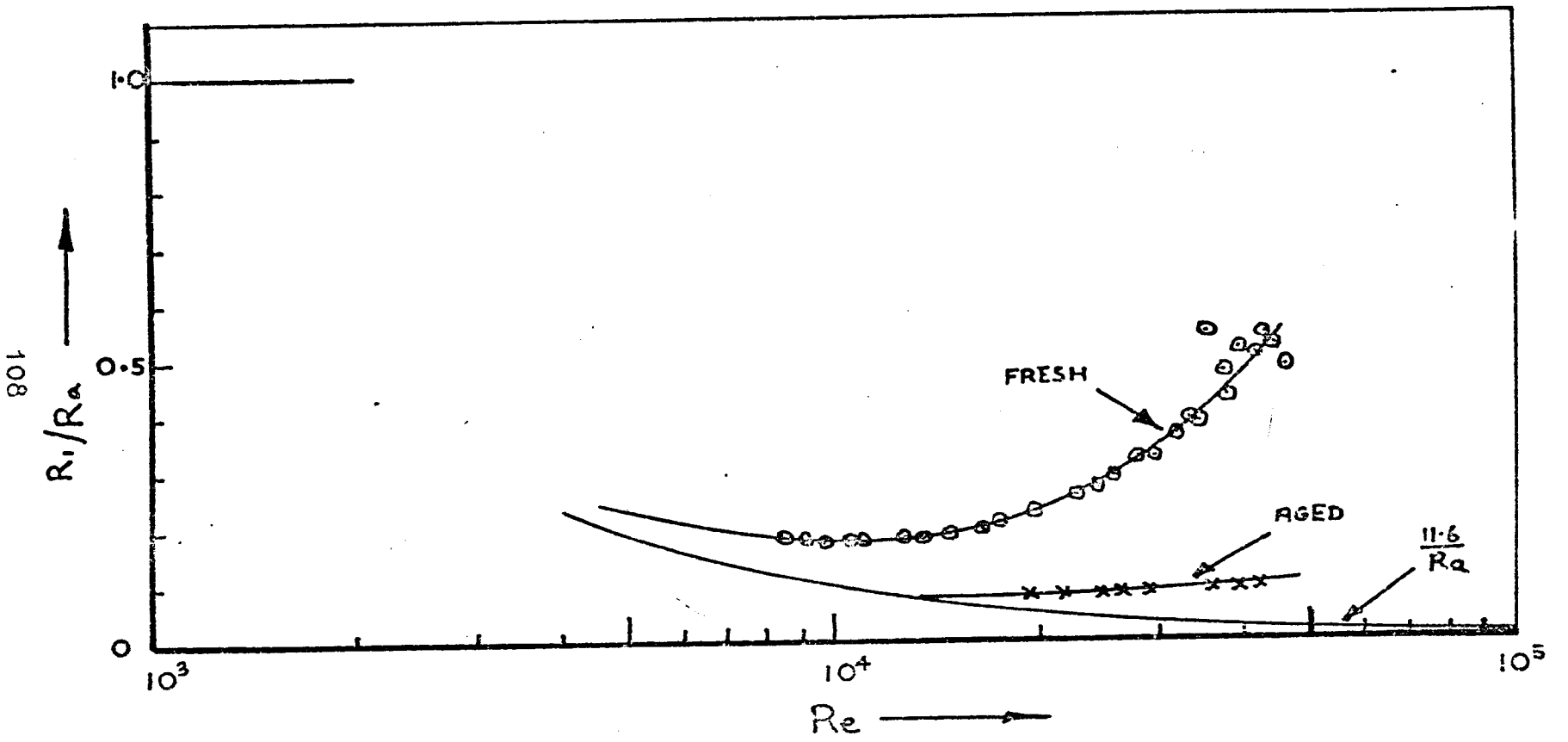

WALL LAYER THICKNESS POLYOX WSR 301 PIPE DIA. 3/4 IN.

Fig. 54.

(2.6.0) DRAG REDUCTION WITH A MICELLAR SOAP SYSTEM.

In connection with some fundamental chemistry experiments, Nash (67) - (69) found that when mixtures of cetyltrimethylammonium bromide (CTAB) and derivatives of naphthalene are dissolved in water, highly viscoelastic gels may be formed. However, the proportions and methods of mixing were fairly critical. When correctly mixed, the additives result in the formation of micelles which strongly affect the properties of the solution. It was found that the solution when swirled in a beaker retarded very rapidly, and sometimes after coming to rest, a rotation in the reverse sense was seen.

By using the rotating cylinder apparatus described in ref. (7), Gadd demonstrated that large reductions of frictional drag could be obtained with these additives correctly in solution, and no mechanical degradation was found.

Clearly there were possibilities for practical application of this system, and this led to the comprehensive series of pipe flow experiments described here. The closed circuit pipe flow rig described in fig.7 was used for these tests with additional pipes of 1/4 in. (6.35mm), 1 1/2 in. (38.1mm) dia. and the threaded section which were subsequently added to the apparatus. Equi-molar aqueous solutions of CTAB and 1-naphthol were used for all

the tests since this proportion seemed to be the most effective following the early work by Nash. Pipe friction experiments were carried out with total equi-molar solutions up to 508 p.p.m. concentration, but rheological properties were determined from laminar flow measurements in the 0.090 (2.38mm) in. pipe with higher concentrations.

(2.6.1) Solution Preparation

The solutions were all prepared by first dissolving the weighed quantity of CTAB in water, and then the 1-naphthol which had previously been dissolved in alcohol, was slowly added drop by drop from a burette whilst the solution was circulated around the pipe rig. An insoluble precipitate is formed if the naphthol is added too rapidly.

(2.6.2) Solution Properties.

For shear thinning fluids which obey the Ostwald power law:-

$$\tau_w = K\left(\frac{du}{dy}\right)^n$$

the flow index, n, may be determined from laminar pipe flow results. By making use of the Mooney-Rabinowitsch equation (25) and following the work of Metzner and Reid (26) we can show that:-

$$1/n = \frac{d \ln 8v/d}{d \ln \tau_w}$$

or

$$1/n = \frac{d \ln 8v/d}{d \ln d\,\Delta p/4l}$$

In other words n may be obtained from the slope of logarithmic plots of Δp against the flow rate Q.

Suitable laminar flow measurements were taken in the 0.090 in. pipe which was fed from a small header tank. The derived values for the flow index are shown in fig.55 for equi-molar solutions of CTAB/1-naphthol at various concentrations up to about 2,000 p.p.m. This shows that with concentrations used in the pipe flow experiments (508 p.p.m.), the solutions were Newtonian (n=1), and pseudoplasticity was found only with the higher concentrations. Values for the viscosity of the dilute solutions are given in table 6.

TABLE 6

$\frac{\nu}{\nu}$(water)	Total Conc. (p.p.m)
1.05	122
1.07	254
1.13	381
1.18	508

Approx. relative viscosity of an equimolar solution CTAB/1-naphthol.

(2.6.3) The pipe friction results.

The basic pipe flow results are shown in figs. 56 to 59, and these exhibit some most unusual features. The Reynolds number in all these plots is based on the viscosity of water.

This soap system is seen to be an extremely effective drag reducing agent, and there is no evidence of a threshold stress for the onset of friction reduction and the corresponding diameter effect as is found with the polymeric additives. The reduction of drag terminates at a limiting value of the Reynolds number which depends on pipe size and the concentration of the solution. Above this limiting value the flow tends to behave as an ordinary Newtonian fluid, with the experimental points following the line for the solvent. This effect cannot be ascribed to permanent degradation as is found with polymer additives, since drag reduction was again obtained merely by reducing the flow rate. This limiting Reynolds number effect has also been noted by Savins (70) with another more concentrated soap system.

These results were repeatable over a period of several days, however, degradation eventually occurred as a result of oxidation. This is further discussed later.

The limiting Reynolds number for a given solution concentration corresponds roughly to a fixed value of the wall shear stress irrespective of the pipe diameter. This is shown in figs.61 to 63. Values of the limiting wall shear stress for different concentrations are shown in fig.64.

From the preceeding results it seems likely that the micelles are disrupted at high shear rates and re-unite when the stress is reduced. Now if the termination of drag

reduction above the limiting stress does result from a disruption of the micellar structure then the solution viscosity may well be reduced at these high shear rates. This certainly seems to be the case in figs. 56 to 59. since well above the limiting stress the friction factors correlate along the standard pipe friction line with solution viscosity based on that of water. At low Reynolds numbers the viscosity increase above water is apparent from the mis-match with the Poisieulle flow line. It must be mentioned however that some tests carried out in a capillary tube, in which the limiting stress was exceeded under laminar flow conditions showed no marked change in viscosity. This would indicate that scission of the micelles is not simply an effect of high mean shear but is likely caused by some characteristic of the wall layer turbulence dependent on wall shear stress.

Some friction factor results derived from tests in the rough pipe are shown in figs. 56, 57 and 59 for different concentrations, and once again a limiting Reynolds number effect exists, although at lower values than with a smooth pipe of about the same diameter. At high Reynolds numbers the friction results are indestinguishable from water, but before this region is reached a strange plateau exists which has not been explained at present but is certainly a repeatable effect.

(2.6.4) The effect of solution concentration.

In order to show up the effects of concentration changes, some of the preceding results have been re-plotted in figs. 64 and 66. These show pipe friction results with different concentrations in pipes of 1/2 in. (12.7mm) and 1 1/2 in. (38.1mm) diameter respectively. It is seen that a reduction of concentration causes a decrease in the limiting stress as was previously noted, but has little effect of the drag reduction below this stress until the concentration is reduced below about 200 p.p.m. when drag reduction disappears completely and rather suddenly.

(2.6.5) Correlation of friction data.

If the reduced friction results obtained with these micellar soap systems are compared with polymer additive findings, we see that the soap systems follow the maximum drag reduction asymptote found with the polymers. This is clearly shown in figs.68 to 71. These figures show results only below the limiting stress values, in order to avoid confusion, and the Reynolds numbers in these cases are based on the solution viscosities. It is seen that for the effective concentrations (greater than 200 p.p.m.) the frictional drag is given very closely by Virk's semi-logarithmic asymptote expression:-

$$1/\sqrt{f} = 19 \log_{10}(Re\sqrt{f}) - 32.4$$

This equation holds irrespective of pipe diameter or solution concentration, and would make practical application of these results very simple.

(2.6.6) Temperature effects.

The high drag reductions obtained with these CTAB/1-naphthol solutions together with their resistance to mechanical degradation gives strong possibilities for useful practical applications. This fact was seized upon by Fitzgerald (71), who suggested that there may be an important application in the heating and ventilating field.

In this connection the effect of temperature on these solutions is of practical interest, and some results are shown in figs. 72 and 73. In order to obtain these results both the 1/2 in. diameter, and threaded pipes were lagged with asbestos lagging, together with the associated supply piping. The solution in the sump was heated by a secondary circuit consisting of a tank and electric immersion heater, circulating pump, and a coil of copper tube which was immersed in the main sump. This was preferable to the alternative method of placing the immersion heater directly in the main sump since any local high temperature or boiling around the heater may have caused premature degradation of the test solution.

It is seen from figs.72 and 73 that moderate heating has little effect on the drag reducing properties

of the solution apart from causing a small reduction in the limiting stress value. Between 35 and 40°C, a complete breakdown occurs and above 40°C, the solution is completely ineffective. This is consistent with the observations by Nash (68) during early experiments with this system.

This loss of effectiveness with temperature seems due to a breakdown of the micelle structure, but when the temperature was reduced below 35°C after previous heating, then drag reduction was once again obtained.

(2.6.7) Effect of age of the solution effectiveness.

After conducting these heating tests the same solution was re-tested on the following and successive days, when the solution had cooled to room temperature. Fig.74 shows that when cooled the solution practically regained its initial effectiveness and remained effective for over one week. During this period of time the solution took on a brown colour due to oxidation, and a precipitate slowly formed. After about nine days oxidation rendered the solution completely ineffective.

The lack of thermal stability, and the fact that this soap system degrades with age, reduces the likely field of practical application. Nash* has suggested that other naphthol derivatives may produce solutions which are more stable towards oxidation, and these certainly require further investigation.

*(Nash, T. Private communication).

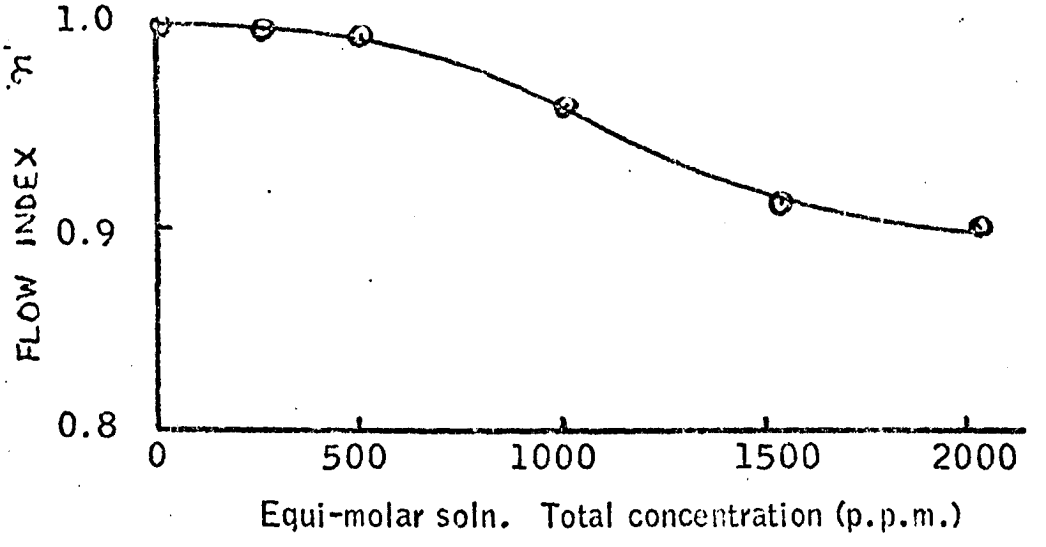

VARIATION OF FLOW INDEX WITH CONCENTRATION FOR CTAB/1-NAPHTHOL SOLN.

Fig. 55.

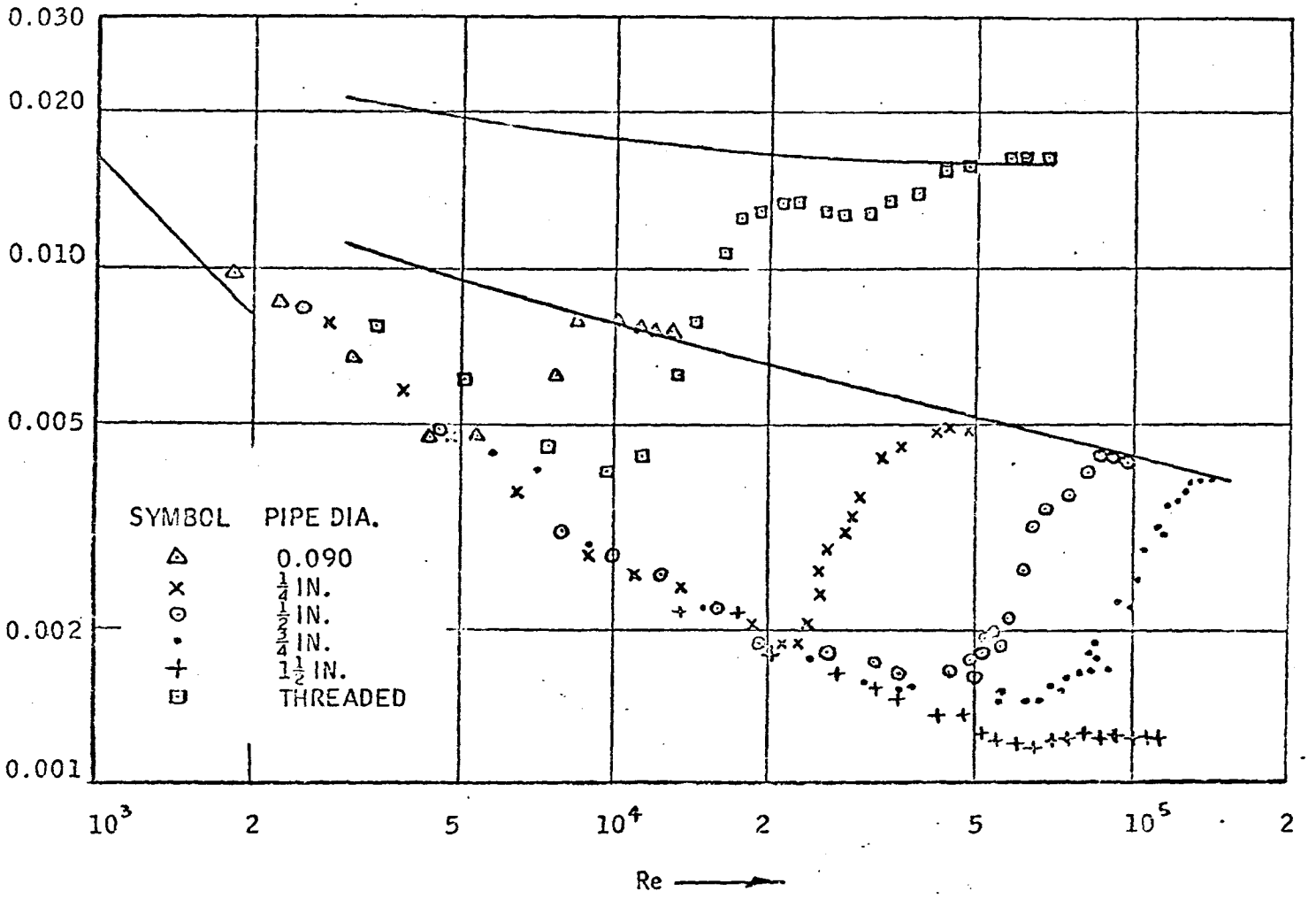

PIPE FRICTION REDUCTION WITH CTAB/1-NAPHTHOL; EQUIMOLAR SOLN.
TOTAL CONC. 508 P.P.M.

Fig. 56

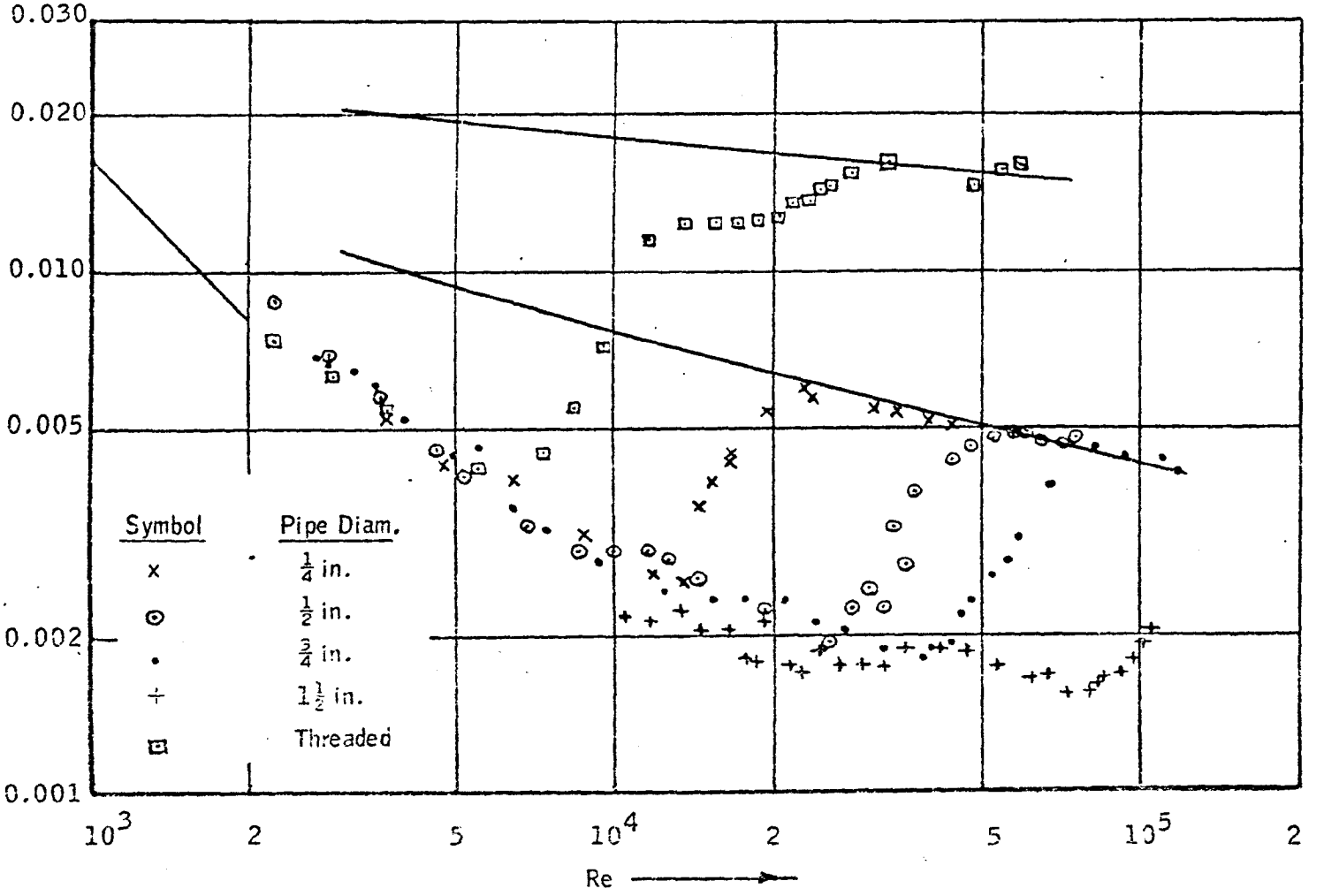

PIPE FRICTION WITH CTAB/1-NAPHTHOL; EQUIMOLAR SOLN.
TOTAL CONCENTRATION 318 P.P.M.

Fig. 57.

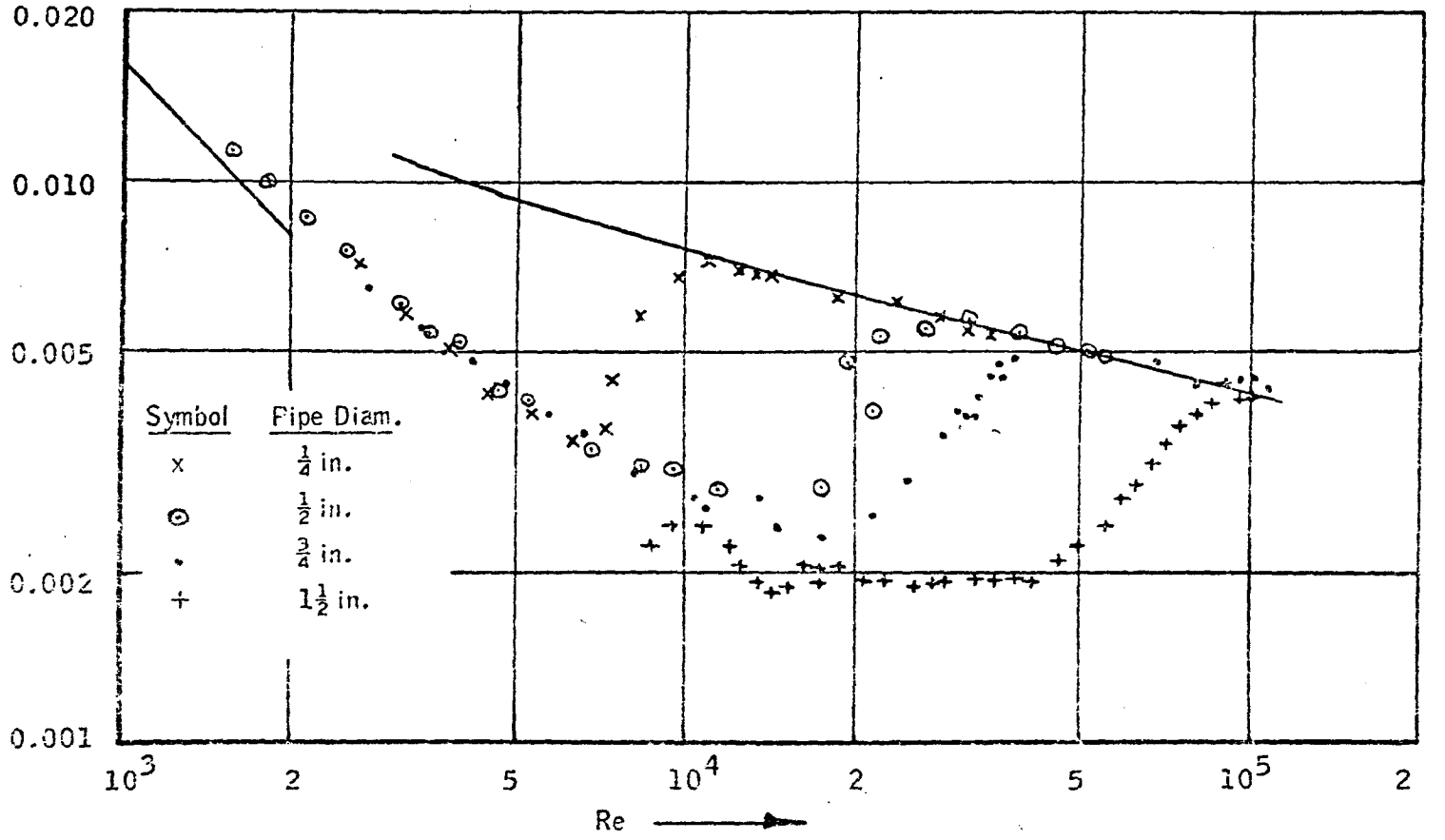

PIPE FRICTION WITH CTAB/1-NAPHTHOL; EQUIMOLAR SOLN.
TOTAL CONC. 250 P.P.M.

Fig. 50.

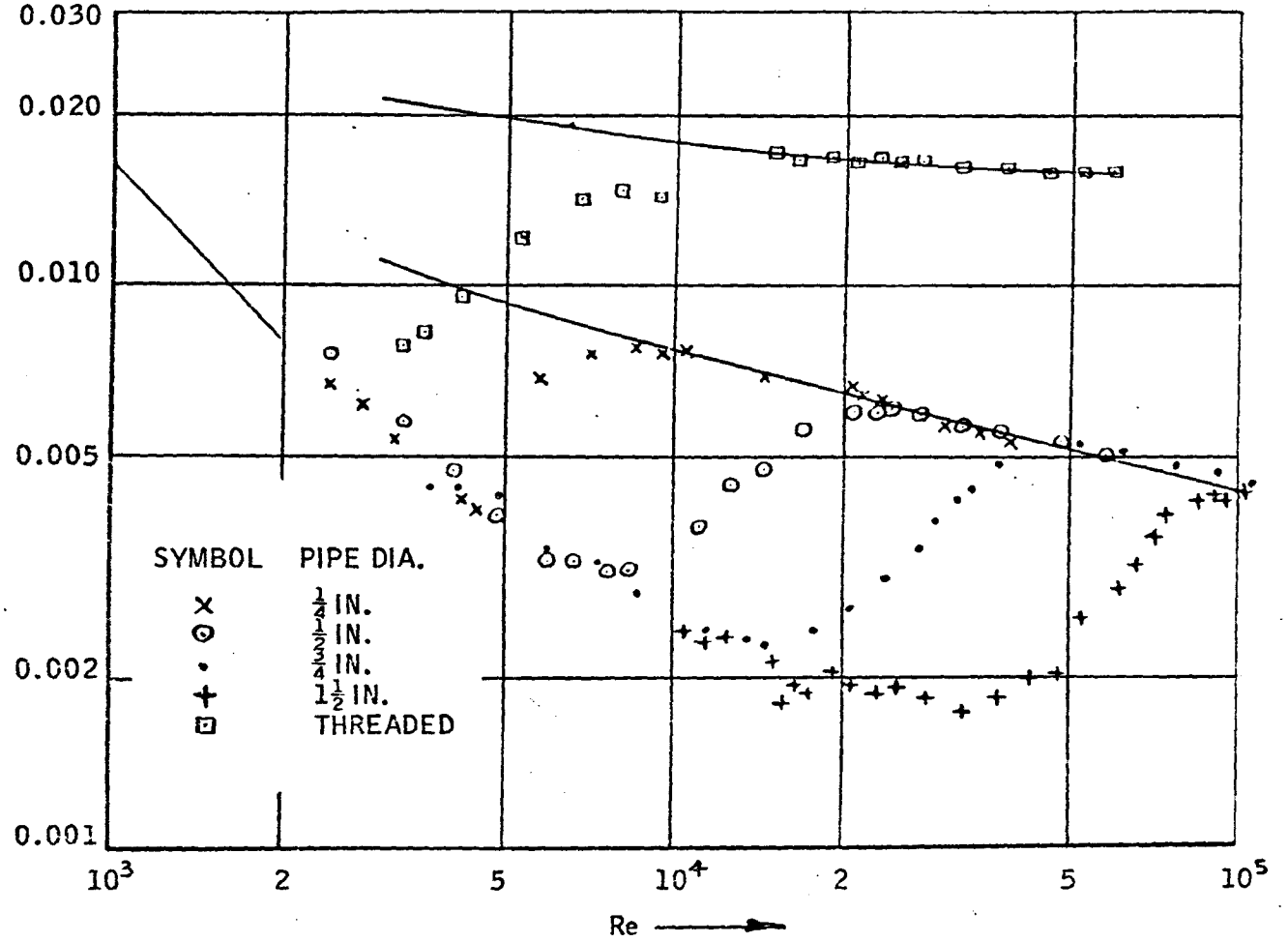

PIPE FRICTION WITH CTAB/1-NAPHTHOL; EQUIMOLAR SOLN.
TOTAL CONC. 222 P.P.M.

Fig. 59.

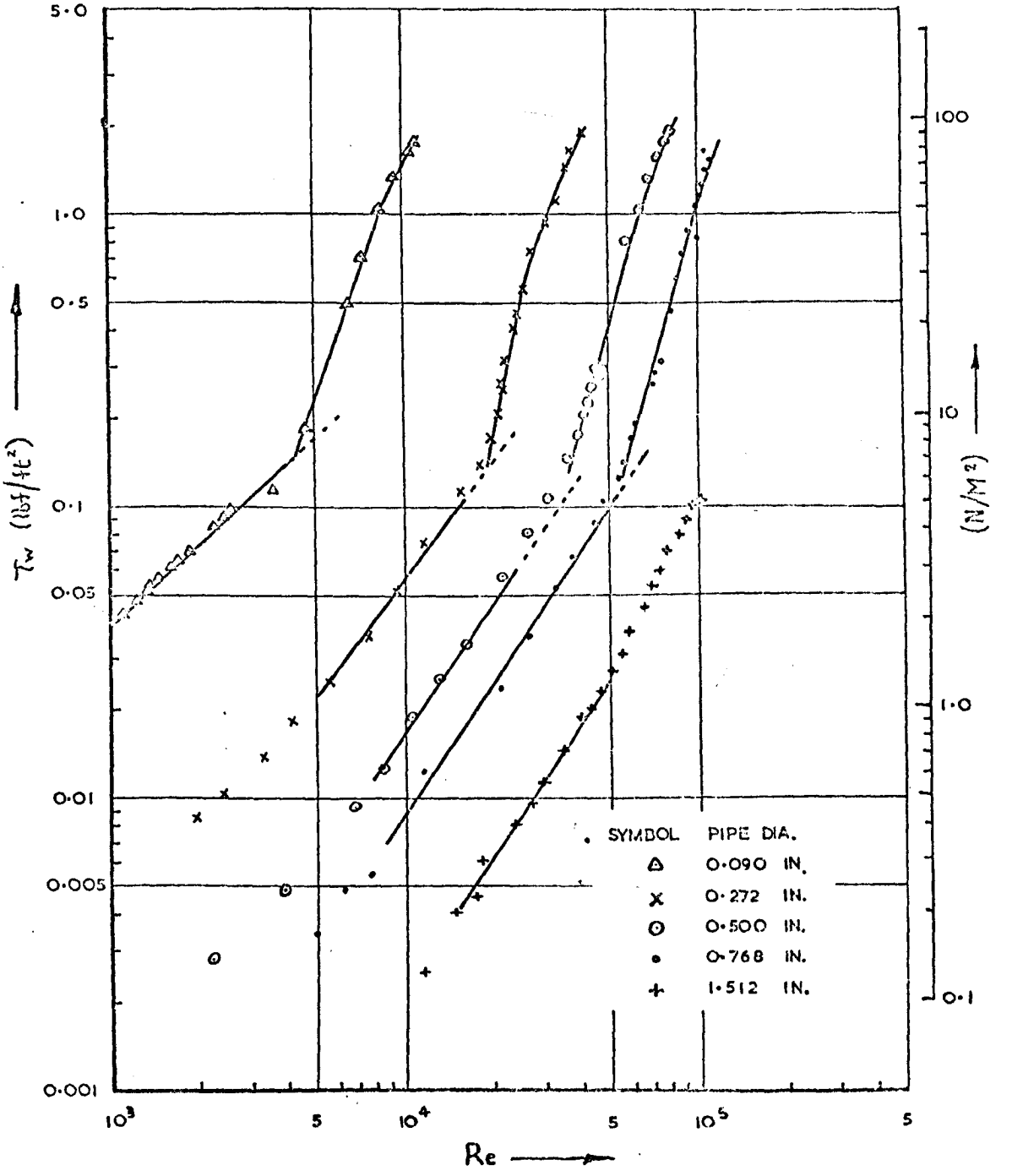

LIMITING WALL SHEAR STRESS WITH CTAB/1-NAPHTHOL EQUIMOLAR SOLN. TOTAL CONC. 508 p.p.m.

Fig. 60.

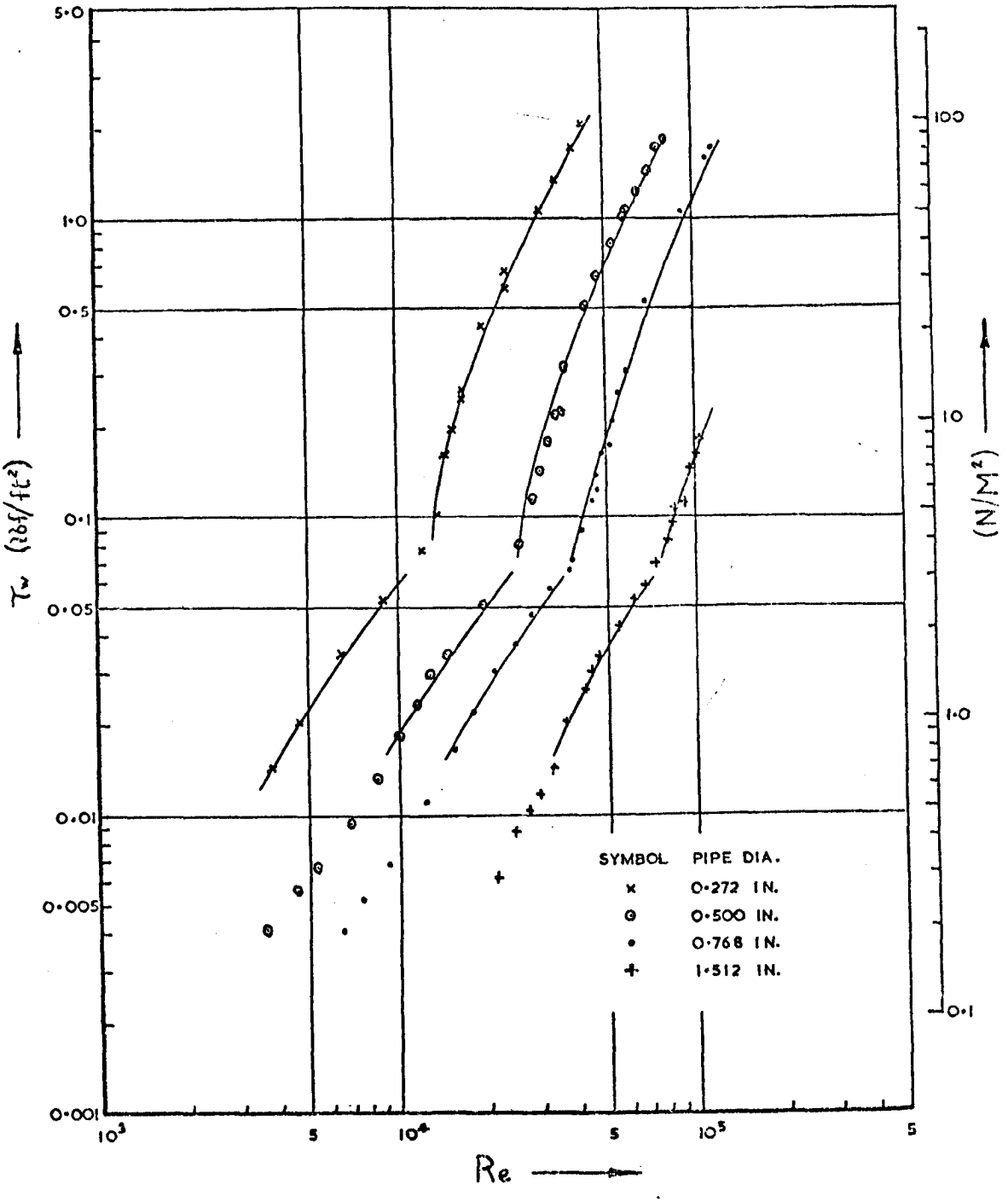

LIMITING WALL SHEAR STRESS WITH CTAB/1-NAPHTHOL EQUIMOLAR SOLN. TOTAL CONC. 318 p.p.m.

Fig. 61.

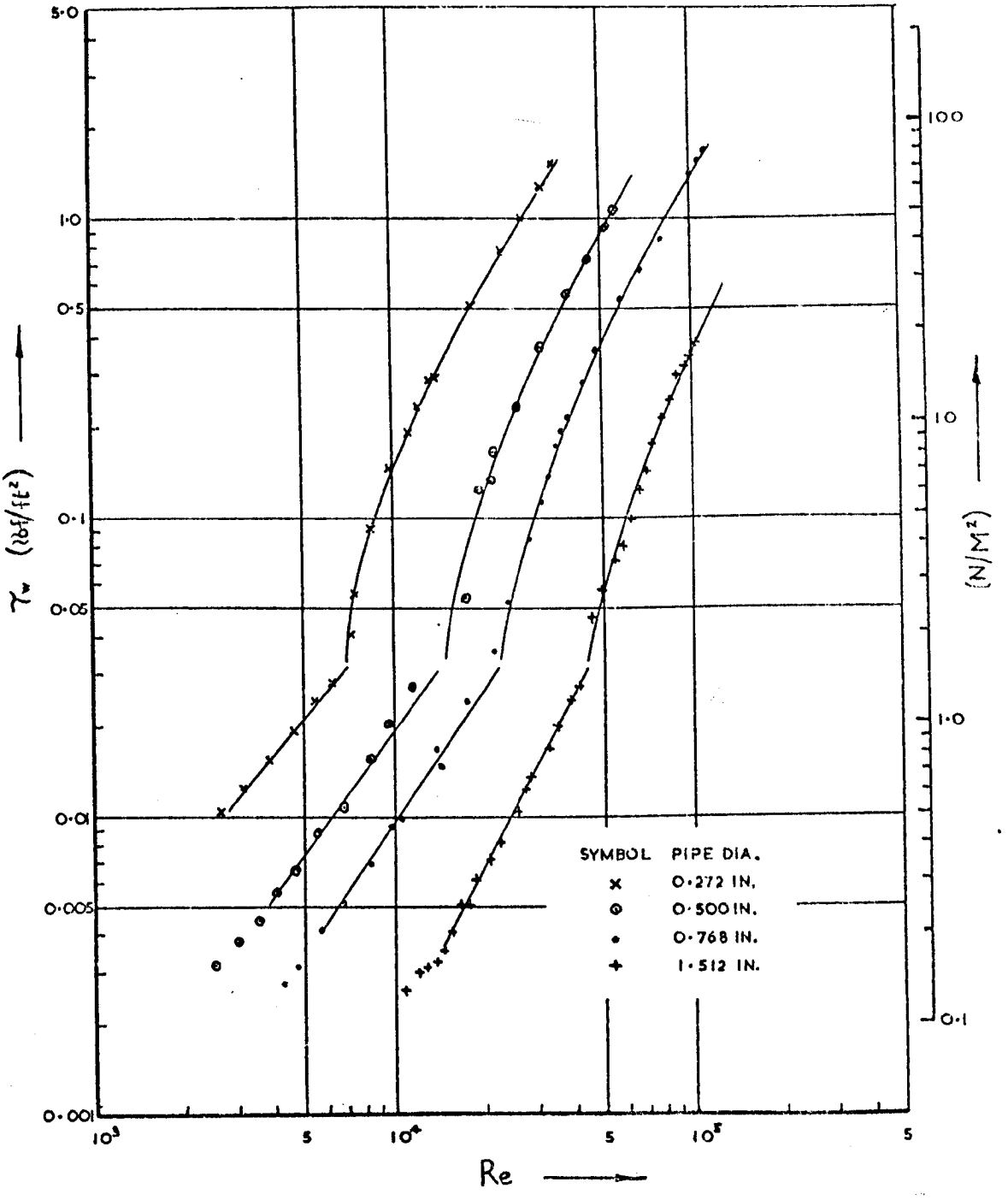

LIMITING WALL SHEAR STRESS WITH CTAB/1-NAPHTHOL EQUIMOLAR SOLN. TOTAL CONC. 250 p.p.m.

Fig. 62.

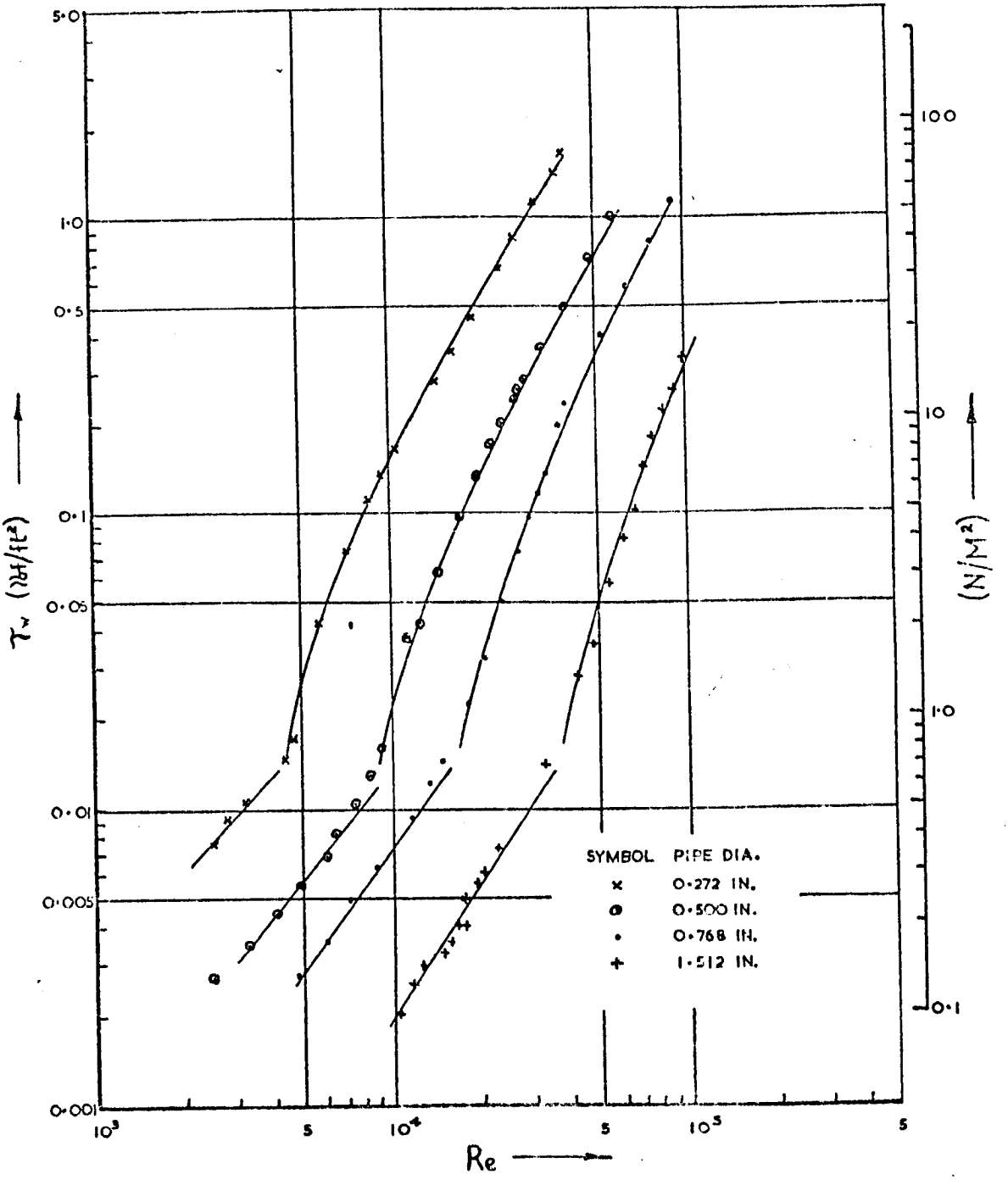

LIMITING WALL SHEAR STRESS WITH CTAB/1-NAPHTHOL EQUIMOLAR SOLN. TOTAL CONC. 222 p.p.m.

Fig. 63.

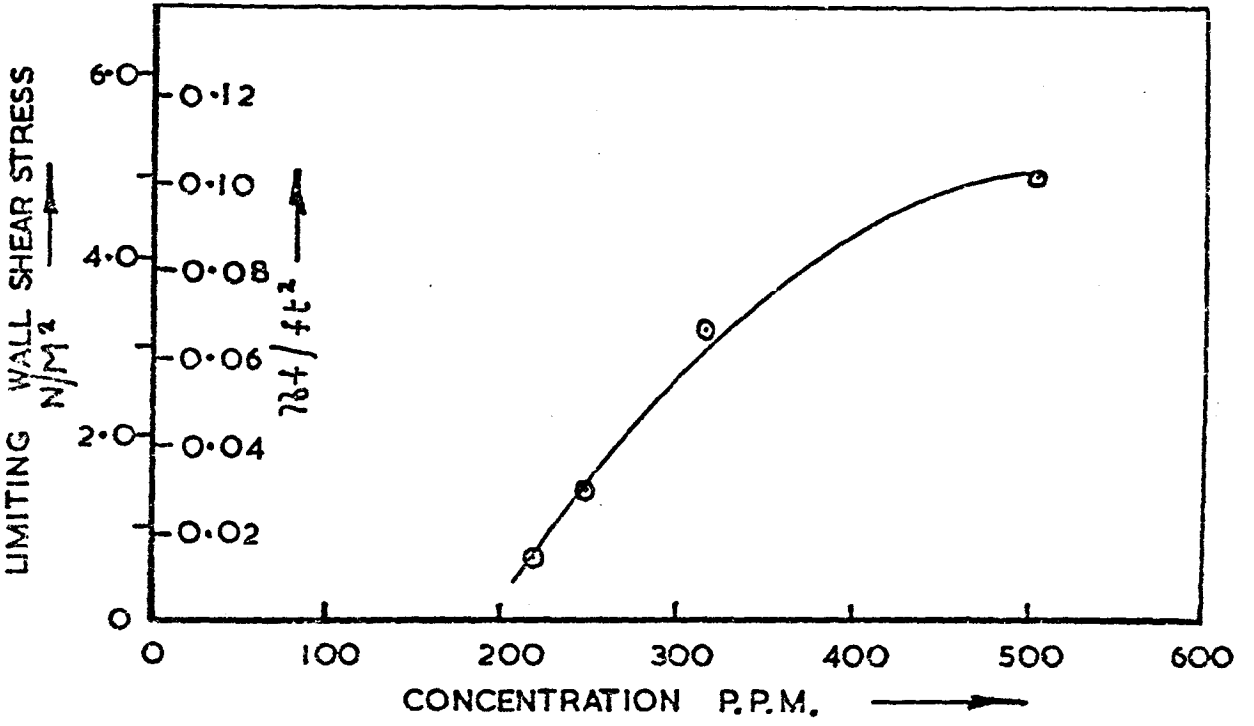

VARIATION OF LIMITING WALL SHEAR STRESS WITH CONC.
EQUIMOLAR SOLN. CTAB/1-NAPHTHOL.

Fig. 64.

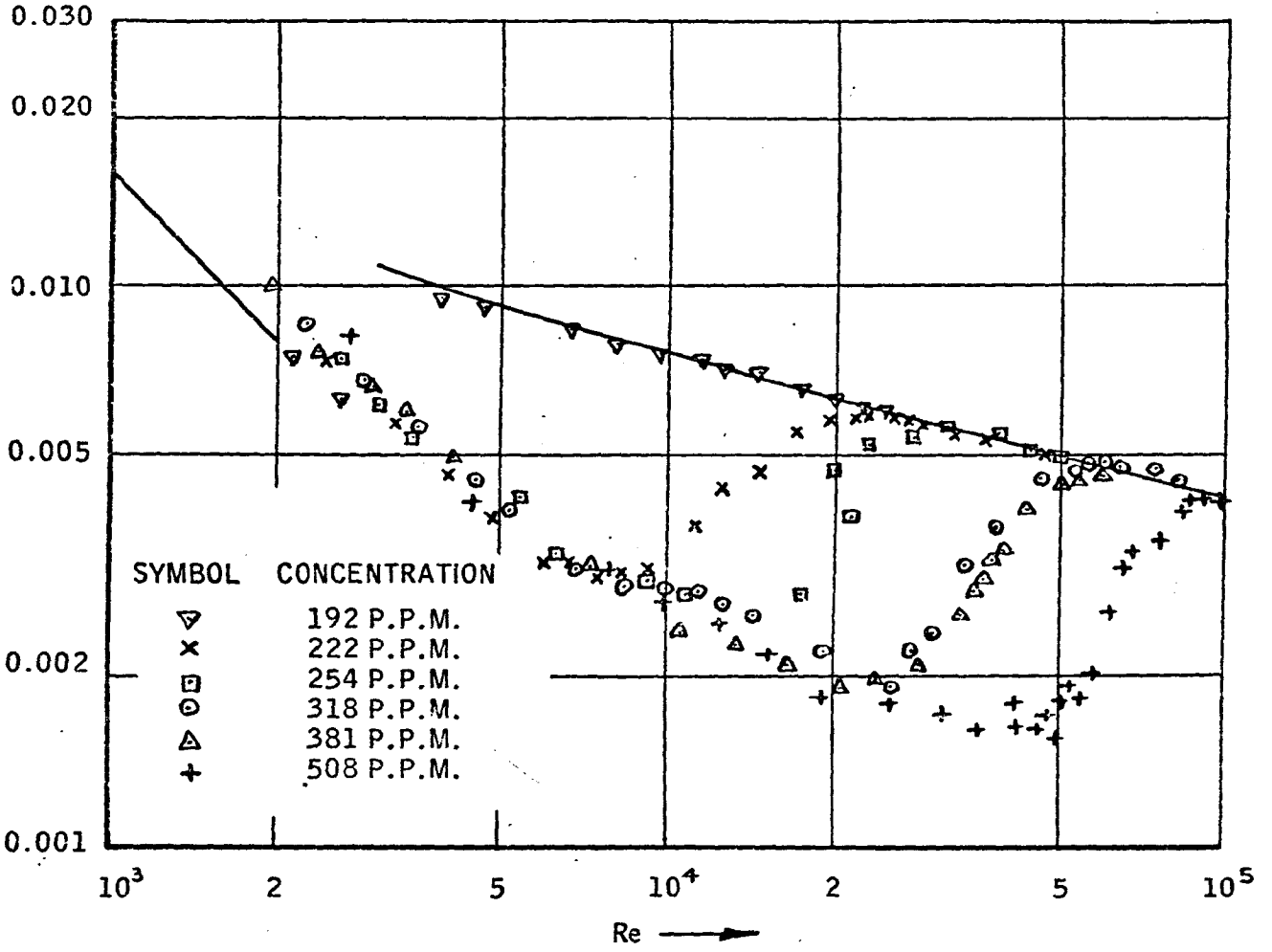

CONCENTRATION EFFECT - EQUIMOLAR SOLN. CTAB/1-NAPHTHOL
(PIPE DIA. $\frac{1}{2}$ IN.)

Fig. 65.

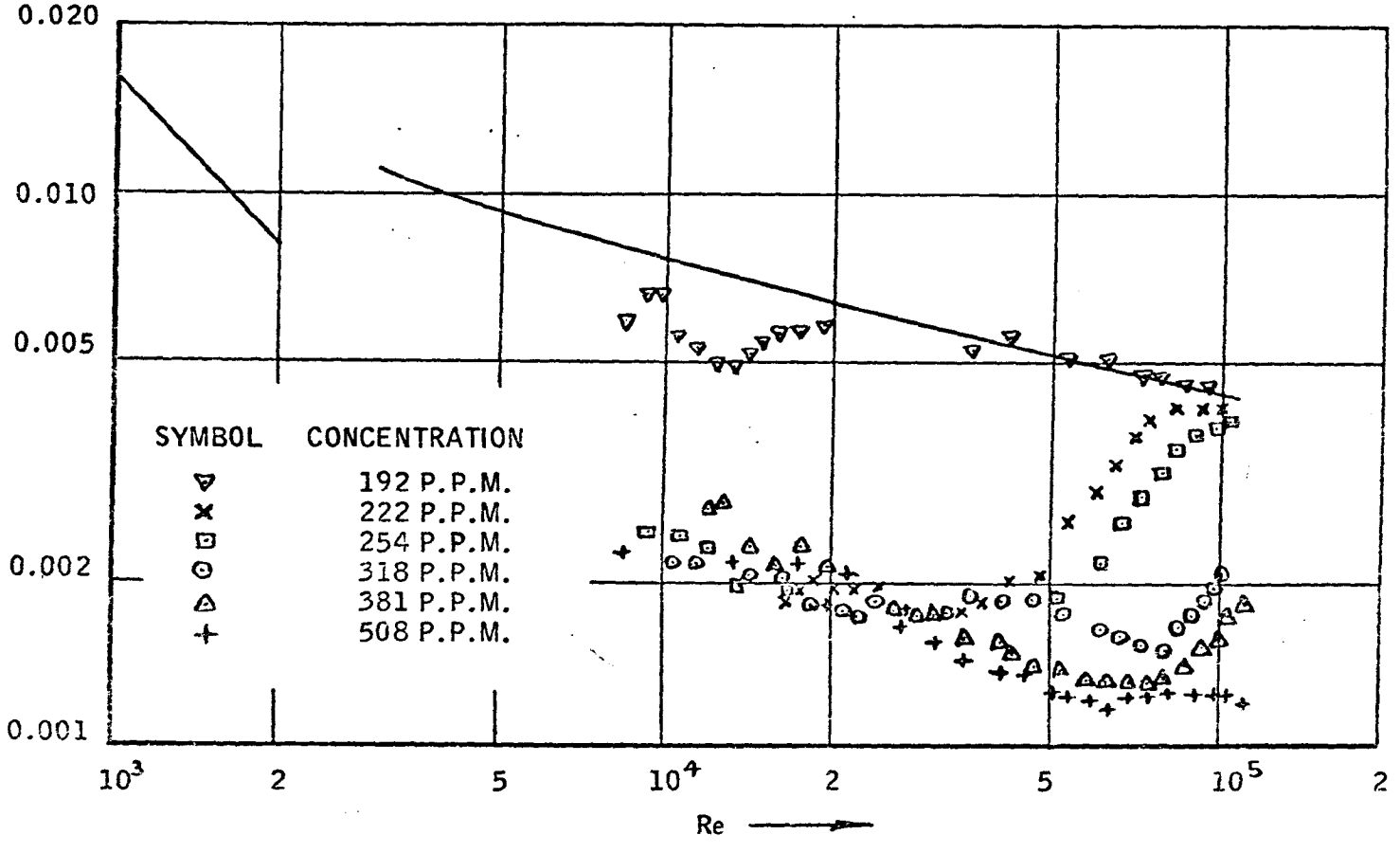

CONCENTRATION EFFECT - EQUIMOLAR SOLN. CTAB/1-NAPHTHOL
(PIPE DIA. $1\frac{1}{2}$ IN.)

Fig. 66.

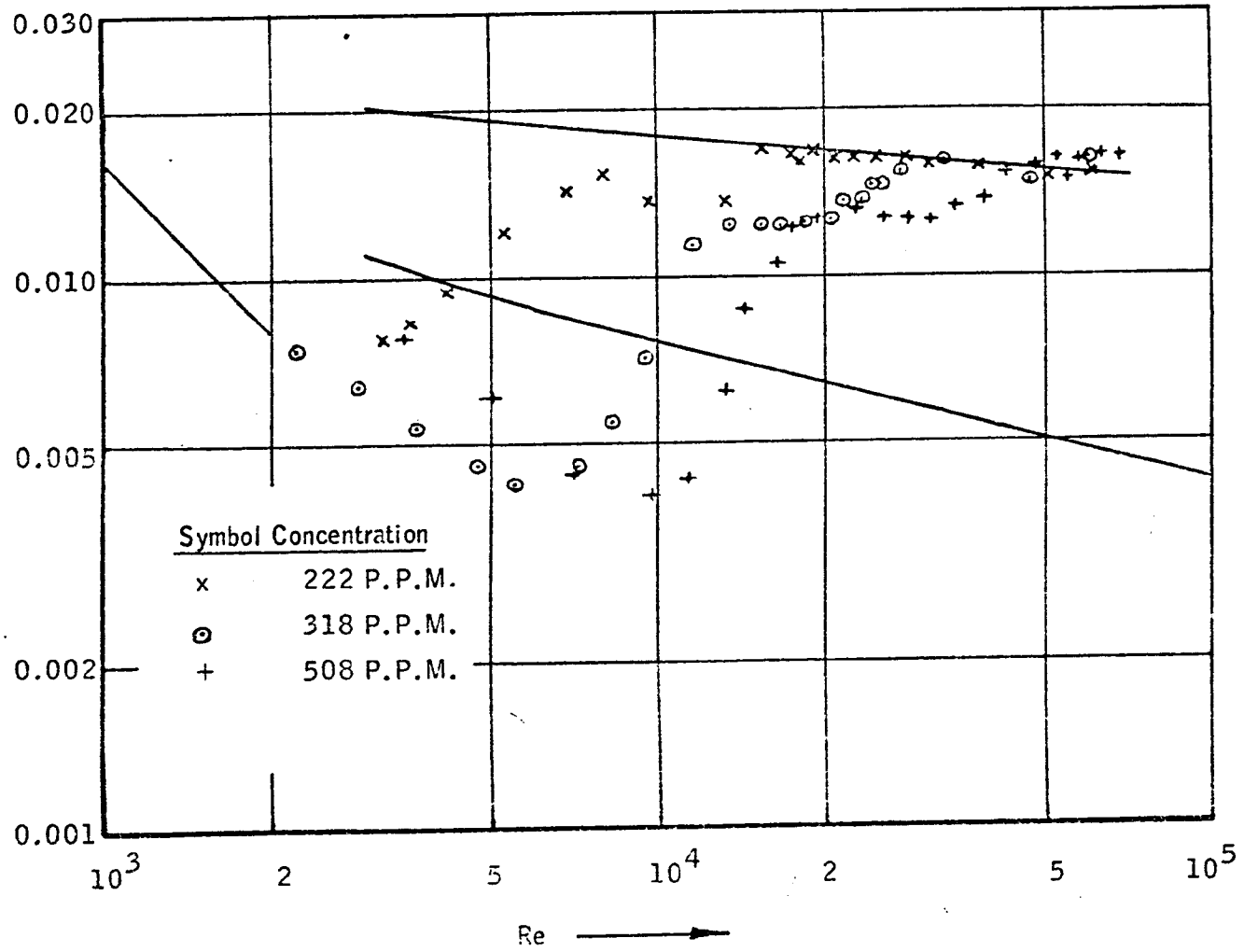

DRAG REDUCTION IN THREADED PIPE : CONCENTRATION EFFECT
(EQUIMOLAR SOLUTIONS OF CTAB/1-NAPHTHOL)

Fig. 67.

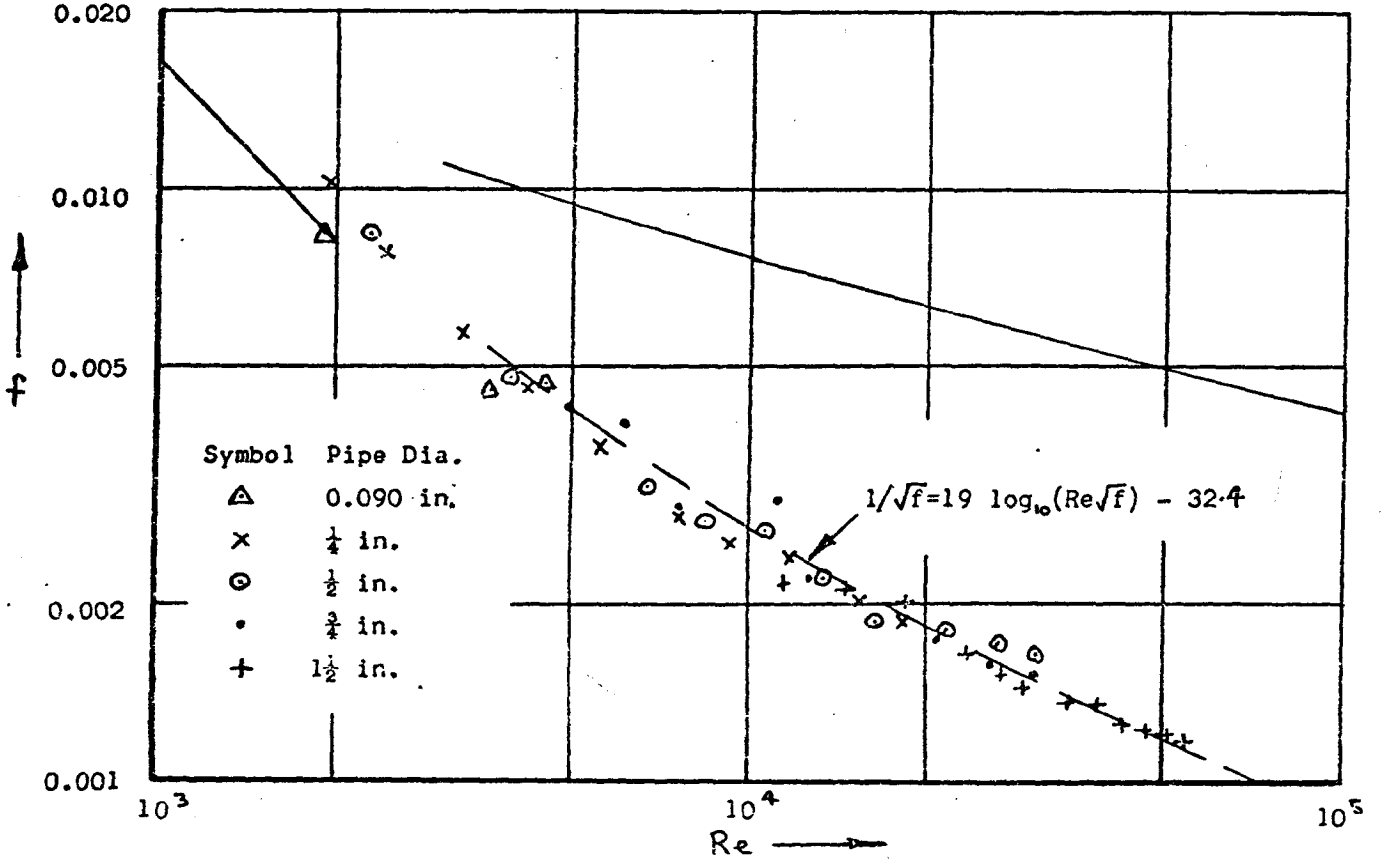

PIPE FRICTION DATA BELOW LIMITING WALL SHEAR STRESS.
EQUIMOLAR SOLN. CTAB/1-NAPHTHOL TOTAL CONC. 508 p.p.m.
Re BASED ON SOLUTION VISCOSITY.

Fig. 68.

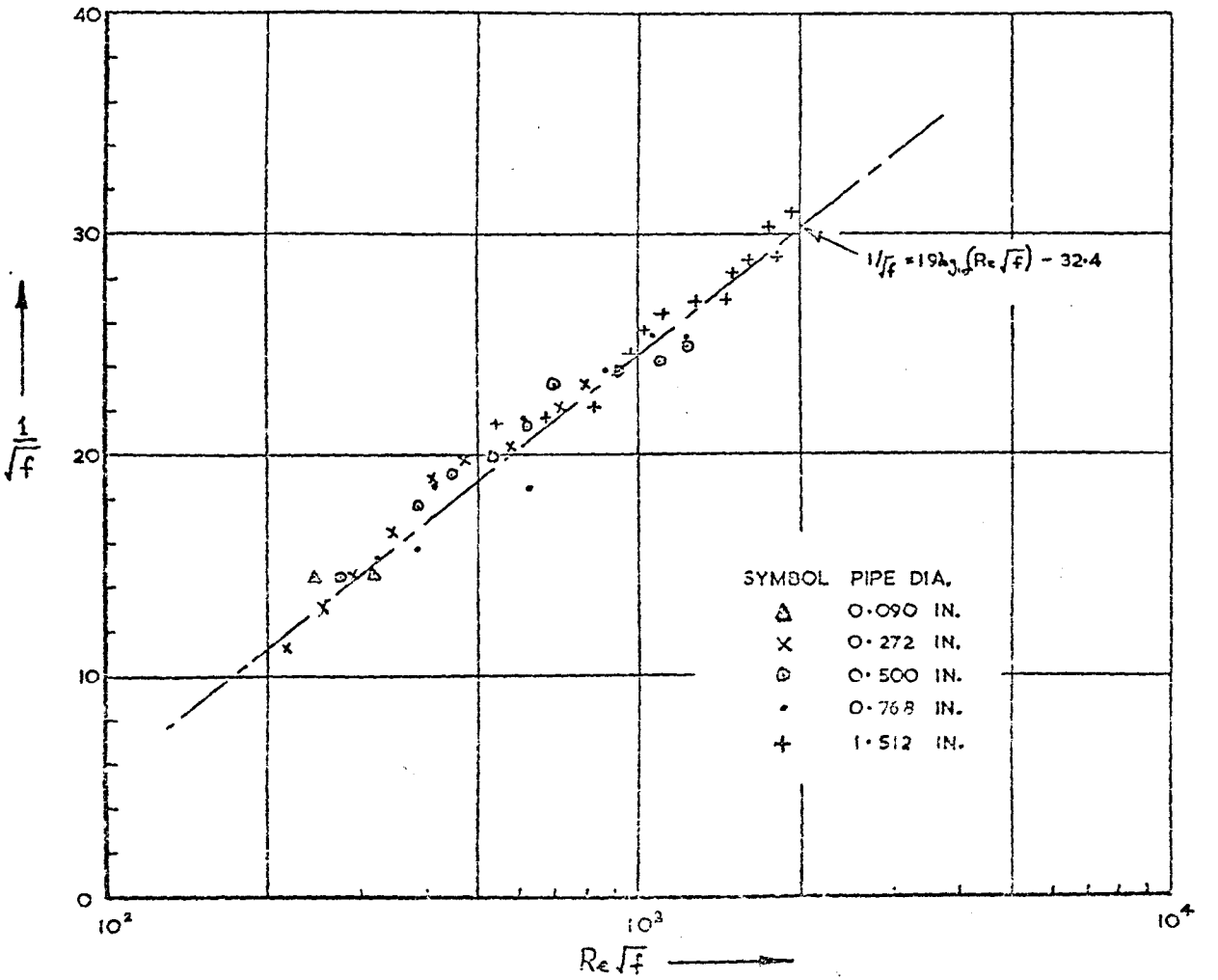

PIPE FRICTION DATA BELOW LIMITING WALL SHEAR STRESS.
EQUIMOLAR SOLN. CTAB/1-NAPHTHOL TOTAL CONC. 508 p.p.m.
Re BASED ON SOLUTION VISCOSITY.

Fig. 69.

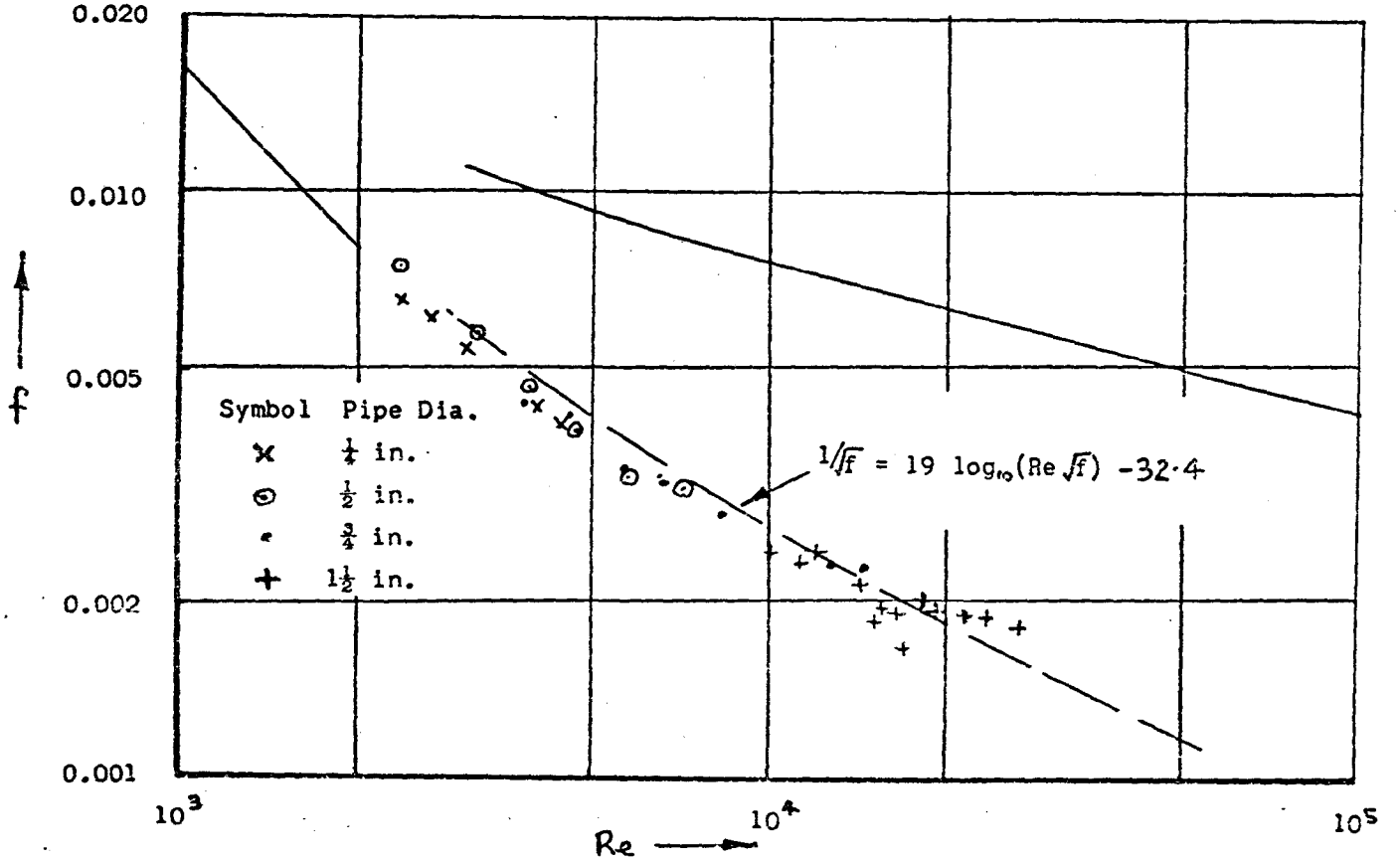

PIPE FRICTION DATA BELOW LIMITING WALL SHEAR STRESS.
EQUIMOLAR SOLN. CTAB/1-NAPHTHOL TOTAL CONC. 222 p.p.m.
Re BASED ON SOLUTION VISCOSITY.

Fig. 70.

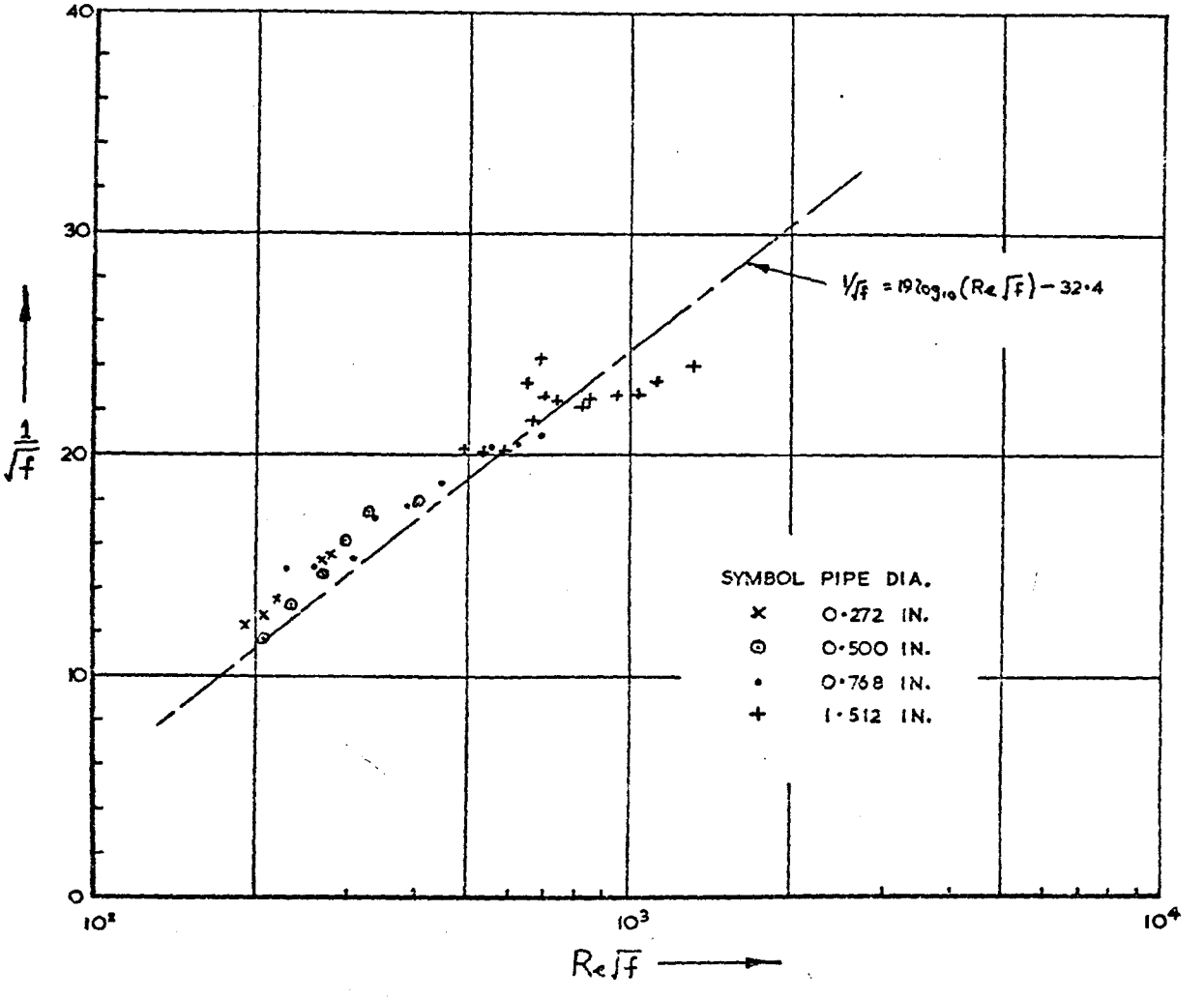

PIPE FRICTION DATA BELOW LIMITING WALL SHEAR STRESS
EQUIMOLAR SOLN. CTAB/1-NAPHTHOL TOTAL CONC 222 p.p.m.
Re BASED ON SOLUTION VISCOSITY.

Fig. 71.

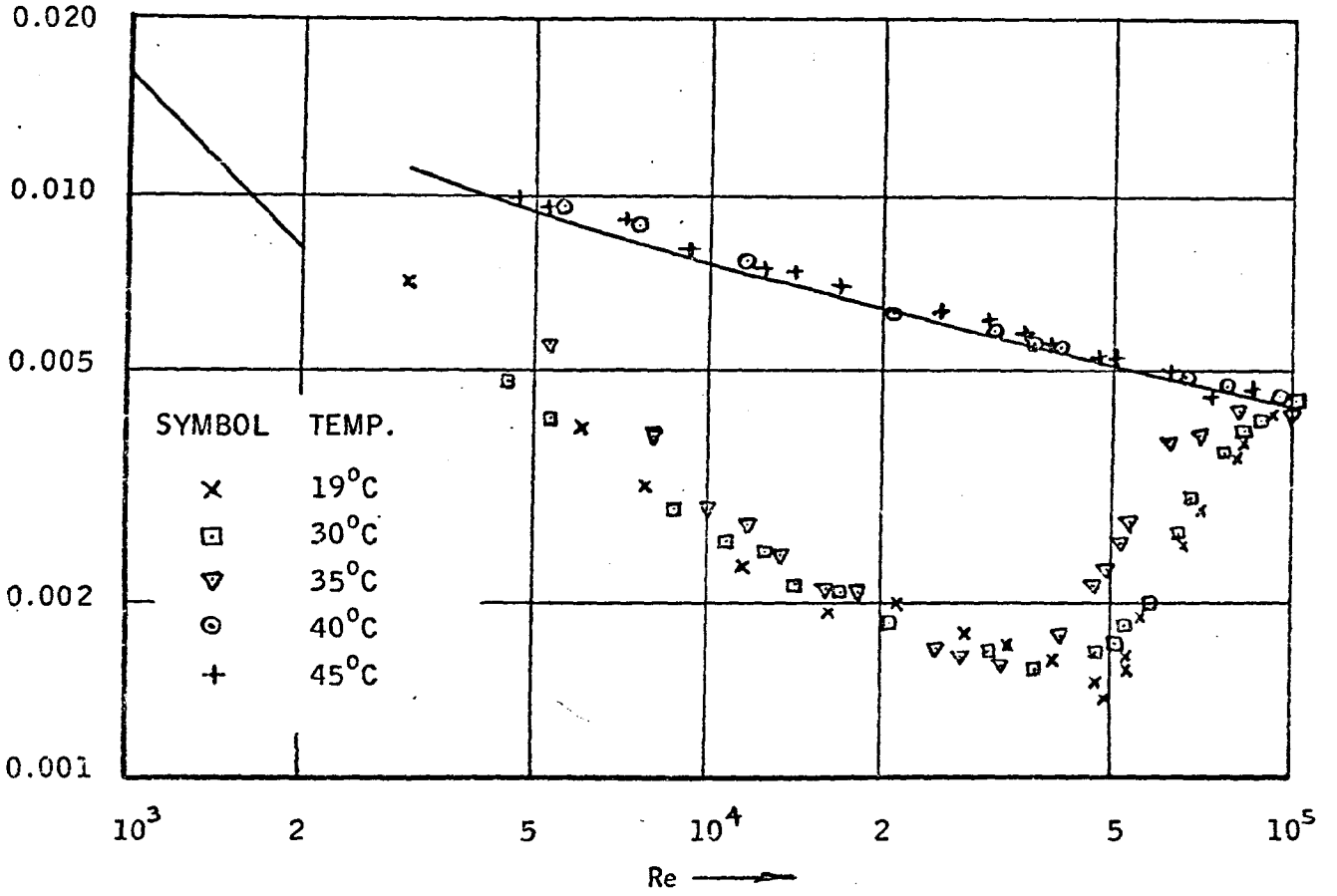

TEMPERATURE EFFECT - EQUIMOLAR SOLN. CTAB/1-NAPHTHOL
TOTAL CONC. 508 P.P.M. (PIPE DIA. $\frac{1}{2}$ IN.)

Fig. 72.

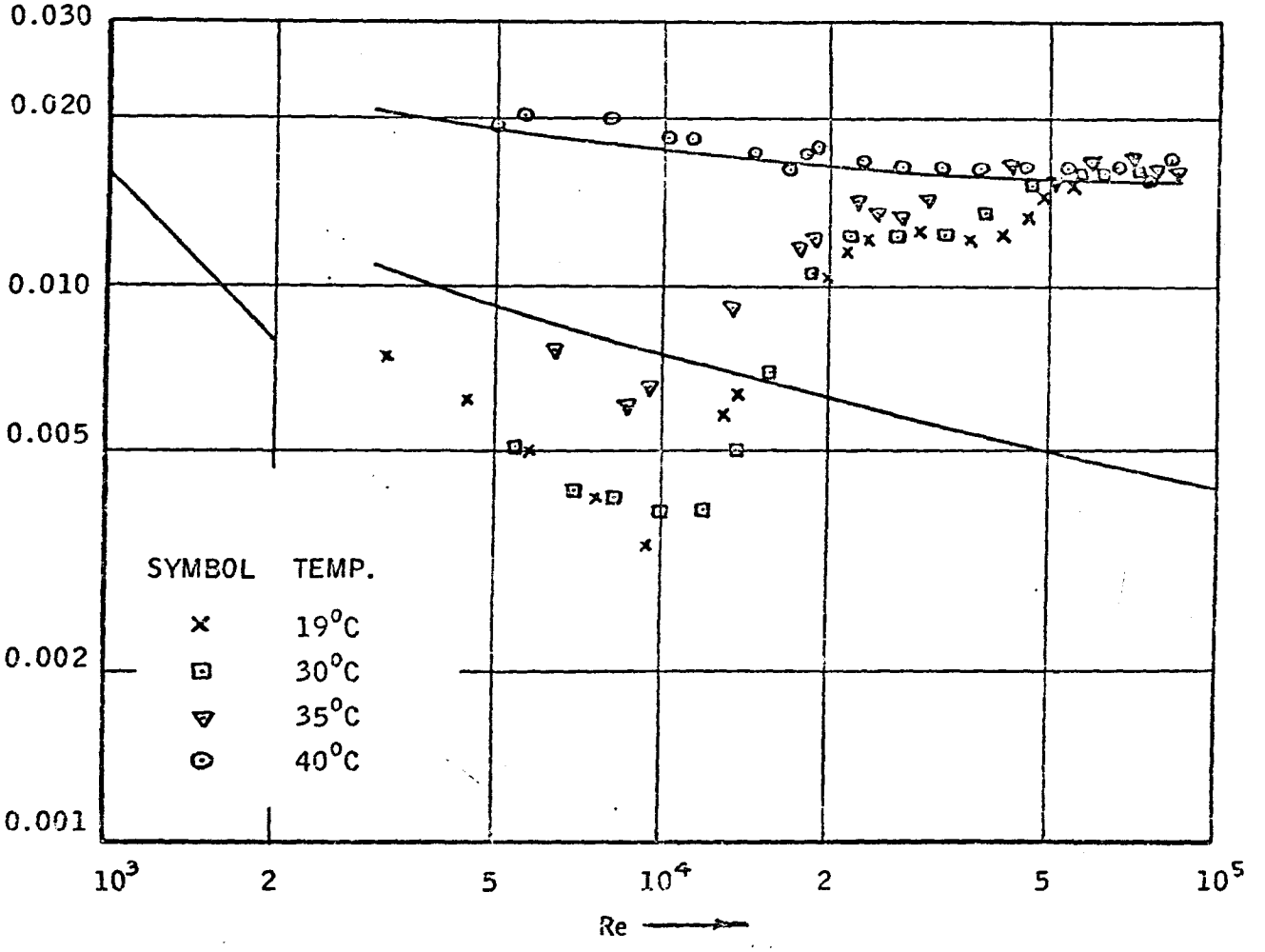

TEMPERATURE EFFECT - EQUIMOLAR SOLN. CTAB/1-NAPHTHOL
TOTAL CONC. 508 P.P.M. (THREADED PIPE).

Fig. 73.

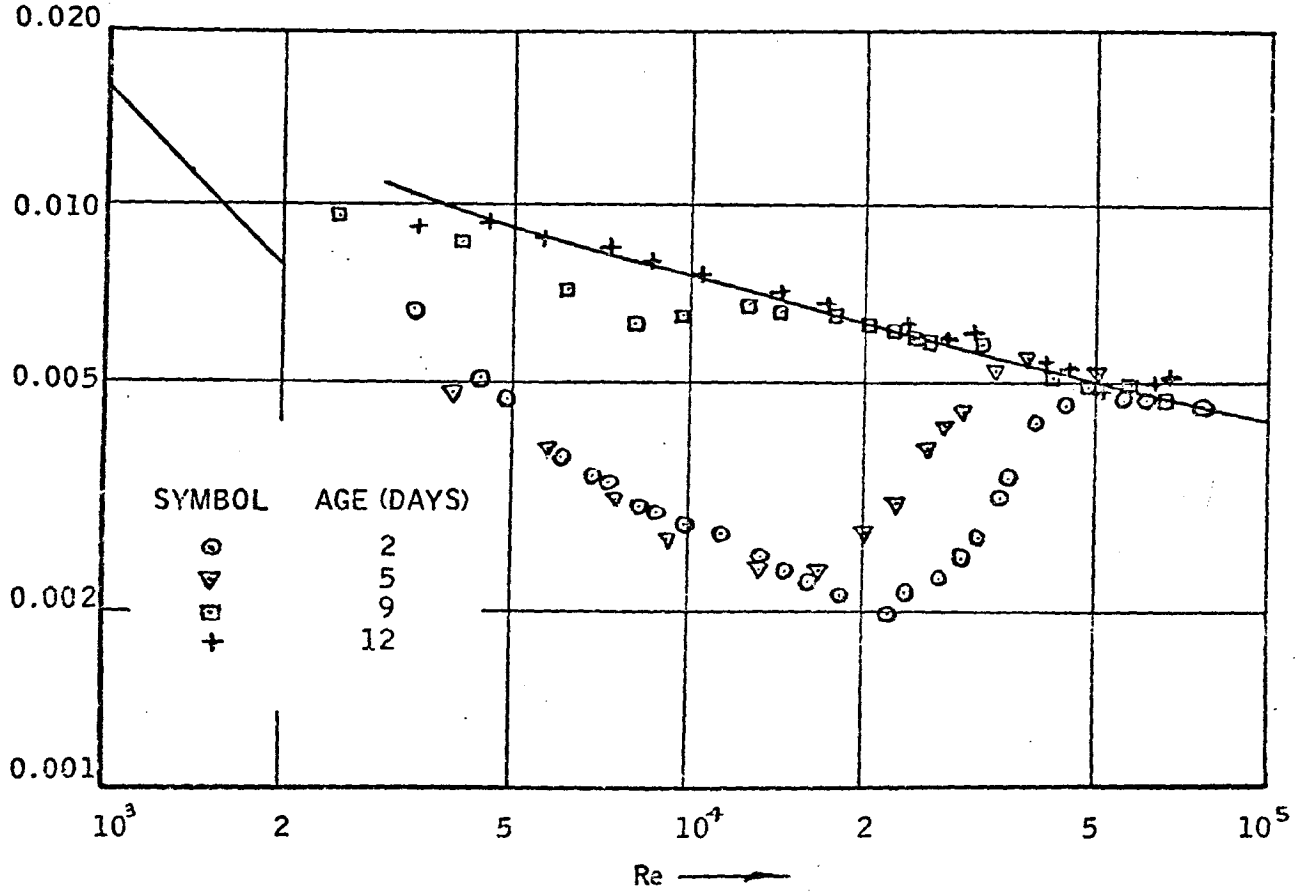

DEGRADATION WITH AGE - EQUIMOLAR SOLN. CTAB/1-NAPHTHOL
TOTAL CONC. 508 P.P.M. (PIPE DIA. $\frac{1}{2}$ IN.).
(N.B. These tests were carried out with the same soln. after heating experiments - see Fig. C.1)

Fig. 74.

(2.7.0) OBSERVATIONS ON THE FLOW STRUCTURE AND VELOCITY PROFILES OF THE COMPLEX SOAP SYSTEM IN PIPE FLOW

We have previously seen that the CTAB/Naphthol solutions produce reduced drag given by Virk's asymptotic expression, irrespective of pipe diameter or concentration within the range investigated. As far as the available evidence goes this represents the maximum drag reduction obtainable, and the flow characteristics under asymptotic conditions are therefore of high interest. A qualitative and quantative picture of such flows have been obtained by using the pulsed hydrogen bubble technique (72). It is very convenient to use the present micellar system for such an investigation because asymptotic conditions are achieved with low concentrations in large diameter pipes, and furthermore the solutions are not susceptible to mechanical degradation.

(2.7.1) The test rig and test procedure.

Fig.75 shows a schematic layout of the apparatus used for this investigation. A drawn Perspex pipe of internal diameter 1 1/2 in. (38.1mm) was fed from a sump by a centrifugal pump and a 0.055mm dia. wire was stretched across a diameter about 150 pipe diameters from the entry to act as the cathode as shown. A copper tube downstream from the wire completed the flow circuit back to the sump

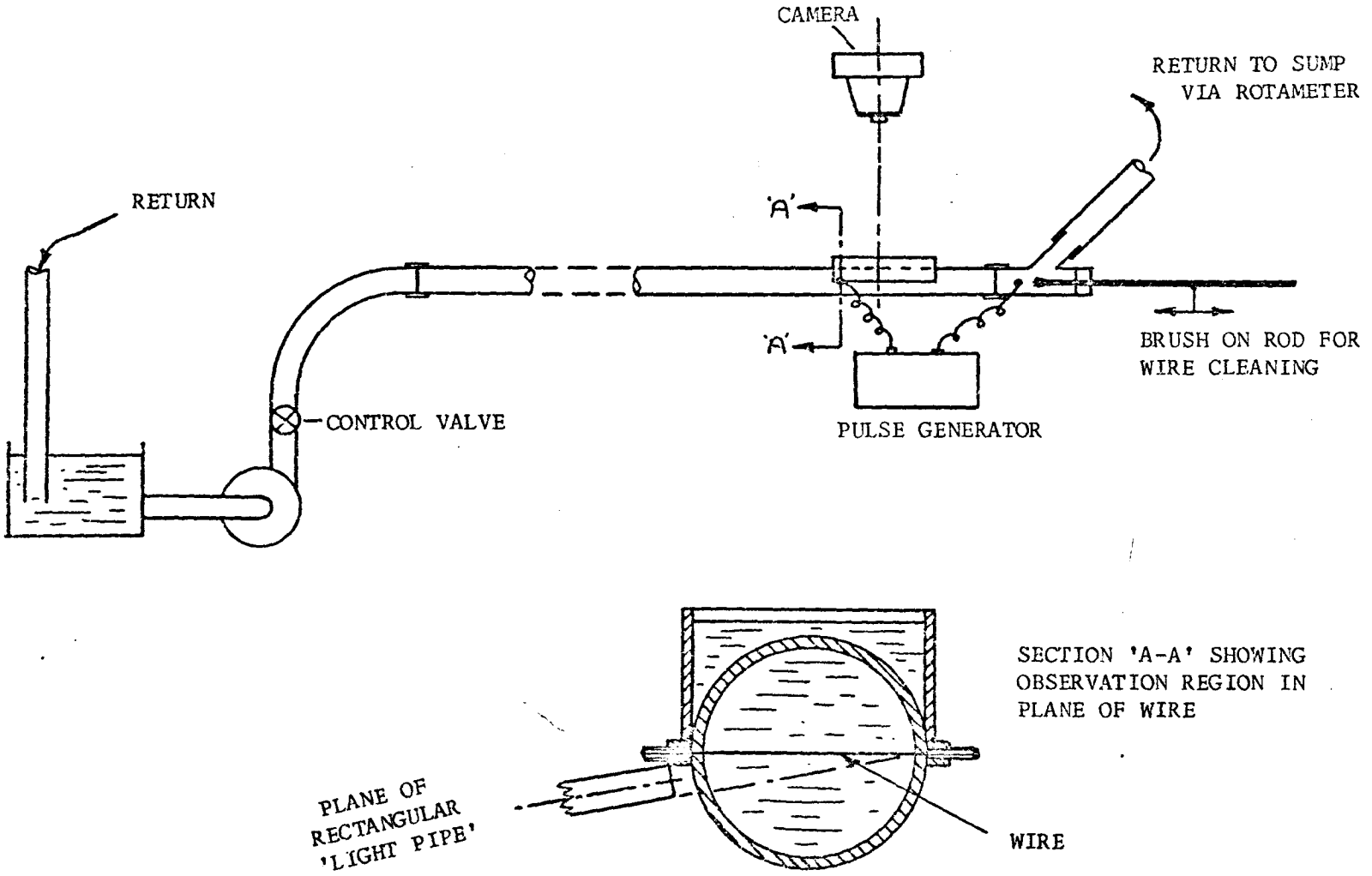

SCHEME OF HYDROGEN BUBBLE PIPE-FLOW RIG.

Fig. 75.

and also served as the anode. Flow rates were measured by timed weighing and were monitered with a rotameter. A pulsed voltage of square wave form (0 - 30v) was applied between the anode and cathode, and the pulses of small hydrogen bubbles swept downstream from the wire were illuminated by a transverse sheet of intense light just below the plane of wire.

A series of photographs was taken of the flow patterns at various flow rates, and from these the axial velocity at a given distance from the pipe axis was determined by measurement of the displacement between two successive pulses, knowing the pulse frequency. Optical aberation was minimized by surrounding the observation region of the pipe by a rectangular Perspex box filled with water.

(2.7.2) Experimental results.

Some typical photographs obtained with water are shown in fig.76. With Reynolds numbers above 3,000 the flow is noticeably turbulent and velocity profiles are quite flat. At high Reynolds numbers the pulses have become quite diffused by the turbulence.

Fig.77 shows some corresponding results obtained with an equi-molar solution of CTAB/1 naphthol at 508 p.p.m. total concentration. The velocity profiles are generally much more peaky than with water, and small scale turbulence has been considerably suppressed by the additives. The fact

that large turbulent eddies remain is seen from the distortion of the pulse shapes.

A comparison of the photographs, figs.76 and 77 shows that the bubble pulse lengths with the soap system are considerably shorter than those for water although the pulse unit settings were identical for both. Bubbles grow on the wire and are not swept from it until the drag force on them becomes sufficiently great. The drag force on the hydrogen bubbles in the soap system is likely to be less than in water, see section 2.10.4. Since the bubble dynamics are similar for successive pulses this does not affect velocity measurements from the photographs.

Typical instantaneous velocity profiles for the micellar solution in turbulent flow are shown in figs.78 and 79. Only three profiles are shown in each figure to avoid confusion but the dashed lines representing the temporal mean velocities were averaged from seven random instantaneous profiles. Deviations from the mean due to turbulent eddies are quite significant, and an estimate of the r.m.s. perturbations is shown in fig.80. The scatter is quite large due to the very limited sample, but the turbulence intensities with the solution are roughly the same order of magnitude as for water in pipe flow when compared with some results by Wells (74). We deduce therefore that the micelles only suppress the very small scale turbulence (high wave numbers). This is apparent from

visual observations of the flow photographs, but it should be emphasized that the present technique will not allow quantitative measurement of turbulent eddies whose periodic time is less than that of the pulses - in this case 0.125 sec.

Fig.81 shows temporal mean velocity profiles obtained for a range of flow rates in the turbulent regime. Again these were all averaged from seven random photographs at each flow rate. The volume flow rates determined from an integration of these profiles agree fairly well with the values obtained by timed collection into a measuring vessel. The differences are all less than $\pm$ 5%, except for the highest flow rate which is -8% in error. This is considered to be satisfactory in view of the rather limited number of flow photographs, and gives some confidence to the validity of the velocity profiles.

These mean velocity profiles are seen to be more laminar like in shape than the usual 1/7th power law form, characteristic of normal flow at corresponding Reynolds numbers. Differences in profile shape between normal turbulent flow, laminar flow and the soap solution profiles are clearly seen in fig.82 where the average and peak velocities are compared.

As previously stated the pipe friction data for the soap solution is well correlated by Virk's asymptotic expression:-

$$f^{1/2} = 19 \log_{10}(Re\ f^{1/2}) - 32.4 \quad (Re\ 4000)$$

This correlation implies the existence of a semi-logarithmic velocity profile given by:-

$$U^+ = 11.7 \ln Y^+ - 17.0$$

The form of this limiting velocity profile was predicted by Virk (59) but with no corroberating velocity measurements under asymptotic limit conditions.

Fig.82 shows the present results plotted in this dimensionless form, and these provide a fairly good confirmation to the existance of the asymptotic profile. Values for the wall shear stress were deduced from the preceding pipe friction results.

Fig. 76. PLATES (i) to (ix)

PIPE FLOW VISUALIZATION USING HYDROGEN BUBBLE TECHNIQUE.

WATER.

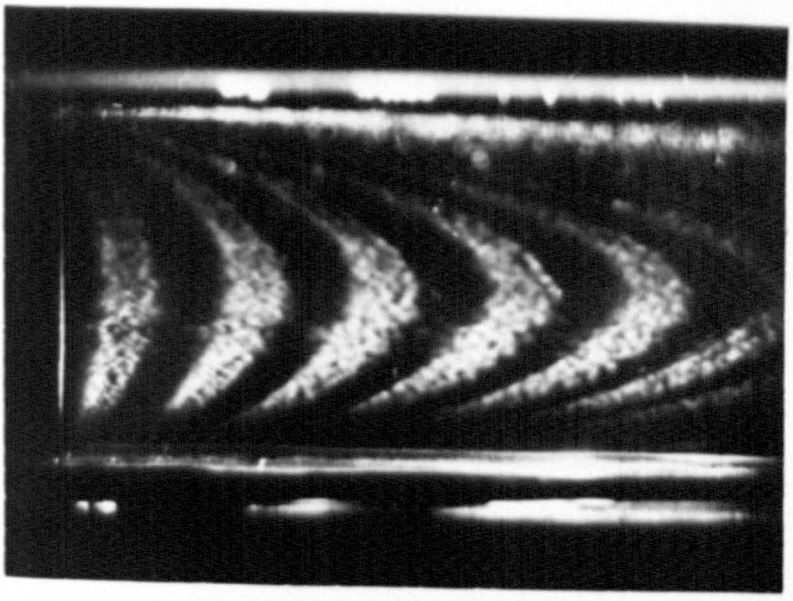

(i) Re = 1600

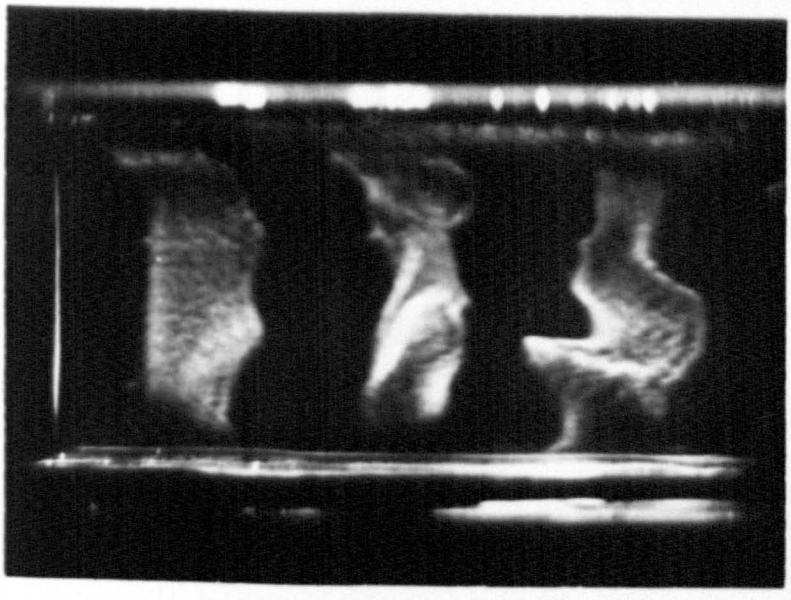

(ii) Re = 3700

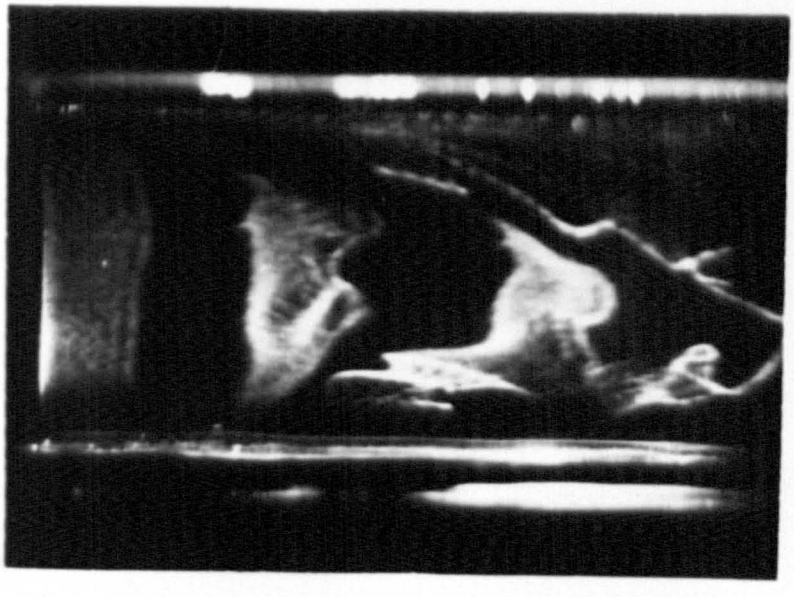

(iii) Re = 3700

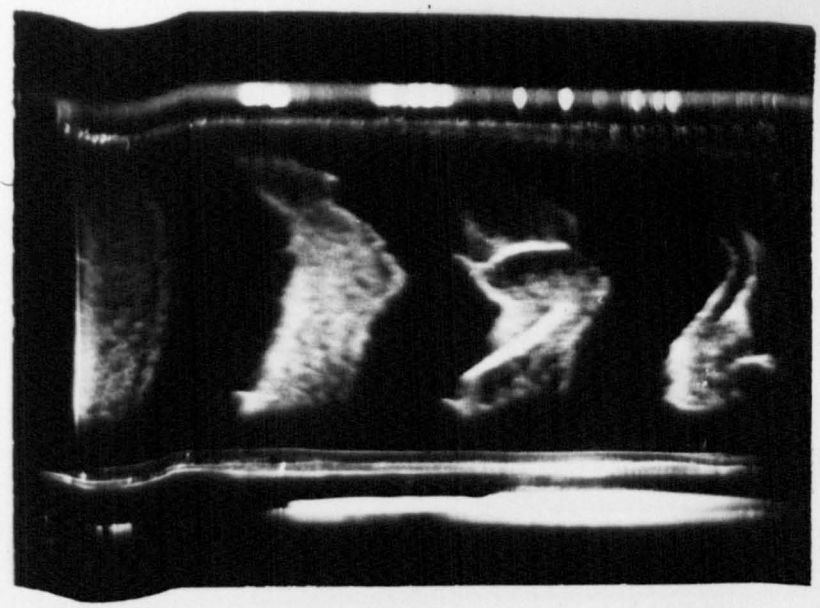

(iv) Re = 3700

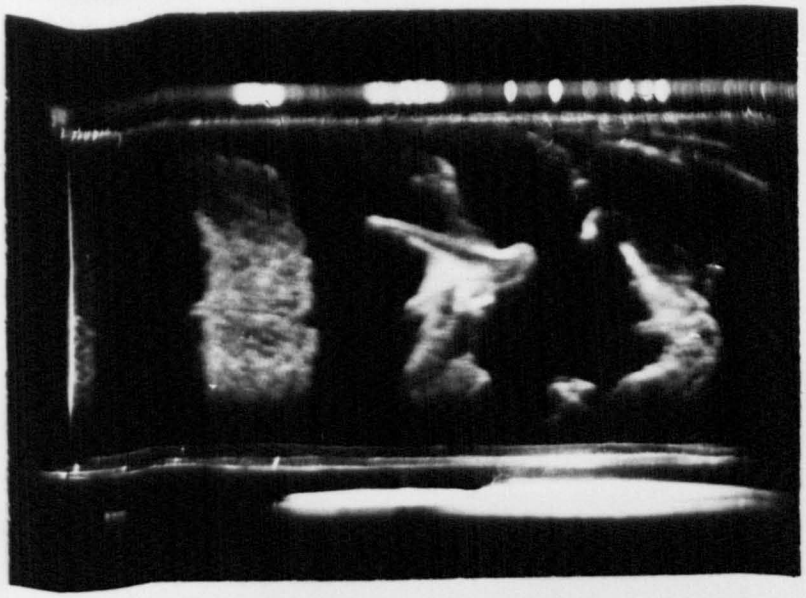

(v) Re = 3700

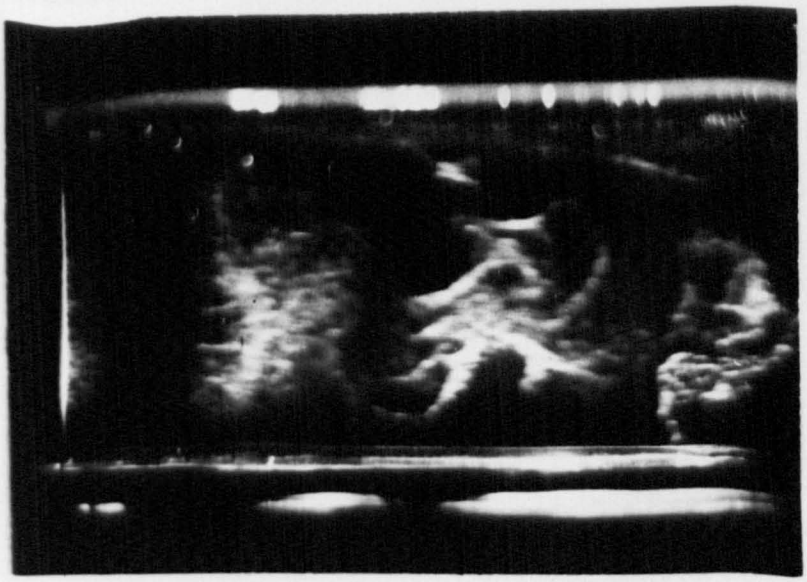

(vi) Re = 4540

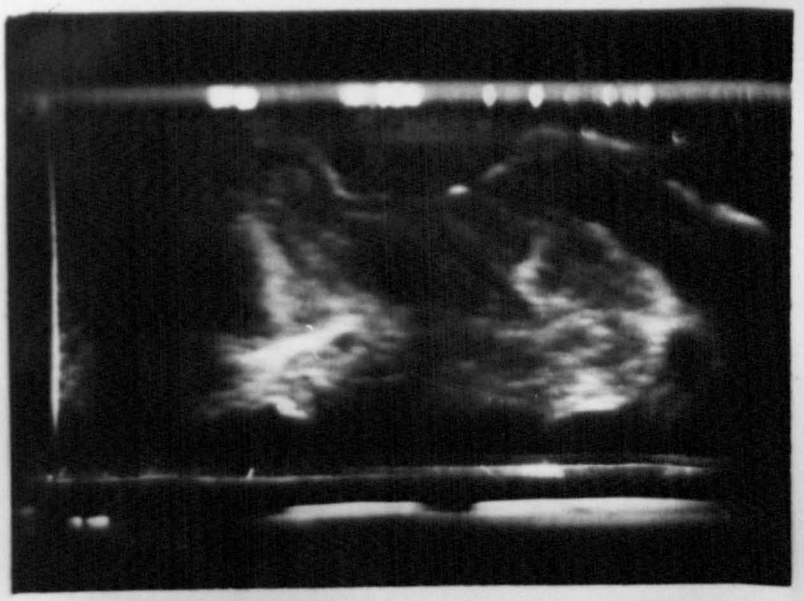

(vii) Re = 5200

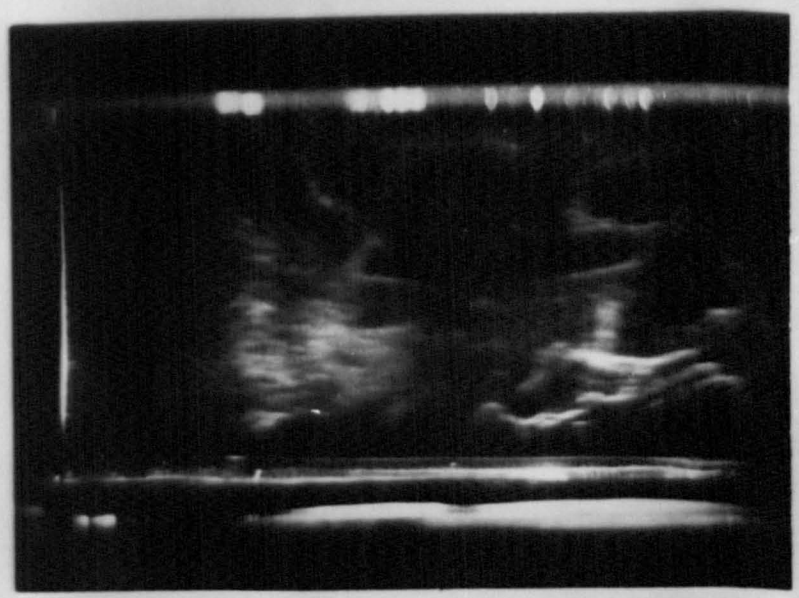

(viii) Re = 6300

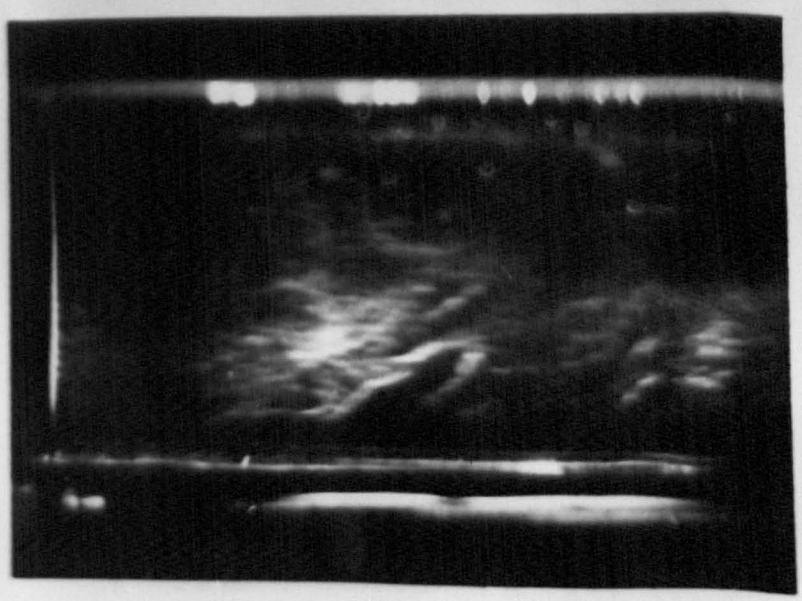

(ix) Re = 7500

Fig. 77. PLATES (i) to (xi)

PIPE FLOW VISUALIZATION USING
HYDROGEN BUBBLE TECHNIQUE.
EQUIMOLAR SOLN. CTAB/1-NAPHTHOL.
TOTAL CONC. 508 p.p.m.

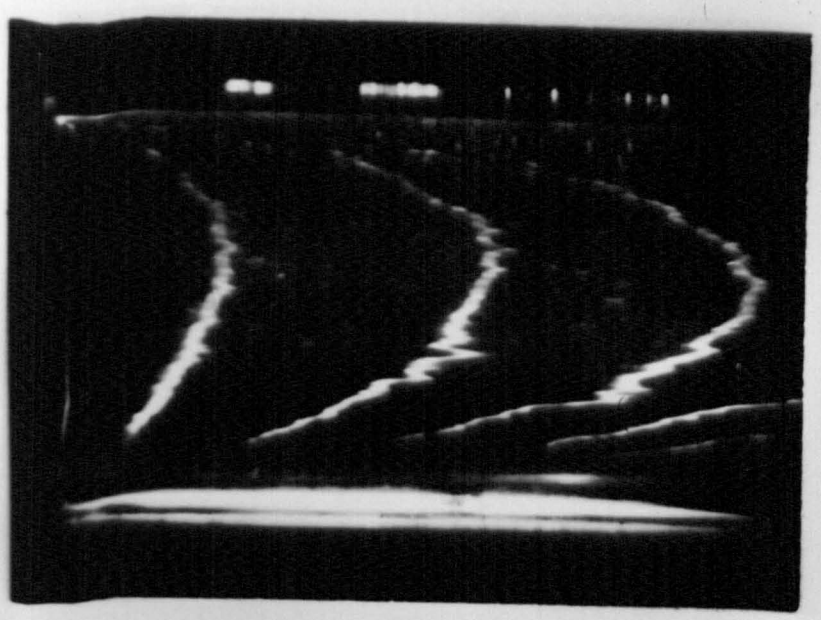

(i) Re = 3140

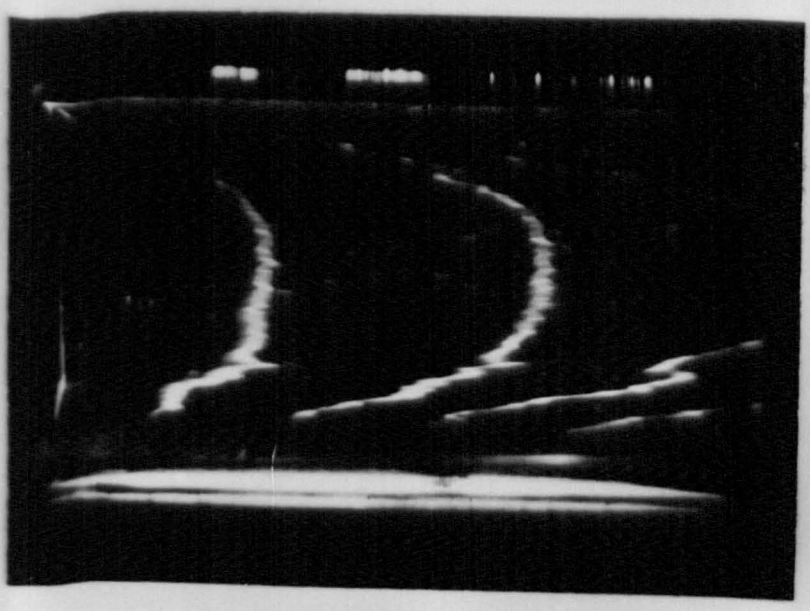

(ii) Re = 3140

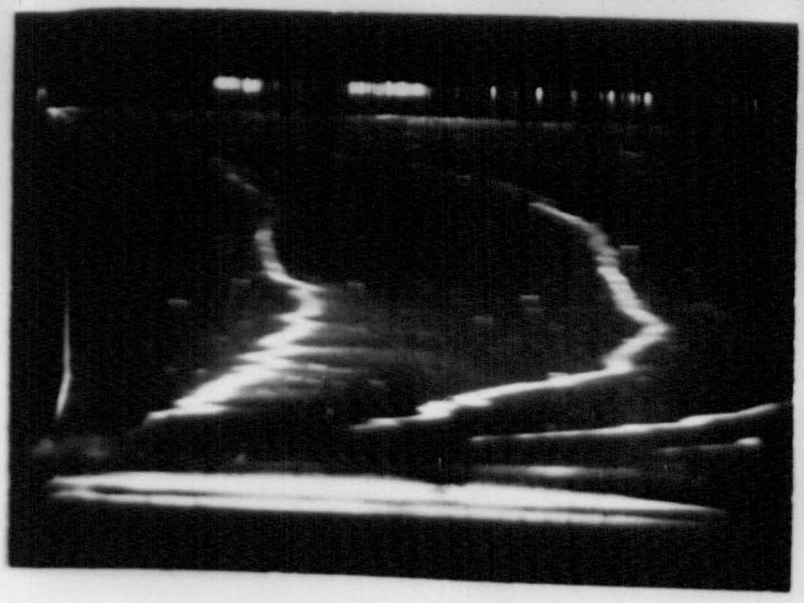

(iii) Re = 3860

(iv) Re = 3860

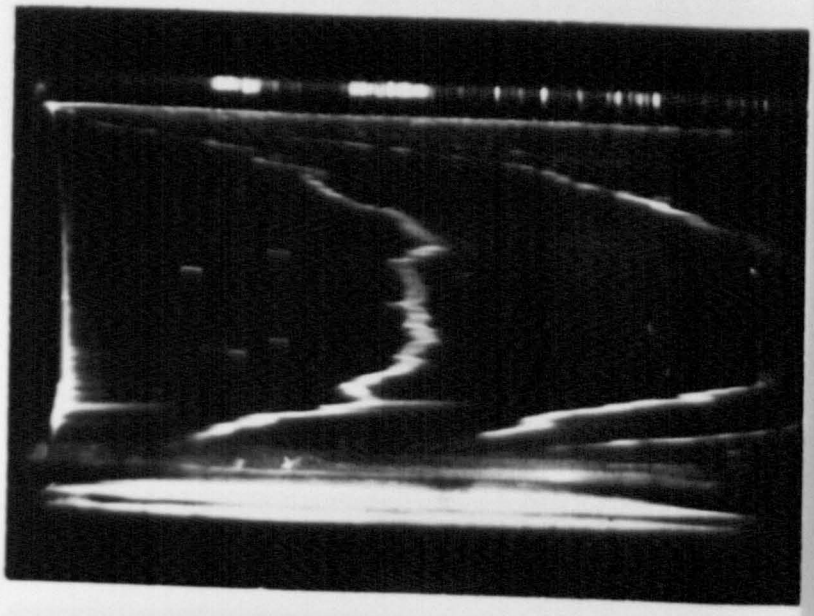

(v) Re = 4440

(vi) Re = 4440

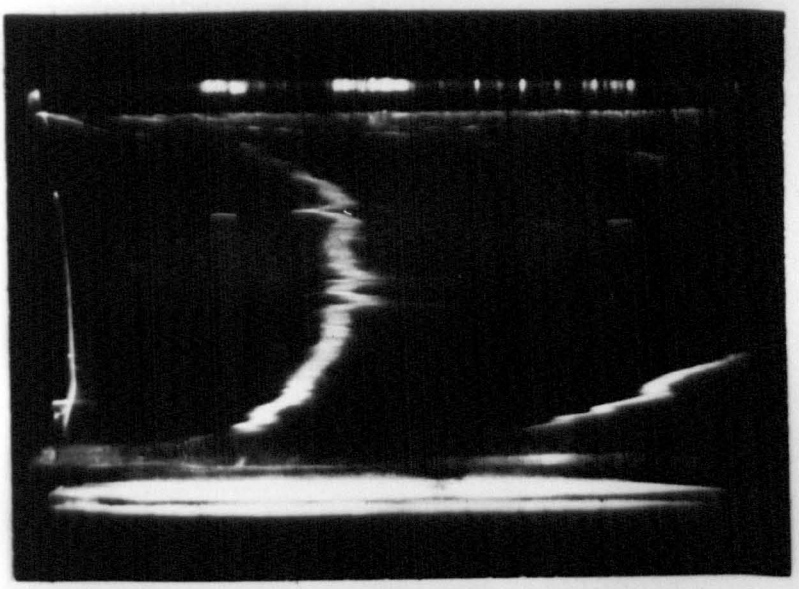

(vii) Re = 5300

(viii) Re = 5300

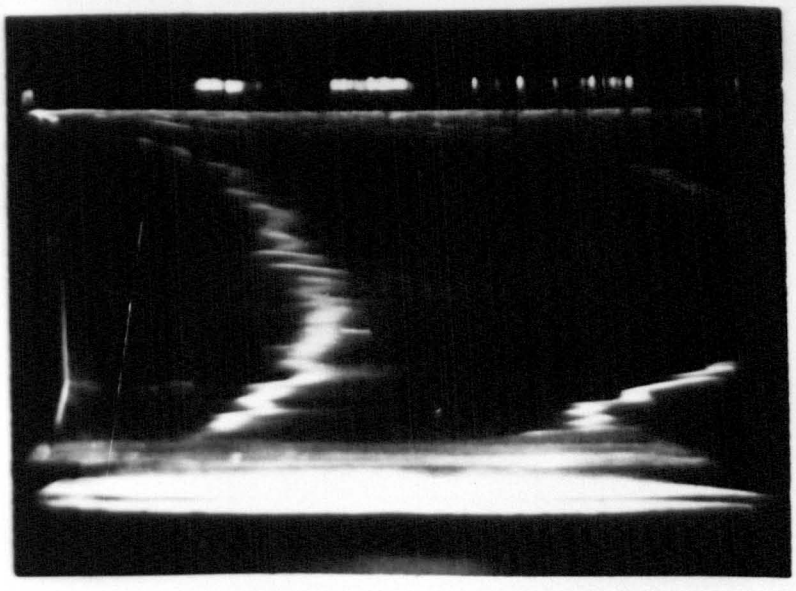

(ix) Re = 6410

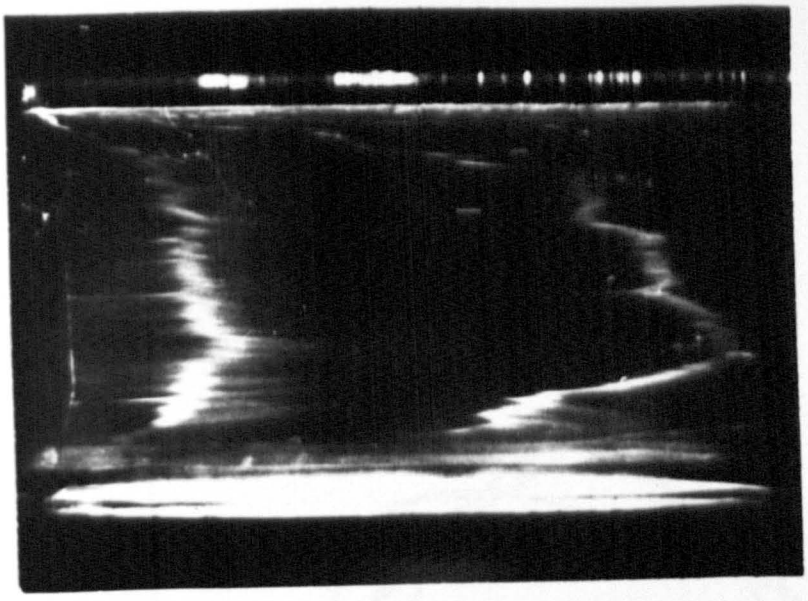

(x) Re = 6410

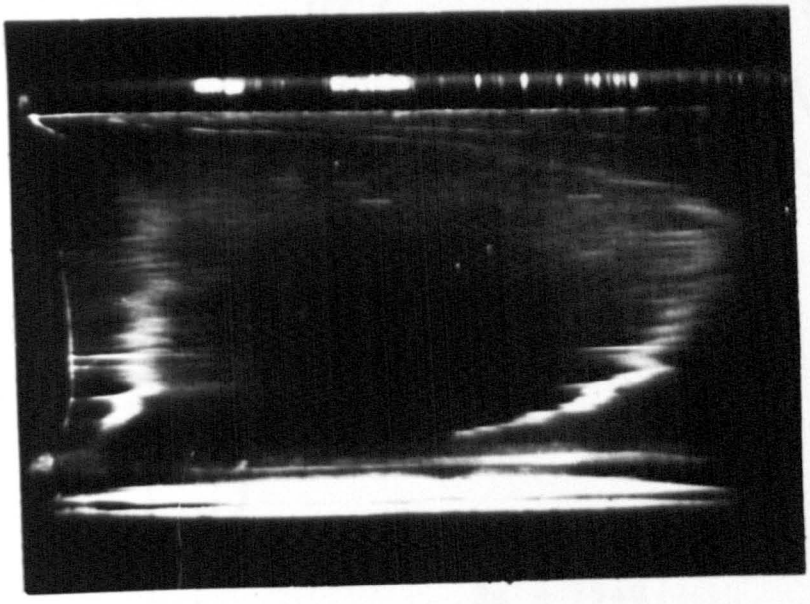

(xi) Re = 7540

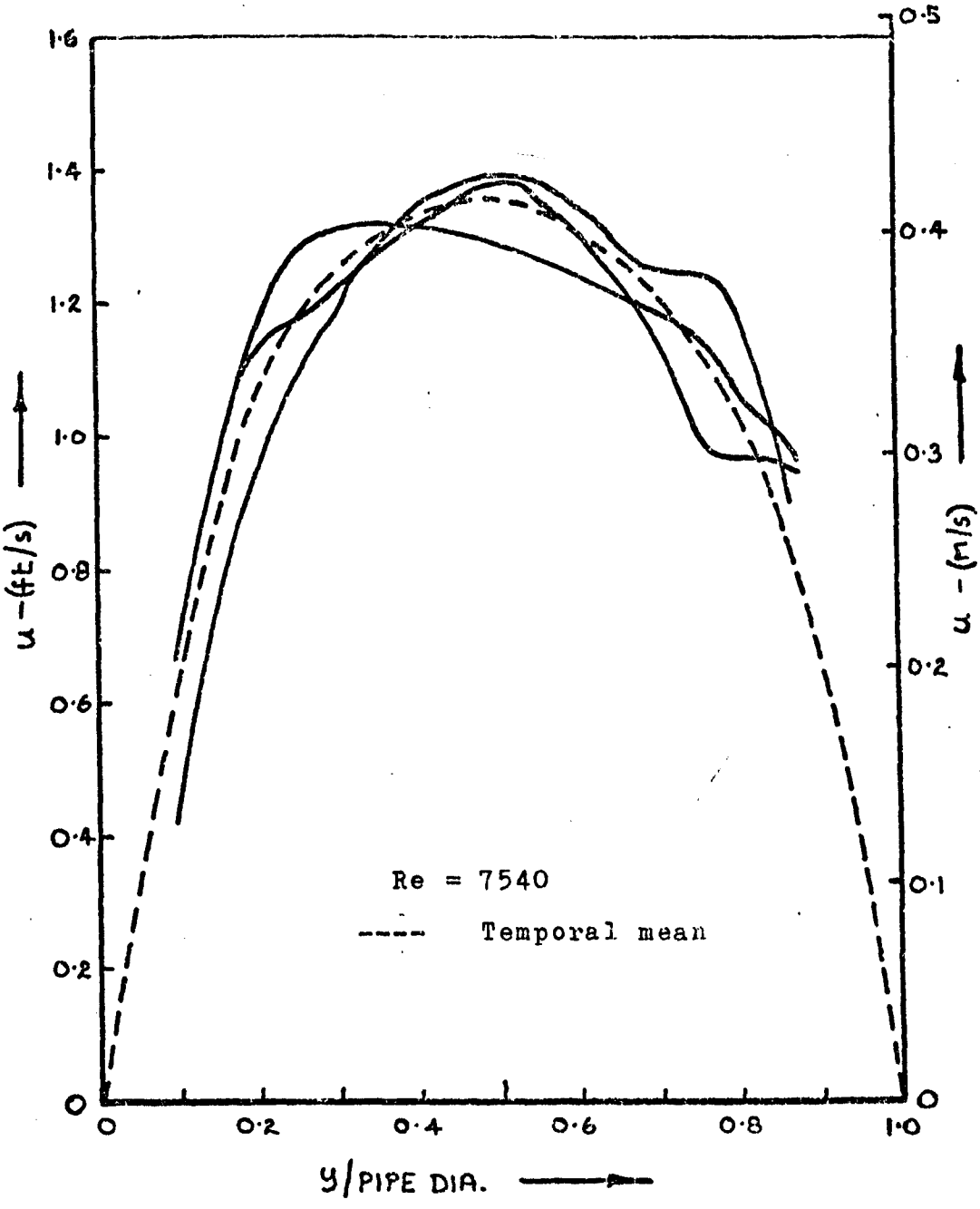

INSTANTANEOUS VELOCITY PROFILES

(Equi-molar soln. CTAB/1-naphthol, 508 p.p.m.)

Fig. 78.

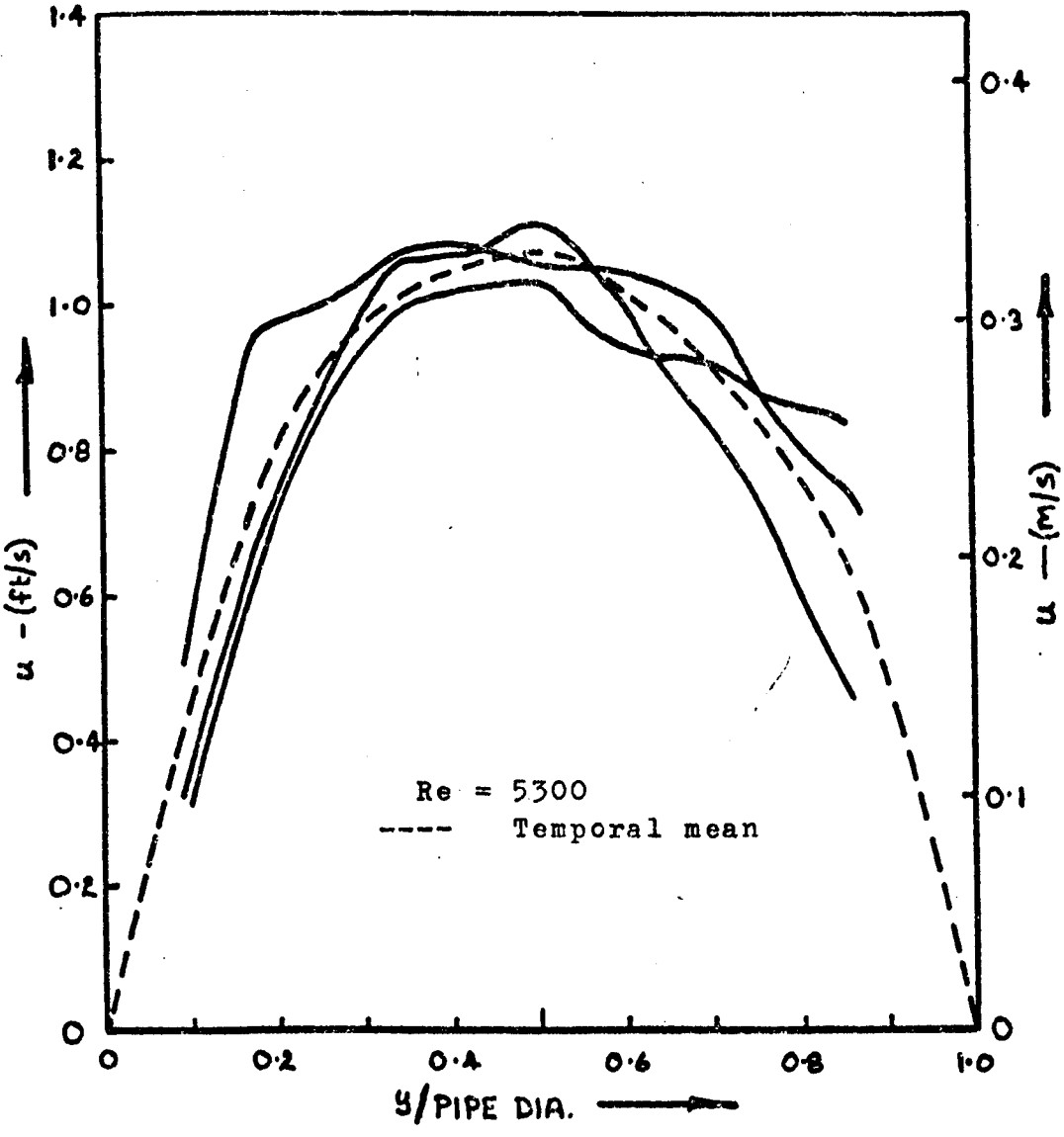

INSTANTANEOUS VELOCITY PROFILES

(Equi-molar soln. CTAB/1-naphthol, 508 p.p.m.)

Fig. 79.

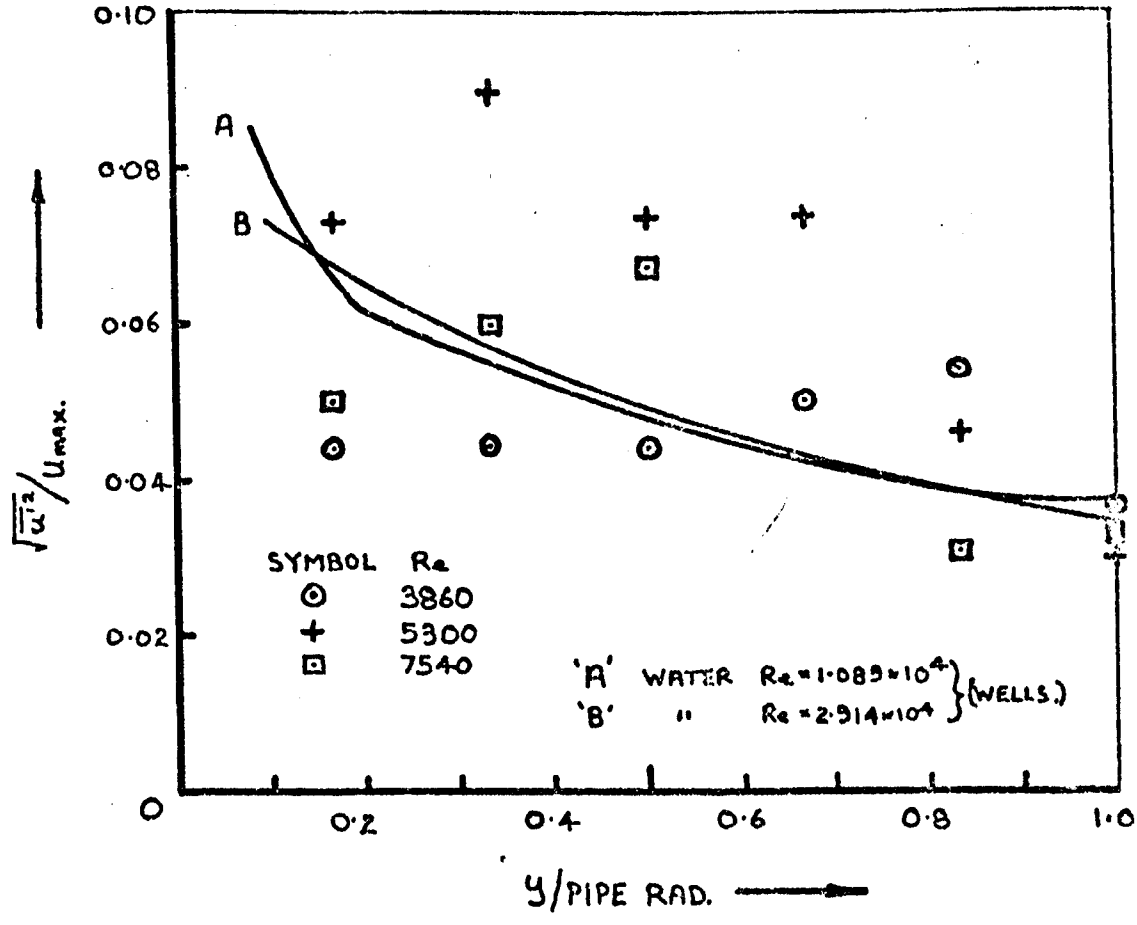

R.M.S. TURBULENCE INTENSITY.

(Equi-molar soln. CTAB/1-naphthol, 508 p.p.m.)

Fig. 80

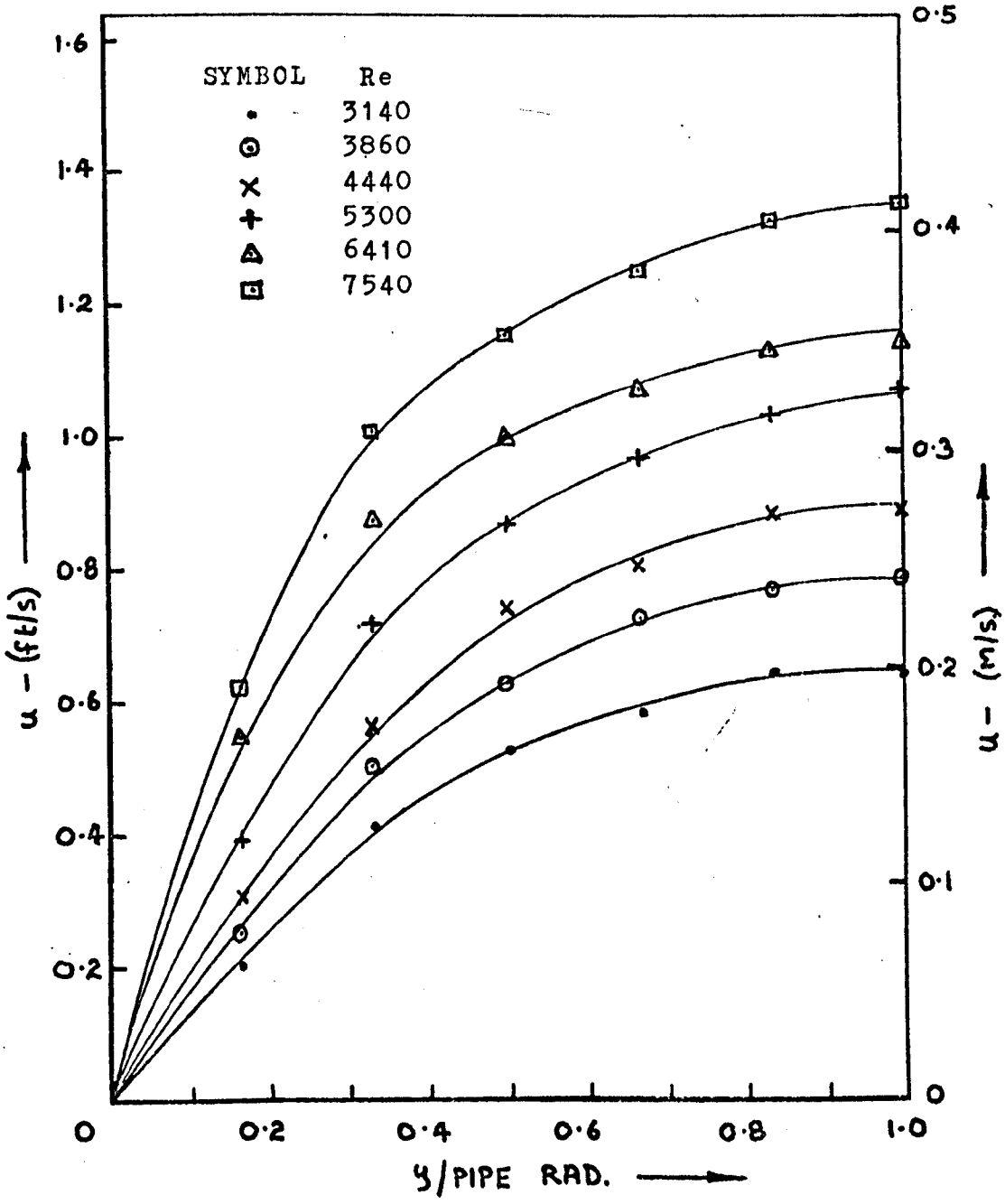

MEAN VELOCITY PROFILES.

(Equi-molar soln. CTAB/1-naphthol, 508p.p.m.)

Fig. 81.

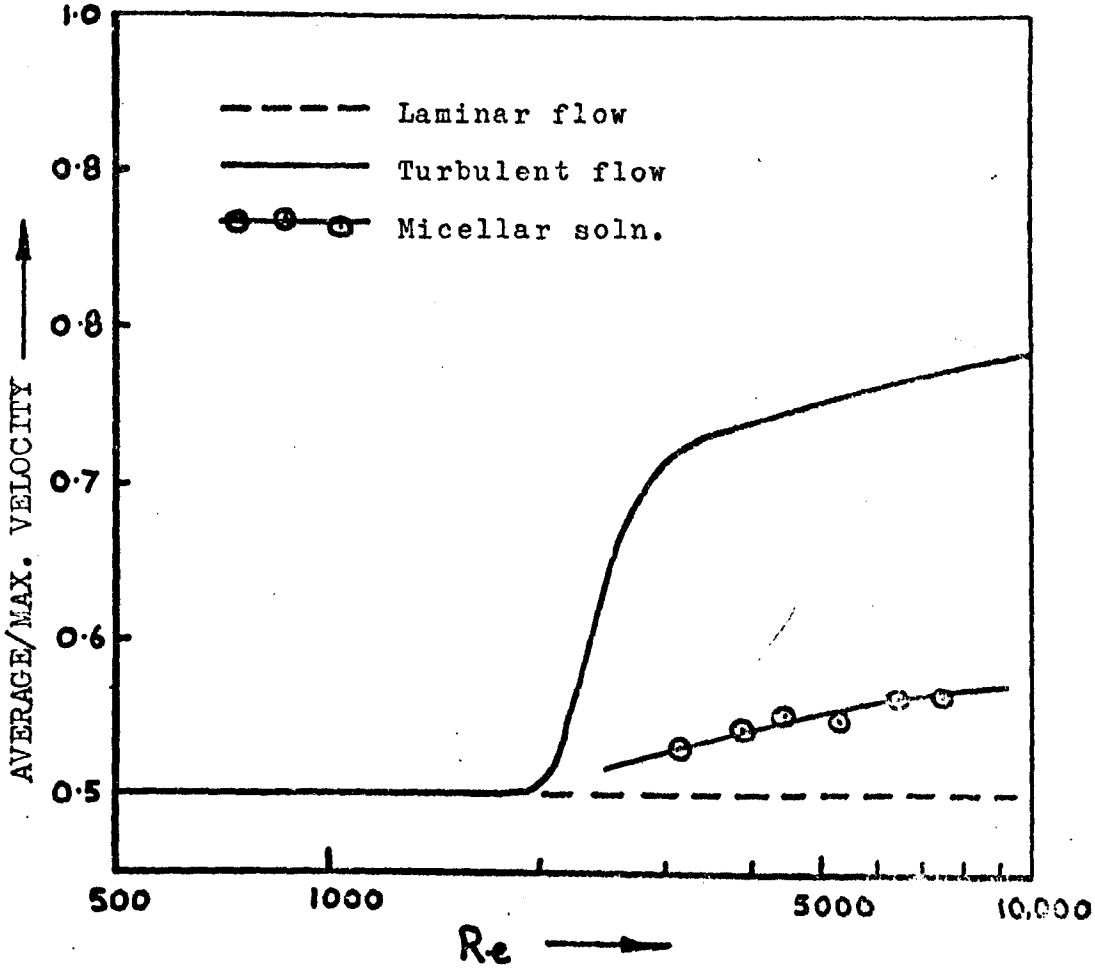

Ratio of average to maximum velocity.

Pipe flow.

Fig. 82.

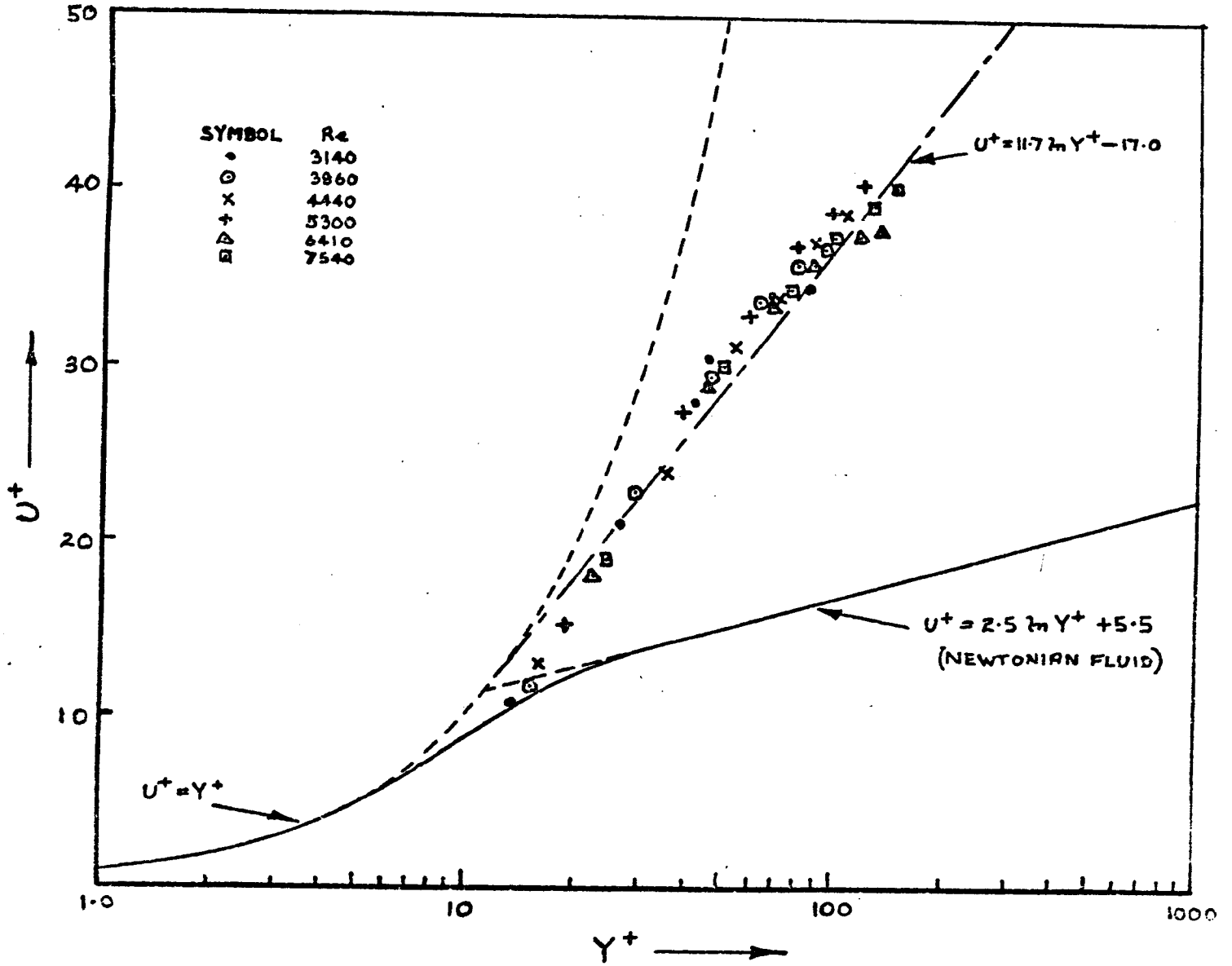

Fig.83. DIMENSIONLESS VELOCITY PROFILES

(2.8.0) THE EFFECT OF THE MICELLAR SOAP SYSTEM ON THE STRUCTURE OF A FLAT PLATE BOUNDARY LAYER

Kline and his co-workers have produced much qualititive and quantitive information on the structure of turbulent boundary layers in water by making use of the pulsed hydrogen bubble technique (72), (73). In view of the remarkable effects exhibited by the CTAB/1-naphthol solutions in pipe flow, it was decided that much useful information could be obtained from boundary layer observations on a flat plate using Kline's technique.

(2.8.1) The experimental rig and test procedure.

A small open channel was adapted for the tests as shown in fig.84. The fluid was circulated by a centrifugal pump and the flow passed through a bed of glass marbles upstream from the working section to even out the approach velocity.

Observations were made in the boundary layer on a flat plate placed at the bottom of the observation region. Due to the limited flow velocity obtainable, a trip wire was placed at the upstream end of the plate to induce turbulence in the boundary layer.

Pictures of the flow were obtained from pulses of hydrogen bubbles emitted from a 0.055mm dia. stainless steel wire stretched across a fork of 4in. (102mm) span as

shown, the distance of the wire from the plate being measured with a Vernier traverse mechanism. The bubbles were illuminated by an intense sheet of light just below their plane, as in the pipe flow experiments. The wire was situated 12in. (305mm) from the leading edge of the plate.

A series of photographs of the flow patterns with water and an equi-molar solution of CTAB/1-naphthol at 508 p.p.m. concentration were taken for several rates of flow with the wire at known distances from the wall.

(2.8.2) Experimental results.

A typical set of flow photographs with water are shown in fig.84. Unfortunately the channel velocity was not great enough to produce a full turbulent boundary layer with a logarithmic region. However, the present flow patterns near to the wall are very similar to those previously published by Kline et.al. (72), (73). These show the characteristic streaky appearance within the viscous sublayer, with regions of high and low velocity and periodic bursts away from the wall.

An end view shown in fig.86 gives some indication of the spanwise spacing and penetration of these bursts, which Kline et.al. (73) believe gives rise to the bulk of turbulence production.

The flow pictures obtained with the micellar

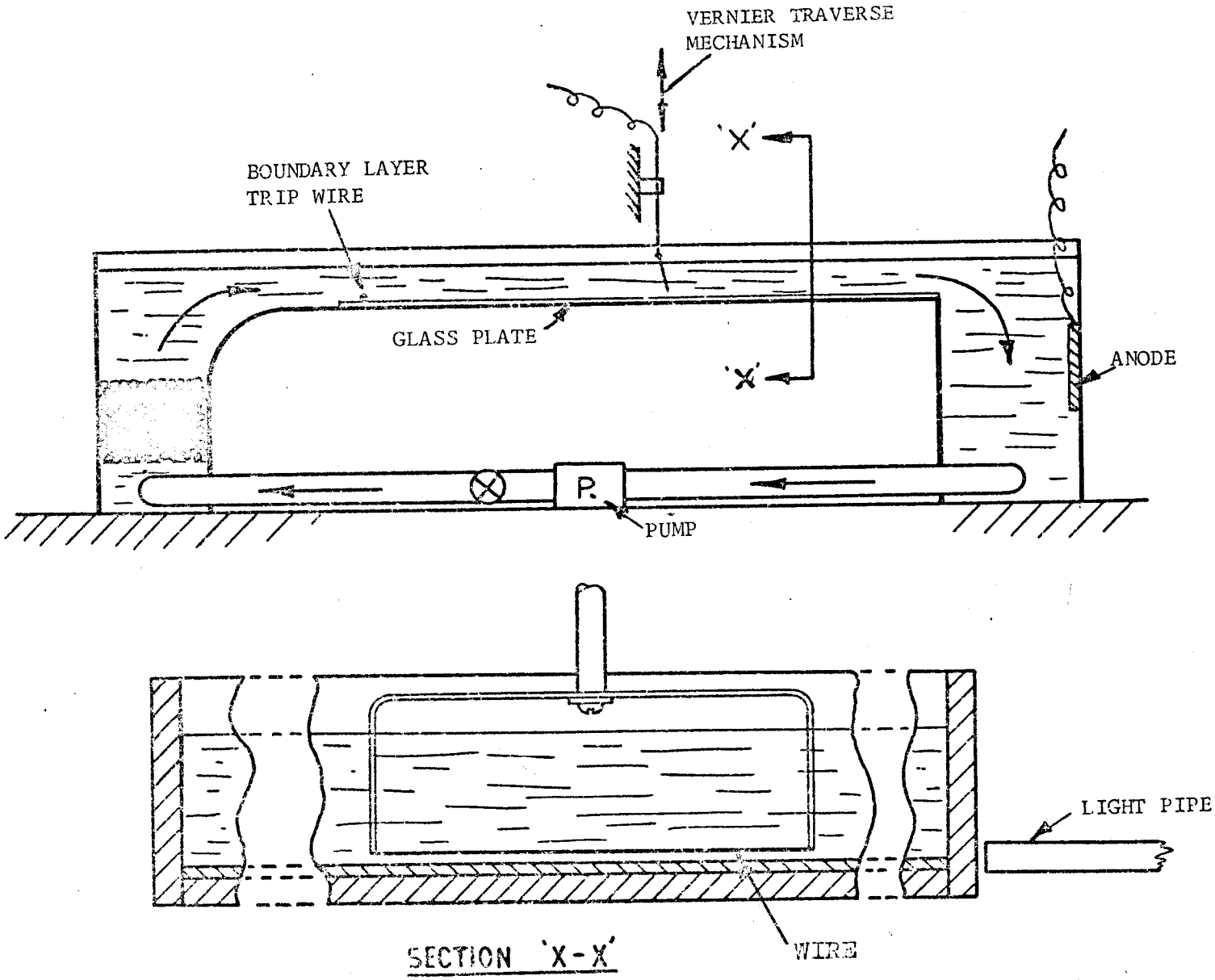

RIG LAYOUT FOR FLAT PLATE BOUNDARY LAYER OBSERVATIONS

Fig. 84

soap system seen in fig.87 are quite different in nature. Bursts of turbulence from the wall are much more passive and less frequent, and generally the flow within the sublayer is more truly laminar.

If, as suggested by Kline, the turbulence production depends mainly on the bursts, then clearly production with the soap solution is very much reduced. It was unfortunately not possible to take an end view picture with the soap solution because of slight turbidity over the relatively long distance through the fluid.

Average local velocities were determined from the flow photographs just as in the preceding pipe flow tests, and deduced velocity profiles are shown in fig.88. Curves (1) and (2) compare the soap solution and water at the same wall shear rate, which was determined from the slope of the velocity profiles at the wall. The soap solution profile is much more peaky than that with water, and this would imply a reduced wall shear stress if the soap solution were tested at the same free-stream velocity as water.

The individual photographs may be related to points on the dimensionless velocity profiles shown as fig.88

All of these present results lie within the viscous sublayer and transition regions due to the limitation of the flow rate in the small channel. The results are

useful in so far as they show reduced turbulence production and important qualitative differences between the solutions and water. It is suggested that much more information could be obtained from tests carried out in a much larger channel, to facilitate observations in the logarithmic region. Such a channel was not available when the present work was carried out.

Fig. 85. PLATES (i) to (vi)

FLAT PLATE BOUNDARY LAYER.

FLOW VISUALIZATION BY HYDROGEN BUBBLE TECHNIQUE.

WATER.

(i) $Y^+ = 0.67$

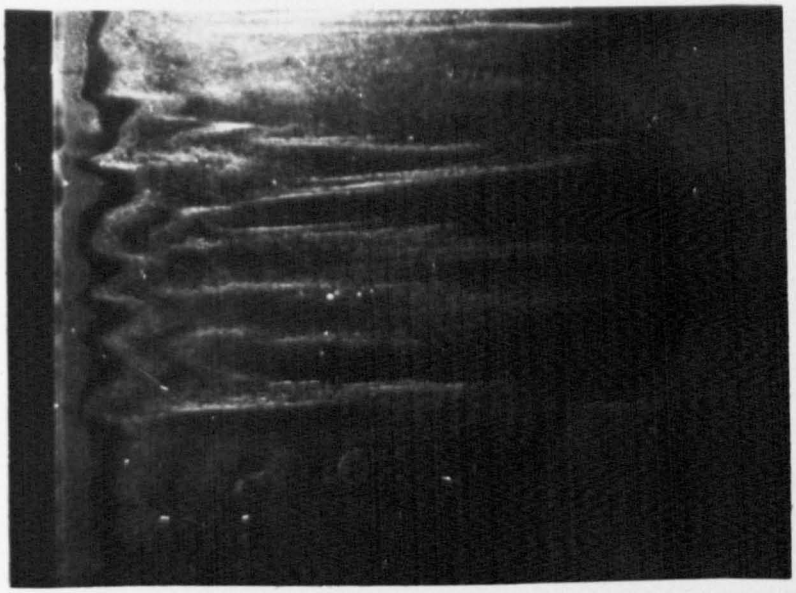

(ii) $Y^+ = 3.53$

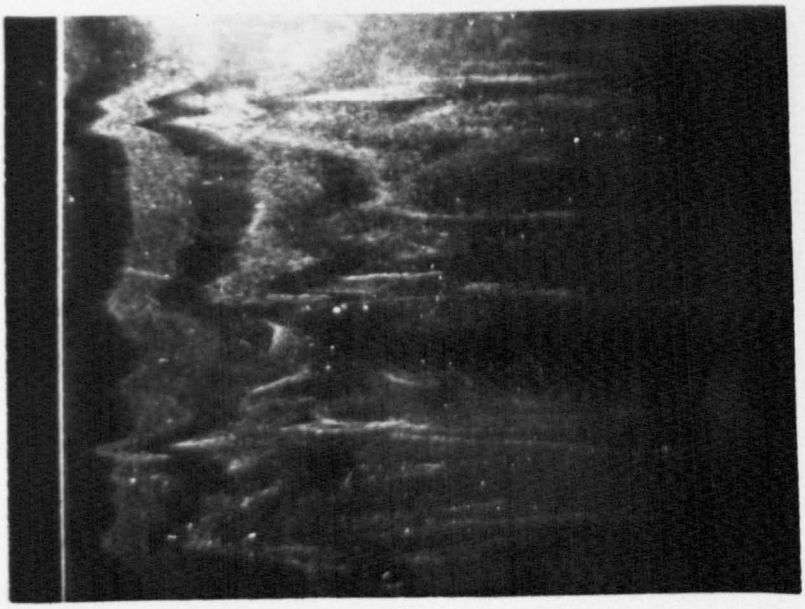

(iii) $Y^+ = 7.61$

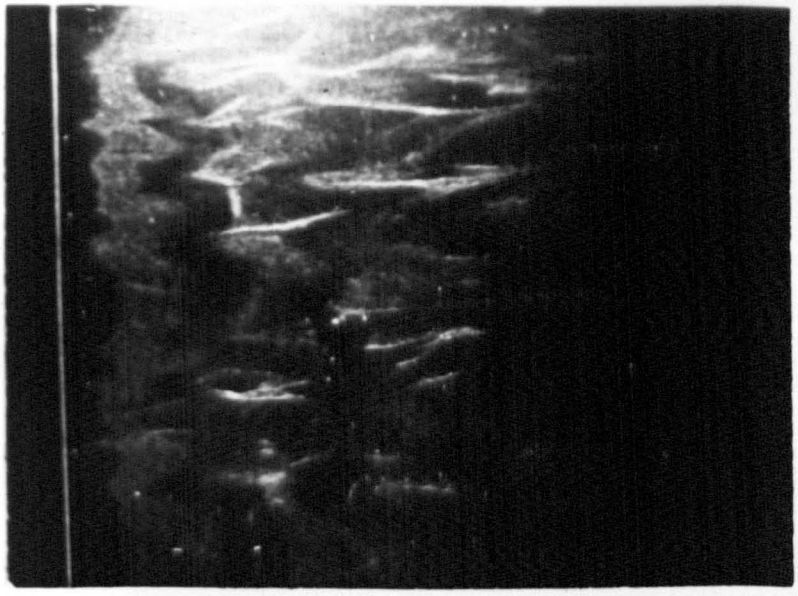

(iv) $Y^+ = 11.0$

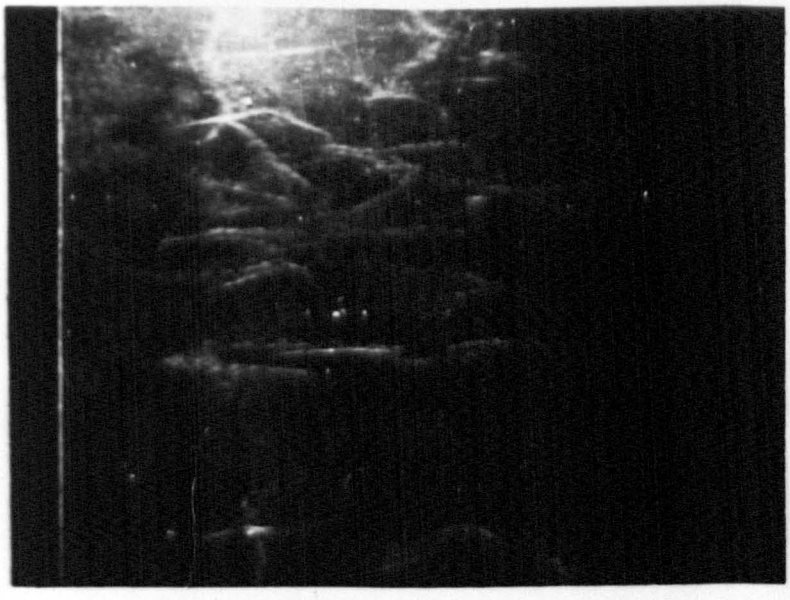

(v) $Y^+ = 17.5$

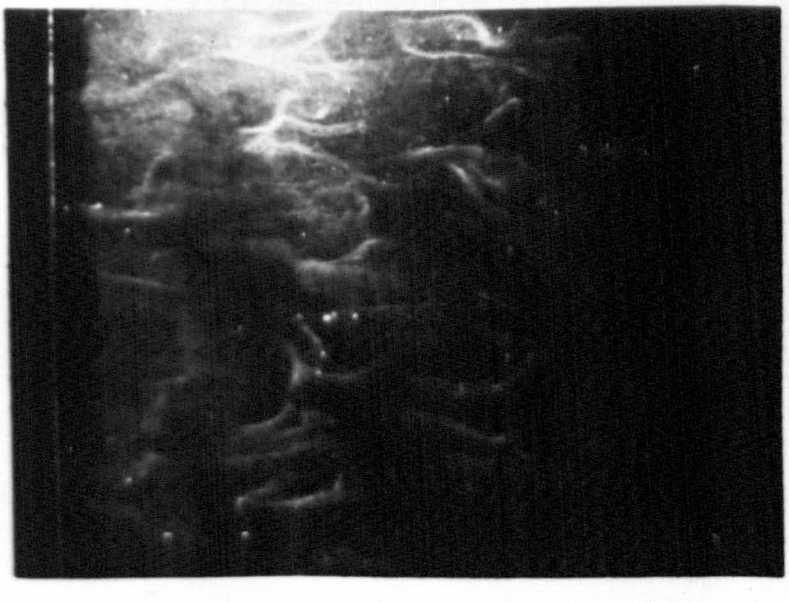

(vi) $Y^+ = 27.0$

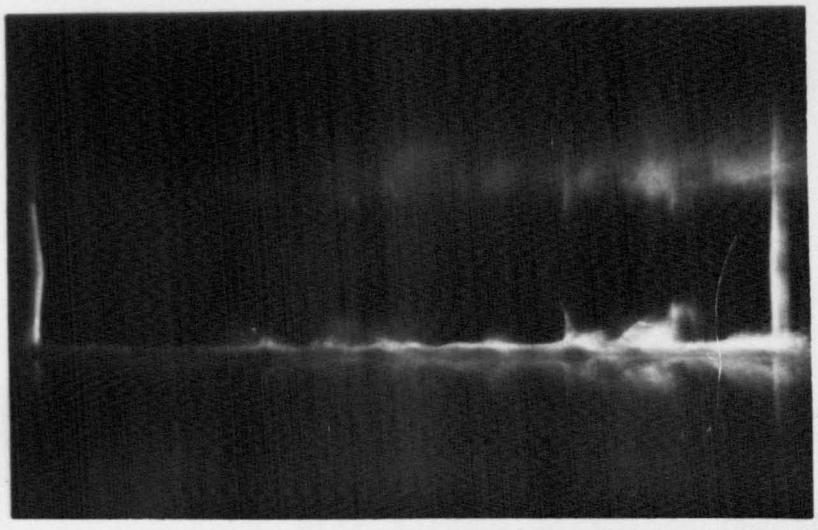

END VIEW WITH WATER SHOWING 'BURSTS'.
WIRE AT $Y^+ = 3.53$, CORRESPONDING TO
FIGURE 85 PLATE (ii).

Fig. 86

Fig. 87. PLATES (i) to (v)

FLAT PLATE BOUNDARY LAYER,
FLOW VISUALIZATION BY HYDROGEN
BUBBLE TECHNIQUE.
EQUIMOLAR SOLN. CTAB/1-NAPHTHOL
TOTAL CONC. 508 p.p.m.

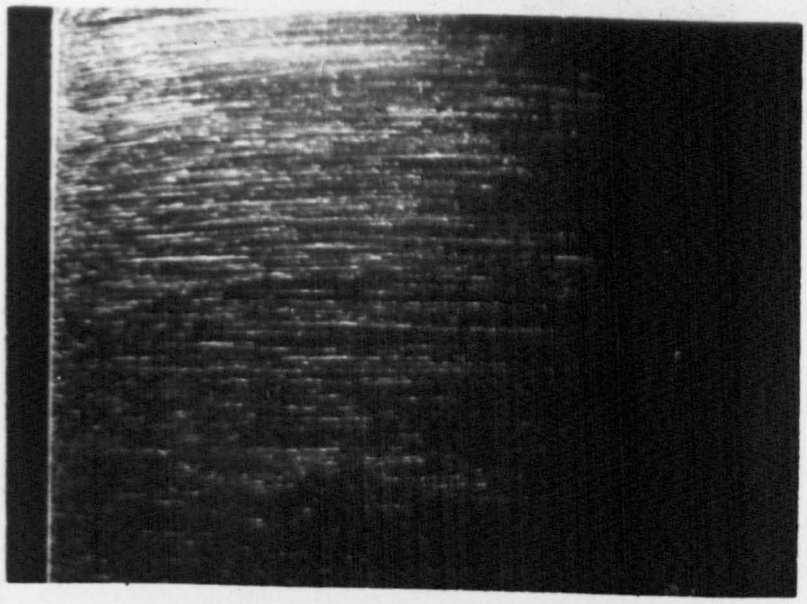

(i) $Y^+ = 1.0$

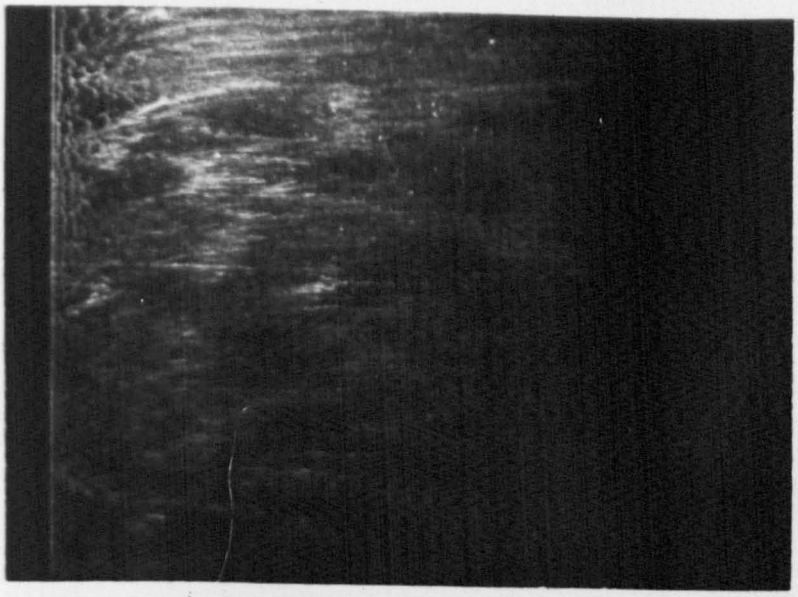

(ii) $Y^+ = 1.13$

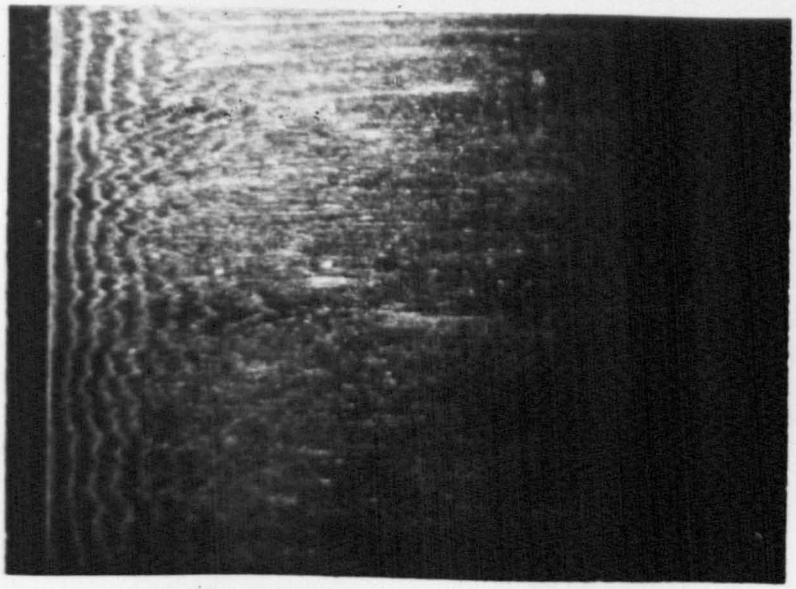

(iii) $Y^+ = 2.44$

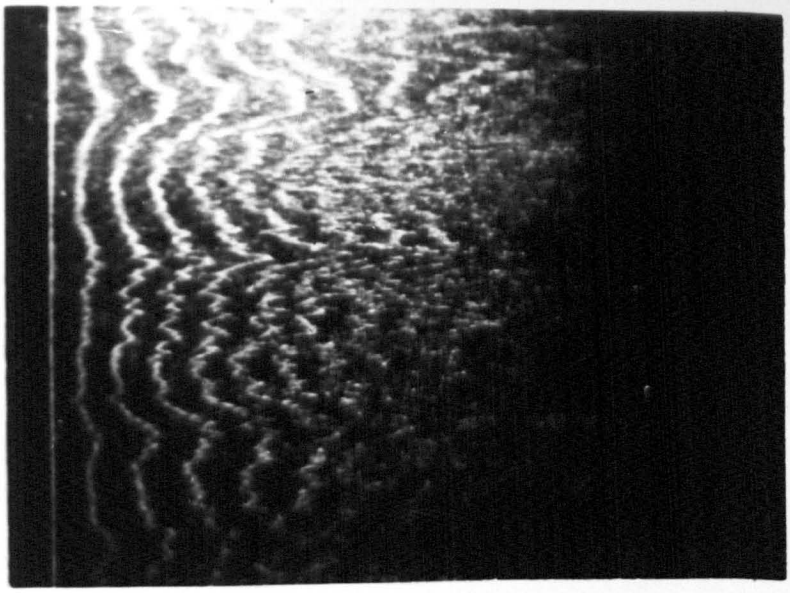

(iv) $Y^+ = 5.06$

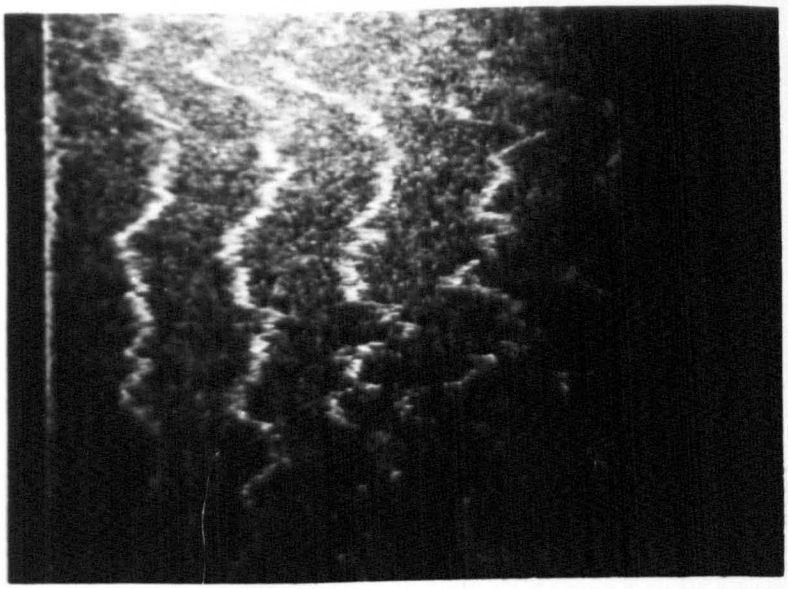

(v) $Y^+ = 16.5$

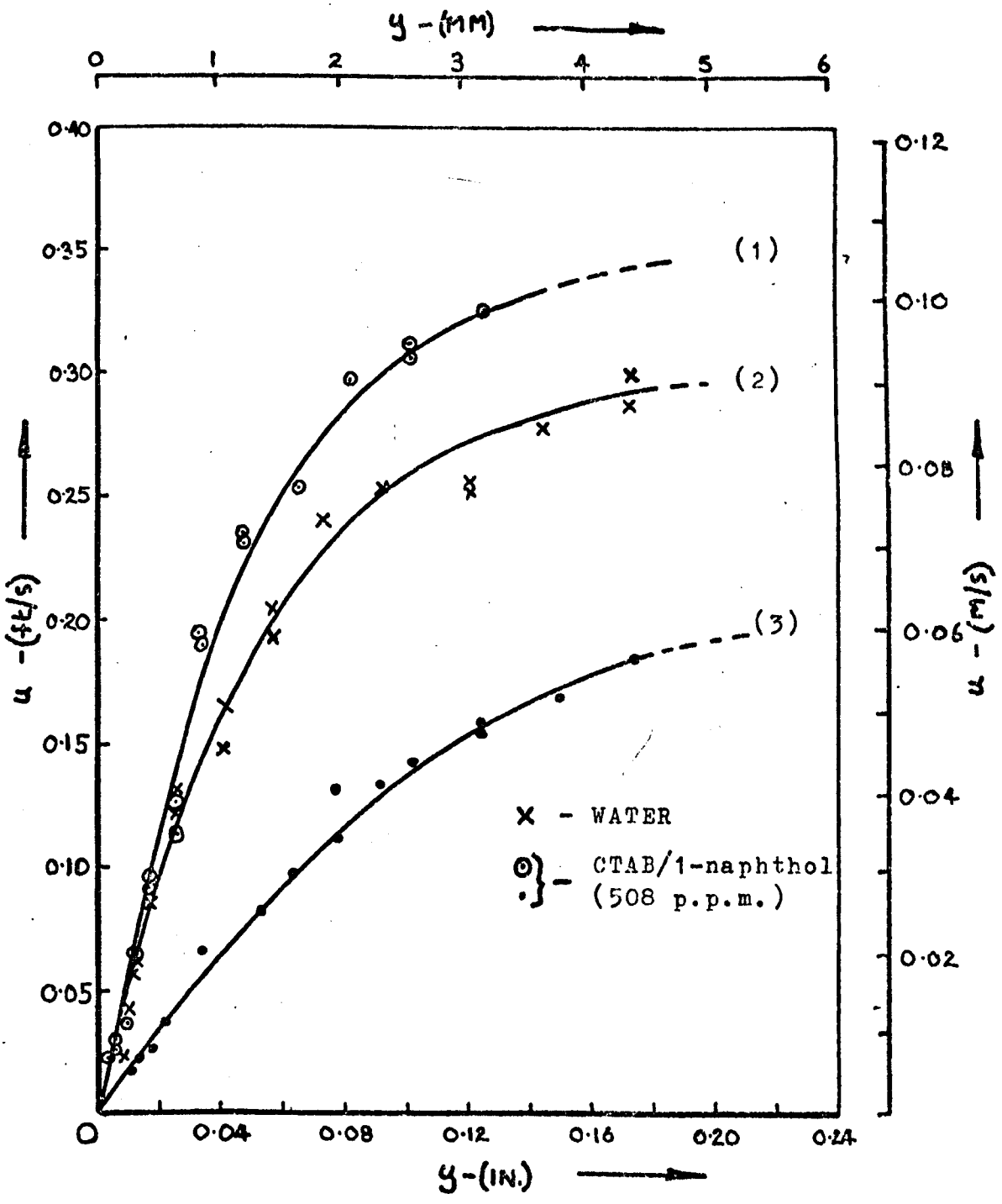

VELOCITY PROFILES - FLAT PLATE.

Curves (1)&(2) - Wall shear rate 57sec^{-1}
Curve (3) - Wall shear rate 17.5sec^{-1}

Fig. 88.

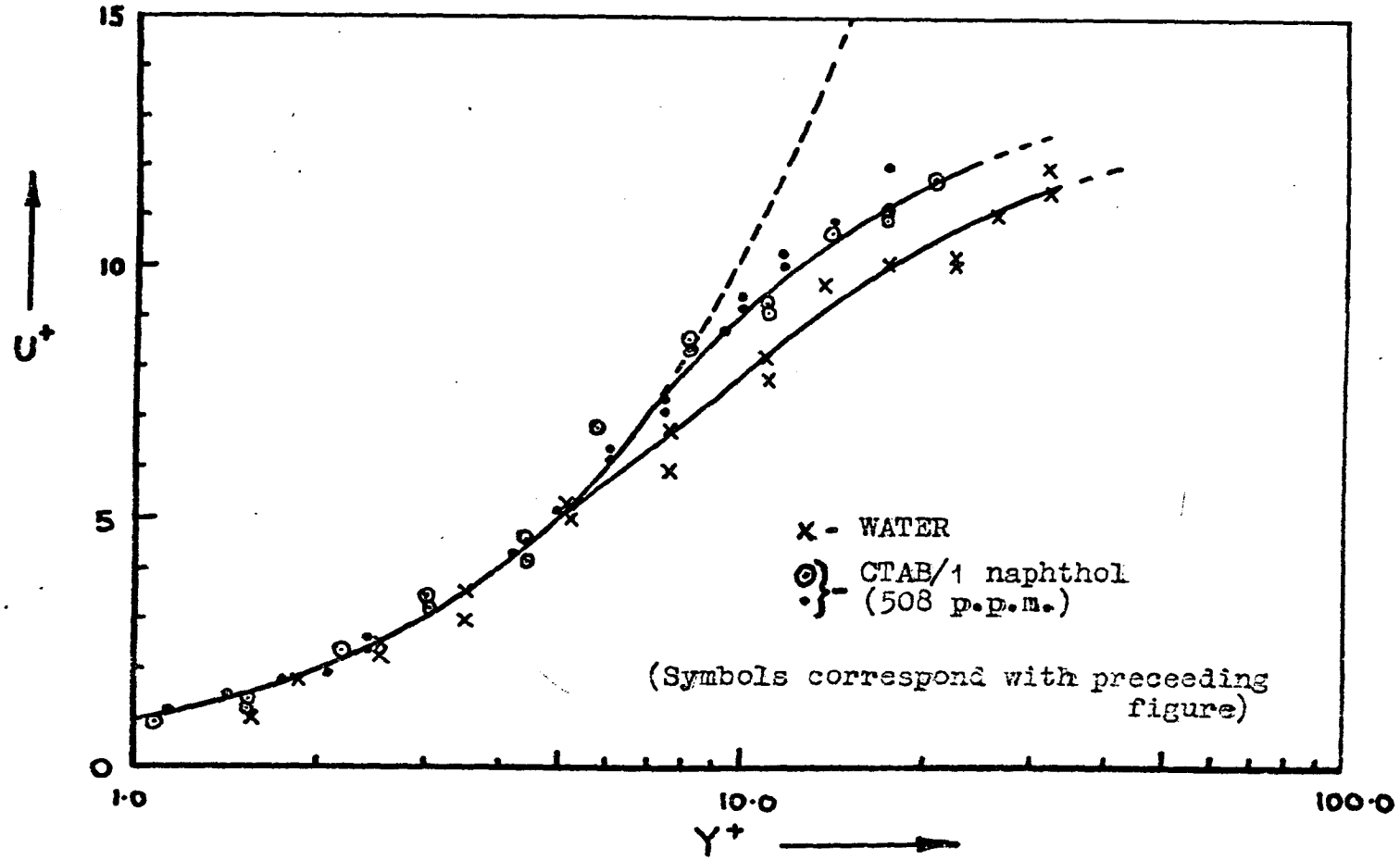

Fig. 89. DIMENSIONLESS VELOCITY PROFILES Flat plate

(2.9.0) SUBMERGED JET EXPERIMENTS.

The preceding experimental evidence suggests that the large reductions in frictional drag obtained under turbulent flow conditions with dilute polymer solutions is brought about by an increase in the thickness of the 'interactive' layer adjacent to the wall, the structure of the turbulent core being little changed. It is therefore of interest in this connection to study the turbulence structure of these solutions without the influence of a solid wall.

Submerged jets provide a means to study the flow characteristics of various additive solutions with no wall effect. Goren (61) Jackley (75) both found little difference between a polymer jet and one of water using respectively Polyox and a polyacrylamide. Gadd (76) on the other hand had previously observed that the small scale turbulence was greatly diminished with Polyox at 30 p.p.m. concentration.

In an attempt to resolve these differences some further flow visualization studies of jets were carried out with a small jet and a much larger one, using solutions of Guar gum, Polyox WSR 301, and the nonionic polyacrylamide Separan NP 10.

The small jet was produced by a rounded entry nozzle, 24mm in diameter. which was supplied with either water or polymer solution from a constant head tank, and the

jet discharged into a Perspex vessel containing a solution identical to the jet. A dye (either Fluorescein or Indian ink) was injected into the supply pipe just upstream from the nozzle in order to render the jet patterns visible.

The experiments carried out with Guar gum solution up to a concentration of 500 p.p.m. showed no apparent difference from a pure water jet, although as previously shown this concentration brings about an enormous drag reduction in turbulent pipe flow. Polyox jets on the other hand were quite different in structure with concentrations greater than about 10 p.p.m., although the difference was not really apparent with lower concentrations. With higher concentrations much of the small scale turbulence appeared to be suppressed, and flow patterns similar to Gadd's were observed. This certainly indicates a change in the spectrum of turbulent kinetic energy. The submerged jets of Separan solution were similar in nature to the Polyox jets except that a concentration of about 70 p.p.m. was required to produce an observable damping effect. No significant differences in the jet patterns were observed over the whole of the Reynolds number range investigated - between 3,500 and 20,000 (based on the nozzle diameter). Photographs of some of the jet patterns are reproduced in fig.90.

For the larger scale experiments, the jet was produced by a straight length of 3/4 in. (19.05mm) dia. pipe, which was again supplied with fluid from a header

tank and discharged into a transparent container. Dye was injected into the centre of the jet pipe 8 in. (203mm) from the exit end. This apparatus is shown in fig.91.

From all the tests the jet patterns were very similar to those observed with the smaller apparatus. The effect of Polyox concentration on the flow structure is clearly shown in figs.92 and 98. Once again much of the small scale eddying disappears with concentration increase and only very large eddies remain. Furthermore, with the water jet the dye has diffused completely across the pipe at the exit, but this is not the case with the higher concentrations of Polyox solution. This could be partly due to reduced diffusion in the core region, or possibly could be caused by the greatly thickened interactive layer along the pipe wall.

The jets with Guar gum solution at 500 p.p.m. were not distinguishable from those with water. It was also found that after ageing the Polyox solutions for about one week these jets too were indistinguishable from water, but the same solutions still produced considerable friction reduction in turbulent pipe flow.

Although these observations are at best only rough and qualitative, they are clearly related to the flow characteristics of Polyox solution in the threaded pipe previously discussed.

Fig. 90. PLATES (i) to (iv)

SUBMERGED JETS.

(SMALL JET RIG.)

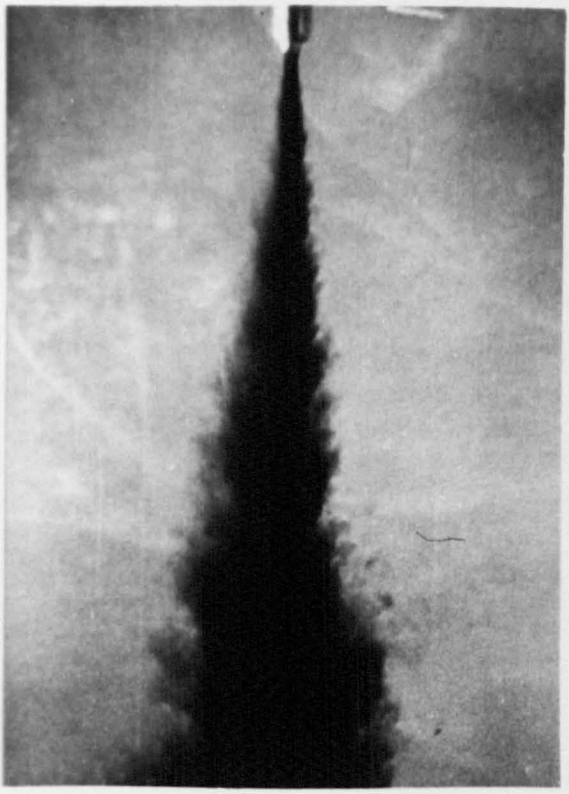

(i) WATER

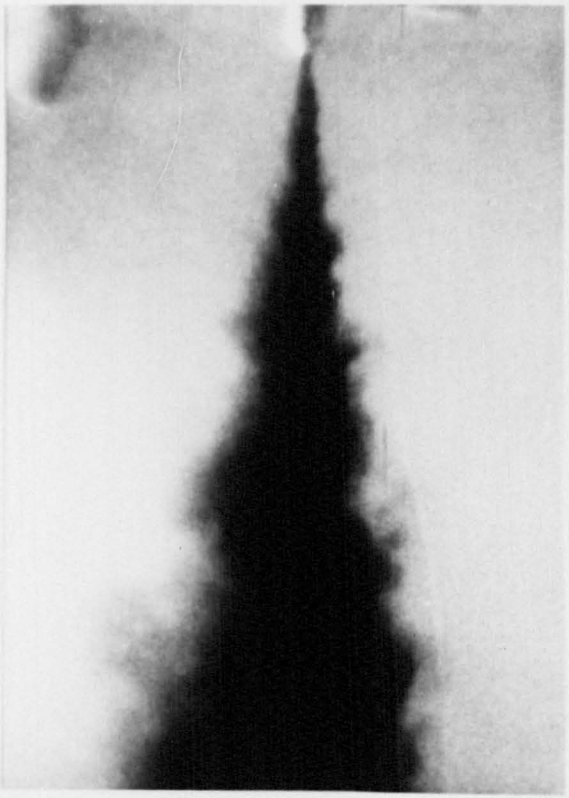

(ii) GUAR GUM SOLN.
500 p.p.m. Conc.

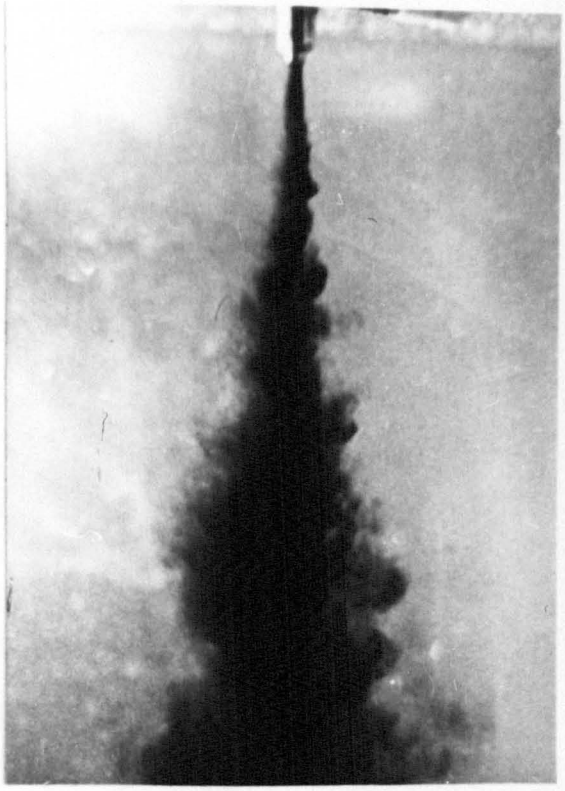

(iii) POLYOX WSR 301
SOLUTION
10 p.p.m. Conc.

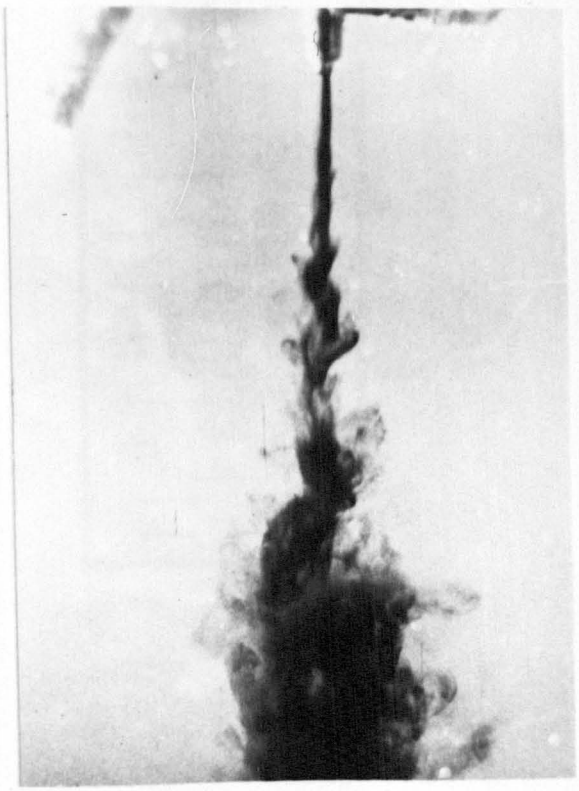

(iv) POLYOX WSR 301
SOLUTION
30 p.p.m. Conc.

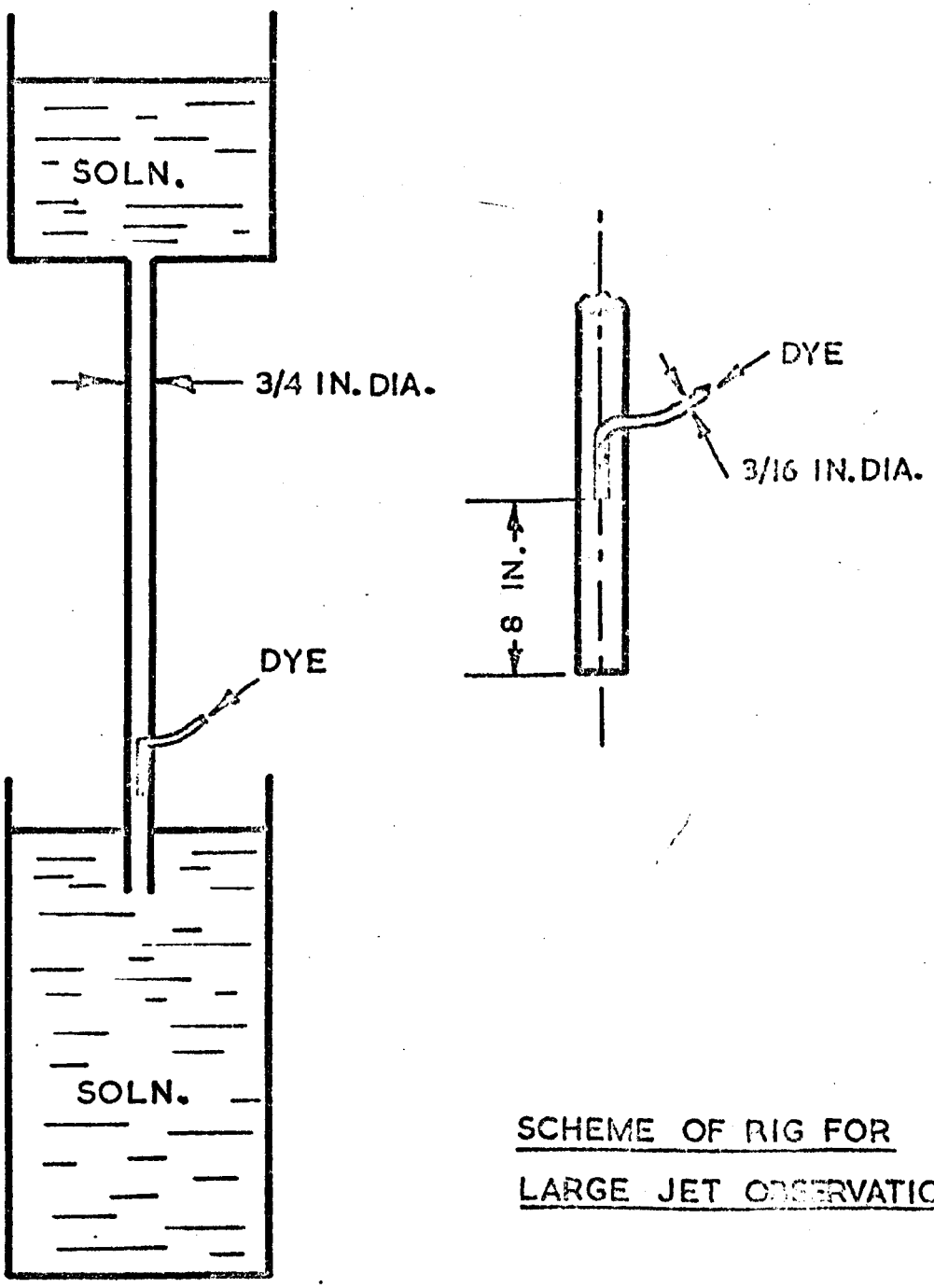

SCHEME OF RIG FOR LARGE JET OBSERVATIONS

Fig. 91.

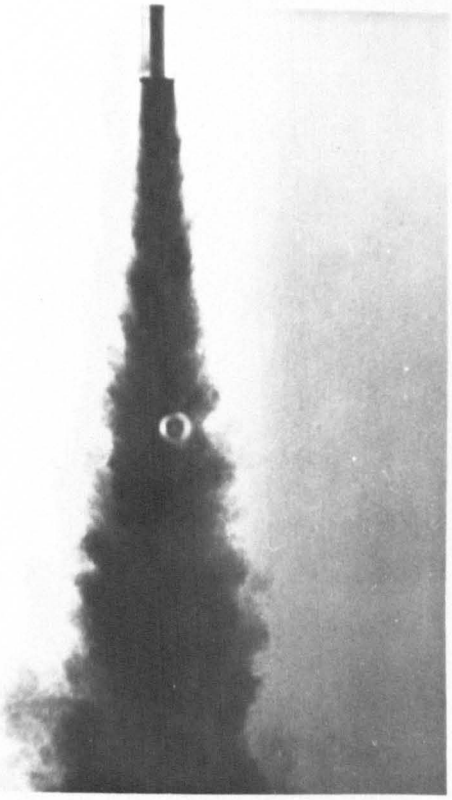

WATER
Fig. 92

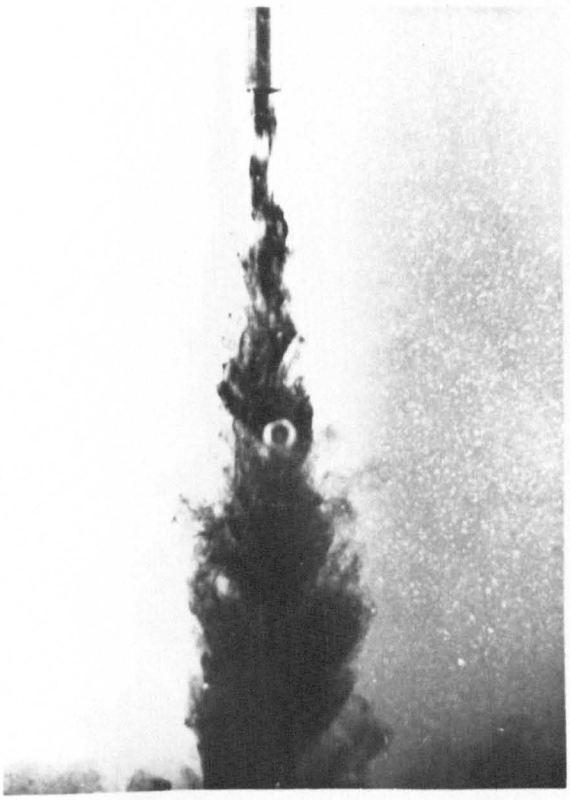

POLYOX WSR 301 SOLN.
50 p.p.m. Conc.
Fig. 93

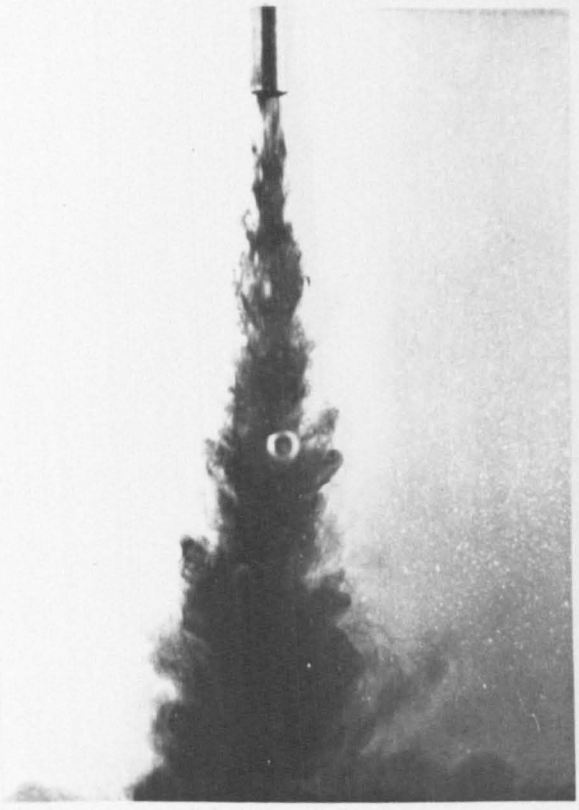

POLYOX WSR 301 SOLN.
20 p.p.m. Conc.
Fig. 94

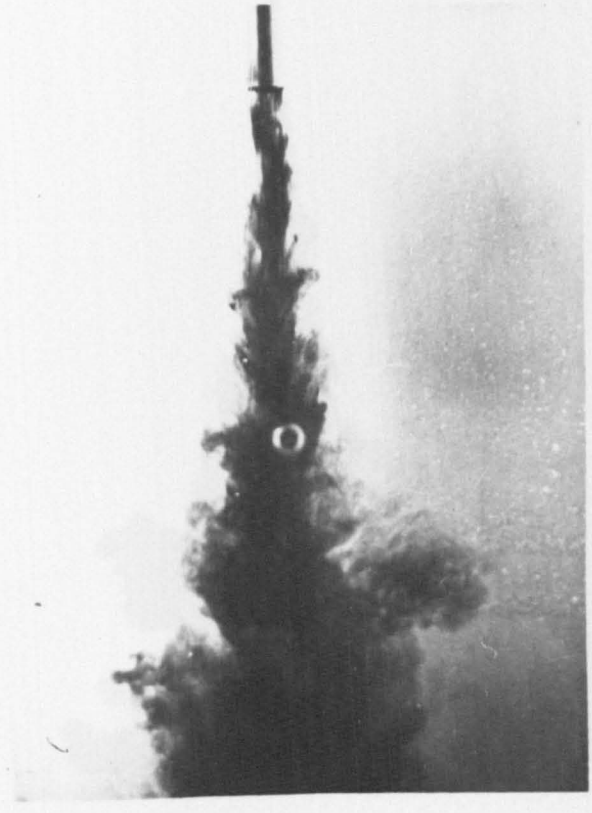

POLYOX WSR 310 SOLN.
15 p.p.m. Conc.
Fig. 95

POLYOX WSR 301 Soln.
10 p.p.m. Conc.
Fig. 96

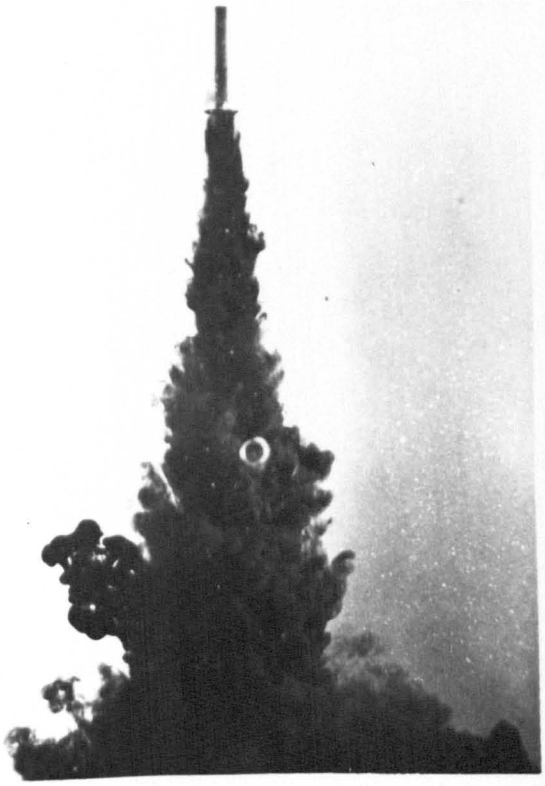

POLYOX WSR 301 Soln.
8 p.p.m. Conc.
Fig. 97

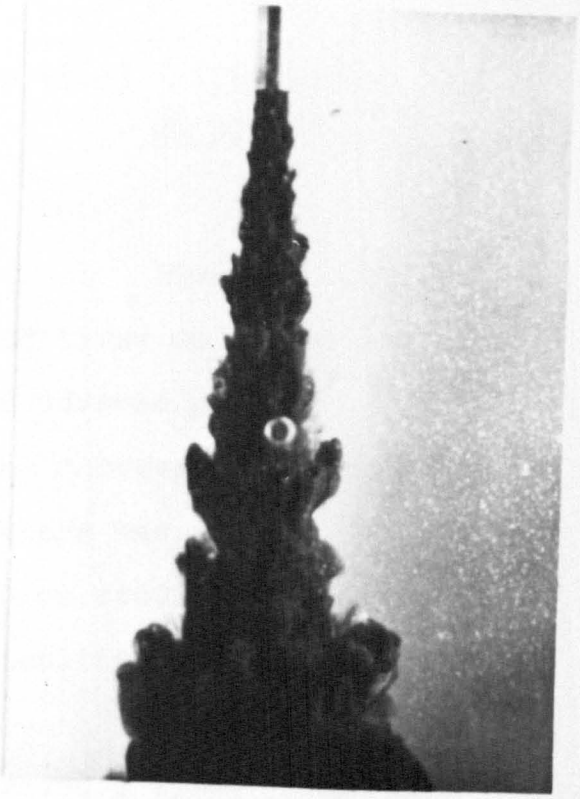

POLYOX WSR 301 SOLN.
50 p.p.m. Conc.
Whole of jet solution pre-dyed prior to test.
Fig. 98

(2.10.0) THE EFFECT OF DRAG REDUCING ADDITIVES ON BOUNDARY LAYER SEPARATION AND FORM DRAG ON SUBMERGED BODIES.

In this section the effects of drag reducing additives on the separation of boundary layers in regions of adverse pressure gradient are discussed, together with the corresponding effects on wake size and form drag. A sphere was selected as the simple geometrical shape for these studies since this minimized the experimental difficulties.

The characteristics of ordinary Newtonian flow around a sphere are shown in fig.99, and are well documented, see for example Goldstein (14), Schlichting (13) or any basic text on fluid dynamics. Briefly, at very low Reynolds numbers the drag is given by Stokes law, flow separation occurs as the Reynolds number increases, the boundary layer becomes turbulent when the Reynolds number reaches about 2.10^5 and above this value the wake size and drag is much reduced. This transitional Reynolds number may be reduced somewhat by freestream turbulence or by roughness on the sphere surface.

We have seen that polymeric additives can drastically change the structure of a turbulent boundary layer by greatly thickening the interactive zone close to the wall. If we now consider the case of a sphere in a flow with the Reynolds number exceeding the critical value, i.e.

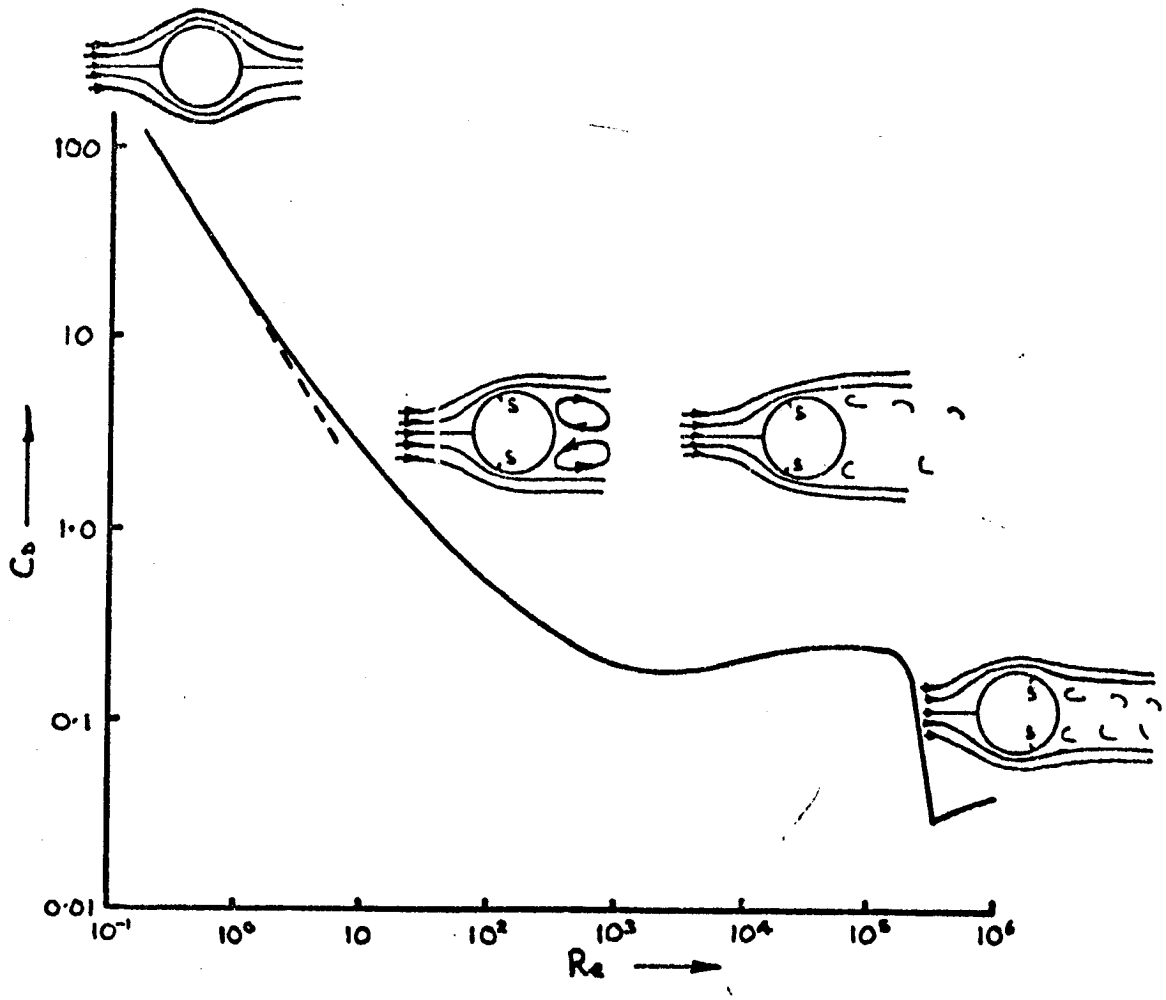

NEWTONIAN FLOW AROUND A SPHERE.

Fig. 99.

with a turbulent boundary layer, the addition of some polymer additives could possibly increase the drag. The reason being that the additive could result in a much thicker, more 'laminar like' interactive layer adjacent to the surface, with a consequent earlier separation point and increased wake size. This should be particularly apparent with freshly mixed solutions of Polyox at moderate concentrations. The following simple experiment was carried out in order to verify this hypothesis:-

(2.10.1) An experiment to demonstrate the effect of Polyox on boundary layer separation.

For this experiment a concrete sphere was dropped into a Perspex sided tank which contained either water or dilute Polyox solution, and the wake patterns were recorded by high speed cine photography. A very rough comparison of the drag coefficients was also determined from the rate of retardation after impact with the fluid.

The sphere was cast in a selected glass lampshade, which was broken away after the mix had cured. The model was then made hydrodynamically smooth by filling, rubbing down with abrasive paper, and painting with several coats of black paint.

Fig.100 shows the arrangement of the rig used for these tests, the sphere being released from a suitable height so that the Reynolds number on impact with the fluid

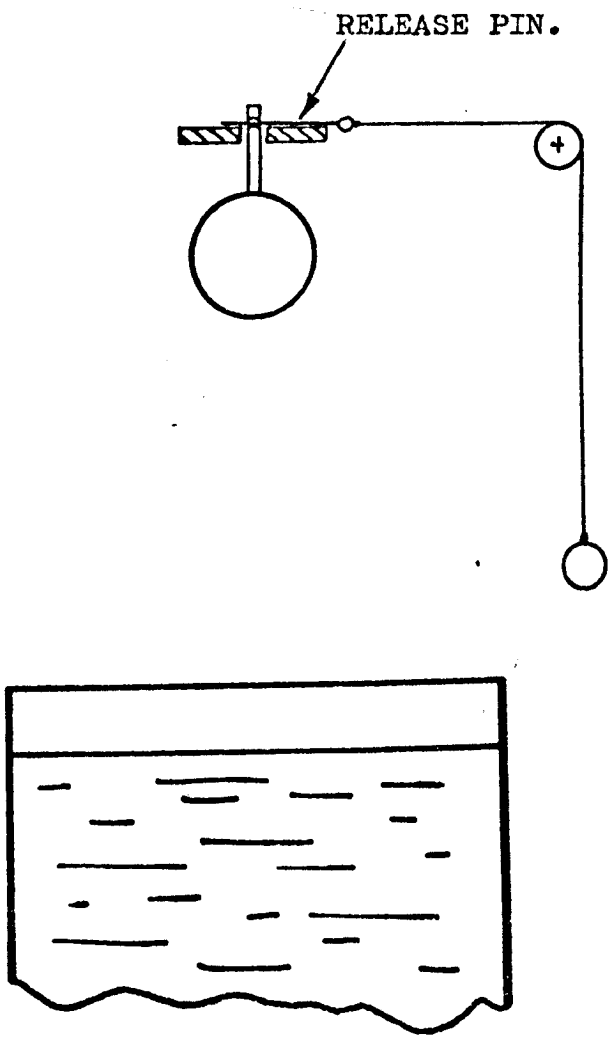

Drop Arrangement For Large Sphere.

Fig. 100.

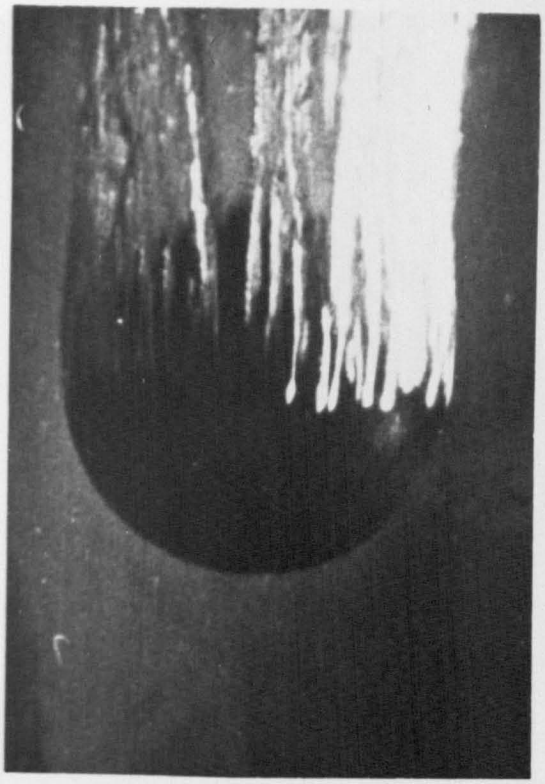

WATER - LAMINAR
BOUNDARY LAYER

Fig. 101

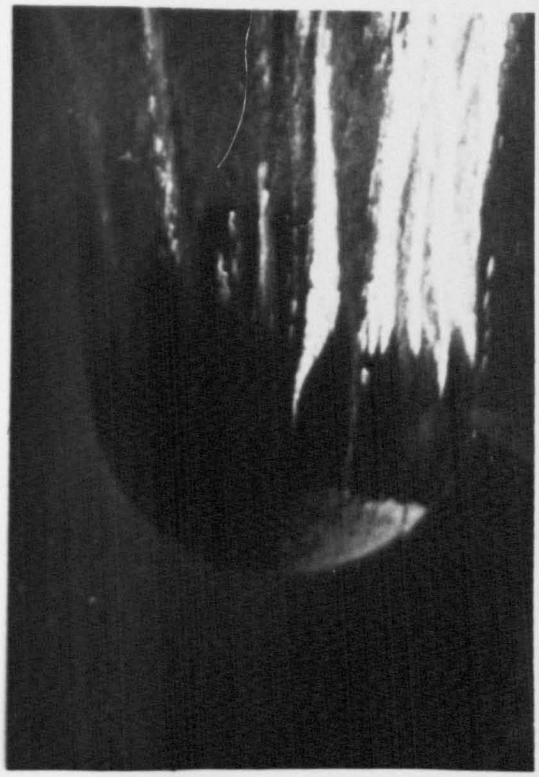

WATER - TURBULENT
BOUNDARY LAYER

Fig. 102

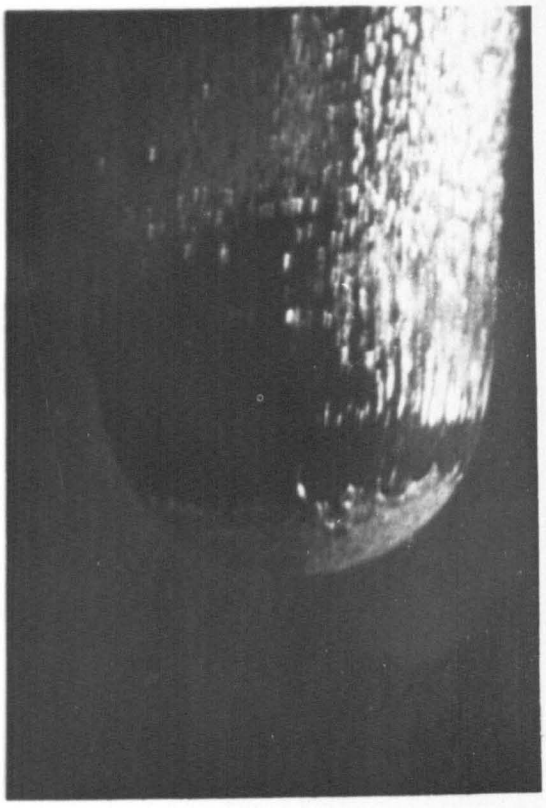

POLYOX WSR 301 SOLN.
60 p.p.m. Conc.
Fig. 103

was just below the critical value ($Re = 2.10^5$).

For the first test the sphere was dropped into water, and fig.101 shows a single frame from the ciné film. This indicates a laminar boundary layer with characteristic early separation.

The front of the sphere was then roughened by glueing on a patch of sand, and the sphere was again dropped into the water from the same height. Fig.102 shows the wake pattern from this test which exhibits a much later separation point caused by the turbulent boundary layer. The drag coefficient was roughly half the value found from the previous test.

These results are of course as expected, and indeed similar pictures have been reported by the U.S.Naval Undersea Test Station (77), see also ref. (78).

For the third test the sphere was dropped into a freshly mixed solution of Polyox at 60 p.p.m. concentration. Fig.103 shows that polymer additive has drastically affected the boundary layer and caused the separation point to move forward again with a resulting increase in form drag. The drag coefficient was of the same order as the first test.

It is therefore seen from this rather basic experiment that although polymer addition can significantly reduce skin friction, the effect can in certain circumstances be more than offset by an increase in form drag caused by a change in the separation point and wake size. We must

note of course that the sphere was followed by an air filled cavity in these experiments whereas in the following we have a liquid filled wake. The two situations are not necessarily the same.

(2.10.2)Sphere drop tests in friction reducing solutions.

Some experimental results reported by D.A.White (79), Lang and Patrick (80) and Sanders (81) showed that the drag on a sphere in water was considerably reduced by adding Polyox. Their experiments were all carried out below the critical Reynolds number, where the boundary layer is laminar, and the results were somewhat surprising since friction reduction in pipe flow only occurs in the turbulent flow regime. Flow visualization studies by Lang and Patrick showed delayed boundary layer separation and smaller wake size with the Polyox solutions which is consistent with the measured reduction of drag.

The experimental results from the preceding section indicated that drag could be increased when working above the critical Reynolds number, and in order to relate this to the above results a comprehensive series of experiments were planned to cover a wider range of Reynolds number and to span the critical region.

The technique of measurement was simple, and similar to that used by the previous investigators. Steel spheres were dropped down through cylinders containing the

test liquid, the spheres being released from a point just below the liquid surface by an electro-magnet. The apparatus was kept in a darkened room and for each test the falling sphere was illuminated by a strobo-flash unit operating at mains frequency (50 hz). Measurements from multiple image photographs on high speed 'Polaroid' film of 10,000ASA rating enabled the terminal velocities to be determined, from which the corresponding drag coefficients were calculated.

Two rigs were used: spheres between 0.25 in. (6.35mm) and 1.5 in. (38.1mm) in diameter were dropped into a Perspex tube 10ft. (3.05m) high by 6 in. (152.4mm) in diameter, and the larger spheres ranging in diameter from 1.5 in. (38.1mm) to 4.5 in. (114.3mm) were dropped into a steel vessel 22ft (6.7m) high by 2ft (0.61m) in diameter which had Perspex windows at the bottom for observation purposes. The arrangement of this larger rig is shown in fig.104. The spheres were retrieved after use by means of a catch net which was lowered to the bottom of the containers prior to each test. It was found that frequently the spheres deviated from a vertical path during their descent and struck the sides of the containers: in all such cases the results were discarded.

(2.10.3) Sphere drag characteristics in Polyox solutions.

The results obtained from both rigs with water

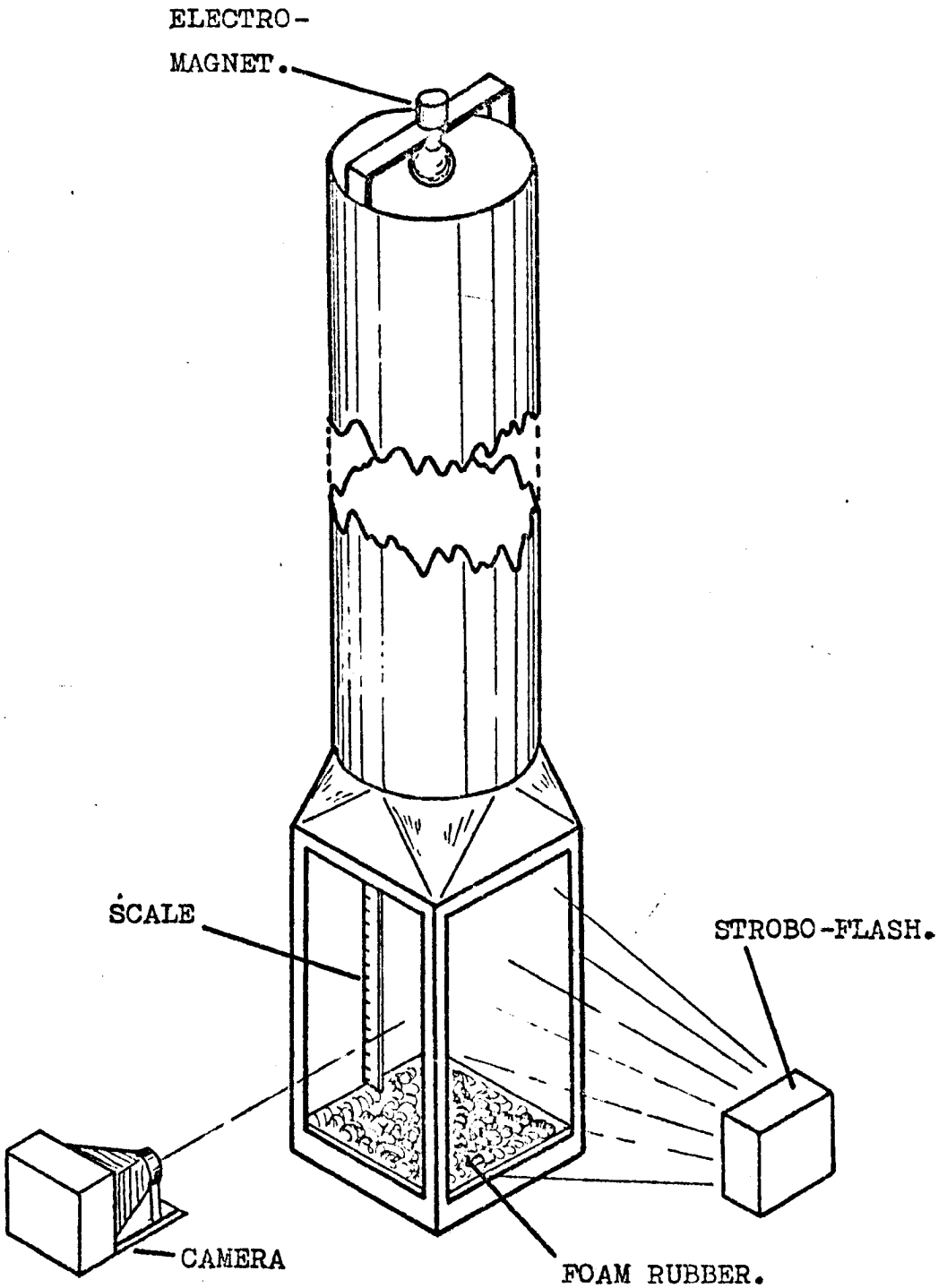

LARGE RIG FOR SPHERE DROP TESTS.

Fig. 104.

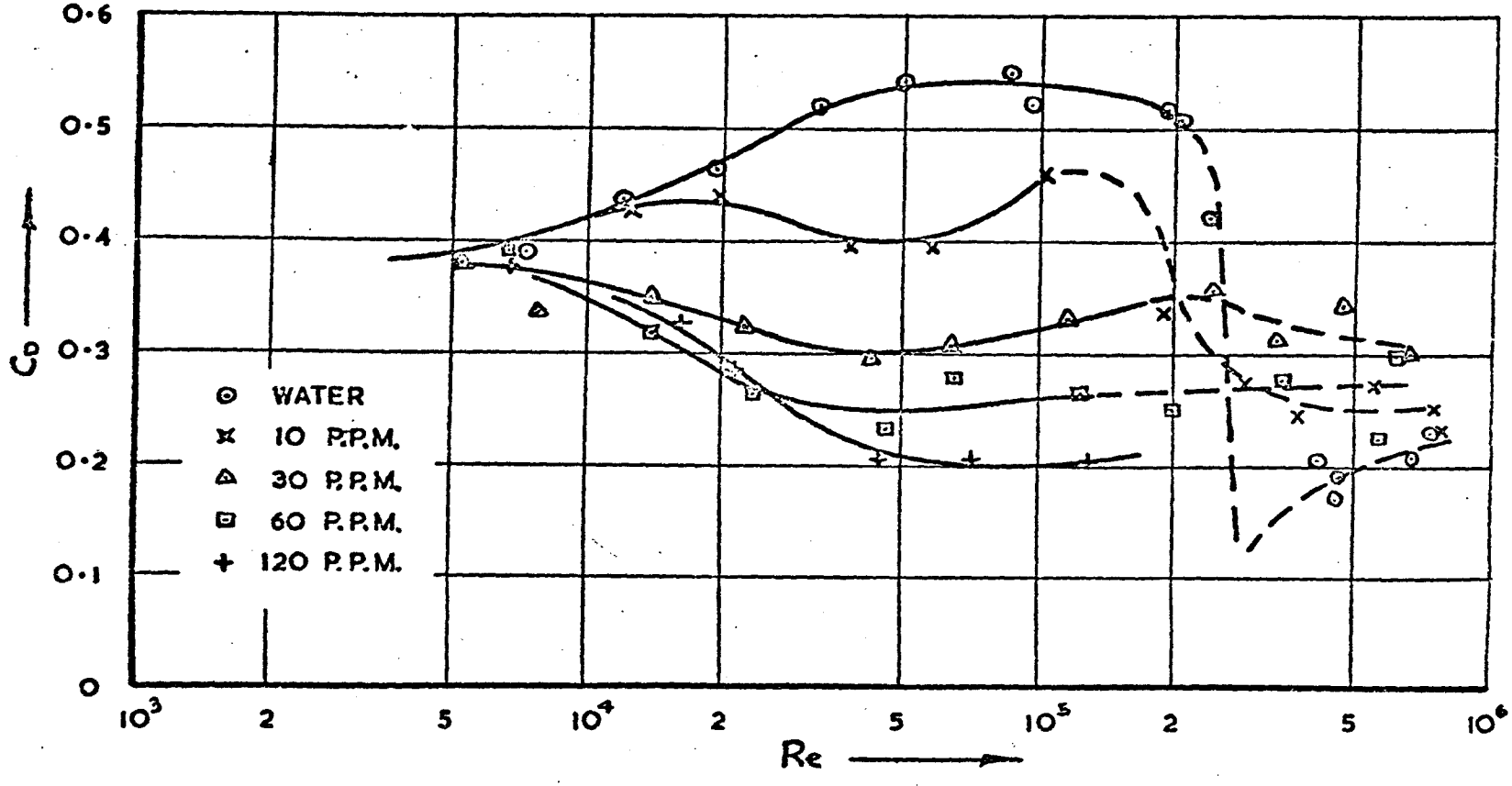

SPHERE DRAG COEFFICIENTS IN POLYOX WSR 301 SOLN.

Fig. 105.

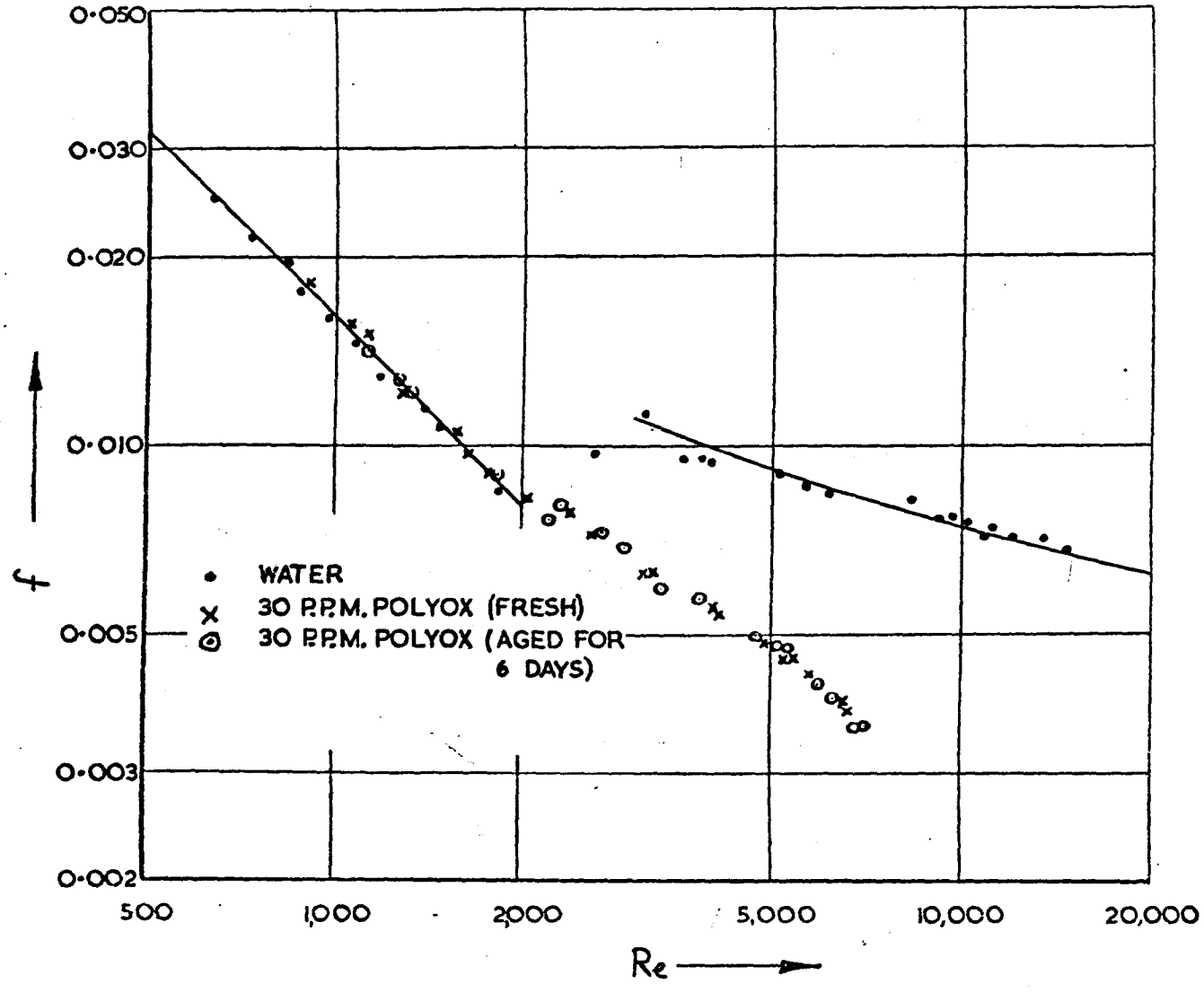

EFFECT OF AGE ON POLYOX WSR 301 SOLN. USED FOR SPHERE TESTS
PIPE DIAMETER 0.090 IN.

Fig. 106.

and freshly mixed solutions of Polyox WSR 301 are shown in fig.105, and the Reynolds numbers are based on the viscosity of the solutions using the values from table 4. Results from the large rig are shown connected by dashed lines. Drag coefficients determined for water from these tests agree well with results by other workers over the whole Reynolds number range. The drag coefficients in Polyox solution at low values of Reynolds number also agree to a large extent with the results of previous investigators (79), (80), (81). It can be seen from fig.105 that at high Reynolds numbers the sphere drag is greater in Polyox solution than in the solvent, as the previous experiment suggested.

We have already discussed to some extent the effect of age on the performance of Polyox solutions in connection with pipe flow. It has also been found that ageing has a serious effect on the drag with the present experiment. A 1/2 in. (12.7mm) diameter steel sphere was periodically dropped over a period of one week into a 30 p.p.m. solution of Polyox using the small rig. These ageing effects are shown in table 7, and is is seen that after about one week the sphere drag reduction has virtually disappeared.

TABLE 7

Sphere dia. 1/2 in. (12.7mm) (Cd in water = 0.475

AGE	Cd
Fresh	0.324
1 Day	0.346
2 Days	0.362
3 Days	0.390
6 Days	0.445

This same solution was afterwards tested in a pipe flow apparatus, and practically identical pipe friction results were obtained with the aged solution and a freshly mixed one (see fig.106). This might seem to indicate that the loss of effectiveness in reducing sphere drag is not due to degradation. It should be emphasized however that a small bore pipe had to be used for this test because only a limited quantity of aged solution was available from the small drop rig. Tests in a small bore pipe are not always effective in showing up changes in friction characteristics if working near to saturation conditions, i.e. near to the asymptote.

(2.10.4) Sphere drop tests with other additives.

Sphere drag experiments have also been carried out in the small rig with equimolar solutions of cetyltrimethyl-ammonium bromide (CTAB) and 1-naphthol. This complex soap system has previously been shown to produce very large drag

reductions in turbulent pipe flow, although the effect terminates when the wall shear stress exceeds a certain value because of changes in or disruption of the micelle structure. Results are shown in fig.107 and drag reductions are very much less than those found with Polyox solutions. Because the highest concentration of the soap system was slightly pseudoplastic (n=0.95), and because possible structure changes at high shear rates make viscosity difficult to interpret, the Reynolds numbers in fig.88 have been based on the viscosity of water.

These results have been criticized by D.A.White (82) who found no drag reduction on spheres in this CTAB-naphthol system. He suggested that if fig.107 were based on the solution viscosity instead of the solvent, then apparent drag reduction would disappear. However, one cannot escape the fact that with the present tests the sphere terminal velocities were actually increased in the soap solutions. This is clearly seen in fig.108. Indeed even if corrections are made to fig.107 allowing for viscosity increases, the lines for the additive solutions still lie slightly below, and to the right of the line for water.

In order to resolve this difference an additional experiment was carried out to determine the effect of the CTAB-naphthol system on boundary layer separation. A circular cylinder 2.5 cm in diameter was mounted transversely across a square section water tunnel of 5.0 cm side. In

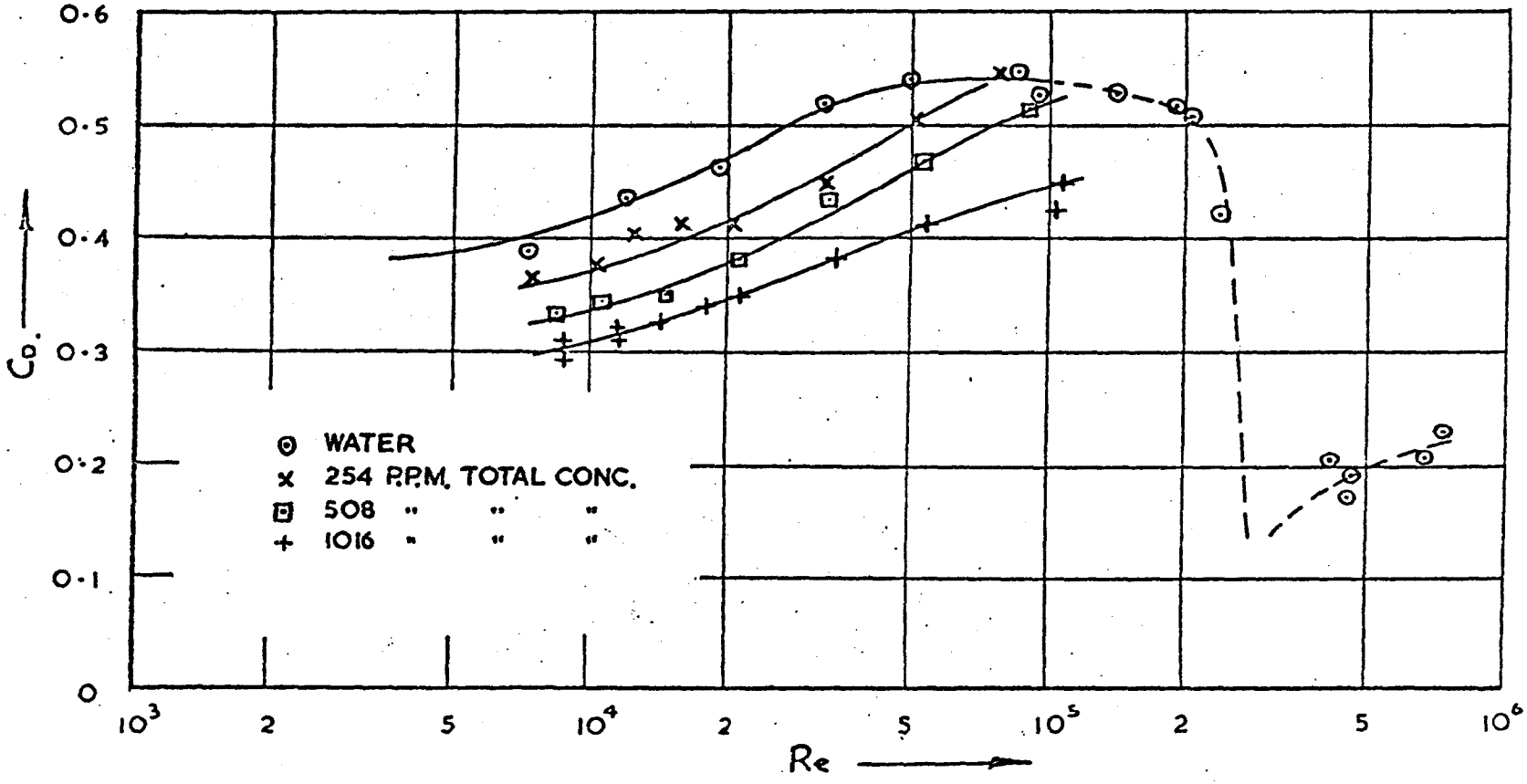

SPHERE DRAG COEFFICIENTS IN EQUIMOLAR SOLN. CTAB/1-NAPHTHOL

Fig. 107.

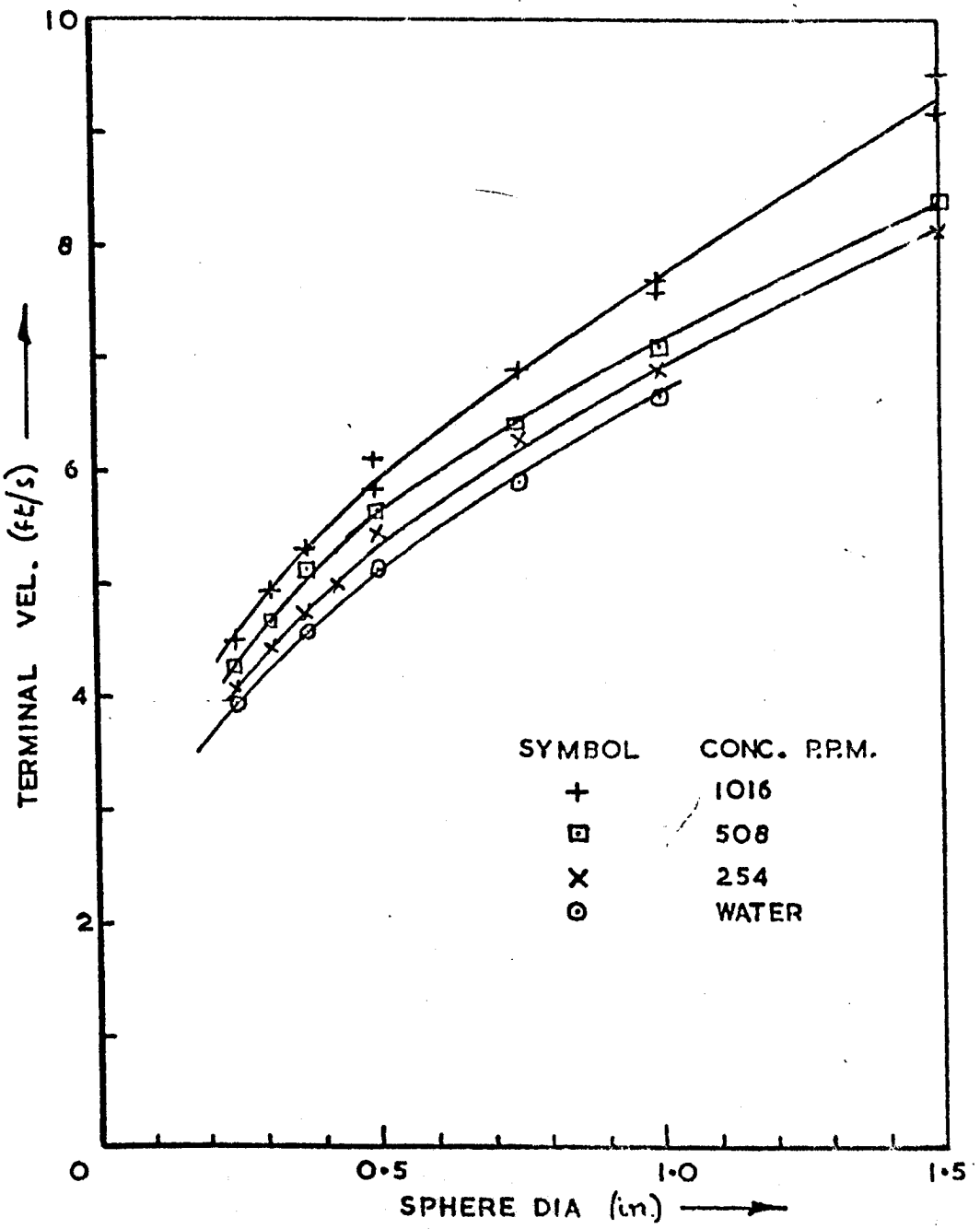

TERMINAL VELOCITIES OF STEEL SPHERES IN EQUIMOLAR SOLUTIONS OF CTAB/1-NAPHTHOL

Fig. 108.

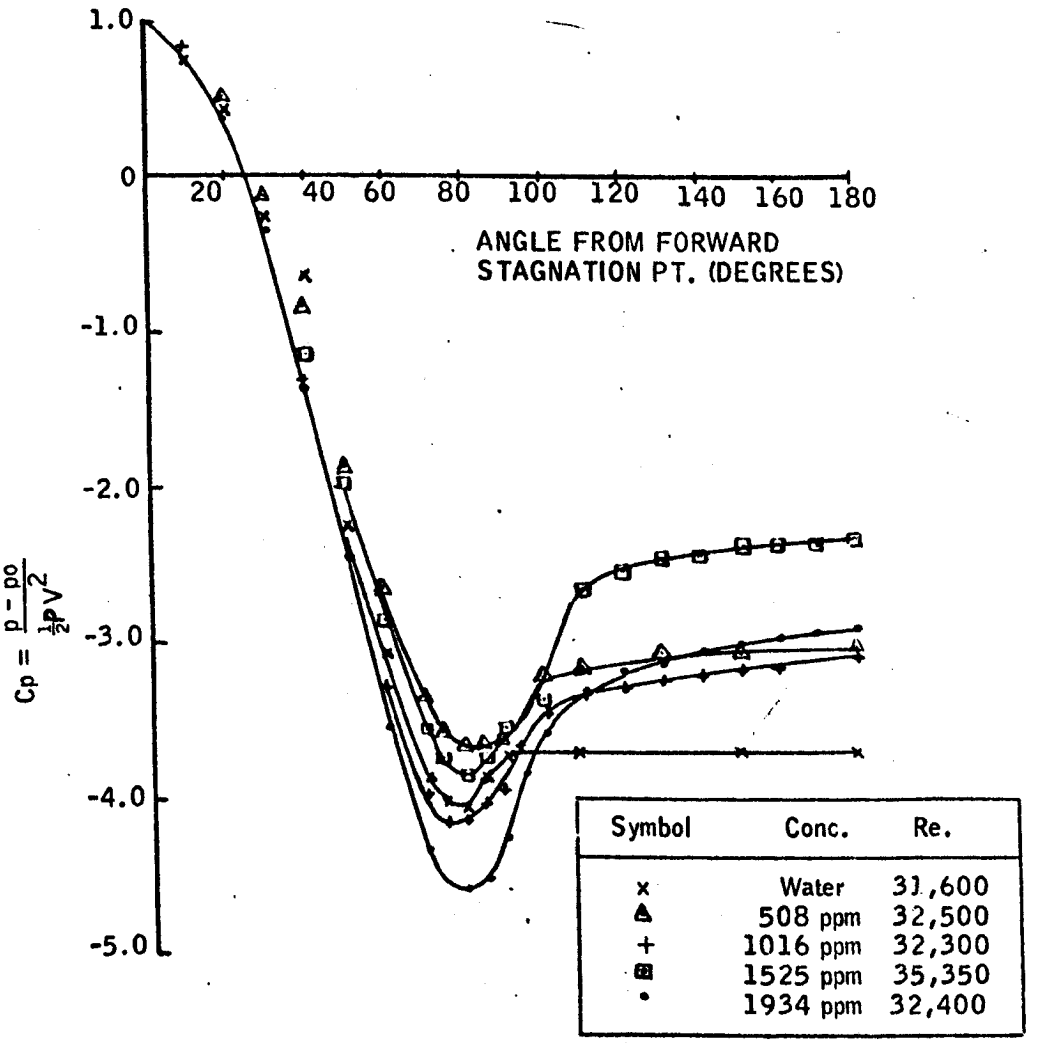

VARIATION OF PRESSURE COEFFICIENT AROUND CYLINDER FOR VARIOUS CONCENTRATIONS OF C.T.A.B./1-NAPHTHOL SOLN.

Fig. 109.

order to measure the pressure distribution around the cylinder a 1/16 in. (1.58mm) diameter pressure tapping was provided mid-way along its axis, the angular position being adjusted by rotating the cylinder. A static pressure tapping was provided in the tunnel wall just upstream from the cylinder.

It should be emphasized that the blockage effects with this arrangement are extremely large and the results obviously cannot be applied to a cylinder in an unbounded stream. At best they can merely indicate the likely trend.

Fig.109 shows a typical set of results for the pressure distribution with a range of concentrations at a roughly constant Reynolds number (based on water). In all cases the pressure coefficient at the forward stagnation point was assumed equal to unity, but this is not likely to be true for the higher concentrations where normal stress differences will probably invalidate the Bernoulli equation. However, despite the uncertainties it can be seen that the additives have delayed boundary layer separation and produced a smaller wake at higher pressure, thereby reducing the drag force. These results then are consistent with the observed small drag reductions found for spheres in the micellar soap system.

Finally in this connection we turn to experiments on the drag spheres in dilute Guar gum solution. Although Guar gum solution is very effective in reducing skin friction

it was found to have NO effect on the drag of spheres for concentrations up to 500 p.p.m.

Gadd (83) and Brennan and Gadd (66) showed that freshly mixed Polyox in dilute solution exhibited elastic effects through measurable normal stress differences, but these measureable differences disappeared on ageing the solutions. Furthermore, they found no detectable elastic effects with dilute Guar gum solutions.

From these results it certainly seems that the delayed laminar separation found with fresh Polyox and the micellar solutions is caused by elastic effects, since the phenomenon only occurs with solutions which exhibit detectable normal stress differences in shear flow.

It should be noted that sphere drag reduction has been measured by Ruszczycky (49) using Guar gum solution at very much greater concentrations. Now at these high concentrations Guar gum is certainly viscoelastic, shown by the Weissenberg effect, and it is also extremely pseudoplastic. Bizzell and Slattery (84) have also shown that for a power law fluid the separation point would move towards the rear of a sphere as the flow index is decreased. These effects then can account for Ruszczycky's results.

(2.11.0) ANOMOLOUS HEAT TRANSFER CHARACTERISTICS OF DILUTE POLYMER SOLUTIONS IN FULLY ROUGH PIPE FLOW.

Metzner and Friend (85) modified Reichardt's analogy and proposed the semi-empirical expression:-

$$St = \frac{f/2}{1.2 + 11.8(Pr-1)(Pr)^{-\frac{1}{3}}(f/2)^{\frac{1}{2}}}$$

This relationship showed good agreement with experimental data for Newtonian and purely viscous non-Newtonian fluids in pipe flow.

Pruitt et.al. (86) found that the above relationship failed with drag reducing solutions and empirically modified it to the following form:-

$$St = \frac{f(1-FR)/2}{1.2 + 11.8(Pr-1)(Pr)^{-\frac{1}{3}}[f(1-FR)/2]^{\frac{1}{2}}}$$

where $FR = (f_o-f)/f_o$, f_o and f being solvent and solution friction factors respectively at the same pipe flow rate.

Poreh and Paz (87) showed that the Pruitt et.al. correlation was reasonably successful within $\pm$ 20%, and in turn analyzed the heat transfer characteristics in terms of a three zone velocity profile model with thickened viscous sublayer and an assumed expression for the buffer zone. Their final results is:-

$$St = \frac{(f/2)^{\frac{1}{2}}}{\left\{y_1^+\left(\ln\left[Pr-(Pr-1)\,y_1^+/y_2^+\right] + (Pr-1) + (2/f)^{\frac{1}{2}}\right\}}$$

This too correlated the available data within ± 20 %.

It may be noted that for unity Prandtl number this reduces to the basic Reynolds analogy St = f/2.

One assumption made by Poreh and Paz was the equality between the eddy diffusivities of heat and momentum, which may not always be justified in view of the experimental results shortly to be described.

(2.11.1) The heat transfer rig.

Heat transfer experiments have been carried out in a tube with a very rough wall to eliminate any viscous sublayer. The scheme of the apparatus is shown in fig.110.

Lengths of 3/8 in. (9.52mm) o.d. brass rod were internally threaded ¼ in. Whitworth and joined together to produce a working section 32 in. (0.81m) long. Pressure tappings were provided in short lengths of smooth tube upstream and downstream of the threaded section, together with mixing cups for mean temperature measurement. The working section was provided with an insulated jacket and was externally heated by condensing steam at atmospheric pressure. Axial conduction was minimized by isolating the mixing cups from the working section by short lengths of rubber tube.

Fluid was supplied to the pipe from a large header tank and the flow rate was determined from timed collection into measuring cylinders.

(2.11.2) The experimental results.

The pressure drop and fluid temperature rise were measured over a range of flow rate with water, 50 p.p.m. solution of freshly mixed Polyox WSR 301 and a 500 p.p.m. solution of Guar gum.

Fig.111 shows a comparison of the overall heat transfer coefficients for water and the polyox solution. These coefficients have been based on the log. mean temperature difference between the fluid in the pipe and the heating steam, and the mean diameter at half thread depth.

The results are quite remarkable: whereas the coefficient for water increases with Reynolds number as expected, the coefficient for Polyox solution DECREASES. In fact less heat is carried away from the wall by a greater flow of Polyox than by a lesser flow.

Results with the Guar gum solution were practically identical to those with water which is consistent with the previously discussed results in a rough pipe of larger diameter.

By allowing for conduction through the pipe wall and estimating the outer coefficient for film condensation on a horizontal pipe using Nusselts expression, the internal film coefficients were roughly determined. (Internal properties being based on the bulk mean temperature of the fluid). Results are shown in fig.112. Again whereas the Polyox has reduced the friction factor considerably, the

Stanton number has been reduced by an even greater amount.

(2.11.3) Discussion of the heat transfer results.

Before attempting an explanation of the anomolous heat transfer results we must first consider the flow in more detail.

For the turbulent core region in pipe flow, i.e., outside the sublayer, we may write:-

$$\frac{\tau}{\rho} = (\nu+\varepsilon_m)\frac{du}{dy} = \frac{u^{*2}}{\nu}(\nu+\varepsilon_m)\frac{du^+}{dy^+}$$

$$= \frac{\tau_w}{\rho}\left(1+\frac{\varepsilon_m}{\nu}\right)\frac{du^+}{dy^+} \quad \text{——} \quad (2.11.i)$$

A force balance for steady flow yields:-

$$\frac{\tau}{\rho} = \frac{\tau_w}{\rho}\left(1-\frac{y}{a}\right) = \frac{\tau_w}{\rho}\left(1-\frac{y^+}{Ra}\right) \quad \text{——} \quad (2.11.ii)$$

Equating 2.11.i and 2.11.ii gives:-

$$\left(1+\frac{\varepsilon_m}{\nu}\right)\frac{du^+}{dy} = \left(1-\frac{y^+}{Ra}\right)$$

$$i.e. \quad \frac{\varepsilon_m}{\nu} = \left[\frac{1-y^+/Ra}{du^+/dy^+}\right]-1 \quad \text{——} \quad (2.11.iii)$$

The logarithmic velocity profiles for Newtonian flow and for flow with drag reducing additives away from the interactive wall region imply:-

$$\frac{du^+}{dy^+} = \frac{2.5}{y^+} \quad \text{——} \quad (2.11.iv)$$

For drag reducing solutions within the interactive zone or under completely asymptotic conditions, previously discussed work indicates:-

$$\frac{du^+}{dy^+} = \frac{11.7}{y^+} \qquad \text{(2.11.v)}$$

Expression 2.11.iii enables an estimate to be made of ε_m from velocity profile measurements. Fig.113 shows the variation of $\frac{\varepsilon_m}{\nu}$ with y^+ for Newtonian fluids and is based on eqns. 2.11.iii and 2.11.iv. In this figure $Ra = \frac{au^*}{\nu} = \frac{Re\sqrt{f}}{8}$ and we see that for small pipes at moderately low Reynolds numbers, ν may not always be negligible compared with ε_m although the assumption is certainly justified at high Reynolds numbers.

Fig.114 is an estimate of conditions in the threaded pipe at a Reynolds number of 10 000, results for the Polyox solution being based on the asymptotic velocity profile. The dotted line represents the variation of eddy viscosity for water at the same wall shear stress (i.e. same Ra) as the Polyox results. The assumption of the asymptotic velocity profile for the Polyox solution in this small pipe seems justified from the previously discussed work. There may be an upward jump to the dotted line in fig.114 close to the pipe axis if the interactive zone has not spread completely over the whole pipe radius. The important deduction is that certainly over the bulk of the flow the kinematic viscosity is the same order of magnitude

as the eddy viscosity and cannot be neglected away from the wall as is customary in heat transfer work. Fig.114 emphasizes the enormously reduced values of eddy viscosity compared with water.

We may describe the heat transfer characteristics for turbulent pipe flow using the analogy between heat and momentum transfer. Since there is no viscous sublayer present in the threaded pipe, we will use the general anology:-

$$St = \left(\frac{\alpha + \varepsilon_q}{\nu + \varepsilon_m}\right) f/2$$

which reduces to the basic Reynolds anology for unity Prandtl number if $\varepsilon_q = \varepsilon_m$

The relationship may be written in alternative form:-

$$St = \left(\frac{1/Pr + \varepsilon_q/\nu}{1 + \varepsilon_m/\nu}\right) f/2 \qquad \text{(2.11.vi)}$$

We will now use equation 2.11.vi to provide a tentative explanation for the anomolous heat transfer results.

Taking data from fig.112, at a flow Reynolds number of 10 000 we have the following values for f/2 and St:-

	f/2	St	St/(f/2)
Water	0.012	0.0032	0.267
50 p.p.m. Polyox	0.0045	0.0001	0.022

Comparing the solvent and solution results through equation 2.11.vi we see that the bracketed term is reduced by a factor of 0.022/0.267 = 0.0825 with Polyox addition.

Taking a Prandtl number value of 8.0 for the solvent and solution and making a very rough mean order of magnitude estimate of ε_m/ν from fig.113 as 8.0 and 1.0 respectively and finally assuming that $\varepsilon_\ell = \varepsilon_m$ for the solvent, then insertion of these values into equation gives:-

$$0.0825 = \left(\frac{0.125 + \varepsilon_\ell/\nu}{1 + 1}\right)_{\text{Soln.}} \times \left(\frac{8 + 1}{0.125 + 8}\right)_{\text{Solvent}}$$

This implies that $\varepsilon_\ell/\nu = 0.024$ for the solution.

We see therefore that for the Polyox solution $\varepsilon_\ell/\varepsilon_m = 0.024$, in other words the additive has caused ε_ℓ to reduce very much more than ε_m.

It must be emphasized that this analysis is far from rigorous, being merely a demonstration, but it is possible to picture the result intuitively. We have seen that Polyox can suppress the very small eddies in turbulent flow, and it seems that the remaining large eddies whilst effective in momentum transfer would be less effective in heat transfer. This is because the 'lump' of fluid would not have time to reach an equilibrium temperature with its surroundings before moving off to some other position.

This simple experiment demonstrates clearly the need for further detailed work on the heat transfer charac-

teristics of the very effective drag reducing solutions, particularly near to asymptotic limit conditions.

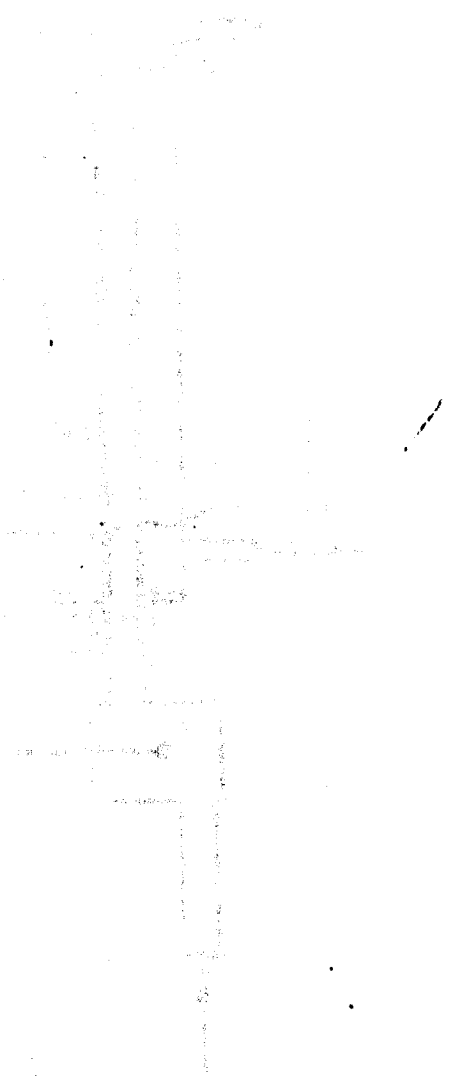

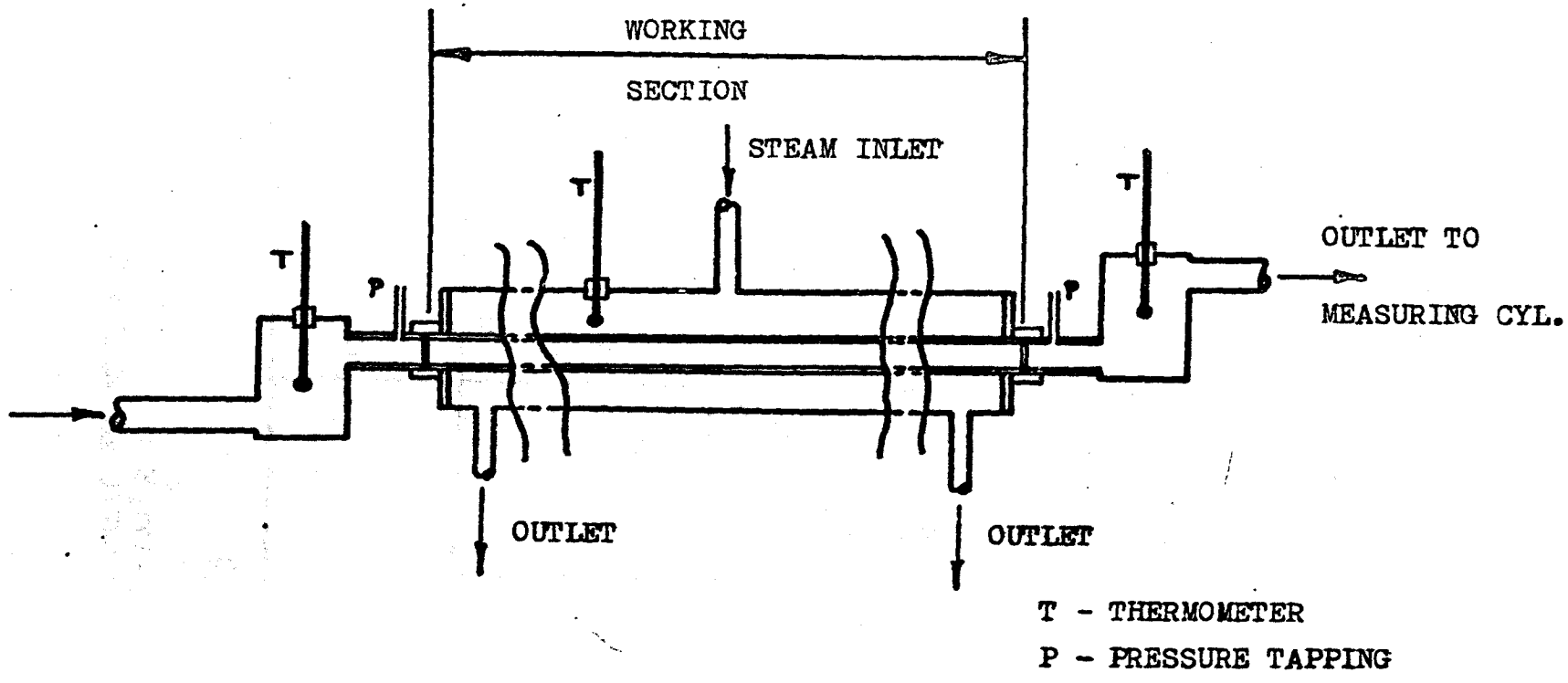

RIG FOR HEAT TRANSFER EXPERIMENT - THREADED PIPE

Fig. 110.

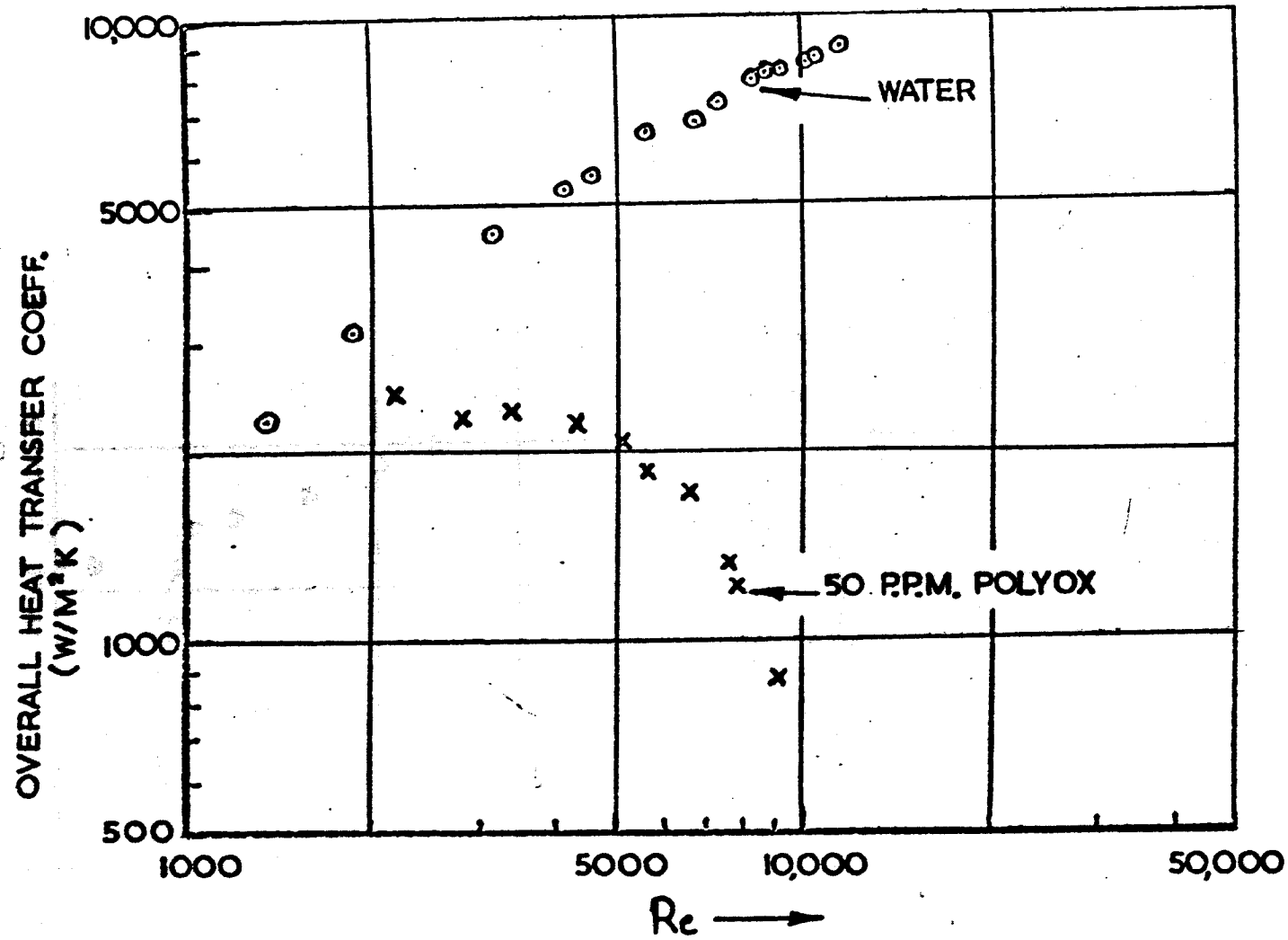

OVERALL HEAT TRANSFER COEFFICIENT. BASED ON INNER MEAN DIA.

Threaded pipe $\frac{1}{4}$ B.S.W. - Brass, $\frac{3}{8}$ IN. O.D.

Fig. 111

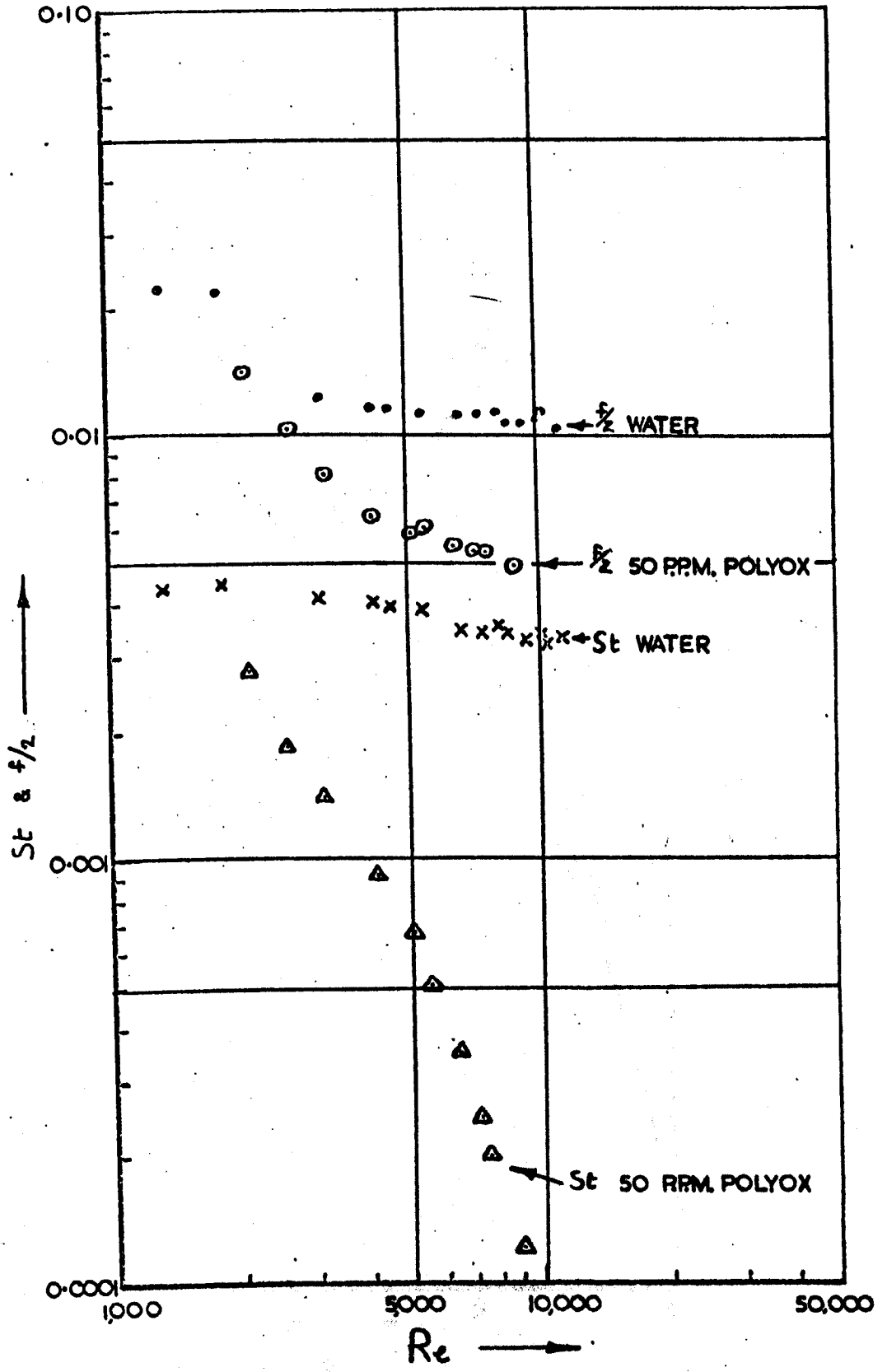

FRICTION AND HEAT TRANSFER CHARACTERISTICS

FULLY ROUGH PIPE.

FIG. 112.

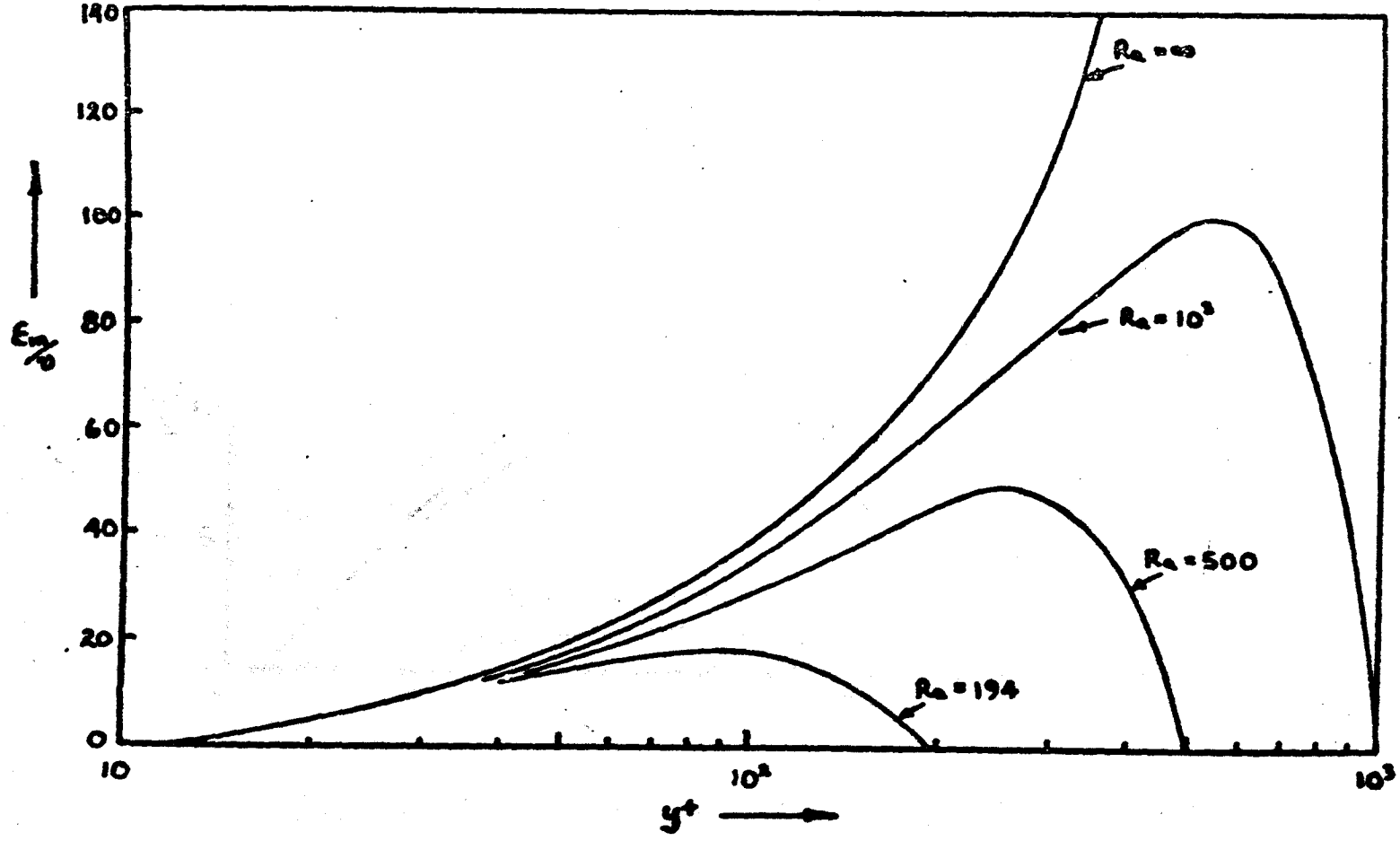

PLOT OF EQN. 2.11.11 - WATER

Fig. 113.

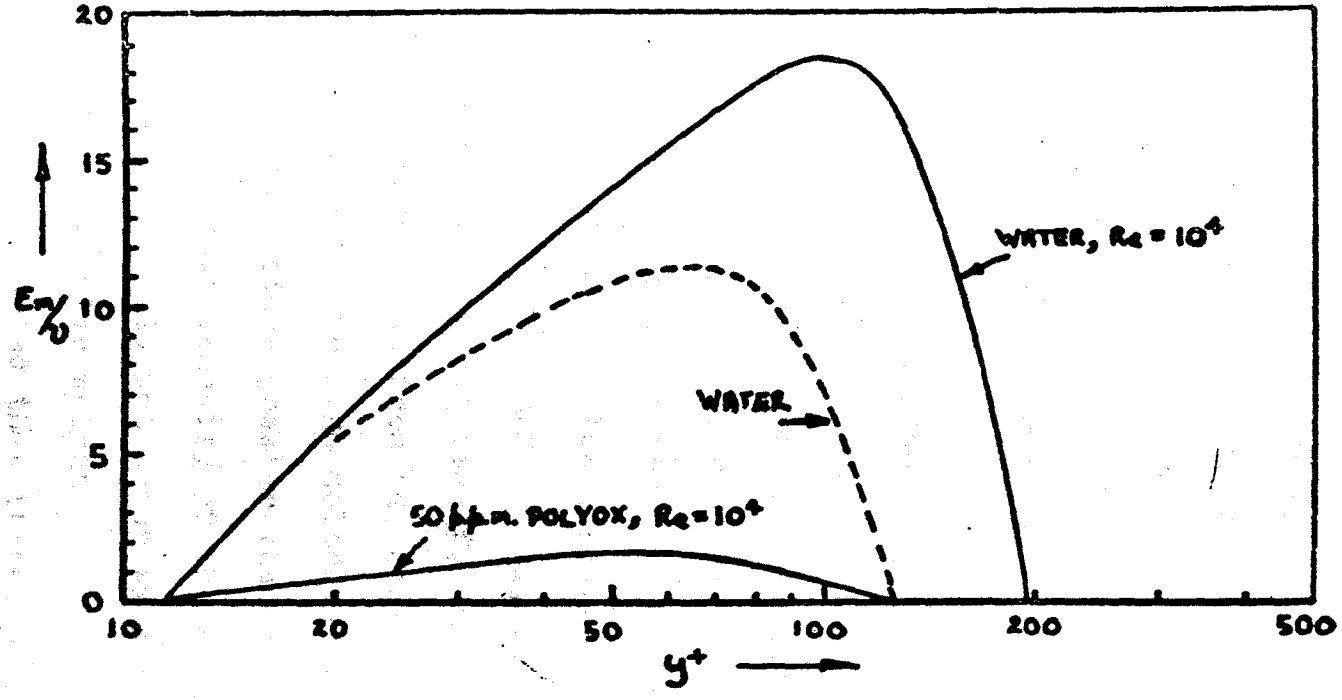

COMPARISON OF EDDY DIFFUSIVITIES IN SMALL PIPE WITH WATER AND POLYOX SOLUTION UNDER ASYMPTOTIC CONDITIONS.

Fig. 114.

(2.12.0) OTHER ANOMOLOUS EFFECTS WITH DRAG REDUCING ADDITIVES.

Apart from reducing turbulent friction many of the effective additives exhibit other anomolous effects, particularly at the higher concentrations. Several of these miscellaneous phenomena were briefly investigated during the course of the present study.

(2.12.1) Open syphon and suspended syphon.

A very spectacular demonstration of the cohesive effect between Polyox molecules was reported by James (88). A beaker was completely filled with Polyox solution and then tipped slightly to start the fluid flowing over the lip. Once established, the flow continued, and provided that the overflow head was sufficiently great it was possible for the beaker to empty itself, the stream offalling fluid "pulling" more fluid from the container. The effect was only observed with the high molecular weight Polyox WSR 301, at concentrations greater than about 0.2%, and illustrates the extreme tenacity of the additive molecules in a flow. The effect did not occur with poly (ethylene oxides) of lower molecular weight.

James also showed that it was possible to syphon Polyox solution through a suspended syphon pipe.

These experiments were easily repeated and results are pictorially described in publication (P.4)

*Using a 0.4 solution of Polyox it was found possible to completely empty a standard 600 ml beaker with a syphon pipe near to the top.

Some similar tests with Guar gum solution at high concentration showed no tenacity effect at all, and Separan N.P.10 solution, although very stringy in appearance was not sufficiently tenacious to form an open channel or suspended syphon.

(2.12.2) Enhanced Coanda effect.

Differences in behaviour between Guar gum and Polyox solutions are also apparent from observations made during some wall attachment (Coanda effect) experiments.

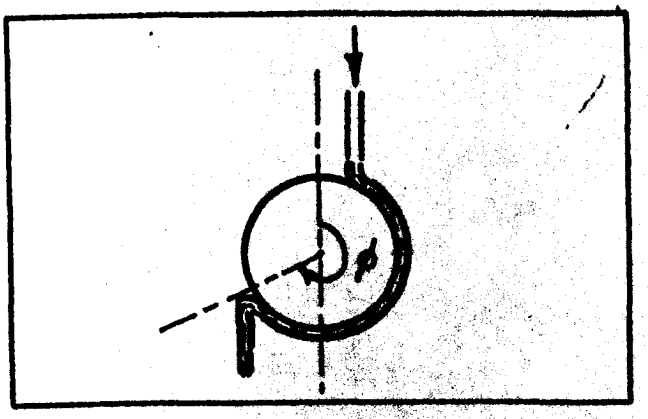

Fig.115 APPARATUS FOR WALL ATTACHMENT EXPT.

Fig.115 shows the layout of the apparatus used. Liquid was supplied to a 1/8in. (3.17mm) diameter pipe from a constant head container and the jet from this pipe was directed on to a 3 1/2 in. (89mm) diameter cylinder.

The flow rate was slowly increased and the

*(Publications at end of this thesis).

maximum value of the angle $\emptyset$ to the "peel off point" was noted. Although the flow oscillated only the maximum value of $\emptyset$ was recorded. The same maximum value, $\emptyset=240°$ was obtained with both water and filtered Guar gum solutions up to 500 p.p.m. concentration. With fresh Polyox solution on the other hand a value of $\emptyset=270°$ was easily achieved for concentrations between 30 and 150 p.p.m. With higher concentrations the energy dissipation caused by the increased viscosity resulted in $\emptyset$ becoming less than that observed with water.

(2.12.3) Cavitation Suppression.

It has been found that some of the additives effective in drag reduction can also delay the onset of cavitation. This was demonstrated using a transparent venturi-tube, fed from a header tank and fitted with a 20ft. (6.1m) vertical pipe at the downstream end in order that the throat pressure would reach low values at moderate rates of flow. The feed pipe from the tank was short and of large diameter so that pressure losses were negligible.

Freshly mixed polyox solutions were found to delay the onset of cavitation to higher flow rates, and the noise level was much reduced. The lowest concentration used was 12.5 p.p.m. and the delay of cavitation was more effective as the concentration was increased to 200 p.p.m., the highest tested. These phenomena were much less notice-

able with Polyox solutions which had been stored for several days prior to use.

An equi-molar solution of CTAB/1-Naphthol at 508 p.p.m. concentration delayed cavitation onset by about the same order as fresh Polyox solution at 12.5 p.p.m., but noise reduction was comparable with Polyox at 50 p.p.m.

Cavitation suppression has also been noted by Hoyt (89), (90), Ellis (91) and Breenen (92).

(3.0). GENERAL DISCUSSION AND CONCLUSIONS.

The fundamental characteristics of the effective dilute high polymer solutions in pipe flow can now be described from the present work and the results of others. In order to produce significant drag reduction the polymers should be of high molecular weight (order 10^6), flexible and linear with few side branches. The degree of solubility is also important, greater drag reduction being obtained with very good solvents than with poorer ones. Friction reduction only occurs in the turbulent flow regime and laminar flows are not affected by the additives, except for small viscosity increases. Generally the transitional Reynolds number is not changed and remains around 3,000 - 4,000 as with the solvent.

An interesting result in polymer solution drag reduction is the "Diameter effect." For a given polymer species and concentration the drag reduction increases with reduction of the pipe size and conversely reduces with an increase of the pipe diameter. Indeed drag reduction does not commence at all until a certain value of the wall shear stress has been exceeded. This threshold wall shear stress seems dependent on the polymer molecular weight and solution concentration and its value is reduced if the latter are increased in magnitude. Virk (93) has related the onset condition to the polymer properties (weight and r.m.s. dia-

meter in solution), but this analysis does not account for variations due to concentration change.

With pipes of a very small diameter the wall shear stress may be sufficiently high to occur in the laminar region and in this case normal turbulent flow is never established. On the other hand with very large diameter pipes operating at practical flow velocities, the threshold wall stress may never be reached, and consequently no drag reduction would occur.

The present work has shown that for a given polymer and concentration the percentage drag reduction depends purely on the value of the wall shear stress, apparently irrespective of pipe diameter. This form of correlation is extremely convenient for practical use since a few laboratory tests carried out in a moderately sized apparatus could be used to predict prototype plant behaviour if wall shear stress is used as a scaling parameter. However, extrapolation to extremely large pipe sizes is still rather uncertain as no experimental results are available.

Friction factor reduction is limited by an asymptote curve which seems to apply to all of the drag reducing additives. This asymptotic limit is approached by increasing the concentration of the polymer additive and may also be approached with moderately low concentrations in small pipes. The concentration required to reach limiting conditions depends on the polymer type - particularly on the

molecular weight, and on the diameter of the pipe. The expression for the asymptote proposed by Virk (59) is:-

$$1/f^{\frac{1}{2}} = 19 \log_{10}(Re\ f^{\frac{1}{2}}) - 32.4 \quad (Re>4000)$$

This seems to fit all of the experimental data with reasonable accuracy. All reduced drag data for smooth pipes consequently lies between this expression as the lower limit and the normal turbulent flow relationship as the upper limit viz.:-

$$1/f^{\frac{1}{2}} = 1.765 \ln(Re\ f^{\frac{1}{2}}) - 0.6 \quad (Re>4000)$$

Most of the effective drag reducing solutions are very susceptible to permanent degradation if the solution is subjected to excessive shearing. The drag reduction decays rapidly at first presumably due to scission of the higher molecular weight fractions which are the most effective ones, and then more slowly. This is a most serious drawback to the practical exploitation of these additives since it practically rules out any closed circuit application. Degradation also causes drag reduction to decrease at high shear rates even in a once through system.

Some natural polymers such as Guar Gum appear quite resistant to mechanical degradation and Poreh, et.al. (58) report successful runs in a closed circuit rig for long periods of time. The present work indicates that

Guar Gum solutions lose their effectiveness quite rapidly in a system which is not chemically clean, the loss of drag reduction being apparently due to adsorption and agglomoration into a jelly like precipitate.

Velocity profile measurements of other workers and the pipe friction results of the present study are consistent and lead to the view that this form of drag reduction is primarily due to an increase in the thickness of the wall layer, - i.e. sublayer plus some buffer or interactive zone, the core region well away from the wall being little affected by the additives.

Correlations based on the two zone velocity profile model, with increased thickness of the linear sublayer seem to work satisfactorily for cases of moderate drag reduction. In the limit however this model would result in a laminar flow with a linear velocity profile, which is not consistant with the limiting asymptotic conditions. This objection is overcome with the three zone model proposed by Virk et.al.(59). In this model the linear sublayer remains unchanged and the interactive buffer zone increases in thickness and eventually reaches the pipe axis when the asymptotic limit is achieved. The limited velocity profile data available supports the adoption of this model as a good approximation to the actual profile.

Provided that the wall layer thickness is known the pipe friction may be determined from the velocity

profile by integration. For the two zone model both Meyer (62) and Elata et.al. (57) indicated that their dimensionless sublayer thickness Ro was a unique function of a Deborah number (which is a ratio of elastic to viscous forces), or for a given polymer and concentration to the wall shear stress irrespective of pipe diameter. The present data and that of Elata et.al. do show a small but significant diameter effect, and the same trend is also shown with the interactive zone thickness R_1 using the three zone model.

A particular advantage of correlations based on the increased wall layer thickness is the ease with which they can be applied to flat plate boundary layer calculations. This has been carried through by Granville for the two zone velocity profile model and the limiting asymptotic condition (94), (95), (96).

With some additives the method of solution preparation and its pre-history play an important part in the form of the flow characteristics. This is particularly so with Polyox and considerable differences have been found between the behaviour of freshly mixed and aged solutions. The results previously discussed here would indicate the presence of large clusters of molecules in the fresh solutions which are particularly effective in drag reduction and turbulence suppression in general. Freshly mixed solutions exhibit strong elastic effects which are not so

readily detectable with the aged solutions.

At quite an early stage viscoelasticity was considered as a very possible explanation of the drag reduction mechanism. If the polymer molecules (or clusters of them) are viscoelastic, then they are capable of storing kinetic energy from the main flow as potential energy of deformation. Now if the time scale of a turbulent disturbance is less than the relaxation time of the molecule or molecules, then the solvent flows around the additive thereby dissipating energy and reducing the kinetic energy of the disturbance. In other words turbulence damping would occur. If on the other hand the time scale of the disturbance is great compared with the relaxation time of the additive then little damping would occur as the molecules would move with the disturbance. In order for the former effect to occur the dimensions of the molecules would have to be of the same order as the Kolmogorov turbulent microscale, - Lumley (97). This is not the case for single molecules of even the very high molecular weight additives such as Polyox, so for this mechanism to be effective either the molecules are not randomly coiled (which seems unlikely) or they exist as agglomorates of more than one. This theory does indicate that only the small scale turbulence is affected such as that near to the wall in pipe flow. Certainly only the small scale eddies are affected by Polyox in the free jet experiments.

There is growing evidence that surface adsorption may also be responsible for many of the anomolous results, as discussed by Kowalski (56), and in the recent paper by Arunachalam and Fulford (98).

The CTAB soap system in pipe flow behaves rather differently from the dilute polymer solutions. No drag reduction occurs with very low solution concentrations but above a certain critical concentration the drag reduces very rapidly and follows approximately the limiting asymptote line irrespective of pipe diameter or further concentration increase.

It is believed that above this critical concentration the molecular structure associates itself into micelles of large but unknown size, and that these colloidal agglomorations interfere with the turbulence structure in a similar way to clusters of polymer molecules.

Reversible scission of the micelles appears to occur above a certain value of the wall shear stress (which depends on the solution concentration), which can explain the sudden disappearance of drag reduction above this stress value.

Velocity profile measurements with the soap system have confirmed the existence of Virk's predicted asymptotic velocity profile law.

Although the small scale turbulence is suppressed by the micellar system, rough measurements indicate that

the overall mean turbulence is still the same order as with the uncontaminated fluid.

Observations on the turbulent boundary layer of a flat plate immersed in the soap system would indicate reduced turbulence production, judging from the fewer more passive 'Bursts' from near the wall.

Some evidence has been presented which suggests that the heat eddy diffusivity reduces very much more than the corresponding momentum eddy diffusivity with fresh polyox solution. This could have an important bearing on heat transfer calculations.

External flows around bluff bodies such as spheres and cylinders only appear to be affected by additive solutions which exhibit detectable elastic effects. Generally these delay boundary layer separation and reduce form drag although in special circumstances the drag may be increased.

Future work in this field should be aimed at obtaining a clearer insight into the mechanism responsible for the drag reduction. Much useful information could be obtained from studies of the turbulence structure of drag reducing solutions in shear flow. This is admittedly a difficult task with liquids, particularly since hot film probes and the like have proved unreliable in polymer solutions. However, the hydrogen bubble technique used in the present preliminary experiments could be usefully extended together with laser anemometry in order to provide

key information on the turbulence structure.

(4.0) SOME PRACTICAL APPLICATIONS.

Since the early discovery of skin friction reduction by the use of soluble macromolecular additives many practical applications have been suggested. Unfortunately many of the initial hopes for the practical exploitation of the effect have been unfulfilled, largely due to the rapid shear degradation of many of the effective drag reducers, and due to economic considerations. Some of the more obvious practical applications which are being considered are listed below:-

(4.1) Marine applications.

Much of the early work with drag reducing additives was carried out at naval establishments with a view for application in this field. The quantity of additive required for continuous routine injection into a ships boundary layer makes such an application uneconomic although for peak wartime emergency use possibility may still be considered. Full size trials have been carried out by the British Admiralty.

One possible civil application is with hydrofoils, and short term drag reduction would be of use whilst the vessel accelerates to become foil-borne. This would then enable a smaller, lighter and cheaper engine to be installed. The use of additives in ship model tests has also been considered (6).

(4.2) Oil well fracturing.

Early use of drag reducing fluids was made for hydraulic fracturing operations in oil wells (30). The reduction of friction along the relatively small bore down-pipe improved the efficiency of the fracturing operation, and enabled the process to be successfully carried out in wells which were hitherto too deep.

(4.3) Firefighting.

Reduction of firehose pipe friction results in a greater throughput, nozzle pressure and jet throw. Although most fire tenders have pumps with normally excess performance in reserve, the use of additives may be considered for exceptional cases or in circumstances where the supply pressure is limited for some reason. Polyox is being used by the New York fire brigade to enable smaller and lighter hoses to be utilized. Studies are still being carried out in this field.

(4.4) Irrigation.

Some test results have been reported by Union Carbide Corp. (99) with Polyox injected into a typical crop spraying system. An increase of 215% in crop coverage was reported.

(4.5) Sewage and floodwater disposal

Polyox has been successfully used in one of the

Southern States of the U.S,A. to increase the throughput of city sewers at times of peak rainfall.

(4.6) Heating and ventilating.

A detailed stuy has been carried out by Fitzgerald (71). Unfortunately most of the polymeric additives are easily degraded by mechanical shearing which rules them out for use in closed circuits. It was initially hoped that the cetrimide-naphthol system discussed earlier might prove useful in this application, but the present experiments showed that drag reduction disappeared when the temporature exceeded about 40°C. Application in this field will not be possible unless an effective additive can be found which is stable both thermally and mechanically.

(4.7) Pumping of slurries.

Bulk hydraulic transport is widely used and experiments are being carried out with additives by a number of investigators to see if the pipe friction can be economically reduced. Little data is available at the present time, apart from the few results of Poreh, et.al. (100) and Arunchalam and Fulford (98).

(4.8) Pipeline transport of crude oil.

Several oil soluble effective additives have been found and the possibility exists for reducing pumping power

and increasing throughput (101). Studies have shown that use of the presently known additives is probably not an economic proposition.

REFERENCES.

1. Mysels, K., "Flow of thickened fluids," U.S.Patent No. 2,492,173 (1947).

2.(i) Toms, B.A., "Some observations on the flow of linear polymer solutions through straight tubes at large Reynolds numbers," Proc. 1st. Int. Congr. on rheology, Scheveningen, 135, (1949).

(ii) Oldroyd, J.G., A suggested method of detecting wall-effects in turbulent flow through tubes." Proc. 1st. Int. Congr. on Rheology, Scheveningen, 130, (1949).

3. Savina, J.G., Symp. on drag reduction, A.I.Ch.E. meeting, Atlanta, (Feb.1970).

4. Fabula, A.G., "The Toms phenomenon in the turbulent flow of very dilute polymer solutions," 4th. Int. Congr. on rheology, Brown Univ. Providence, R.I. (Aug.1963).

5. Hoyt, J.W. and Fabula, A.G., "The effect of additives on fluid friction," 5th Symp. Naval Hydrodynamics, O.N.R.- Skipsmodelltanken, Bergen, (Sept.1964).

6. Emerson, A., "Model experiments using dilute polymer solutions instead of water," Trans. N.E.C. Inst. of Eng. and Shipbuilders, 81,4,201, (1965).

7. Gadd, G.E., "Turbulence damping and drag reduction promoted by certain additives in water," Nature, 206,4983, 463, (1965).

8. Rouse, H and Ince, S., "History of Hydraulics" Dover, (1957).

9. Von Kármán, T., "Aerodynamics," Cornell U.P.,(1954)

10. Giacomelli, R. and Pistolesi, E., Historical Sketch in "Aerodynamic theory," Ed. W.F.Durand, Vol.1, 305, Dover, (1963).

11. Goldstein, S., "Fluid mechanics in the first half of this century," Ann. Rev. Fluid Mechanics., Vol 1, 1, Annual reviews Inc.,(1969)

12. Tokaty, G.A., "A history and philosophy of fluid-mechanics," Foulis, (1971).

13. Schlichting, H., "Boundary layer theory," McGraw Hill,(1968).

14. Goldstein, S., "Modern developments in fluid dynamics," Dover,(1965).

15. Hoerner, S.F., "Aerodynamic Drag," Pub. by Author (1965).

16. Lumley, J.L., "The reduction of skin friction drag," Int. Symp. of Naval Hydrodynamics, Bergen, (1964).

17. Hoyt, J.W., "A survey of hydrodynamic friction-reduction techniques," AIAA 3rd. Propulsion Joint Conf. Washington, D.C. Paper No.67-431, (July 1967).

18. White A., "The flow of fluid in rotating pipes," M.Sc.Thesis. University of Durham. Kings College, Newcastle-upon-Tyne (1963).

19. White, A., "Flow of a fluid in an axially rotating pipe," J.Mech.Eng.Sci., 6, 1, 47, (1964).

20. Hoyt, J.W. and Fabula, A.G., "Frictional resistance in towing tanks," 10th. Int. Towing tank Conf. London, (1963).

21. Rao, P.V., "Nineteenth-Century concepts of boundary-layer flow," La Houille Blanche, 25, 15, (1970).

22. Agostan, G.A. et.al., "Flow of gasolene thickened by napalm," Ind. and Eng. Chem.,46, 5, 1017, (1954).

23. Savins, J.G., "Some comments on pumping requirements for non-Newtonian fluids," J. Inst. Petroleum, 47, 454, 329, (1961).

24. Wilkinson, W.L., "Non-Newtonian fluids," Pergamon, (1960).

25. Skelland, A.H.P., "Non-Newtonian flow and heat transfer," Wiley, (1967).

26. Metzner, A.B. and Reid, J.C., "Flow of non-Newtonian fluids - Correlation of the laminar, transition and turbulent-flow regions," A.I.Ch.E.Jour., 1, 434, (1955).

27. Dodge, D.W. and Metzner, A.B., "Turbulent flow of non-Newtonian systems," A.I.Ch.E.Jour., 5, 2, 189, (1959).

28. Shaver, R.G. and Merrill, E.W., "Turbulent flow of pseudoplastic polymer solution in straight cylindrical tubes," A.I.Ch.E. Jour., 5, 2, 181, (1959).

29. Hershey, H.C. and Zakin, J.L., "Existance of two types of drag reduction in pipe flow of dilute polymer solutions," Ind. and Eng. Chem. Fund., 6, 3, 381, (1967).

30. Ousterhout, R.S. and Hall, C.D., "Reduction of loss in fracturing operations," J. Petr. Tech., 13, 217, (1960).

31. Lummus, J.L., et.al. "New type of mud reduces drilling costs," World Oil, 154, 68,(1962).

32. Ripken, J.F. and Pilch, M., "Studies of the reduction of pipe friction with the non-Newtonian additive C.M.C.," Univ. Minnesota, St. Anthony Falls, Hyd. Lab. Tech. Paper, 42,Ser.B. (1963).

33. Elata, C. and Tirosh, J., "Frictional drag reduction," Israel J. Tech., 3, 1, 1, (1965).

34. Metzner, A.B. and Park, M.G., "Turbulent flow characteristics of viscoelastic fluids," J.Fluid Mech., 20, 2, 291, (1964).

35. Savins J.G., "Drag reduction characteristics of solutions of macromolecules in turbulent pipe flow," Soc. Petr. Eng. Jour.,p.203, (Sept.1964).

36. Lumley, J.L., "Turbulence in non-Newtonian fluids," Phys. of fluids, 7, 3, 335, (1964).

37. Wells, C.S., "On the turbulent shear flow of an elasticoviscous fluid," A.I.A.A. preprint No. 64-36, (1964).

38. Thurston, S. and Jones, R.D., "Experimental model studies of non-Newtonian soluble coatings for drag reduction," A.I.A.A. paper No. 64-466, (1964).

39. Lummus, J.L. and Randall, B.V., "Development of drilling friction additives for Project Mohole," Pan Am. Petr. Corp. Report F 64-P-54 (1964).

40. Astirita, G., "Possible interpretation of the mechanism of drag reduction in visco-elastic liquids," Ind. and Eng. Chem. Fund., 4, 354, (1965).

41. Hoyt, J.W., "A turbulent flow rheometer." Paper at Rheology Symp., A.S.M.E. Applied Mech.,-Fluid Mechanics joint conf. Washington D.C. (June 1965).

42. Hoyt, J.W. and Soli, G., "Algal cultures: Ability to reduce turbulent friction in flow," Science, 149, 3691, 1509, (1965).

43. Pruitt, G.T. and Crawford, H.R., "Effect of molecular weight and segmental constitution on the drag reduction of water soluble polymers," Rep.No.DTMB-1, Western Co. Texas. (1965).

44. Pruitt, G.T. and Crawford, H.R., "Investigation for the use of additives for the reduction of pressure losses," A.D. 613345 (1965).

45. Vogel, M.W. and Patterson, A.M., "An experimental investigation of the effect of additives injected into the boundary layer of an underwater body," 5th Symp. Naval Hydrodynamics, O.N.R. Skipsmodelltanken, Bergen, (1965).

46. Wu, J. "Experiments on free turbulence in visco-elastic fluids," Hydronautics Inc. Tech. Rep. 353-1, (1965).

47. Barenblatt, G.I. et.al. "The effect of solutions of high molecular weight compounds on the lowering of resistance around bodies during turbulent flow," Prikl Mekh.i Tek. Fiz., 3, 95, (1965).

48. Barenblatt, G.I. et.al., J.Prikl. Mekh. i Tek. Fiz., 5, 147, (1965).

49. Ruszczycky, M.A., "Sphere drop tests in high polymer solutions," Nature, 206, 4984, 614, (1965).

50. Lindgren, E.R., "Friction reduction effects on turbulent flows of water in rough pipes by dilute additive of high molecular weight polymer," A.D. 621070, (1965)

51. Bradshaw, P., "An introduction to turbulence and its measurement," Pergammon press (1971).

52. Hinze, J.O., "Turbulence," McGraw-Hill (1959)

53. Kline, S.J., "Some remarks on turbulent shear flows," Proc. I.Mech.E. 1965-1966, 180 part 3J p.222.

54. Lighthill, M.J., "Turbulence," Paper in "Osborne Reynolds and engineering science today." Manchester U.P. (1970).

55. Phillips, O.M., "Shear flow turbulence," Ann. Rev. of Fluid Mech. 1, (1969)

56. Kowalski, T., "Turbulence suppression and viscous drag reduction by non-Newtonian additives," R.I.N.A. Trans., 10, 2, 207, (April 1968).

57. Elata, C., et.al., "Turbulent shear flow of polymer solutions," Israel Jour. of Tech. 4, 1, 87, (1966).

58. Poreh, M., et.al. "Studies in rheology and hydrodynamics of dilute polymer solutions," Technion, Faculty of Civil Eng. Publication No. 126, (March 1969)

59. Virk, P.S., et.al. "The ultimate asymptote and mean flow structure in Toms' phenomenon," Trans. A.S.M.E., J.Appl. Mech.,37, 488, (1970).

60. Ernst, W.D., "Turbulent flow of an elasticoviscous non-Newtonian fluid," AIAA Jour. 5, 5, 906, (1967).

61.(i) Goren, Y and Norbury, J.F., "Turbulent flow of dilute aqueous polymer solutions," Trans A.S.M.E. J.Basic Eng.,89, Ser.D,4, Dec. (1967).

(ii) Goren, Y., "The effect of polymer additives on turbulent shear flow," Ph.D. Thesis, Univ. of Liverpool, (Oct.1966).

62. Meyer, W.A., "A correlation of the frictional characteristics for turbulent flow of dilute viscoelastic non-Newtonian fluids in pipes," A.I.Ch.E.Jour., 12, 3, 478 (1966).

63. Gadd, G.E. "Turbulence suppression," N.P.L. Ship T.M.228. (Sept.1968).

64. Vlasov, S.A. and Kalashnikov, V.N., "Turbulent diffusion of heat in jets of dilute polymer solution," Nature, 224, 1195 (Dec.1969)

65. Kalashnikov, V.N. and Belokon, V.S., "Polymer additives and turbulent friction near rough surfaces," Nature, Phys.Sci. 229, 55, (Jan.1971).

66. Brennen, C. and Gadd, G.E., "Ageing and degradation in dilute polymer solutions," Nature, 215, 5108, 1368, (1967).

67. Nash, T., "Modification of the bulk mechanical properties of water by complex formation in dilute solution," Nature, 177, 948 (1956).

68. Nash, T., "Conjugation with lone pair electrons. II The absorption of naphthols by cationic micelles in dilute aqueous solution," J.App.Chem., 6, 519, (Dec.1956).

69. Nash, T., "The interaction of some naphthalene derivitives with a cationic soap below the critical micelle concentration," J.Colloid Sci., 13, 2, 134, (1958).

70. Savins, J.G., "A stress controlled drag reduction phenomenon," Rheo. Acta, 6, 4, 323,(1967).

71. Fitzgerald, D., "Drag reduction in central heating," Paper at Brit. Soc. Rheology Conf. Shrivenham, (1967).

72. Kline, S.J., et.el. "The structure of turbulent boundary layers," J.Fluid Mech., 30, 4, 741, (1967).

73. Kline, S.J. et.el. "The production of turbulence near a smooth wall in a turbulent boundary layer," J.Fluid.Mech., 50, 1, 133, (1971).

74. Wells, C.S., et.el. "Turbulence measurements in pipe flow of a drag reducing non-Newtonian fluid," AIAA Jour. 6, 2, 250, (1968).

75. Jackley, D.N., "Drag reducing fluids in a free turbulent jet," Int. Shipbuilding Prog. 14, 158, (1967).

76. Gadd, G.E., "Reduction of turbulent friction in liquids by dissolved additives," Nature, 212, 5065, 874, (1966).

77. U.S.Navy photograph from Naval Ordnance Test Station, Pasadena, Calif.

78. Streeter, V.L., "Fluid Mechanics," McGraw-Hill (1966) p.243.

79. White, D.A., "Drag coefficients for spheres in high Reynolds number flow of dilute solutions of high polymers," Nature,212, 5059, 277, (1966).

80. Lang, T.G. and Patric, H.V.L., "Drag of blunt bodies in polymer solutions," ASME preprint 66-WA/FE-33, (1966).

81. Sanders J.V., "Drag coefficients of spheres in Poly (Ethylene Oxide) solutions," Int. Shipbuilding Prog., 14, 140, (1967).

82. White D.A. and Bond, J.A., "Terminal velocities of balls dropping through dilute colloid solutions," Nature, 226, 5240, 72, (1970).

83. Gadd, G.E., "Differences in normal stress in aqueous solutions of turbulent drag reducing additives," Nature, 212, 5069, 1348, (1966).

84. Bizzell, G.D. and Slattery, J.C., "Non-Newtonian boundary layer flow," J. Chem. Eng. Sci., 17, 177, (1962).

85. Metzner, A.B. and Friend, P.S., "Heat transfer to turbulent non-Newtonian fluids," Ind. Eng. Chem., 51, 879, (1959).

86. Pruitt, G.T., et.al. "Turbulent heat transfer to viscoelastic fluids," Western Co. Dallas, Texas, Report. (1966).

87. Poreh, M. and Paz, U., "Turbulent heat transfer to dilute polymer solutions," Int. Jour. Heat and Mass Trans., 11, 805, (1968).

88. James, D.F., "Open channel syphon with viscoelastic fluids," Nature, 212, 5063, 754, (1966).

89. Hoyt, J.W., "Effect of high polymer solutions on a cavitating body," Paper at 11th. Int. Towing tank Conf.

90. Hoyt, J.W., "The influence of natural polymers on fluid friction and cavitation," Paper at Symp. on Testing techniques in ship cavitation research. Skipsmodelltanten, Bergen, (June 1967).

91. Ellis, A.T., "Some effects of macromolecules on cavitation inception and noise," Div. of Eng. and Appl. Sci. California Inst. Tech. (June 1967) - (U.S.Naval Ord. Test Sta. Contract N60530-12164).

92. Brennen, C., "Some cavitation experiments with dilute polymer solutions," N.P.L. Ship Rep. 123, (Nov.1968).

93. Virk, P.S., and Merrill, E.W., "The onset of dilute polymer solution phenomena," Paper in "Viscous Drag Reduction," ed. C.S.Wells, p.107, Plenum press (1969).

94. Granville, P.S., "The frictional resistance and velocity similarity laws of drag reducing dilute polymer solutions," Naval Ship Res. and Dev. Washington, Report. 2502, (Sept.1967).

95. Granville, P.S., "Limiting conditions to similarity law correlations for drag reducing polymer solutions," Naval Ship Res. and Dev.Center. Washington, Report, 3635, (Aug.1971)

96. Granville, P.S., "Maximum drag reduction at high Reynolds number for a flat plate immersed in polymer solution," Naval Ship Res. and Dev. Center, Washington, Ship performance dept., TN 205, (Aug.1971).

97. Lumley, J.L., "Drag reduction by additives," Annual Rev. of Appl. Mech. Vol. 1, 367, Annual Reviews Inc. (1969).

98. Arunachalam, Vr. and Fulford, G.D., "Pressure drop reduction in turbulent pipe flow by soap and polymer additives," La Houille Blanche, 26, 1, 33, (1971).

99. Union Carbide Corp. Polyox friction reducing agent FRA Applications Bulletin, March 1966.

100. Poreh, M., et.al. "Drag reduction in hydraulic transport of solids," J. Hydraulics Div., Proc. Am. Soc. Civil Eng. April 1970, 903.

101. Ram, A., et.el. "Reduction of friction in oil pipelines by polymer additives," I. and E.C. Process design and development, 6, 3, 309, (1967).

SEPARATE BIBLIOGRAPHIES.

Progress in frictional drag reduction, Summer 1966 to summer 1967, P.S.Granville. U.S.Naval ship research and development center, Washington, D.C. Presented at ORDHAC meeting, Sept.1967.

Progress in frictional drag reduction, Summer 1967 to summer 1968. P.S.Granville. U.S Naval ship research and dev. center, Hydromechanics lab. T.N.118, (Oct.1968).

Progress in frictional drag reduction, Summer 1968 to summer 1969, P.S.Granville, U.S.Naval ship research and dev. center, Hydromechanics lab. T.N.143, (Aug.1969)

Progress in frictional drag reduction, Summer 1969 to summer 1970, P.S.Granville, U.S.Naval ship research and dev. center, Dept. of ship performance, T.N.184, (Oct.1970).

Progress in frictional drag reduction, Summer 1970 to summer 1971, P.S.Granville, U.S.Naval ship research and dev. center, Ship performance dept., R. and D. report No.3761, (Jan.1972).

A bibliography of Drag Reduction and related subjects, University of Exeter. Tech. Report FD/DR No. 1, (June 1970).

APPENDIX 1. INTEGRATION OF TWO ZONE VELOCITY PROFILE MODEL.

(Pipe flow)

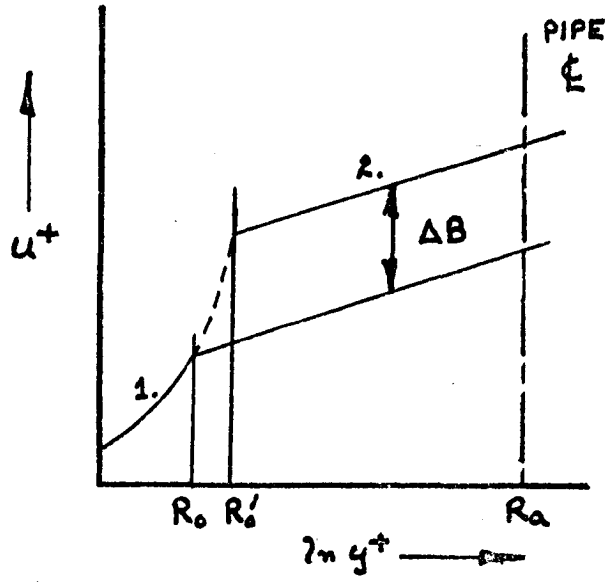

1. $u^+ = y^+$
2. $u^+ = A \ln y^+ + B + \Delta B$

At the intersection of 1 and 2 we have:-

$$R_0 = A \ln R_0' + B + \Delta B$$

Integration across the pipe radius (a) yields the volume flow rate, viz:-

$$Q = \pi a^2 \bar{U} = \int_0^a 2\pi r \, u(r) \, dr$$

Since $y = (a-r)$ and $dy = -dr$ this becomes:-

$$\pi a^2 \bar{U} = \int_0^a 2\pi (a-y) \, u(y) \, dy$$

The above expression is put into dimensionless form:-

$$\frac{a\bar{U}}{2u^*} = \int_0^{Ra} \left(1 - \frac{y^+ \nu}{a u^*}\right) u^+ \frac{\nu}{u^*} \, dy^+$$

and the integration is carried out in two parts using expressions for zones 1 and 2 respectively.

Noting also that $R_e = \frac{2\bar{U}a}{\nu}$ and $R_a = \frac{a u^*}{\nu}$ we may write:-

$$\frac{R_e}{4} = \int_0^{R_0'} \left(1 - \frac{y^+}{Ra}\right) y^+ dy^+ + \int_{R_0'}^{Ra} \left(1 - \frac{y^+}{Ra}\right)(A \ln y^+ + B + \Delta B) \, dy^+$$

Integration then yields:-

$$\frac{Re}{4} = \left[\frac{y^{+2}}{2} + \frac{y^{+3}}{3Ra}\right]_0^{R_0'} + \left[A y^+ (\ln y^+ - 1) + (B+\Delta B) y^+ \cdots \right.$$
$$\left. \cdots - \frac{A}{Ra}\frac{y^{+2}}{2}(\ln y^+ - \tfrac{1}{2}) - \frac{B+\Delta B}{Ra}\cdot\frac{y^{+2}}{2}\right]_{R_0'}^{Ra}$$

Insertion of the limits gives:-

$$\frac{Re}{4} = \frac{R_0'^2}{2} + \frac{R_0'^3}{3Ra} + \left[\frac{ARa}{2}\ln Ra + \frac{BRa}{2} - \frac{3}{4}ARa\right] \cdots$$
$$\cdots - \left[-R_0'\{A-(B+\Delta B)\} + AR_0'\ln R_0 - \frac{A}{Ra}\cdot\frac{R_0'^2}{2}\ln R_0' - \frac{R_0^2}{2Ra}(B+\Delta B - \frac{A}{2})\right]$$

Noting that $Ra = Re\sqrt{\frac{f}{8}}$ we may write:-

$$\frac{1}{\sqrt{f}} = \frac{2R_0^2}{Re\sqrt{f}} + \frac{4}{3}\frac{R_0^3}{Re^2 f}\cdot 2\sqrt{2} + \frac{A}{\sqrt{2}}(\ln Re\sqrt{f} - \ln 2\sqrt{2}) + \frac{B}{\sqrt{2}} - \frac{3A}{2\sqrt{2}} \cdots$$
$$\cdots + \frac{4R_0'\{A-(B+\Delta B)\}}{Re\sqrt{f}} - \frac{4AR_0'\ln R_0'}{Re\sqrt{f}} + \frac{4AR_0'^2\cdot 2\sqrt{2}}{2Re^2 f}\ln R_0' \cdots$$
$$\cdots + \frac{4R_0'^2}{2Re^2 f}(B+\Delta B - \frac{A}{2}).$$

On collecting terms and eliminating $B+\Delta B$ we have:-

$$\frac{1}{\sqrt{f}} = \frac{2R_0'^2}{Re\sqrt{f}} + \cancel{\frac{B\sqrt{2}}{3}\frac{R_0^3}{Re^2 f}} + \frac{A}{\sqrt{2}}(\ln Re\sqrt{f} - \ln 2\sqrt{2}) + \frac{R_0' - A\ln R_0'}{\sqrt{2}} \cdots$$
$$\cdots - \frac{3A}{2\sqrt{2}} + \frac{4R_0'[A-(R_0'-A\ln R_0')]}{Re\sqrt{f}} - \frac{4AR_0'\ln R_0'}{Re\sqrt{f}} \cdots$$
$$\cdots + \cancel{\frac{4A\sqrt{2}}{Re^2 f}R_0^2\ln R_0'} + \cancel{\frac{4\sqrt{2}}{Re^2 f}R_0^2}\left[\cancel{R_0' - A(\ln R_0' + \tfrac{1}{2})}\right]$$

The three terms struck out are small compared with the remaining ones and are hence neglected.

This equation then simplifies to:-

$$\frac{1}{\sqrt{f}} = \frac{A}{\sqrt{2}}\left(\ln Re\sqrt{f} - \ln 2\sqrt{2} + \frac{R_0'}{A} - \ln R_0' - \frac{3}{2}\right) + \frac{R_0'}{Re\sqrt{f}}(4A - 2R_0') \quad \text{---[A1]}$$

The last term is small provided that R_0' is not too large.

For a Newtonian fluid we note that $\Delta B = 0$,

i.e. $Ro' = Ro = 11.6$, and $A = 1/k = 2.5$

Substitution of these values into eqn.A1 yields:-

$$\frac{1}{\sqrt{f}} = 1.768 \ln Re\sqrt{f} - 0.619 - \frac{153.12}{Re\sqrt{f}}$$

This agrees with Von Kármán's integration which ignored flow through the sublayer:-

$$\frac{1}{\sqrt{f}} = 1.768 \ln Re\sqrt{f} - 0.60.$$

APPENDIX 2. INTEGRATION OF THREE ZONE VELOCITY PROFILE MODEL.

(Pipe flow)

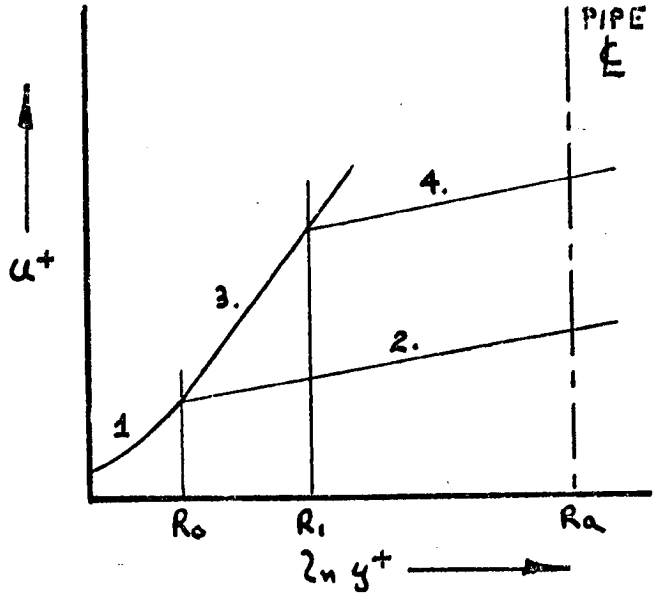

Zone 1-2 for Newtonian fluid.
Zone 1-3-4 for Drag reducing fluid.

Equations for zones:-

1. $u^+ = y^+$
2. $u^+ = A \ln y^+ + B$
3. $u^+ = A_1 \ln y^+ - B_1$
4. $u^+ = A \ln y^+ + B + \Delta B$

Where $A = 1/k = 2.5$ $\quad B = 5.5$ $\quad B = f(\gamma_w)$

$A = 11.7$, $B = 17.0$ } Virk

At the intersection of 3 and 4:-

$$A_1 \ln R_1 - B_1 = A \ln R_1 + B + \Delta B$$

$$(B + \Delta B) = (A_1 - A) \ln R_1 - B_1 \quad -18.$$

Working as in appendix 1, integration across the pipe radius gives the volume flow rate, and we can hence show:-

$$\frac{Re}{4} = \int_0^{Ra} \left(1 - \frac{1}{Ra} y^+\right) u^+ dy^+$$

The integration is carried out in three parts:-

$$\frac{Re}{4} = \int_0^{R_0} \left(1 - \frac{y^+}{Ra}\right) y^+ dy^+ + \int_{R_0}^{R_1} \left(1 - \frac{y^+}{Ra}\right)\left(A_1 \ln y^+ - B_1\right) dy^+ \ldots$$

$$(I_1) \qquad\qquad (I_2)$$

$$\ldots + \int_{R_1}^{Ra} \left(1 - \frac{y^+}{Ra}\right)\left[A \ln y^+ + (A_1 - A)\ln R_1 - B_1\right] dy^+$$

$$(I_3)$$

$$I_1 = \frac{R_0^2}{2} - \frac{R_0^3}{3Ra} \quad \text{(See appendix 1.)}$$

$$I_2 = \int_{R_0}^{R_1} \left(A_1 \ln y^+ - B_1 - \frac{A_1}{Ra} y^+ \ln y^+ + \frac{B_1}{Ra} y^+\right) dy^+$$

$$= \left[A_1 y^+ (\ln y^+ - 1) - B_1 y^+ - \frac{A_1 y^{+2}}{2Ra}\left(\ln y^+ - \tfrac{1}{2}\right) + \frac{B_1}{2Ra} y^{+2}\right]_{R_0}^{R_1}$$

$$= \left\{A_1 R_1 (\ln R_1 - 1) - B_1 R_1 - \frac{A_1 R_1^2}{2Ra}\left(\ln R_1 - \tfrac{1}{2}\right) + \frac{B_1 R_1^2}{2Ra}\right\} \ldots$$

$$\ldots - \left\{A_1 R_0 (\ln R_0 - 1) - B_1 R_0 - \frac{A_1 R_0^2}{2Ra}\left(\ln R_0 - \tfrac{1}{2}\right) + \frac{B_1 R_0^2}{2Ra}\right\}$$

$$I_3 = \int_{R_1}^{Ra} \left[A \ln y^+ + (A_1 - A)\ln R_1 - B_1 - \frac{A}{Ra} y^+ \ln y^+ \ldots\right.$$

$$\left. \ldots - \left(\frac{A_1 - A}{Ra} \ln R_1\right) y^+ + \frac{B_1 y^+}{Ra}\right] dy^+$$

$$= \left\{A y^+ (\ln y^+ - 1) + \left[(A_1 - A)\ln R_1 - B_1\right] y^+ - \frac{A y^{+2}}{2Ra}\left(\ln y^+ - \tfrac{1}{2}\right) \ldots\right.$$

$$\left. \ldots - \frac{1}{2Ra}\left[(A_1 - A)\ln R_1 - B_1\right] y^{+2}\right\}_{R_1}^{Ra}$$

So:-

$$I_3 = \left\{A Ra (\ln Ra - 1) + \left[(A_1 - A)\ln R_1 - B_1\right] Ra - \frac{A Ra^2}{2Ra}\left(\ln Ra - \tfrac{1}{2}\right) - \frac{1}{2Ra}\left[(A_1 - A)\ln R_1 - B_1\right] Ra^2\right\}$$

$$\ldots - \left\{A R_1 (\ln R_1 - 1) + \left[(A_1 - A)\ln R_1 - B_1\right] R_1 - \frac{A R_1^2}{2Ra}\left(\ln R_1 - \tfrac{1}{2}\right) - \frac{1}{2Ra}\left[(A_1 - A)\ln R_1 - B_1\right] R_1^2\right\}$$

Continued- - -

On collecting terms we find:-

$$\frac{R_e}{4} = \frac{R_0^2}{2} + R_0\left[B_1 - A_1(2nR_0 - 1)\right] + \frac{R_0^2}{R_a}\left[\frac{A_1}{2}(2nR_0 - \tfrac{1}{2}) - \frac{R_0}{3} - B_1\right] \cdots$$

$$\cdots + R_a\left[\frac{A\,2nR_a}{2} - \frac{3A}{4} - \frac{B_1}{2}\right] + R_1(A - A_1) \cdots$$

$$\cdots + R_1^2\left[\frac{A_1}{2R_a}2nR_1 - \frac{A}{R_a}2nR_1 + \frac{1}{4R_a}(A_1 - A) - \frac{B_1}{2R_a}\right] \cdots$$

$$\cdots + \frac{R_a}{4}(A_1 - A)2nR_1$$

Noting that $R_a = R_e\sqrt{\frac{f}{8}}$ we get:-

$$\frac{1}{\sqrt{f}} = \frac{4}{R_e\sqrt{f}}\left\{\frac{R_0^2}{2} + R_0\left[B_1 - A_1(2nR_0 - 1)\right\} + \frac{8R_0^2}{R_e^2 f}\left[\frac{A_1}{2}(2nR_0 - \tfrac{1}{2}) - \frac{R_0}{3} - B_1\right] \cdots\right.$$

$$\cdots + \frac{A}{\sqrt{2}}\left[2nR_e\sqrt{f} - 2n2\sqrt{2}\right] - \frac{3A}{2\sqrt{2}} - \frac{B_1}{\sqrt{2}} + \frac{A_1 - A}{\sqrt{2}}2nR_1 \cdots$$

$$\cdots + \frac{4R_1}{R_e\sqrt{f}}(A - A_1) + \frac{2\sqrt{2}}{R_e\sqrt{f}}\left[2nR_1\left(\frac{A_1}{2} - A\right) + \frac{A_1 - A}{4} - \frac{B_1}{2}\right].$$

Terms struck out are small compared with the others, and are neglected leaving:-

$$\frac{1}{\sqrt{f}} = \frac{A}{\sqrt{2}}2nR_e\sqrt{f} - \frac{4}{\sqrt{2}}2n2\sqrt{2} - \frac{3A}{2\sqrt{2}} + \frac{A_1 - A}{\sqrt{2}}2nR_1 \cdots$$

$$\cdots + \frac{4}{R_e\sqrt{f}}\left\{\frac{R_0^2}{2} + R_0\left[B_1 - A_1(2nR_0 - 1)\right] + R_1(A - A_1)\right\}.$$

On inserting numerical values for the constants we find:-

$$\frac{1}{\sqrt{f}} = 1{\cdot}768\,2nR_e\sqrt{f} - 16{\cdot}5104 + 6{\cdot}5054\,2nR_1 + \frac{268{\cdot}095}{R_e\sqrt{f}} - \frac{9{\cdot}2R_1}{R_e\sqrt{f}}$$

Foe a Newtonian fluid $R_1 = R_0 = 11.6$, and the equation reduces to:-

$$\frac{1}{\sqrt{f}} = 1{\cdot}768\,2nR_e\sqrt{f} - 0{\cdot}565 + \frac{161{\cdot}3}{R_e\sqrt{f}}$$

This agrees with the Von Karman result, $1/\sqrt{f} = 1{\cdot}768\,2nR_e\sqrt{f} - 0{\cdot}60$. and thus provides a check on the integration.

APPENDIX 3

COURSES AND CONFERENCES ATTENDED DURING THE PRESENT PERIOD OF STUDY.

It is a requirement of the C.N.A.A. that candidates for post graduate research degrees should attend relevant courses and conferences during the period of the research work. The following were attended during the period of this study. In some cases a paper was presented by the present author, and these are marked with an asterisk.

----------oOo----------

1) I.Mech E. Symposium on Boiling Heat transfer, sponsored by the Steam Plant, Nuclear Energy and Thermo, and Fluid Mechanics groups. Manchester, Sept.1965.

2) Convention and Symposium sponsored by the Thermodynamics and Fluid Mechanics groups of I.Mech.E. Liverpool, April 1966.

3) Euromech Colloquium, The Structure of Turbulence, Southampton, March 1967.

4) I.Mech.E. Conversazione, Novel instrumentation in Thermodynamics and Fluid Mechanics. London, April 1967.

5) British Society of Rheology conference, Non-Newtonian flow through pipes and passages. Shrivenham, (Sept.1967).

* Paper by author - "Turbulence and suppression and drag reduction with macromolecular additives."

6) Convention and symposium sponsored by the Thermodynamics and Fluid Mechanics groups of I.Mech.E. Bristol, March 1968.

7) Symposium on turbulence suppression, with reference to Polyox type additives. Sponsored by Union Carbide U.K.Ltd. Bradford, April 1968.
   * Paper by author - "Studies of the flow characteristics of dilute Polyox solutions."

8) Symposium on viscous drag reduction, sponsored by U.S. Office of Naval Research and N.A.S.A. L.T.V. Research Center, Dallas, Texas, Sept.1968.
   * Invited lecture presented by author - "Flow characteristics of dilute macromolecular solutions."

9) I.Chem.E. Graduates and Students section annual Symposium, "Recent developments in fluids handling." London, Oct.1968.
   * Paper by author - "Pipe friction reduction with macromolecular additives."

10) Polyox conference, sponsored by Union Carbide U.K.Ltd. London, Sept.1969.

11) Discussions on Drag Reduction, a conference Admiralty Materials Laboratory, Holton Heath, Dorset, Nov.1969.
   * Informal paper presented by author.

12) Symposium on internal flows, sponsored by the N.P.L. and I.Mech.E. Salford, April 1971.

APPENDIX 4

PUBLICATIONS.

These are enclosed in a flap at the end of this thesis.

P1) "Turbulent drag reduction by using dilute polymer solution instead of water." Hendon Coll. Tech. Res. Bull. 3,58, (Jan.1966)

P2) "Turbulent drag reduction with polymer additives." J.Mech.Eng.Sci., 8,4,452, (1966)

P3) "Effect of polymer additives on boundary layer separation and drag of submerged bodies." Nature, 211, 5056, 1390, (1966)

P4) "Turbulence and drag reduction with polymer additives." Hendon Coll.Tech.Res.Bull. 4, 75, (Jan.1967).

P5) "Flow characteristics of complex soap systems." Nature, 214, 5088, 585, (1967)

P6) "Drag of spheres in dilute high polymer solutions." Nature, 216, 5119, 994, (1967)

P7) "Studies of the flow characteristics of dilute high polymer solutions." Hendon Coll.Tech.Res.Bull. 5, 113, (Mar.1968)

P8) "Pipe friction reduction with macromolecular additives." I.Chem.E. - Graduates and Students section, Symp. "Recent developments in fluids handling." London, (Oct.1968)

P9) "Some observations on the flow characteristics of certain dilute macromolecular solutions." (Nominated paper at Symp. on viscous drag reduction, LTV Research Center, Dallas, Sept.1968) Published in 'Viscous Drag Reduction.' ed. C.S.Wells, Plenum press, (1969).

P10) "Heat transfer characteristics of dilute polymer solutions in fully rough pipe flow."
Nature, 227, 5257, 486, (1970)

P11) "The flow of viscoelastic micellar solution around circular cylinders."
Hendon Coll.Tech.Res.Bull. 7, 115,(Nov.1970)

P12) "Velocity profiles of a complex soap system in turbulent pipe flow."
Nature, Phys.Sci., 235, 60, 154, (1972)